THE PERFORMANCE OF LABYRINTH WEIRS

by

Geoffrey Taylor, B.Eng.

Thesis submitted to the Faculty of Applied Science,

University of Nottingham, for the degree of Doctor of Philosophy.

October, 1968

CONTENTS

SECTION I EXPERIMENTAL WORK

APPENDIX.

SYNOPSIS

The purpose of the labyrinth weir is to increase the discharge per unit length of structure normally obtained from a conventional weir when operating under identical head conditions. This is achieved by compressing a large length of crest in concertina form, into the space available on site.

The investigation carried out as described in this thesis aimed to provide comprehensive performance data covering all aspects of labyrinth weir behaviour. This has been achieved by a series of experimental model tests.

The initial experimental work was confined to basic labyrinth weir configurations and the significance of the parameters of fundamental importance has been determined. This allowed the definition of the most useful ranges of weir design and subsequent experimental tests were confined to within these ranges.

Following the initial experimental work tests were conducted to determine the significance of all the parameters of secondary importance including various refinements to the weir designs such as sloping channel inverts and alternative crest sections etc.

A comprehensive set of experimental performance data covering all aspects of labyrinth weir design and behaviour are thus contained in the thesis.

A mathematical model representing the behaviour of the weirs has been constructed and translated into a computer programme. Close correlation has been achieved between the theoretical and experimental results and the programme will accurately predict the performance of any labyrinth weir subject to some minor restrictions.

The computer programme is included in the thesis so that it will be available to anyone wishing to use it.

A design method using two design charts has been developed. This enables the design and performance prediction of any weir designed in accordance with recommendations contained in the thesis. The design charts are included in the text together with a worked example illustrating their use.

ACKNOWLEDGEMENTS

The work described in this thesis was carried out in the Mechanical Engineering Department of the University of Nottingham and was financed by the Science Research Council.

Thanks are due to Professor A.G. Smith for the facilities provided.

I would like to express my sincere thanks to Dr. N. Hay who supervised the work and whose advice and assistance were greatly appreciated.

Thanks are due to the Technicians of the Fluid Mechanics Laboratory for their practical assistance and for their tolerance on the occasions when the laboratories were flooded.

I would also like to express my gratitude to my wife and parents for their encouragement, and to Miss M.B. Williams who typed the script.

LIST OF TABLES

LIST OF PHOTOGRAPHS

LIST OF FIGURES

The Figures are situated at the end of thesis.

NOMENCLATURE

The nomenclature has been adequately described where necessary in the text but the following symbols and ratios are of fundamental importance.

Dimensions in f.p.s. units.

h	- upstream head over the crest.
h_d	- downstream head over the crest.
l	- developed length of one cycle of weir.
w	- width of one cycle of weir.
p	- crest height.
n	- number of weir cycles in plan.
α	- angle of side walls to main flow direction.
QL	- discharge over labyrinth weir.
QR	- discharge over a corresponding linear weir operating under identical head conditions to those which determine the discharge QL of the labyrinth weir.
l/w	- length magnification factor = ratio of the developed crest length of the labyrinth weir to the crest length of the corresponding linear weir. (see Descriptive Terms).
w/p	- vertical aspect ratio = ratio of width of weir cycle in plan to the crest height.
QL/QR	- flow magnification (see Descriptive Terms).
E	- effectiveness of the labyrinth weir = $\frac{QL/QR}{l/w} \times 100\%$

d - change in channel bed elevation between the upstream and downstream sides of the weir.

a - half length of tip sections normal to the flow.

b - length of side walls of weir.

c - crest coefficient.

Descriptive Terms

The following terms have been widely used throughout the text and their meaning is therefore fundamental to the understanding of the text.

Corresponding linear weir: A straight weir occupying the same channel width as the labyrinth weir.

Flow magnification - QL/QR: The ratio of the discharge of the labyrinth weir to the discharge of a corresponding linear weir operating under the same head.

Length magnification (factor) - l/w: The ratio of the developed crest length of the labyrinth weir to the width of channel occupied by the labyrinth weir (Figure 1)

Side wall angle - α : The angle of the side walls of the weir to the main flow direction (Figure 1).

Vertical Aspect Ratio - w/p: The ratio of the width of one cycle of weir (or pitch) to the crest height.

Weir tips: The end sections of the weir normal to the main flow direction.

Rectangular weir: A labyrinth weir with a zero side wall angle so that the tips are perpendicular to the side walls (Figure 2).

Triangular weir: A weir in which the side walls meet at a point so that the length of the tips is zero and the weir consequently assumes a triangular form in plan (Figure 2).

Trapezoidal weir: A weir having a trapezoidal plan form somewhere between the limits of the rectangular and triangular plan forms described above.

Apron Ratio: The ratio of the maximum height of the apron above the channel bed to the crest height.

CHAPTER 1

INTRODUCTION

1.1 Weirs as Control Devices

In any construction involving the retention of water, means of allowing the passage of excess water must be provided so that flooding and weakening of the dam structure is prevented. In rivers and canals weirs are almost invariably used for this purpose, and are also generally used to supplement mechanically operated gates in large dam structures.

Low level gates have the advantage of being unaffected by ice and floating debris but maintenance costs can be high. Non-automatic gates are only suitable for climates where flooding can be reliably predicted, unless personnel are standing by at all times. A further disadvantage of gates is that they can discourage the movement of migratory fish, and for this reason it is often necessary to provide an alternative spillway.

Weirs, being simple and fixed, have the major advantage of being completely automatic in operation and require only a minimum of attention unless there are large quantities of floating debris.

The discharge capacity of a weir is directly proportional to the length of the weir crest. Thus, for a given head, the discharge is limited by the maximum crest length which can be built in a given situation. This limitation can be overcome by the use of siphon spillways, but these are expensive to construct and have a serious disadvantage in their mode of operation. A siphon reaches its maximum discharge shortly after priming, and maintains this discharge until the siphon suddenly 'vents'. Priming and venting can give rise to waves which travel down the river, causing erosion and also presenting a hazard to shipping.

1.2 The Labyrinth Weir

A labyrinth weir is characterised by a broken axis in plan (Figure 1), the total crest length thus being compressed in concertina form into the space available on site. (Photographs 1 and 2).

The purpose of this type of weir is to present the water flow with a greater crest length than that of a normal linear weir occupying the same space. The discharge capacity is increased and the weir provides a simple alternative to the siphon overflow.

Labyrinth weirs are particularly useful in situations where it is necessary to discharge large quantities of water with

the head over the weir restricted to a relatively small value. In these cases, even though the site conditions may allow the construction of a normal straight overflow of equivalent discharge capacity, it may be found more economic to adopt the labyrinth plan form.

Labyrinth weirs have similar advantages to linear weirs in their mode of operation, but have the disadvantage that they may be more prone to damage and obstruction by ice and floating debris.

As the purpose of the labyrinth weir is to increase the discharge that would normally be obtained over a straight weir operating under the same head and occupying the same width of channel, it is logical to define the performance of the labyrinth weir in terms of flow magnification. The flow magnification is defined as the ratio of the discharge of the labyrinth weir to that which would be obtained from the corresponding linear weir. Ideally the flow magnification will be equal to the crest length magnification of the labyrinth weir. (See descriptive terms, page xiv).

1.3 Basic Considerations

The discharge of a normal linear weir is primarily dependent on the crest height p, the head h, and the length of the weir

crest. It is reasonable to assume therefore that the behaviour of labyrinth weirs will also be dependent on these variables, but will also be influenced by the parameters defining the plan form.

Infinite variations of weir plan forms are possible but the simplest and most favoured is the trapezoidal form shown in Figures 1 and 2. Furthermore, if the plan form is symmetrical, that is with upstream and downstream tips of equal length, then the shape of the plan form is completely defined by the length magnification of the weir ($^{l}/_{w}$), and the side wall angle α .

The parameters considered fundamental in determining the labyrinth weir discharge (QL), are therefore:-

$$h,\ p,\ l,\ w,\ \alpha,\ g,\ n.$$

where l is the developed crest length of one cycle of weir

w is the width of one cycle of weir

g is the acceleration due to gravity

n is the number of weir cycles.

These may be reduced to the following non-dimensional groups:-

$$^{h}/_{p},\ ^{w}/_{p},\ ^{l}/_{w},\ \alpha,\ ^{gh^5}/_{QL^2},\ n.$$

The significance of the geometrical parameters, $^{l}/_{w}$, $^{w}/_{p}$, α, is indicated in the following sections and a discussion of the remaining parameters in included in Chapter 4.

1.3.1 The Length Magnification Factor $^{l}/_{w}$

The length magnification factor is fundamentally important in that it represents the theoretical maximum, or optimum, magnification of discharge when compared with a linear weir. The importance of this factor in defining the plan form of the weir has already been indicated.

1.3.2 The Side Wall Angle $\propto$.

Together with the length magnification factor, this parameter defines the weir shape in plan.

Two conditions may severely restrict labyrinth weir discharge, especially at high flowrates:-

(a) Interference between the two nappes issuing from facing side walls of the weir.

(b) Choking of the offtake channels of the weir, producing localised submergence conditions on sections of the side walls and on the upstream tip sections.

An increase in the value of $\propto$ for a given length magnification reduces the lengths of the tips so bringing the side walls into closer proximity in the upstream regions of the weir, (see Figures 1 and 2), and therefore increases any restrictions to the discharge due to nappe interference.

As the problem is one of spatially varied flow, then ideally the area in the offtake channels should increase with distance in direct proportion to the flow. Regarding condition (b) the side wall angle is therefore of immediate significance.

The effect of the side wall angle on the flow in the upstream channels is not readily apparent.

1.3.3 The Vertical Aspect Ratio $^{w}/_{p}$.

This parameter defines the size of the weir cycles in plan, relative to the height of the crest. If labyrinth weir performance is related to the head to crest height ratio, then when the $^{w}/_{p}$ ratio is small, the size of the weir cycles in plan can become small in comparison with the head. Under such conditions true side flow can be prevented by interference between the opposing nappes, with a consequent loss in performance. Furthermore with $^{w}/_{p}$ very small the size of the weir cycles can become so small that the labyrinth form will not be 'seen' by the flow and the performance will approach that of a normal linear weir.

1.4 Review of Work by Other Researchers

To the author's knowledge, only three investigations directly concerned with labyrinth weirs had been conducted prior

to the present work, although a large number of tests have been carried out on linear weirs placed obliquely to the main flow direction. It should be noted that the oblique weir can be regarded as a special case of the triangular labyrinth weir, where the number of cycles, n, is $\frac{1}{2}$.

1.4.1 Kozák and Sváb. (Reference 1).

In 1961, Kozák and Sváb conducted tests on a series of labyrinth weir models within the following design ranges:-

length magnification:	$1.23 \leqslant {}^{l}/_{w} \leqslant 4.35$
vertical aspect ratio:	$1.15 \leqslant {}^{w}/_{p} \leqslant 4.61$
side wall angle:	$5.7^{o} \leqslant \propto \leqslant 20.6^{o}$
head to crest height ratio:	$0.05 \leqslant {}^{h}/_{p} \leqslant 0.25$

All the models were trapezoidal in plan and were constructed from sheet material 6 mm. thick. The crests were flat with the edges chamfered on both sides so that the width of the flat was $4\frac{1}{2}$ mm. Refinements to the models such as sloping channel inverts, or alternative crest sections, were not considered. In all, eleven models were tested and the design parameters used are indicated in Figure 17.

The results of these tests have been replotted in the form of flow magnification against head to crest height ratio in Figure 3. This method of presentation is more meaningful than

that employed by Kozák and Sváb and is discussed more fully in Chapter 6.

It should be noted that a standard 'sharp' crested weir coefficient has been used to calculate the flow magnification in this figure. Strictly, to allow comparison with the corresponding linear weir, the coefficient of the actual labyrinth weir crest section should have been used; but considering that the results were read from a small scale graph then with the consequent errors such further refinements were hardly relevant.

Kozák and Sváb concluded from their tests that the discharge of a labyrinth weir can be appreciably greater than that obtained from a corresponding straight weir operating under the same head. They further concluded that it was practicable to increase the number of cycles of weir, (i.e. decrease the $^{w}/_{p}$ ratio) without an appreciable decrease in the discharge capacity, the advantage being that weirs having a greater number of smaller cycles are more economical.

Investigations by other workers have shown that this conclusion only applies under conditions where there is little interference between the nappes issuing from the facing side walls of the weir. It will be seen from the present work that Kozák and Sváb's conclusions resulted from the relatively small heads on the weirs compared with the size of the weir cycles.

It was also stated by Kozák and Sváb that due to the complexity of labyrinth weirs their discharge capacity could only be determined experimentally.

The main criticism of the work is that the ranges of designs and performance covered by the tests were too small. Consequently the significance of the various weir parameters was not fully apparent and so the conclusions reached by Kozák and Sváb are only applicable within the limits of their experimental tests.

From the results shown in Figure 3 it can be seen that the flow magnification tends to fall with increase in head to crest height ratio, especially for the models with high length magnifications. The ability of the labyrinth plan form to increase the discharge capacity of weirs is clearly demonstrated.

Apart from the effect of the length magnification factor however, no general conclusions or design recommendations regarding the optimum design of this type of weir can be deduced from the results.

1.4.2 Gentilini (Reference 2)

Following earlier experimental work on oblique (straight) weirs by Boileau (Reference 3) in 1854, Aichel (Reference 32) in 1907, Escande and Sabathé (Reference 4) in 1937 and Istomina

(Reference 5) in 1937, Gentilini (Reference 2) in 1941 extended the idea of the oblique weir into a number of oblique sections, resulting in triangular plan form labyrinth weirs.

Three plan forms with side wall angles (α) of 60°, 45° and 30°, corresponding to length magnifications of approximately 1.15, 1.42, and 2 respectively were considered.

Various values of the $^{w}/_{p}$ ratio were used with each plan form this factor being varied by using different combinations of the crest height and the number of cycles in plan.

The models were sharp crested and the crest height in every case was large in comparison with the width of the channel. Consequently the tests were conducted using small $^{w}/_{p}$ ratios so the operating head was large in comparison with the size of the weir cycles. The results, unlike those obtained by Kozák and Sváb, were therefore very dependent on the vertical aspect ratio used. (Figure 4).

The effect of the small $^{w}/_{p}$ ratios was so large in the case of Gentilini's tests that the flow magnification obtained was a function of $^{h}/_{w}$ and not $^{h}/_{p}$ as in Kozák and Sváb's experiments.

1.4.3 Tison and Fransen (Reference 6)

The main purpose of the experimental tests conducted by

Tison and Fransen was to determine the performance of weirs simply constructed from standard pile planks welded edge to edge so as to form a trapezoidal shape in plan.

Tests were conducted on a number of scale models but only one plan form (determined by the shape of the standard pile plank) was used.

Figure 5 indicates the form of the results obtained. It can be seen that again, unlike Kozák and Sváb's work, the head was large in comparison with the weir cycle size in plan, and the performance of the weirs was therefore very dependent on the magnitudes of the $^{w}/_{p}$ ratios. Thus as the head increased the performance of the weirs rapidly approached that of a normal weir occupying the same width of channel.

Models of different scales were tested and no significant change in performance resulted.

In their paper (Reference 6) Tison and Fransen have also published the results of experimental tests on a scale model of the labyrinth weir installed on the R. Belia in the Congo (see 1.5). A large $^{w}/_{p}$ ratio was used in the design of this weir and the operating head is small in relation to the size of the weir cycles in plan. Almost ideal performance has resulted, in that, over the flow range considered, the magnification of the weir compared with that of the alternative straight weir is approximately equal to the crest length magnification.

1.4.4 Discussion

The ranges of the variables covered by the investigations described above were not sufficiently large to provide any general conclusions or design data concerning labyrinth weir performance. The investigations do however indicate the significance of the $^{w}/_{p}$ ratio on the performance of this type of weir.

As the dimensions of a weir are defined in terms of the crest height, it follows that under similar operating conditions (defined by $^{h}/_{p}$), decrease in the value of $^{w}/_{p}$ necessarily reduces the size of the weir cycles in plan relative to the head over the weir, i.e. for the same $^{h}/_{p}$ ratio, $^{h}/_{w}$ increases in inverse proportion to $^{w}/_{p}$. Thus as $^{w}/_{p}$ is decreased free side flow is prevented by interference between the nappes issuing from facing side walls of the weir. If the vertical aspect ratio ($^{w}/_{p}$) is very small the plan form of the weir becomes a mere ripple in comparison with the head and the discharge obtained becomes effectively that of a normal straight weir.

This is clearly shown by the results in Figures 3, 4, and 5. In Kozák and Sváb's work (Figure 3) the values of $^{h}/_{w}$ were small and consequently the $^{w}/_{p}$ ratio seemed of small significance. The tests conducted by Gentilini and by Tison and Fransen (Figures 4 and 5) clearly indicate on the other hand, that the $^{w}/_{p}$ ratio becomes of primary importance when $^{h}/_{w}$ is relatively large.

1.5 Existing Labyrinth Weirs

A number of labyrinth weirs have been constructed as a direct result of individual model tests and these give a good indication of the range of application of this type of weir.

The majority of labyrinth weirs have been designed either with small length magnifications or to operate under small head to crest height ratios, with the result that the performance obtained is, in general, almost ideal i.e. for the same head an equivalent discharge would be obtained from a linear weir equal in length to the developed crest length of the labyrinth weir.

In Great Britain, the Trent River Authority has constructed two labyrinth weirs, one at Clay Mills (R. Dove)and the other at Mountsorrel (R. Soar). Both weirs are similar in construction and are trapezoidal in plan, except that the weir at Mountsorrel has been built with an irregular plan form in order to utilise existing foundation works from an old mill. Length magnifications in the region of 2 have been used, the weirs being formed by straight walls surmounted by a Crump section crest.

Model tests on these weirs indicated very little error in assuming the discharge to be given by using the developed crest lengths in normal weir formulae, although during extensive flooding

Clay Mills weir was found to be operating under a high degree of submergence.

A good indication of the application and advantages of labyrinth weirs is given by the weir constructed for the Central Electricity Authority at Skelton Grange, near Leeds. (Photographs 1 and 2). This weir, built in 1950, is situated on the side of a canal and comprises some 20 cycles in plan with a length magnification in the region of 5. The small maximum design head of the weir (3"), allows almost ideal operation. The advantages of the design in reducing structural costs are clearly apparent when one considers that a linear weir of equivalent discharge capacity would need to be five times the length of the present structure.

Photograph 1 indicates however, the possible disadvantages of labyrinth weirs in their tendency to become obstructed by floating debris, although in this case obstruction is made worse by the very small operating head of the weir. Further design details for the Skelton Grange weir may be found in Reference 7.

A weir with a labyrinth form has been constructed on the R. Belia in the Congo, (Reference 6). The weir is situated between two rocky escarpments which prevent the use of a normal straight overflow. A trapezoidal plan form with rounded upstream tips has been used, giving a length magnification in the region of 2. The

crest has been constructed with a Creager profile and almost ideal performance has been obtained.

A special design of overflow using labyrinth weir principles has been constructed at Beni Bahdel in Algeria, (References 8 and 9). The overflow is situated on the side of a large dam structure and consists of 20 rectangular sloping lips, referred to as 'duck bills', over which the water flows into tunnels through the dam and then into a very large stilling pool below the downstream face of the dam.

The 'duck bills' are some 30 metres in length and 2 metres wide, the overflow being equivalent to a normal weir of approximately 1250 metres in length. A discharge of 1000 m^3/sec occurs on this overflow at the design head of 0.5 metres. The principles involved in labyrinth weirs have also been applied to shaft spillways.

1.6 Purpose of the Investigation

The previous work on labyrinth weirs clearly indicates the ability of these designs to magnify the discharge for a given head normally obtained from a linear overflow. The scope of the previous work is not however sufficiently large to enable the effects of the various design parameters to be fully determined nor to allow the performance of a new design to be predicted.

Ideally the performance of a labyrinth weir will be equal to that of a linear weir having an equivalent length of

crest. However it is evident that ideal performance will not normally be obtained, nevertheless the high potential of the labyrinth weir justifies the acquisition of comprehensive design and performance data.

The purpose of this investigation is to provide the weir designer with the information necessary for deciding on the most efficient design of labyrinth weir for any given situation.

For cases where the available site area may not allow the use of what would be the most efficient design, a comprehensive set of characteristics covering a wide range of weirs will be required.

The investigation aims at providing this information and in addition obtaining an understanding of the fundamental factors appertaining to labyrinth weir behaviour so that a theoretical solution to the problem can be effected.

1.7 Method of Approach

It was intended to achieve the objectives of this investigation by carrying out a series of experimental tests on labyrinth weir models, and then to develop a theoretical analysis of labyrinth weir behaviour with the aid of the results obtained.

In order to ensure that the work was kept at a practical and generally useful level, contact was established and maintained

with the various organisations likely to benefit from the results of the investigation.

PAGE NUMBERING AS ORIGINAL

SECTION 1

EXPERIMENTAL WORK

CHAPTER 2

EXPERIMENTAL FACILITIES

2.1 General Layout

The layout of the test plant occupied two floors, as shown on the assembly drawing, (Figure 6).

The experimental channel, (Figure 7, and Photographs 6 and 8), was 16 ft. long, 3 ft wide, and 1 ft. 2" deep and was supplied with water from a large, deep, concrete header tank of approximately 550 cu. ft. capacity.

The channel was hinged onto the header tank and supported at the other end by a screw jack, thus allowing simple adjustment of the channel slope.

Gates at the downstream end of the channel permitted control of the flow depth within the channel and uniform flow was achieved by flow straighteners situated immediately after the elliptical entry section.

On leaving the channel, the flow cascaded into a diverting tank (hopper) and thence into the pump feed tank located underneath the test channel and just beneath the roof of the ground floor pump room.

Two axial pumps, (Photograph 3), recirculated the water back to the concrete header tank, the whole flow path forming a closed loop system. The two pumps were powered by d.c. motors and could be operated independently, one, the south pump, being maintained at adjustable constant speeds by a Ward-Leonard control set. Each pump had a maximum discharge capacity of approximately 4 cusecs. It was considered that only one pump need be used for the purposes of the investigation.

Flow control was effected by a hand operated Saunders valve on the north pump, and by an electrically operated needle valve on the south pump, (Photograph 3). Operation of the needle valve was possible from either the ground floor or the first floor by remote control. Sensitive adjustment of the valve was provided for by means of mag-slip motors and digital revolution counters.

On exit from the pumps and control valves, the flowswere merged into a single 14 in. diameter pipe with a built in flow straightener section, comprising a large number of 'nested' small bore tubes, immediately downstream of the junction.

In the subsequent plain pipe section four blanking plates, equidistantly spaced on the pipe circumference, allowed the admission of Pitot-static tubes for use in calibration and velocity profile checks.

Immediately downstream of the Pitot tubes locations was a Dall-tube, (a shortened form of the venturi tube, Photograph 4), which when calibrated, enabled accurate flow measurement.

Two 60" manometers were connected to measure the pressure differential produced by the Dall-tube and these were conveniently situated one on each floor, beside the needle valve controls.

The water level in the pump feed tank being lower than that in the concrete header tank necessitated the inclusion of a non return device in the circuit. This was achieved by pumping the water over the top of the concrete tank and incorporating an anti-siphon valve at the highest point so that on shutdown, the valve opened and broke the induced vacuum, thus destroying the siphon effect and preventing backflow to the pump feed tank.

From the main 14" diameter delivery pipe the flow was divided equally into two 10" diameter pipes running vertically to the bottom of the concrete header tank. These two pipes were symmetrically positioned and the water was discharged through holes drilled in the pipe walls near their open ends and also through the open ends themselves.

The concrete tank was designed with a large vertical dimension to minimise turbulence and so provide steady uniform flow to the test channel. Ideally the tank should have had a large surface area so that any head variation due to fluctuation

of the flow would be minimised but, this was impracticable due to space limitations. However it was considered that the pump control was sufficient to provide the constant steady head required.

A traversing depth gauge system, Figure 8, was mounted on rails running the length of the channel. Vernier scales and locking screws enabled the gauge to be locked in any position in a plane parallel to the channel floor, to an accuracy of 0.01". The depth gauge itself was capable of measuring to an accuracy slightly in excess of 0.01 inches. The cross beam carrying the depth gauge remained horizontal for any channel position, but to enable operation of the depth gauge in a vertical direction for any channel slope, rotational adjustment of the beam was provided.

2.2 Development of the Apparatus

Basically the hydraulic circuit functioned as planned but certain modifications, not indicated in the general description, were necessary.

2.2.1 Air Entrainment

At high flowrates, air entrainment occurred in the system. This was apparent as a homogeneous mixture of air bubbles in the

water flow, seen through both a perspex pipe section immediately upstream of the south pump, and through the perspex Dall-tube. The degree of air entrainment could not be measured quantitatively but it was estimated to constitute a percentage of the flow of the order of 5%. It was considered that this resulted in an effective decrease in the density of water, giving rise to errors in flow measurement of the same order as the percentage of air entrainment. Modification of the circuit was therefore necessary to minimise the air entrainment.

A number of factors contributed to the occurrence of air in the water flow. Initial introduction occurred due to the excessive turbulence created by the cascading overfall from the channel and also from the downfall between the hopper and the pump feed tank.

During running, large quantities of water were transferred from the pump feed tank to the vented sections of the pipes and to the channel, especially when water was constrained in the channel by the use of the gates. This reduction in feed tank water level gave rise to the formation of a vortex at the outlet pipes to the pumps, and the consequent admission of large quantities of air to the flow.

A number of modifications, Figure 9, were made to the circuit to eliminate the entry of air from the sources mentioned above.

A baffle was fitted in the hopper to provide a form of stilling pool for the channel overfall. To further increase the level of water in the hopper, the outlet section was modified by the use of a 9" dia. pipe which extended below the surface level in the pump feed tank. The flow path in the pump feed tank was extended by the use of a further baffle, Figure 9, to allow a greater time for the air to float out.

Anti-swirl vanes were constructed over the outlet pipe leading to the south pump, and these successfully destroyed the vortex formed at this point. Then, to promote further separation of air and water, a $^{1}/_{16}$" wire mesh cage, in the form of a truncated frustum of a square pyramid, was fitted over the anti-swirl vanes. This latter device was intended to increase the uniformity of the flow, so allowing air in the previously high velocity regions of the flow, to float out due to the decrease in velocity.

As only the flow from the south pump was considered necessary for the purposes of the investigation, the modifications were made accordingly.

With the above alterations to the circuit, and by replacing water transferred from the pump feed tank during running by overfilling the circuit after start up, all air was eliminated from the flow through the pumps and the Dall-tube. On shutdown,

excess water introduced after start up, was temporarily stored in the pump feed tank until discharged by the overflows.

2.2.2 Anti-siphon Device

The original anti-siphon device was a simple poppet valve held open by a light spring. During running, the water pressure at the valve was less than atmospheric pressure due to the position of the valve and the nature of the circuit. The circuit therefore remained vented at this point, with the result that large quantities of air were drawn into the system.

Whilst this air did not affect the accuracy of flow measurement it produced a very turbulent head on the concrete tank, making head measurement in the channel impractical to a high degree of accuracy.

The valve was replaced by an open ended pipe which under static conditions reached down to just above the water level in the concrete tank.

During operation the end of the pipe became submerged thus preventing the admission of air. Although water was drawn into the vent pipe by the main suction pressure, air trapped in the top loop of the pipe prevented steady flow.

On shutdown water was allowed to siphon back to the pump feed tank until the normal static level in the concrete

tank was reached. At this point the system was vented and the siphon effect destroyed.

This modification proved extremely satisfactory not only in producing a smooth steady head in the channel but also in improving the pump performance by reducing the pump delivery head.

2.2.3 Stationary Depth Gauges

Two non-travelling depth gauges, of the type used on the traversing system, were fixed to measure the flow depth in the channel from tappings in the channel floor, upstream and downstream of the weir positions. These enabled more accurate depth measurement than the traversing system by the exclusion of errors due to surface ripples etc..

Instead of the normal sharp point, the gauges were blunt and rounded as recommended by the Hydraulic Research Station, Wallingford. On contact with the water surface, surface tension produces a readily visible meniscus, permitting accurate and repeatable measurements.

2.2.4 Flow Straighteners

The original flow straightener arrangement is shown in Figure 7, and this consisted of two sections of aluminium honey-

comb approximately 3" thick and $2\frac{1}{2}$ ft. apart. A wooden board, floating between these sections, was intended to smooth the water surface.

This system proved unsatisfactory, in that the honeycomb sections restricted the flow so that a difference in flow depth existed across each section, producing waves in the channel.

On removal of the downstream section of honeycomb, waves still persisted in the channel but this time due to the weight of the wooden board which produced an effective flow contraction followed by a sudden expansion.

The wooden board was replaced by a large sheet of expanded polystyrene so that the final flow straightener arrangement consisted of one honeycomb section followed by the floating sheet of expanded polystyrene. This system resulted in a satisfactory velocity distribution and a smooth ripple free surface.

The velocity distributions obtained in the channel are discussed in Chapter 3.

2.3 Preparations Prior to Experimental Work

Surveys were conducted of the channel floor and also of a static water surface within the channel, using the travelling depth gauge. These surveys indicated that the slope of the

channel floor was less than 1 in 800 when set for the horizontal position, and that variations in the surface of the channel bed were of the order of ± 0.05 in.

The head of water over the crest of a model was to be determined independently of the depth of flow, so that errors in depth measurement would only affect the velocity head on the weir and would therefore represent very minor second order effects in the weir flow.

The conditions of the test channel were considered satisfactory and the channel was maintained in this state throughout the experimental work.

Due to non-linearity of the guide rails and cross beam, it was found necessary to zero the travelling depth gauge at each measurement point by using a static water surface. Failure to do this would have incurred errors in the region of ± 0.09 in.

A number of test runs of the circuit confirmed that the depth in the channel was maintained constant due to the excellence of the pump control, and also that all three depth gauge readings were repeatable and in agreement to within their maximum degree of accuracy.

Some fluctuation occurred in the Dall-tube manometer columns but this was not excessive and accurate readings were obtainable. Modifications to the arrangement of the manometers are discussed in Chapter 3.

Further development of the apparatus and the accuracy of flow measurement are also discussed in Chapter 3.

CHAPTER 3

CALIBRATION OF THE DALL-TUBE

The calibration of the apparatus has been included at this point in the thesis because the tests conducted served also as commissioning tests of the experimental facilities.

The only means of flow measurement provided in the hydraulic circuit is the Dall-tube, and the key to the success of the investigation rested on the accurate calibration of this device.

No direct volumetric means of calibrating the Dall-tube were available due to space limitations. It was decided therefore, to use as many different alternative methods of calibration as possible.

3.1 Calibration by Standard Crump Section Weirs

Recent work on Crump section weirs by the Hydraulic Research Station, Wallingford, (1966), indicated that an accurate Dall-tube calibration could be made by using weirs of this type in the test channel.

The following discharge formula was supplied by the H.R.S:-

$$Q = 3.55\ L\ (H-0.001)^{3/2} \qquad \ldots (1)$$

where H is the total head above the crest

and L is the length of the weir crest.

An accuracy of $\pm \frac{1}{2}\%$ was claimed for the coefficients in this formula so that on using this type of weir for the calibration the overall accuracy was expected to be within $\mp$ 1%.

Two weirs of standard Crump section were constructed, one with a crest height of 6 inches and a crest length equal to the width of the channel (3 ft.), the other having a crest height of 5 inches and a crest length of 1 ft.

The smaller weir was designed for greater accuracy at low flows and was used in conjunction with two flume boards, Photograph 6, clamped into the channel as shown to reduce the effective channel width to 1 ft. Both weirs were made of wood and secured in position by Evostik adhesive.

Several readings of the crest height were taken along the length of the crest, together with readings of a static water surface sufficiently far from the crest, about 1 inch, to avoid surface tension errors.

The average difference of these readings allowed a correction to be made to the depth gauge readings at the point of head measurement, so giving a zero depth gauge reading corresponding to the weir crest level. This procedure was adopted for all the tests.

To justify the point chosen for head measurement several other positions were tried. No difference in the test results were observed. The pressure tapping was therefore sufficiently far upstream to eliminate 'draw down' effects and close enough to the weir for frictional head losses to be negligible.

The depth gauge designed for use in conjunction with the tapping in the channel floor was not available for the early tests on the large Crump weir. When this depth gauge did become available, testing was continued using both this and the travelling depth gauge. While both gauges gave the same results, ripples on the water surface at the higher flowrates increased the scatter in the results obtained from the travelling depth gauge.

The accuracy of the fixed depth gauge having been established, the use of the travelling depth gauge was discontinued.

From measured values of the static head, h, the discharge was calculated from Equation 1. The calculations were done on a digital computer using an iterative procedure - each step being successively corrected for the velocity head until the correction became less than 0.0001 cusecs.

3.1.1 Initial Tests on the Large Crump Weir

A total of 59 readings were taken using the travelling depth gauge and vertical manometer under normal flow conditions. The results are displayed in Figure 10, whereit can be seen that the flow, Q, through the Dall-tube is directly proportional to the square root of the manometer reading.

For flows exceeding 1 cusec a scatter of $\pm$ 1% exists about the line given by:-

$$Q = 0.6105 \sqrt{h} - 0.0233 \text{ cusecs} \qquad \ldots (2)$$

where h is the manometer reading in inches of water. A much greater scatter occurs for flows below 1 cusec.

To simplify the presentation of the calibration results Equation (2) has been used as a datum calibration formula against which the percentage differences obtained from other calibration methods have been plotted, Figures 11 and 12.

3.1.1.1 Air Entrainment Tests

Although the hydraulic circuit had been successfully modified to eliminate air entrainment in the flow, it was felt that the effects of this factor on flow measurement should be determined in case the effect reappeared after calibration.

A quantity of water was expelled from the pump feed tank which resulted in air entrainment to such a degree that

the pump inlet pipe ran only partially full. Tests were carried out therefore under normal intolerable conditions. Further results were obtained with the system vented at the anti-siphon device.

The effect of this air entrainment was apparent in the channel by the unsteady head, (turbulent in the case of the vented system), and unsteady flow at high flowrates.

The results obtained from the Crump weir under these conditions, obeyed the same relation as that previously obtained except that a greater scatter occurred as shown in Figure 10.

It was concluded that the behaviour of the Dall-tube would be unaffected by any air entrainment likely to be encountered during the investigation.

3.1.2 Tests on the Small Crump Weir

At this point in the calibration programme the fixed depth gauge became available and this was incorporated in the apparatus.

The small Crump weir, being only one third the crest length of that previously tested, allowed greater accuracy in head measurement for the same flow due to the increased head over the crest. Some 65 readings were taken with this arrangement.

Results obtained from the vertical manometer readings display a scatter of the same order as that previously obtained in the testing of the large Crump weir. This indicated that the scatter was due to manometer errors rather than errors in head measurement.

An attempt was made to increase the accuracy of the manometer readings by connecting an inclined manometer in parallel to the vertical manometer. Despite the use of several wetting agents in the tubes of the inclined manometer, the scatter of the results obtained from this instrument was in fact greater than that of the vertical manometer, (Fig. 11).

The use of the inclined manometer was abandoned and it was replaced by a bi-fluid manometer which was simply a second 60" manometer with commercial manometer fluid replacing the air in the normal vertical manometer.

This arrangement successfully magnified the fluid column displacements but again the scatter of the results was greater than that obtained with the normal manometer, (Figure 11).

In a final series of low flow tests on the small Crump weir, a double Betz manometer was used and the scatter obtained was very small, again this is indicated on Figure 11. The double Betz manometer was incorporated in the circuit for use with small flows, together with the normal 60" vertical manometer for higher flowrates.

It is evident from Figure 11 that the small Crump weir indicated a flow/manometer reading relation between 1 and 2% higher than the large Crump weir. This could be accounted for in that friction losses would be greater for the small weir, thus resulting in higher head measurements. The discrepancy however, being small, did not invalidate the use of the Crump weirs and the flow formula supplied by H.R.S., any error common to both weirs necessarily lying in the coefficient (3.55) of Equation 1.

3.1.3 Final Tests on the Large Crump Weir

In view of the discrepancy obtained in the calibration from the two Crump weirs and as a repeatability check, the large Crump weir was retested. It was also required to confirm the original test results using the more accurate double Betz manometer and the fixed depth gauge not previously available.

A further 70 readings were obtained, (shown in Figure 12), confirming the original results and proving the accuracy and repeatability of the instrumentation.

3.2 Calibration by Velocity Traversing Methods

On the recommendations of the Hydraulic Research Station, a miniature current flowmeter was purchased for use as a velocity measuring device.

Basically the instrument consisted of a five bladed Cobex plastic rotor mounted in jewelled bearings at the end of a probe. (Photograph 5). An electronic measuring unit connected to the probe counted the number of revolutions of the rotor over a predetermined time, (normally 10 seconds), allowing the flow velocity at the probe head to be read directly from a calibration curve supplied with the instrument.

The rotor, being of small dimensions,had an extremely short response time and the very low friction in the bearings provided an almost linear calibration curve.

The manufacturers claimed that the accuracy of the instrument was within:-

$\pm$ 5% for 0.9 < velocity < 3 inches/sec

$\pm$ 2% for 3 < velocity < 6 inches/sec

$\pm$ 1% for 6 < velocity < 60 inches/sec

The flowmeter had therefore obvious advantages over the alternative Pitot-static tube both in accuracy and in the response time of the system, although one disadvantage was that the probe had to be immersed to a depth of at least 1 inch.

To enable accurate positioning of the measuring head, the probe was clamped to the depth gauge on the traversing system, Photograph 5.

For each test the flow in the channel was allowed to steady and accurate readings of the depth taken. The flow area was then divided into 100 equal parts, each part being geometrically similar to the total flow area. A velocity measurement was taken at the centre of each section, in accordance with the recommendations of the British Standards Institution on flow measurement, (Reference 15).

It was found that individual 10 second counts could vary by as much as 10% and so the count time was extended to 50 seconds throughout the tests.

The mini-flowmeter could not be used to determine the velocities in the 10 areas forming the free surface due to probe immersion depth limitations and so these had to be found by extrapolation of the velocity distribution curves.

As the calibration curve for the flowmeter was linear over the range of each test then the mean flow velocity was simply determined by averaging the 100 flowmeter readings obtained, the mean velocity then being read directly from the calibration curve.

Six tests were conducted with the large Crump weir in the channel and with the original flow straightener arrangement described in Chapter 2 (2.2.4).

Results from these tests indicated a flow between 10 and 11% higher than that of the datum calibration obtained from the

Crump weirs. This large discrepancy between the two calibration methods clearly necessitated further investigation, and a consideration of the possible sources of error.

As stated previously results obtained from the two Crump weirs were in close agreement, the only source of error common to both weirs being in the coefficient of the flow relation used. The large Crump weir continued to repeat the results of the previous tests during the velocity traverses and the Crump weir flow formula had been reconfirmed by the Hydraulic Research Station. It was therefore considered that the error causing the discrepancy most probably existed in the velocity traversing method.

Possible sources of error in the velocity traversing tests were considered to be:-

(a) depth measurement

(b) incorrect operation of the dekatron counter unit

(c) incorrect functioning of the flowmeter probe

(d) inherent errors in the method

(e) incorrect instrument calibration

Although small errors in the depth measurement were inevitable these could not account for the observed discrepancy of 10%.

As the flow readings were too high then it was unlikely that the error would be due to faulty operation of either the probe or the counting unit.

Inherent errors are present in techniques of the type used if the flow is not uniform, due to approximations involved in the averaging procedure. In general these errors are positive, indicating a higher flow than actually exists.

Some errors must have been incurred in extrapolating the velocities in the surface layer sections but to account for the discrepancy of 10% these would have been of the order of 100%, which was clearly not the case.

The most probable sources of error were therefore considered to be:-

(a) inherent errors due to non-uniform velocity

(b) incorrect calibration of the flowmeter

Sample velocity distribution curves obtained from three of the above tests are indicated in Figure 13, where it can be seen that the flow was subject to relatively large boundary effects. The velocity fall off at the free surface resulted from the drag of the wooden board in the flow straightener arrangement. Further, this board had a clearance of about 2 inches with the side walls of the channel and its weight produced flow contraction and tended to increase the velocity

of the core of the flow while allowing slower velocities at the side walls.

In order to investigate the effect of non-uniform flow on the velocity traversing method, the flow straighteners were removed from the channel. It was expected that this would have an adverse effect on the velocity distributions, so increasing the discrepancy between the velocity traverse calibrations and the datum calibration. In fact the reverse occurred, in that a more uniform flow resulted, indicated by the velocity distributions shown in Figure 13.

Results of four tests conducted without flow straighteners displayed a shift of some 3% towards the datum calibration, the actual discrepancy from the datum then being between 7 and 8%.

The original velocity traverse results were reconfirmed by two tests conducted with the flow straighteners replaced so ensuring that no change had occurred in the flowmeter itself.

To assess the accuracy of the flowmeter calibration, a similar velocity traverse test was conducted with a Pitot-static tube connected to the double Betz manometer. Flow straighteners were used in this test.

The traverse with the Pitot-static tube indicated a discrepancy compared with the datum of 6.8% suggesting a mini-flowmeter calibration error of between 3% and 4%.

Due to the long settling time required by the Betz manometer, this latter test took approximately eight hours to complete and no further tests of this type were contemplated as a recalibration of the mini-flowmeter appeared more important.

The flowmeter calibration was checked by the Hydraulic Research Station, Wallingford, using standard rotating arm apparatus and the suspected calibration error was confirmed to be approximately + 3.5%.

The results of the velocity traverses were therefore corrected and are shown on Figure 12.

In the light of the above results modifications were made to the flow straighteners as indicated in Chapter 2, (2.2.4). Although results obtained with the new arrangement did not indicate a great improvement in the velocity distribution of the flow, it was decided that the advantages gained in having a smooth, steady measuring surface, outweighed the disadvantages of non uniform flow. In spite of the various arrangements of the flow straighteners used in the traversing tests the Crump weir continued to repeat the results previously obtained.

In conclusion, the velocity traverse method of calibration indicated a flow approximately 4% greater than that indicated by the Crump weir calibrations.

3.3 Pitot-static Tube Traverse Across the Flow in a Pipe Section

Four Pitot-static tubes were manufactured in accordance with the recommendations of the National Physical Laboratory Report, (Reference 16), and positioned equidistantly round the pipe section immediately upstream of the Dall tube. (Chapter 2 (2.1)).

On connecting to a multi-tube inclined manometer however, it was found impossible to maintain steady readings. In view of the difficulties experienced in the channel velocity traverses it was therefore decided to abandon this method of calibration.

3.4 Comparison with Published Work on Dall Tube Behaviour

In a paper titled 'The Dall Flow Tube', (Reference 17), I.O. Miner presented the results of investigations into the behaviour of a number of Dall tubes of different throat/pipe diameter ratios and also dealt with the effects of upstream disturbances.

He found that the Dall tube coefficient remained constant for a pipe Reynold's number exceeding 35×10^4, below which the coefficient increased by about 2.4% at a Reynold's number of 10×10^4. The operating range of the Dall tube being calibrated for use in the present investigation was $5 \times 10^4 < Re < 36 \times 10^4$.

In general the effect of upstream disturbances, in the form of elbows, gate valves etc., were found to further increase the coefficient (for a Reynold's number of 35×10^4) by an order of 1 or 2%.

Denoting the Dall tube coefficient by k then the flow, Q, through the Dall tube is given by:-

$$Q = \frac{k \pi d^2}{4} \sqrt{\frac{2 g H}{1 - \beta^4}}$$

by the elementary application of the Bernoulli equation where:-

d is the throat diameter

β is the throat/pipe diameter ratio

H is the pressure differential (ft.)

Defining a calibration factor (c) for the Dall tube given by $Q = c\sqrt{h}$ where h is the pressure differential in inches, then

$$c = \frac{k \pi d^2}{4} \sqrt{\frac{2 g}{12(1 - \beta^4)}}$$

For the Dall tube under consideration, d is 8 inches and $\beta = 0.571$ and from the paper by Miner, for Reynold's numbers exceeding 35×10^4 then $k = 0.701$

hence $c = 0.600$

and so the calibration formulae based on published work was predicted to be $Q = 0.6\sqrt{h}$ cusecs, where h is the manometer reading in inches of water.

This curve has been plotted against the datum calibration, (Figure 12), from which it can be seen that both are in close agreement, although it should be noted that:-

(a) the operating range of the Dall tube was below a pipe Reynold's number of 35×10^4, (corresponding to a flow of approximately 3.8 cusecs).

(b) a short radius elbow occurred a few pipe diameters upstream of the Dall tube.

Both these conditions would tend to increase the Dall tube calibration factor by about 1% total at maximum flow, (4 cusecs), increasing to an estimated total of 3 or 4% at about 1 cusec.

3.5 Calibration by a Sharp Crested Weir

Although some measure of agreement had been obtained by using the above mentioned calibration methods, some doubt still existed as to the actual calibration formula to be adopted. It was decided therefore to conduct tests on a normal sharp crested weir, partly to throw further light on the Dall tube calibration, and partly as a preliminary to the tests on labyrinth weirs for which it was intended to use sharp crests also.

The actual model weir was machined from half inch thick perspex sheet and had a crest height of 7.1 inches and a length equal to the width of the channel (3 ft.).

Tests were conducted in a similar manner to the Crump weir tests, the weir being ventilated by a number of polythene tubes. The flow was then calculated from the generally accepted Rehbock formula.

The results, plotted on Figure 12, showed reasonable agreement with the results obtained by the other calibration methods except that the discrepancy from the datum calibration increased with decrease in flow and therefore displayed a tendency to follow a relation $Q = c\sqrt{h}$ instead of the datum calibration relation of the form $Q = c\sqrt{h} - K$.

3.6 Volumetric Calibration at Low Flows

A calibration formula for the Dall tube ($Q = 0.6175\sqrt{hm}$) was adopted from the results of the previous tests (see 3.7). However at a later stage in the investigation the one cycle model tests (Chapter 8 (8.2)) cast doubt on the accuracy of this formula at low flowrates and it became apparent that further calibration was necessary.

It had been considered originally that no direct means of calibration were possible due to space limitations. On reconsideration however it was found practicable to seal the outlet of the diverting tank at the end of the flume, to enable the timing of the collection of a known volume of water.

The volume of water in the tank was determined by the use of an inclined tube fitted to the side of the tank. The scale of this tube was calibrated from readings taken after the addition of known quantities of water (50 lbs. each) to the tank. A maximum of 19 cu.ft. of water could be collected, the flow rate being determined from the time taken to collect a specified volume. Flowrate = 0.628 s/t where t is the time of collection over a scale distance of s inches.

An analysis of errors involved in the method indicated an accuracy of within $\pm \frac{1}{2}\%$. The low flow calibration results obtained by this method are shown in Figure 12, and the average difference from the adopted flow formula can be seen to be +1%.

It was concluded that the accuracy of the original calibration was greater than had been estimated and no correction was made to the flow formula.

3.7 Conclusions

In adopting a calibration formula for the Dall tube the following points were taken into consideration:-

(1) Results of the velocity traverse tests were viewed with some reservations as to their accuracy, but the finally adopted formula was slightly biased in their favour.

(2) As no zero errors were present in the manometers, the datum calibration formula (Equation 2) necessarily contained a negative error for small flows due to the constant, -0.0233.

(3) The formula predicted from the published work of Miner, (Reference 17), was estimated to be in error by an order of -3% as the operating range of the Dall tube was below a Reynold's number of 35×10^4 and upstream disturbances were also present.

(4) The results obtained from the tests on the sharp crested weir were considered important as this crest section was to be used in the labyrinth weir models.

The following calibration formula was therefore adopted and is also shown in Figure 12.

$$Q = 0.6175\sqrt{hm} \quad \text{cusecs} \qquad \ldots (3)$$

where hm is the manometer reading in inches of water.

The accuracy of this formula was estimated to be:-

$\pm$ 2% for $Q > 1$ cusec

$\pm$ 4% for $\frac{1}{2} < Q < 1$ cusec

The volumetric calibration tests confirmed the above formula but its estimated accuracy was modified to $\pm$ 2% over the whole flow range.

CHAPTER 4

THE SCOPE OF THE INVESTIGATION

The experimental work was to be conducted in two parts:-

1. An initial investigation to discover the significance of the parameters of primary importance.

2. An investigation to determine the significance of all the remaining parameters likely to influence labyrinth weir behaviour.

The parameters considered to be of primary importance to labyrinth weir behaviour have already been described in Chapter 1, (1.3), and it was intended that the experimental work should cover as wide a range of variation of these parameters as possible. Before the scope of the investigation can be defined however, it is necessary to compile a comprehensive list of all the parameters likely to be of significance. The parameters which are considered of secondary importance are therefore listed below, together with the decisions taken regarding the range of variation of their of their values, (if any), in the initial experimental work.

4.1 Parameters of Secondary Importance

4.1.1 Crest Section

A very wide range of crest sections can be used for labyrinth weirs, but in order to provide an accurate comparison with the behaviour of normal weirs and in view of the extensive work already published on this design, especially on small scale models, (References 10, 11 and 12), it was decided to use a standard sharp crest section for the models in the initial investigations. Further advantages regarding the simplicity of model construction and the independence of the design from a fixed design head, were also considered in this decision.

Apart from the very accurate formulae available for computing the discharge of sharp crested weirs under normal flow conditions, formulae have also been proposed which enable the computation of the discharge under submerged flow conditions, (References 13 and 14). Therefore the use of a sharp crest section simplifies analytical solution not only for general submergence of labyrinth weirs but also for the cases involving localised submergence due to choking of the offtake channels.

4.1.2 Difference between the Elevations of the Channel Beds Upstream and Downstream of the Weir, d

The primary importance of this variable, d, lies in the prevention of downstream interference on the discharge.

If a sufficiently large fall exists on the downstream side of the weir then no interference to the flow will result from choking of the offtake channels.

In a practical situation the maximum allowable value of d will be determined by the site conditions but even so, constructional considerations will probably necessitate the use of a much smaller value in the design.

The initial experimental work was restricted to weirs with no change in elevation between the upstream and downstream channel beds.

4.1.3 Submergence

Drowning seriously affects the performance of normal weirs and other workers, (Reference 7), expected that it would have an even greater effect on the performance of labyrinth weirs. Nevertheless submergence is considered of secondary importance as in practice this condition will be avoided wherever possible. However in view of the lack of any experimental results on labyrinth weirs under submerged flow conditions and because drowning tests could be conducted without alteration to the model construction, it was decided to include this aspect of weir behaviour in the preliminary investigations.

4.1.4 Aprons

Aprons on both the upstream and downstream sides of the weir are constructional details, used to strengthen the structure. Aprons are not therefore a basic feature of labyrinth weir design and were not used in the initial model tests.

4.1.5 Surface Tension and Viscosity

Surface tension is only of minor importance in weir flow but its effect can be significant on small scale models where the head is very small. Care must be taken to ensure that surface tension effects are kept to a minimum as far as possible by the use of sufficiently large scale models.

In a similar manner viscosity is of negligible importance in weir flow. Although frictional energy losses may affect labyrinth weir performance to a small degree this factor has been neglected.

4.1.6 Number of Weir Cycles in Plan, n

Providing the influence of the channel side walls is negligible and these coincide with a longitudinal axis of symmetry then the number of cycles used in the models is of negligible importance. The degree of influence of the side walls was not known to be negligible however, and it was not

known therefore whether the performance of one cycle of weir would be truly representative of a full weir constructed of a number of such cycles, and further, whether this one cycle should be designed as a complete approach channel or a complete offtake channel. A design incorporating an odd half cycle, i.e. the number of cycles n = integer + $\frac{1}{2}$, has the advantage of having an equal number of complete approach and offtake channels plus one half cycle of each.

It was felt necessary to investigate these points in the initial experimental work to ensure that the results obtained were applicable to a weir constructed of any number of cycles in plan.

4.2 Determination of the Scope of the Investigation

The scope of the investigation was determined from the conditions and parameters discussed above and from the limitations imposed by the experimental facilities.

The dimensions of the test channel limit experimental work to weirs not accompanied by a large change in elevation, d, between the upstream and downstream channel beds. Because d is of secondary importance this is not an important limitation.

In the first instance only symmetrical, trapezoidal plan forms were to be considered, (including rectangular and triangular

weirs), incorporating a sharp crest section.

The number of cycles used in the models was to be either an integer or an integer plus one half cycle, but as it was required to work to as large a scale as possible then the number of cycles, n, was kept to a minimum value.

From practical considerations the maximum length of the models in the flow direction was restricted to 4 ft.

The performance of the weirs was to be determined for a range of head to crest height ratio, (h/p), between 0 and 0.5. The maximum allowable crest height was therefore limited to 8 inches by the dimensions of the test channel. Further, to minimise surface tension effects and scale effects in general, the lower limit of the crest height was set at 5 inches.

The length magnification factor, l/w, and the side wall angle, α, are of primary importance and the full ranges of these variables were to be included in the investigation. The maximum value of α is limited however to that giving a triangular plan form and so for a given l/w ratio the maximum value of α is determined from geometrical considerations.

In determining the range of the primary variable, w/p, it was decided that w/p should be sufficiently large to allow unrestricted side flow over the weir but small enough to make

the design a viable economic proposition. As the limits of the variable were not known a full range of w/p was to be covered in the investigation.

The limiting conditions, and the ranges of the variables to be covered in the initial investigation, were therefore as follows:-

(1) $0 < h/p < 0.5$

(2) $5" < p < 8"$

(3) n = integer or integer + $\frac{1}{2}$

(4) $s < 4$ ft.

(5) plan form symmetrical

(6) plan form trapezoidal

(7) crest section - standard sharp crest

(8) $\propto$ - limits imposed by geometry

(9) $d = 0$

To determine the scope of the investigation the ranges of the basic parameters were represented in graphical form.

Figure 14 indicates the maximum allowable value of $\propto$ for a given value of the length magnification factor, so that any combination of $\propto$ and $1/w$ beneath the curve can be used.

The relation between 1 and $1/w$ for various values of n (determined from the test channel width of 3 ft.) is shown in Figure 15. The limiting curves of s = 3, 3.5, and 4 ft.

are also indicated, so that any values of n and 1/w below the line s = 4 ft. could be used.

For a range of n between 1 and $5\frac{1}{2}$ Figure 16 indicates the relation between p and w/p and shows also the optimum design range of p.

Two further Figures, (17 and 18), were constructed from Figures 14, 15 and 16, and these define the scope of the investigation. Figure 17 is for integer values of n and Figure 18 for the case where n = integer + $\frac{1}{2}$. The non-hatched areas define the limits of variation of the fundamental weir design ratios, 1/w and w/p, and hence the available scope of the experimental work.

Also indicated in the Figures are the weir design ratios of weirs already in existence, and also the design ratios used in the experimental work conducted by other researchers. It is evident that the scope of the investigation is more than sufficient to cover both past and probable future labyrinth weir designs.

The scope of the investigation has not been defined in terms of the parameters of secondary importance, except where indicated, as it was not intended that the experimental work should cover a full range of variation of their values. However, having determined the significance of the primary variables it

was intended that the subsequent experimental work should cover sufficient variation of the secondary variables to enable their effect on labyrinth weir performance to be determined.

CHAPTER 5

MODEL CONSTRUCTION AND TESTING PROCEDURE

5.1 Construction

The labyrinth weir models were contructed from perspex sheet both to facilitate manufacture and to overcome the problems of warping previously encountered with wooden weirs. The transparency of the perspex was also considered to be an advantage.

Half inch thick material was used in all cases, the sections being cemented together at their ends with Tensol No. 6 cement.

To economise on material and manufacturing costs, the largest model of each series was manufactured, tested, and then modified to produce the next largest model in the series. As the crest height was constant for all the models in a given series only the ends of the model sections required modification. Waiting time during model construction was kept to a minimum by running a number of test series concurrently.

Evostik adhesive was used to secure the models in the channel and no other means of support were found to be needed. Petrol readily dissolved the Evostik and this greatly facilitated the removal of the models.

A number of polythene tubes, vented to atmosphere, were positioned along the crests to ensure adequate ventilation of the nappe wherever possible (Photograph 8).

Figure 19 indicates the 'sharp' and semicircular crests used in the experiments. The 'sharp' crests were machined to a high degree of accuracy but it was difficult to achieve the same degree of accuracy for the semicircular crests due to variations in the thickness of the perspex. Expanded polystyrene $1\frac{1}{2}$ inches thick was used to construct the aprons in the tests described in Chapter 8 (8.5). This material proved to be easily machined on a bandsaw, even in producing the small angled taper necessary at the weir entry and exit sections. Small adjustments for fitting the aprons were made by rubbing the polystyrene with a cloth damped in petrol.

The aprons were secured to the perspex models and the channel floor by Bostik 299 adhesive and the joints were then further strengthened by the use of waterproof adhesive tape. (Photographs 7 and 8). Once again petrol proved extremely useful for removing the aprons.

5.2 Testing Procedure

With the model under test secured in the channel, a zero depth gauge reading (corresponding to crest level), was obtained

in the manner used for the Crump weir tests.

At least 30 readings of the crest level and corresponding static water surface were taken along the length of the crest using the travelling depth gauge. It was of fundamental importance that these readings should be as accurate as possible.

In all the model crest surveys, the deviation of the crest from the horizontal plane was found to be not greater than $\pm$ 0.02 inches and in many cases much smaller deviations were attained. The accuracy of the model construction was therefore considered to be satisfactory.

Two types of tests were conducted on each weir.

(a) Ventilated tests.

These tests were conducted with the gates at the downstream end of the channel fully open so that the flow depth downstream of the weir was a minimum. This ensured that where possible the nappe issuing from the sharp crest was ventilated. Choking of the offtake channels however, prevented ventilation of the nappe under all flow conditions.

Readings of the depth gauges and manometers were taken over a range of flows up to a maximum of 4 cusecs. Where possible, (for small flows) the double Betz manometer was used to measure the Dall tube pressure differential with the vertical manometer used for comparison.

At high flowrates a second 60" vertical manometer was connected in parallel to the one used for measurement. The wider bore tubes of this second manometer offered little restriction to flow and the instrument damped out the fluctuation otherwise present in the water columns of the measuring manometer.

With the adopted manometer system the errors involved in the measurement of the Dall tube pressure differential were very small. Where comparison was possible the discrepancy between the manometers was found to be less than 0.02 inches of water.

(b) Drowning tests.

The drowning tests were conducted in the same manner as the ventilated tests but with the channel gates adjusted to maintain constant downstream depths greater than the crest height. (The flow over a normal sharp crested weir is unaffected by a downstream depth less than or equal to the height of the crest).

The downstream depth was measured with a second depth gauge connected to a static tapping in the channel floor, some distance downstream of the weir.

Difficulty was experienced both in obtaining accurate depth measurements and also in setting the downstream depth to the required value, due to the turbulence of the flow in these regions.

CHAPTER 6

PRESENTATION OF THE RESULTS

6.1 General Discussion

It was intended throughout the work to compare the performances of the labyrinth weirs with those of the corresponding linear weirs so that the advantages of the labyrinth designs would be readily apparent. The corresponding linear weirs are defined as straight weirs normal to the flow with the same crest height and occupying the same channel width as the labyrinth weir.

Two non-dimensional methods of presentation of the results were considered to be important:-

(a) Direct comparison of the labyrinth weir flow, QL, with the corresponding linear weir flow, QR. This has been achieved by plotting the flow magnification, QL/QR, against the head to crest height ratio, $^{h}/_{p}$, where QR is calculated from standard sharp crested weir formulae using the experimental values of h and p corresponding to the value of QL.

For the case of labyrinth weir submergence the normal weir flow is again calculated from standard submerged weir formulae but account is also taken of the extra parameter hd (downstream head) involved.

In every case therefore QR represents the flow that would be obtained by the corresponding linear weir operating under head conditions identical with those of the labyrinth weir.

(b) An alternative method of presentation to (a) is available by defining the effectiveness, E, of the labyrinth weir as:-

$$E = \frac{QL/QR}{l/w} \times 100\%$$

this factor again being plotted against the head to crest height ratio, h/p.

For the purpose of comparison with the normal sharp crested weir this latter method of presentation is not as useful as method (a), but it does allow simpler comparison between weirs of different length magnification factors.

Some results have been displayed in the form of effectiveness curves, Figure 23 and 25, but it was not felt necessary to use both methods of presentation in every case, and in general effectiveness curves have not been drawn.

6.2 Standard Sharp Crested Weir Formulae

A number of weir discharge formulae are available and a decision had to be taken as to which to use for calculation of QR. The Rehbock formula was adopted at first.

$$QR = \frac{2}{3} c \sqrt{2g}\, h^{3/2} \qquad \text{f.p.s. units.}$$

where $$c = 0{\cdot}605 + 0{\cdot}08\, h/p + \frac{1}{320h - 3}$$

Theoretically for very small flows the labyrinth weir performance should be almost ideal. Thus as h/p approaches O then the flow magnification of the weir, QL/QR, should approach the length magnification value and the effectiveness, E, should approach 100%. This was not verified by the practical results with the Rehbock formula used to determine QR as shown in Figures 22 and 23, for in every case QL/QR and E decreased significantly from their ideal values with h/p small and decreasing. Doubt was therefore cast on the accuracy of these results and an investigation into the possible source of the errors was necessary.

Only three sources of error seemed likely to account for the observed discrepancies. The manometers had been proved reliable and had remained unchanged since the calibration tests, so any errors in flow measurement seemed likely to be in the calibration formula for the Dall tube.

A large number of formulae have been proposed to describe the flow over sharp crested weirs, the majority of these being reported by King (Reference 10). A series of experiments by Yoshinori Shimojama (Reference 11), on small rectangular weirs operating under small heads indicate that of the earlier formulae, that proposed by Rehbock is the most accurate.

The more recent formulae, e.g. those due to the United States Bureau of Reclamation, the Swiss Society of Engineers, the British Standards Institution, Schoder and Turner and Kindsvater and Carter are compared directly with the Rehbock formula in Figure 20. These various formulae all display, for small heads, a marked similar deviation from the Rehbock formula. As the latter had been used for the calculation of the results in Figures 22 and 23 it seemed likely that at least some of the discrepancy observed in the results could be attributed to errors in the Rehbock formula.

In computing the performance of the weirs the corrections in Q_L and h necessary to give ideal performances had been found. It was possible therefore to plot two graphs, one of the Q_L-correction against Q_L, and the other of the h-correction against h. With any error in the calibration formula the Q_L plot would tend to a single curve at points near to the origin for all models, and similarly a tendency to a single curve in the plot of the head correction would indicate an error in the Rehbock formula.

No line common to all the models was apparent in either of the two graphs, (not shown), but for each model the head correction tended towards a constant for small heads, and varied between models, from 0.015 to 0.045 inches.

The effect of a constant head error on the flow calculated from the Rehbock formula is shown in Figure 20. This curve corresponds very closely to the results obtained from the other sharp crested weir formulae.

It was therefore apparent that the two primary sources of error causing the discrepancy in the test results were:-

(a) An inaccuracy in the Rehbock formula.

(b) An error, constant for each model, in the measurement of the head of water, due to inaccurate zero readings of the depth gauges.

It should be noted that both these errors produce significant errors in the performance results for small h/p ratios only.

On reviewing the various formulae available for calculating the performance of sharp crested weirs, that proposed in the paper by Kindsvater and Carter, Reference 12, appears to be the most accurate. This formula was derived from the results obtained from a very wide range of experimental tests, including small scale models, and is considered most representative of the sharp crested weir sections used in the present investigation.

Kindsvater and Carter's formula:-

$$Q = c.L.H^{3/2} \qquad \ldots (4)$$

where Q = discharge in cusecs

c = weir coefficient = 3.22 + 0.4h/p

L = length of weir crest -0.003 (ft)

H = head on the weir +0.003 (ft)

has been used for the calculation of the normal weir flow, QR, in the presentation of the results throughout this investigation.

6.3 Submerged Weir Formulae

Villemonte, (Reference 13), discovered from a series of experimental tests that the performance of weirs under submerged conditions can be determined from the following formula:-

$$\frac{QD}{Q} = \left(1 - \left(\frac{hd}{h}\right)^{1.5}\right)^{0.385} \quad \ldots (5)$$

where QD is the discharge under submerged flow conditions and Q is the discharge under normal free flow conditions given by an upstream head h.

An alternative formula is proposed by Mavis, (Reference 14), but the results obtained from this differ little from those of Villemonte's formula.

The accuracy of these formulae is claimed to be within $\pm$ 5%. Due to the absence of a more accurate method of submerged flow computation, Villemonte's formula has been used throughout the investigation.

6.4 Summary

The generally adopted method of results presentation is to plot the flow magnification, QL/QR, against the head to crest height ratio, h/p, where:-

QL is the experimentally determined labyrinth weir discharge and QR is the calculated discharge over a corresponding linear weir when operating under identical head conditions to those of the labyrinth weir. The formulae proposed by Kindsvater and Carter, (Equation 4), and Villemonte, (Equation 5), are used for calculating QR.

It is interesting to note that as Froude No. $= \frac{v}{\sqrt{g.d}}$ where d is the depth of flow, then for the labyrinth weir the Froude number, FL, is given by:-

$$FL = \frac{QL}{(h+p).w\sqrt{g.(h+p)}}$$

Similarly for the corresponding linear weir the Froude No. FR, is given by:-

$$FR = \frac{QR}{(h+p).w\sqrt{g.(h+p)}}$$

Hence in the adopted methods of presentation as h, p, w, and g are the same for both the labyrinth and linear weirs then:-

$$\frac{QL}{QR} = \frac{FL}{FR}$$

CHAPTER 7

GENERAL LABYRINTH WEIR MODEL TESTS

The experimental work described in this chapter was confined to basic labyrinth weir designsand was intended to determine the significance of the fundamentally important parameters.

7.1 Model Test Programme No. I - Initial Tests

The labyrinth weir models in this programme were designed to give a wide coverage of the scope available in the investigation. The model design ratios are tabulated in Table 1, and are also plotted in Figure 17 ~~and 18~~, to illustrate the amount of scope which they covered.

The purpose of the tests wasto determine the significance of the basic weir parameters so that the useful range of labyrinth weir design could be defined. It was therefore intended that the results obtained should specifically indicate the ranges of the variables most requiring investigation.

Each series of models (A, B, C & D) in Table 1 corresponds to a particular crest height, p, and only the models in series A, B and C were necessary for full coverage of the scope of the programme.

Series D weirs are all geometrically similar to those in series A, except that they have a number of cycles (n) equal to an integer $+\frac{1}{2}$ and are consequently of a slightly different scale. These models were included in the programme to ensure that the experimental tests were representative of labyrinth weirs constructed with any number of cycles in plan, (Chapter 4 (4.1.6)) and also as an indication of any scale effects that may be present in labyrinth weir behaviour.

As the experimental work proceeded it became apparent that the testing of certain models could be discarded for reasons given in the test results, (7.2). The discarded model tests are indicated in Table 1. The shapes of the models tested are shown schematically in Figure 21.

7.2 Ventilated Flow Test Results - Model Programme No. 1

The results of these initial tests are presented separately in Figures 26 - 37, and also in composite form in Figures 22 - 25, to allow comparison between the models.

The Rehbock weir formula was used for the calculation of QR in Figures 22 and 23. These figures are only intended to illustrate the reasons for the choice of the sharp crested weir formula needed for the methods of presentation of the results which have been adopted, (See Chapter 6). The remaining

performance curves have all been obtained by use of the Kindsvater and Carter formula, and these are considered to be more accurate.

Of the 34 models proposed in the test programme, 13 were tested including the normal linear weir, as indicated in Table 1. At this point it was decided that the results gave sufficient indication of the influence of the basic parameters to allow the definition of more specific tests to be conducted in the most useful weir design ranges. The remaining model tests in Programme 1 were discarded.

In general it can be seen that the performance of all the weirs tended to fall with increase in the value of h/p, although with the exception of the rectangular weirs, a small increase in performance occurred at particular points on the curves.

Although these tests have been termed 'ventilated' tests, it was not possible to maintain ventilated conditions over the whole flow range, for although the depth downstream of the weir was maintained below crest height, choking of the offtake channels produced localised drowning along sections of the side walls, (Photographs 10 and 11). At the onset of downstream interference it was found impracticable to maintain ventilated conditions along the whole crest length. The

initial loss of ventilation caused the pressure beneath the nappe to fall below atmospheric pressure which resulted in an increase of flow over the weir corresponding to the 'humped' discontinuity in the performance curves. Beyond this point the crest sections became truly drowned, producing a more rapid fall off in performance than that obtaining under fully ventilated conditions. In general therefore, choking of the downstream channels was detrimental to the weir performance.

It may be argued that, due to the interference in the offtake channels, labyrinth weir performance depends to some extent on the flow depth downstream of the weir. However the drowning tests on these models (7.3) show that little or no change in performance occurs when the downstream depth is maintained at crest level. The performance curves are considered therefore to be representative of the weir configurations irrespective of the depth downstream of the weir providing this does not exceed the crest height.

7.2.1 Influence of the Geometrical Parameters

The programme was designed to indicate the significance of the three basic geometrical parameters, l/w, w/p and α.

As expected, an increase in the length magnification factor, l/w, while possibly increasing the performance of the weirs, nevertheless results in a lower effectiveness of the design and furthermore the small gain in performance obtained in setting $l/w > 8$ is unlikely in practice to justify the extra structural costs involved.

Two models (No.'s 15 and 16), with length magnifications of 2, were tested and both were found to behave almost ideally in that the flow magnification (QL/QR), remained equal to the length magnification over the whole flow range. The remaining models with this length magnification factor were discarded from the programme.

The effect of the vertical aspect ratio, w/p, can be assessed from the performance of models 24, 30 and 31, ($w/p = 3.5$), compared with models 19, 26 and 29, ($w/p = 2$), respectively. No significant difference in performance resulted from the change of w/p involved, although it is known from the results of other workers (Chapter 1), that small w/p ratios can produce significant effects on labyrinth weir behaviour. The results show that providing w/p is sufficiently large any effects due to this factor can be eliminated.

The angle of the side walls to the flow direction (α) was found to be of primary importance. For each length magnifi-

cation the corresponding magnification of flow increases with increase in α, suggesting that for maximum performance the angle α should be as large as possible. Because of the limits imposed on α by the length magnification factor, this implies that maximum weir performance is obtained from the triangular plan form configuration. (Chapter 1 (1.3.2)).

The special case of the rectangular weirs, where $\alpha = 0$, (models 26, 30, 32 and 33), are of particular interest in that the results for different length magnification factors merge into a common curve with increase in h/p. (Figure 24).

Two weirs from series D were tested, (models 29 and 33), where the plan form was of an integer $+\frac{1}{2}$ cycles. No significant differences were observed in the results when compared with the corresponding models in series A and it was concluded that the test channel side walls present no measureable interference to the weir discharge and that the change of scale by $^{6}/_{5}$ also produces no effect on the performance. The remaining models in series D were discarded from the programme.

7.2.2 Conclusions - Programme No. 1 - Ventilated Tests

The conclusions drawn from the initial test programme may be summarised as follows:-

1. The results are representative of the behaviour of

labyrinth weirs where there is no difference between the elevation of the upstream and downstream channel beds, and where the flow depth downstream of the weir is below the weir crest height.

2. The performance of the weirs is primarily determined by the magnification factor, l/w, and the angle of the side walls to the main flow direction, α.

3. Large length magnification factors decrease the effectiveness of the weir designs so that length magnifications greater than 8 are unlikely to be viable in practice. On the other hand, weirs involving small length magnifications behave almost ideally indicating that further experimental work in the range $4 < l/w < 8$ would be most fruitful.

4. Maximum performance for any given l/w ratio can be obtained by use of the maximum value of the side wall angle, α, associated with the triangular plan form.

5. The vertical aspect ratio, w/p, is of little significance in the weir behaviour providing this factor is sufficiently large to exclude effects due to limiting conditions such as nappe interference.

6. The behaviour of the weirs is independent of the number of cycles in plan.

7.3 Test Results - Programme No. 1 - Drowning Tests

The results of the drowning tests are shown in Figures 26 - 37, using the non-dimensional method of presentation described (Chapter 6). The flow magnification refers to the ratio of the flow over the labyrinth weir operating under drowned conditions, to the flow over a corresponding linear weir operating under identical conditions of upstream and downstream heads.

Figure 38 illustrates the results obtained from a number of tests on a normal sharp crested weir compared with the curve given by Villemonte's formula (6.3). Some discrepancy exists between the experimental results and the curve from the equation. Values of hd/h within the range $0.3 < hd/h < 0.9$ give flows with a maximum deviation of 5% - 7% higher than that predicted by the formula, but for higher hd/h ratios the deviation increases, becoming approximately -20% for $hd/h = 0.97$.

In practice, weir drowning conditions generally occur due to excessively high flows, and so the high degree of drowning represented by large values of hd/h (hd/h approaching 1) rarely or never occurs. Consequently for high values of hd/h the discrepancy between the experimental results and those predicted by the formula is considered unimportant. For smaller

hd/h values (hd/h less than 0.9) the discrepancy is within the limits of accuracy claimed by Villemonte.

If should be noted that in calculating the free flow over the normal weir, which is needed to calculate the submerged flow, the problems previously encountered in the choice of the sharp crested weir formula do not arise because of the necessarily high heads required for drowned conditions. The accuracy of the results is therefore independent of the sharp crested weir formula chosen.

With the downstream depth maintained at crest height, (hd = 0), the performance of the labyrinth weirs remained effectively the same as for ventilated flow, except that the 'humped' discontinuity present in the ventilated flow performance curves did not occur. Note that for the sake of clarity only a few representative results have been plotted on the graphs.

In the majority of the tests with hd = 0 and with very high flows, a hydraulic jump formed immediately downstream of the weir so that no further influence on the weir behaviour was produced by the downstream flow conditions.

It can be seen from the results of the tests on models 16, 28, 29 and 31 - 33, (Figures 27, 32, 33 and 35 - 37), that for low flows, i.e. when h/p approached hd/p (hd/h approaching 1),

a rapid fall off in flow magnification occurred.

In the light of the test results obtained from the normal sharp crested weir, it seemed that the likely explanation of these unexpected results is inaccuracy in, or inapplicability of Villemonte's equation in the region where hd/h is greater than 0.9. Whatever the reasons however, these results are considered unimportant because of the non-practical flow conditions under which they were observed. Further, because the results in this region were considered to be in error, testing of subsequent models was confined to drowning conditions where hd/h is less than 0.9. The falloff in performance is not therefore apparent in all the figures.

The remainder of the test results obtained under drowned conditions display a tendency to follow the ventilated performance curves, although in general the flow magnification of the drowned labyrinth weir as referred to a drowned linear weir is greater than the ventilated flow magnification for the same h/p value.

7.3.1 Conclusions - Programme No. 1 - Drowning Tests

The conclusion of major importance is that, like normal weirs, the labyrinth weir performance is unaffected by the down stream depth providing this does not exceed the crest height.

The diversity of the results does not allow any further general conclusions to be drawn, although certain trends are apparent.

Disregarding the fall off in performance for values of hd/h greater than 0.9, the effect of submergence on labyrinth weirs is similar to that on normal weirs, and as a first approximation the flow magnification obtained under drowned conditions can be assumed equal to that obtained under ventilated conditions. Any errors in design calculations based on this assumption would tend to underestimate the performance thus ensuring that the weir would be capable of meeting the design requirements. Thus, contrary to the expectations of other workers, (Reference 7), labyrinth weirs are less seriously affected by drowning than are normal weirs.

The increase in flow magnification under drowned conditions, compared with the ventilated performance, tends to be greater for increasing magnitudes of the side wall angle α, of the w/p ratio and of the degree of drowning (determined by hd/p).

7.4 Model Test Programme No. 2

In view of the results obtained from Model Test Programme No. 1, Test Programme No. 2 was designed primarily to confirm the

indications that for maximum performance, the side wall angle, α, should be a maximum.

To eliminate as far as possible, any secondary effects due to the vertical aspect ratio, w/p, maximum values of w/p, consistent with the scope of the investigation, were used.

The tests were confined to models with length magnifications within the range $4 < l/w < 8$, as this was the range indicated by the initial tests as requiring most investigation.

To achieve the aim of the programme it was originally intended to test models with three different side wall angles for each length magnification and w/p ratio. The angles were $\alpha_{max.}$ (triangular plan form), $0.75\ \alpha_{max.}$ and $0.5\ \alpha_{max.}$.

The design ratios adopted for the models are listed in Table 2 and the shapes of the models are shown schematically in Figure 39.

Models with length magnifications of 4 were not included in the programme as these had already been effectively covered by models 25 ($\alpha = \alpha_{max.}$) and 19 ($\alpha = 0.5\ \alpha_{max.}$) in Test Programme No. 1. The tests on model 41 were abandoned as these had also been covered by model 31 in Programme 1, the small difference in angle of 0.2^{o} between these two models was regarded as being insignificant.

Note that although certain weirs have been designated as triangular in plan form, the thickness of the perspex sections did not facilitate construction with a sharp point at the upstream tips and the side walls were therefore joined at this point with a small triangular fillet. The values of $\alpha_{max.}$ in Table 2 refer to the actual side wall angle obtained with the inclusion of the fillet in the calculation.

For design purposes it was decided to obtain a complete set of experimental results for this programme at least for side wall angles of $\alpha_{max.}$ and $0.75\alpha_{max.}$, even though the aim of the tests be realised at an early stage.

Testing under drowned conditions is very time consuming and as the behaviour of the weirs under these conditions was of secondary importance to the investigation, such tests were restricted to the most efficient weir designs only. Drowning tests were therefore confined to the triangular plan form models in this programme.

7.4.1 Test Results and Conclusions - Programm No. 2

The results have been plotted separately in Figures 40 - 44 and also together, superimposed on the results of Test Programme No. 1, for comparison, Figure 45.

The performance curves have a similar form to those of the previous models tested, but clearly demonstrate that the triangular plan form weirs are more effective than those with a trapezoidal plan form.

For the particular values of w/p used, the greatest flow magnification was achieved by the use of the maximum allowable side wall angle, α, associated with the triangular plan form.

In view of the results obtained from models 35 - 42 ($\alpha = \alpha_{max.}$ or $0.75\,\alpha_{max.}$) and those of the earlier programme it was decided that models 43 - 46 ($\alpha = 0.5\,\alpha_{max.}$) were unimportant for the purposes of the investigation and these were discarded from the programme.

The results of the drowning tests on the triangular models (No.'s 35 - 38) are shown in Figures 40 - 43, and these indicate a significant improvement in performance compared with the earlier drowning tests in Test Programme No. 1(8.3.1). This confirms the original indications that for high values of α the flow magnification obtained under drowning conditions is significantly higher than that obtained under ventilated flow conditions. Therefore for values of α approaching $\alpha_{max.}$, and large w/p ratios, labyrinth weirs are not as seriously affected by drowning as normal straight weirs.

The earlier conclusion (7.3.1), that the performance of labyrinth weirs is independent of the downstream depth, provided this does not exceed crest height, is also confirmed by the triangular weir models.

CHAPTER 8

SPECIAL LABYRINTH WEIR MODEL TESTS

8.1 Introduction

The results obtained from Test Programmes 1 and 2 were sufficient to cover the behaviour of basic labyrinth weir designs, especially in view of the accuracy of the theoretical work, (see Section 2), in predicting the performance of these.

The following series of tests were conducted to determine the significance of the parameters considered earlier to be of secondary importance, (Chapter 4), and also to enable, if possible, extension of the analysis to provide a general theoretical solution for any labyrinth weir configuration.

8.2 One Cycle Model Tests - Test Programme No. 3

The models previously tested, (Programmes 1 and 2), displayed an early tendency to choke on the downstream side, giving rise to interference on the side walls of the weirs. The onset of interference was observed practically, by an inability to maintain ventilation of the nappe along the full length of the crest, coinciding with the discontinuity which occurred in the performance curves.

In a situation involving a large drop on the downstream side of the weir (due to a large difference in the upstream to downstream bed elevations), choking of the weir offtake channels would not produce a sufficiently high flow depth within the offtake channels to create interference with the side wall flow. Ventilated flow conditions over the whole flow range would be obtained in this case and the lower performance associated with interference from the downstream channels would not occur.

Furthermore, difficulty in theoretical representation of interference flow was anticipated and it was considered essential, first, to obtain an analytical solution for the free flow case. It was therefore necessary to obtain fully ventilated (free flow) performance curves for the full flow range of the labyrinth weirs.

Free flow results were obtained in the earlier tests but the corresponding ranges of head to crest height ratios were not large enough to enable development of a theoretical analysis using these for comparison.

Test Programme No. 3 was designed specifically therefore, to determine the degree to which choking of the channels affects the weir performance, so that the significance of a

change in channel bed elevation, d, could be assessed, and also to provide full range ventilated flow performance curves for use in development of the theoretical analysis.

Fully ventilated performance results could have been achieved by constructing a false floor in the test channel upstream of the weir. A change of channel bed elevation, d, equal to the height of the false floor would have resulted. Due to the practical inconveniences involved, this method was discarded in favour of the following one cycle method.

The width of the test channel was reduced by the use of flume boards in a manner exactly similar to that used for the Dall tube calibration with the small 1 ft. Crump weir, (Photograph 6).

One cycle of weir, positioned at the end of the flume boards, gave unrestricted downstream flow so that no downstream interference occurred and the model operated under fully ventilated conditions over the whole flow range.

Apart from the elimination of downstream interference the one cycle models also allowed free expansion of the nappe, due to the absence of facing side walls. In order that the models would be representative of the normal full width labyrinth weirs, nappe interference (normally produced by impingement of the

nappes issuing from facing side walls) was simulated by extending the flume boards beyond the upstream weir sections by flush fitting aluminium plates. A sufficiently large clearance between the plates and the floor of the channel, ensured that the downstream flow remained unrestricted while nappe interference was produced as indicated.

From the results of the earlier tests involving different numbers of cycles in plan, for the same design ratios, and also from the fact that the flume boards and aluminium plates were fitted on longitudinal axes of symmetry, the arrangement was representative of labyrinth weirs subject to a large fall on the downstream side of the weir.

Free nappe expansion was permitted by the removal of the aluminium plates and thus the arrangement enabled quantitative assessment of the influence of nappe interference.

In view of the importance of the triangular plan form (7.4.1) it was decided that four, one cycle models, with identical design parameters to those tested in Programme 2 (models 35 - 38), would be tested. One further model (No. 51) was included in the programme (~~Table 3~~), although this was specifically tested for flow visualisation purposes (Chapter 9). This latter model was a one cycle version of model No. 27 in Model Programme No. 1.

Two tests were conducted on each of the four triangular models, one test with restricted nappe expansion and the other with free nappe expansion.

8.2.1 Results and Conclusions - One Cycle Model Tests

The performance curves of the triangular models are shown in Figure 46.

For low flows, where the full width models operated under ventilated conditions, the performance of the one cycle models and the full width models should have been identical. On comparison of the results however, concern was caused by a discrepancy between them of up to 10%.

A similar fall off in performance for small decreasing h/p values had previously occurred in the full width model tests, but this had been rectified by the use of the sharp crested weir formula proposed by Kindsvater and Carter, (see 6.2). As Kindsvater and Carter's formula had been used in the calculation of the one cycle weir performances it seemed that the discrepancies were due to errors peculiar to these particular tests.

The small width of the models necessitated the use of very small flows in these tests and it seemed therefore that the errors were due to inaccuracies in the Dall tube calibration

formula in the low flow region. The Dall tube was recalibrated at this point in the investigation (see 3.6), and the accuracy of the original calibration formula was confirmed.

The low flow errors present in the one cycle model tests remain unexplained. Nevertheless it was possible to construct satisfactory performance curves over the whole flow range for fully ventilated conditions by use of the one cycle model test results together with the results obtained from the corresponding full width models. These curves are shown in Figure 47.

The discrepancies observed in the results of the triangular weirs did not appear in those for the rectangular one cycle model, (No. 51), which was tested at an earlier time. The test results for this model are shown in Figure 48.

It can be seen from Figure 47 that the interference to the flow produced by choking of the offtake channels reduced the performance of the weirs tested, but not enough to warrant a full experimental investigation into the effects of differences between the elevations of the channel beds upstream and downstream of the weir.

Some slight loss of performance resulted when the aluminium plates were used to simulate nappe interference, (Figure 46), but this loss of performance would become highly

significant for small w/p ratios. (Chapter 1 (1.3.3) and Chapter 14).

It has also been shown (Chapters 1 and 14), that nappe interference has the greatest influence on triangular weir designs and hence it was considered that in all the previous experimental work, the w/p ratio was sufficiently large to exclude all but the most minor effects due to this factor.

8.3 Nappe Interference Tests - Test Programme No. 4

Nappe interference refers to the direct interference to the flow produced when the distance between two facing side walls of the weir is small compared with the head on the weir, such that impingement of the opposing nappes prevents free overfall, (Figure 49).

The preceding tests have shown that if w/p is large, nappe interference can be effectively eliminated. However the results obtained by Gentilini, (Chapter 1), show that when w/p is small, nappe interference becomes a critical factor in determining labyrinth weir performance.

The effect of nappe interference and its relation to the w/p ratio is fully discussed in Chapter 14, but it is easily appreciated that due to the close proximity of the side walls at the upstream tips of triangular weirs, interference

between the opposing nappes is inevitable. Thus although the preceding tests show that triangular plan forms give the greatest performance, these designs are nevertheless, more prone to restrictions due to nappe interference. Moreover as the number of upstream corners per length of weir increases so then must the effects of nappe interference increase.

The number of upstream tips per length of weir is inversely proportional to the w/p ratio, Figure 50, so that as w/p decreases, nappe interference increases, with a consequent loss of performance. This loss of performance is not a linear function of the w/p ratio, see Chapter 14, and it was therefore necessary to determine the effects of the w/p ratio experimentally, especially for the case of triangular plan form weirs.

Maximum values of w/p were used in Test Programme No. 2 with the intention of minimising any nappe interference effects present. Test Programme No. 4 was designed to repeat the triangular models tested in Programme 2 but with $w/p = 2$ in each case.

The design parameters for Programme No. 4 have been summarised in Table 3 and the shapes of the models shown schematically in Figure 51.

The results obtained from these tests (described in 8.4) did not seem to conform to the general pattern of those obtained for other designs and to confirm their validity it was decided to repeat the tests in full. In fact however, tests were repeated on only the first three models (52, 53 and 54).

8.3.1 Results and Conclusions - Nappe Interference Tests

Performance curves for the weirs are shown in Figures 52 and 53.

Figure 52 allows comparison with the performance of the corresponding triangular models with high w/p ratios and Figure 53 allows comparison with the trapezoidal models where $\alpha = 0.75\,\alpha_{max}$.

The change in performance due to the change in w/p ratio is shown in Figure 54.

Clearly a significant fall in performance occurred due to the reduction of the w/p ratios to 2 and as this fall in performance had not been detected in similar tests on trapezoidal weirs, (Test Programme No. 1), the results confirmed that triangular weirs are more prone to nappe interference effects than trapezoidal weirs of equivalent length magnifications. Further, Figure 53 indicates that the performance advantages gained by the use of triangular designs are lost for w/p = 2

and so if w/p is sufficiently small for nappe interference to become a significant factor then it will be necessary to revert to the trapezoidal plan form for optimum performance.

The major conclusion is that in weir design the adopted value of the w/p ratio should be as large as possible and in general not less than 2.

for triangular weirs.

The performance curves indicate that the increase in performance produced by the loss of ventilation, (at the onset of downstream interference), is maintained for h/p values far in excess of those expected and that downstream interference is generally beneficial to the weir behaviour.

The tests were repeated to check the validity of the results and the results of both sets of tests are displayed in Figure 55. A small discrepancy (less than 1.5%) can be seen between the performance curves and it was concluded that this was due to a difference in ventilation conditions between the tests. Observations during the second series of tests indicated that interference due to choking of the offtake channels was not as great as that previously obtained with large w/p ratios. The increased performance which resulted after the onset of downstream interference in these tests, was due to the loss of ventilation of the nappe which existed for the remaining ranges of flow.

The two separate sets of experiments served to demonstrate the repeatability of the model tests and confirmed the validity of the original results.

8.4 Simulated Nappe Interference Test - Linear Weir

A more fundamental understanding of nappe interference was necessary if this aspect of weir behaviour was to be incorporated in the theoretical analysis. In particular, it was required to determine the effect of this interference on the weir coefficient, related to the head and the distance between the side walls at a weir section, Figure 49.

It was considered that the phenomenon could be effectively simulated on a normal linear weir by suitably positioning a board along the axis of symmetry 'XX' in Figure 49. The arrangement is shown in Figure 56.

The wooden board was clamped to the test channel in a vertical plane, parallel to the weir crest.

A correction factor, f, was defined such that the modified weir coefficient, c', due to nappe interference, was equal to the normal weir coefficient, c, multiplied by the correction factor, i.e. $c' = f.c$:

The parameters, f, c, and c' are all non-dimensional and further consideration suggested that f should be a function

of h/x where h is the head and x is the distance between the weir and the board.

For a range of flows, the distance between the board and the weir was varied between $1\frac{1}{2}$" and 3" and the head and flow determined for each case.

In order that the results should be representative of the conditions existing in labyrinth weirs, ventilation of the nappe was maintained throughout. Failure of the ventilation resulted in a greatly reduced head due to draw down of the flow. This latter condition cannot arise in the labyrinth weir as the flow is confined within the offtake channels.

To ensure that the flow was controlled by conditions at the crest and not by underflow restrictions beneath the board, the clearance between the board and the channel was changed and several tests were repeated.

8.4.1 Results - Linear Weir -- Simulated Nappe Interference

The weir coefficient correction factor, f, was found to be a function of h/x, (see Figure 57). Examination of this figure shows that the relation between f and h/x can be closely represented by the formula

$$f = e^{a(h/x - b)^n} \qquad \ldots (6)$$

where $a = -0.572$, $b = 0.923$ and $n = 0.78$.

The experimental results indicate that nappe interference has negligible effect on the weir coefficient for values of h/x up to 0.6 whereas in using the formula it must be assumed that no nappe interference effects occur until h/x exceeds 0.93.

In the small range $0,6 < h/x < 0.93$ the error introduced by the formula varies from 0 to 5% whereas for the remainder of the curve the discrepancy between the formula and the experimental results is less than 1%.

Increasing the clearance between the bottom of the interference board and the channel floor produced no effects on the results obtained.

It was concluded that the formula could be used in the theoretical analysis to modify the weir coefficient at the labyrinth weir sections where nappe interference occurs. Note that, in the labyrinth weir, as the board was situated in a position corresponding to the centre line of the offtake channels, then h/x corresponds to $\frac{1}{2}(h/w)$.

8.5 Apron Tests - Test Programme No. 5

In discussion with practising weir designers, it was decided that inall probability full scale weirs would be built with vertical crest walls, similar to those used in the model constructions. Unlike the models however, actual weir designs

would most likely incorporate sloping channel floors to strengthen the structure, in the manner shown in Figure 1. These sloping channel floors, referred to as 'aprons', support the crest in such a way that the maximum unsupported height occurs in the centre sections of the weir, this height being equal to the normal crest height less half the maximum rise of the aprons.

The effect of aprons on weir performance was unknown at this stage but it was envisaged that the downstream aprons may be beneficial in reducing localised interference by allowing faster run off, although it was expected that aprons would be, in total, detrimental to overall weir performance.

The apron design is defined in terms of 'apron ratio' which is the maximum apron height divided by the crest height of the weir, (Figure 1).

To achieve a wide range of results three basic plan forms were used with length magnifications of 8, 6 and 4, corresponding to model numbers 39 and 41 in Test Programme No. 2, and model number 24 in Programme 1. Trapezoidal forms were used to minimise any nappe interference effects.

Four tests were conducted on each plan form covering the following apron arrangements:-

(p = crest height)

1. Aprons on the upstream side of the weir only, with a maximum height of:-

(a) 0.75p (apron ratio = 0.75)

(b) 0.5p (apron ratio = 0.5)

2. Aprons on both the upstream and downstream sides of the weir with equal maximum heights of:-

(a) 0.75p (apron ratio = 0.75)

(b) 0.5p (apron ratio = 0.5)

The weir parameters are summarised in Table 4.

Tests with aprons on the upstream side of the weir only, were conducted mainly as an aid to the development of the theoretical analysis. These configurations are not of practical importance.

8.5.1 Results and Conclusions - Apron Tests

The performance curves for the tests are shown in Figures 58 - 60, where it can be clearly seen that both the upstream and downstream aprons are greatly detrimental to labyrinth weir performance.

The loss of performance due to the upstream apron only, was slightly greater than half that recorded when both upstream and downstream aprons were present, but it cannot be assumed that upstream aprons are more detrimental than aprons on the

downstream side of the weir. The curves clearly show however, thataprons are more detrimental to the behaviour of labyrinth weirs with high flow magnifications and in practice, the smallest permissible aprons should be used.

Note that aprons have been considered to alter the basic design by 'filling up' the weir channels and the results have accordingly been plotted against the h/p ratio where p is the maximum crest height. If it had been considered that the aprons were formed by 'opening out' the weir channels, then the minimum crest height would have been used to calculate h/p, and consequently the reverse conclusion - that aprons improve labyrinth weir behaviour - would have resulted.

8.6 Semi-circular Crests - Test Programme No. 6

The purpose of these tests was to determine the applicability of the previous results to various crest sections.

A wide range of sectional crest shapes was possible but it was decided to continue the investigation with vertical walled crests. This decision was taken on the advice of consultants, who expressed the opinion that expensive, large scale structures, (requiring the use of a Creager profile for example) would necessarily involve specific model tests by the weir designers themselves.

It was decided that just one crest section other than the sharp crest type would be tested, in the hope that should the performance curves already obtained not be applicable to the new crest, suitable modification of the theoretical analysis would enable prediction of labyrinth weir performance irrespective of the crest shape used in the design.

The semicircular crest section described in Chapter 5 (5.1) was adopted for the tests (Figure 19).

Two tests were conducted with length magnifications of 6 and 4 respectively, corresponding to the designs of models 31 and 24 in Test Programme No. 1. Again nappe interference effectswere minimised by the use of trapezoidal designs incorporating large w/p ratios, (3.5).

In addition to these two labyrinth weirs, a normal linear weir was tested under both free and submerged flow conditions, in order to determine the weir coefficient for the semi-circular crest section. This was necessary to enable presentation of the results in the form of flow magnification against head to crest height ratio.

8.6.1 Results and Conclusions - Semi-circular Crests

For the linear weir tests, a correction factor, cf, necessary to modify the normal sharp crested weir coefficient

to that of the semi-circular crest, was calculated and plotted against the head, Figure 61. No account was taken of the crest height as this was the same for all the models with the semi-circular crest. It was not intended that the experimental curves of the performance of these weirs should themselves be used for design purposes. If this had been the case it would have been necessary to investigate scale effects for this particular crest design.

It was found that the coefficient of the semi-circular crest could be determined by multiplying the normal sharp crest coefficient by cf, where cf is given by the equation:-

$$cf = 1.29 - 0.028h \qquad \ldots (7)$$

for the range considered, i.e. $1" < h < 3.2"$.

The results obtained from the drowning tests on the linear weir showed that the Villemonte equation could be applied to the semi-circular crest with only a small degree of inaccuracy involved. (The free flow being determined from the actual crest coefficient).

Results obtained from the semi-circular crested models are plotted in two forms in Figures 62 and 63. Performance curves for the corresponding sharp crested labyrinth weirs are also shown in both cases, for comparison.

The flow magnification, used in Figure 62, was calculated from the labyrinth weir flow divided by the corresponding semi-circular crested, linear weir flow and therefore conforms to the standard method of presentation adopted throughout.

The Figure clearly shows that the performance curves previously obtained for sharp crests are not applicable to any crest section, unless the coefficient of the alternative section is identical to the sharp crest coefficient. In a case in which the crest coefficient is higher than that of the sharp crest a loss in flow magnification occurs over the whole flow range and vice versa.

The above conclusion does not mean that a greater flow, for the same head, occurs over a labyrinth weir constructed with a small crest coefficient, as can be seen in Figure 63. Calculation of the flow magnification in this figure was achieved by dividing the semi-circular crested labyrinth weir flow by the flow over a corresponding sharp crested linear weir. It can be seen that an increase in discharge occurs due to the higher coefficient of the semi-circular crest, although the gain in discharge compared with the sharp crested labyrinth weir decreases with increase in the head to crest height ratio.

The fall in performance observed in Figure 62 and 63, for small values of h/p, was due to errors in the correction

factor, cf, used to determine the coefficient of the semi-circular crest, as these values of h/p, ($h/p < 0.2$), were out of the range for which cf was determined. A repeat test on a linear weir with a semi-circular crest confirmed this, in that for heads below 1" the correction factor falls rapidly from the curve given in Equation (7).

It was concluded that the type of crest used in labyrinth weir design, is of major importance in the determination of the flow magnification of the weir, and that the performance curves presented for sharp crested weirs are not applicable to other crest sections if the coefficient of the crest differs widely from that of the sharp crest.

Further, the gain in discharge produced by the use of a crest with a high coefficient, is most apparent at small h/p ratios and as h/p increases this gain is reduced. For high h/p ratios the discharge becomes to some extent independent of the type of crest used in the design.

It will be seen in Section 2 that the theoretical solution derived for labyrinth weir performance will accurately predict the performance of labyrinth weirs irrespective of the crest type used in the design. No further crest sections were therefore used in the experimental tests.

CHAPTER 9.

FLOW VISUALISATION

9.1 Introduction

The behaviour of rectangular weirs, and weirs of small side wall angle, is characterised by large gradients in the flow surface profiles throughout the weir sections. The contraction at the entry sections produces a reduction in the surface level which then gradually rises along the length of the channel, as outflow effectively expands the flow. As weir flow is primarily dependent upon the head over the crest, then any reduction in surface level results in a loss of performance.

It is shown, Chapter 14, that the theoretical surface profiles for the triangular weir are horizontal, as no entry contractions are present and the rate of outflow is equal to the rate of channel contraction. In this case also, constant uniform velocities should exist throughout the weir sections.

The main purpose of flow visualisation was to provide illustrative confirmation of labyrinth weir behaviour, particularly for the case of the triangular weir. Apart from actual measurement of the surface profiles, it was not considered that flow visualisation would be of any direct benefit to the development of the theoretical

analysis due to the complex, three dimensional nature of the flow.

9.2 Die Injection

A simple die injector was immersed horizontally in the flow upstream of the weir. The injector was designed to produce a number of equidistant jets of die in the flow so that a simple photographic record of the flow pattern could be obtained.

The method was not particularly successful, due to diffusion of the die by turbulence.

Photographs were taken, with various exposure times, and Photograph 14 is representative of the results obtained for a triangular weir using a short exposure time. The photograph clearly demonstrates the linear streamlines obtained in triangular weirs.

9.3 Floating Particles

Photographs with relatively long exposure times, were taken of small black spheres randomly dispersed over the water surface.

Photograph 15 is typical of the results obtained for triangular plan form models - the particle paths, which correspond to the surface streamlines, are linear, except in the vicinity of the crest where the weir influence creates a lateral acceleration.

Perhaps more significant in illustrating the nature of the flow surface are the reflections of the strip lighting, observed in both the photographs (14 and 15). The light reflection provides clear visual confirmation of the linearity of the surface profile obtained in triangular weirs.

9.4 Cine Film

In the theoretical analysis, Chapter 11, transverse channel sections have been used for the application of momentum principles, and transverse velocity components are therefore of minor importance.

To illustrate that uniform velocity in the longitudinal direction, existed across transverse sections and to provide a record of this, die was injected by a moving injector so as to form a continuous straight die line normal to the flow. The progress of this line of die over the weir, was recorded on cine film.

In the areas of the weir upstream of the crest, the die line remained straight and normal to the main flow direction, but after overflow, because of acceleration and turbulence, the die rapidly diffused, as expected.

The behaviour of the die clearly demonstrated the existence of uniform velocities across the flow sections and indicated that

the weir influence merely superimposed a transverse velocity onto the main longitudinal flow velocity.

Cine film was also taken of the normal die injection and of the floating spheres, previously described.

9.5 Surface Profile Measurement

The discussion of the surface profile tests has been confined here to the experimentally observed results and behaviour. A full discussion, concerning the relation between the surface profiles, the weir parameters and the weir performance, is given in Chapter 14.

9.5.1. General Surface Profiles

For a number of models, the flow depth was measured along the centre line of the upstream channels, using the travelling depth gauge system. Surface profiles were plotted graphically from the readings obtained.

Besides providing a visual record of the nature of the weir flow, the tests also allowed direct evaluation of the representative-ness of the theoretical analysis, Chapter 13 (13.5).

Typical surface profiles are shown on Figures 64-65. The vertical scales are greatly magnified in comparison to the horizontal scales and the slight gradients which appear on the profiles for the

triangular model, Figure 64 are therefore negligible. Apart from the draw down effects at the downstream corners, the surface profiles for the triangular weir can be said to be linear and horizontal, further confirming the uniform constant velocities existing throughout the regions of this type of design (see Chapter 14).

The surface profiles obtained for the trapezoidal model, Figure 65, display a drop in head at the entry section due to contraction of the flow, followed by a rising profile which at the far downstream sections rises above the head upstream of the weir. The velocity at the downstream sections is a minimum giving a maximum depth due to the constant specific energy of the flow throughout (Chapter 11).

The models used for the apron tests were trapezoidal in plan form, and two separate shape effects combine to produce the surface profiles shown in Figure 66. The trapezoidal plan form tends to produce a surface profile similar to that shown in Figure 65, whereas the apron itself produces flow contraction with a corresponding falling profile. The overall effect is to create contraction of the flow in the upstream regions of the weir followed by expansion at the sections further downstream. This is clearly demonstrated by the surface profiles in Figure 66 which pass through a minimum depth towards the downstream tips.

The waves which appear on the surface profiles for the apron tests were not apparent upstream of the weir and did not seem to affect the results obtained. (Note that the waves were produced by downstream interference).

9.5.2. Specific Surface Profile Tests

In the development of the theoretical analysis (Chapter 11) the question arose as to whether standard weir coefficients could be applied to side weir flow. The following surface profile tests were designed specifically to clarify this point.

A 3 ft long section of a rectangular weir (model 27), was fixed in the channel with parallel flume boards, as used in the small Crump weir tests, (Photograph 6) positioned as side walls to guide the flow directly into the weir channel, Photograph 13. Overflow at the downstream tip of the weir was prevented by the wooden board also shown in the photograph.

Using this arrangement the flow was restricted purely to side flow, with stagnation conditions at the downstream end of the weir, and so enabled simple evaluation of the applicability of normal weir formulae to side weirs.

Centre line surface profiles were measured for five different flow and these are shown on Figures 67-69.

A number of experimental difficulties led to the non-ideal profiles obtained. The weir supply channel, bounded by the flume boards, seemed incapable of supplying the weir with the entry conditions required for ideal operation (see Chapter 13(13.5)) and large standing waves formed upstream of the weir with a trough existing at the weir inlet in each case.

Waves are also apparent on the surface profiles in Figures 67-69 but the wave length and amplitude of these are very small compared with the waves which occurred upstream of the weir.

It is significant, however, that the inlet depth varies little between the different flowrates and tends to fall with increase in flow beyond a certain point.

The surface profiles display the expected rise as the flow was expanded due to overflow. The surface gradient is not as large as expected in the downstream regions, due to non uniform flow conditions which further, gave rise to a sudden increase in depth on impact with the end board.

The choice of a prismatic rectangular channel for these tests was unfortunate in that the experimental conditions obtained were those probably least likely to correspond to the ideal (uniform flow etc.). Also a tapered channel would have been more representative of the channels actually used in labyrinth weirs.

A full discussion of these results in relation to theoretical performance is given in Chapter 13.

SECTION II

THEORETICAL WORK

CHAPTER 10

REVIEW OF RELATED THEORETICAL WORK

To the author's knowledge only one paper directly concerned with the prediction of labyrinth weir performance has been published, (Reference 18). A number of papers have, however, been published on spacially varied flow, with particular emphasis on side weirs. These are, therefore, related to the side flow conditions encountered in labyrinth weirs.

The following summaries of the more important investigations also include discussion of experimental work. The experimental work contained here was considered relevant to the theory but not to the review of experimental work in Chapter 1.

10.1 Schlag

Schlag, (Reference 18), used the experimental results of Kozák and Sváb (Reference 1) in the derivation of an empirical discharge formula for labyrinth weirs. He showed that the results for each model obeyed the 3/2 power law, common to linear weirs, in that $Q \propto h^{3/2}$, although the graphs of Q 'v' $h^{3/2}$ did not pass through the origin.

By modifying the weir discharge formula, in the manner used by Kindswater and Carter, to $Q = c(h + k)^{3/2}$ he found that c and k could be related independently to l, the developed length of the labyrinth weir crest.

Schlag concluded that the discharge of a labyrinth weir, Q, could be calculated from the formula:-

$$Q = c(h + k)^{3/2}$$

where $$c = 0.0107\ (1 + 115)$$

and $$k = 0.55 - 1/c^{2/3}$$

where the flow, Q, is expressed in litres/sec and the head h and the constants c and k are in centimetres.

The main criticism of this work stems from the criticism of Kozáks experimental results (Chapter 1) in that the ranges of the weir parameters used were not sufficiently large for each to produce a significant effect on the weir performance. The formula proposed by Schlag is applicable, therefore, only within the limited ranges of Kozáks results. No allowance has been included in the formula for variation in side wall angle, w/p ratio, crest shape nor for effects due to choking of the offtake channels, bed elevation changes, aprons, submergence etc.

All the weir parameters and conditions above have been found, in the present investigation, to have significant effects on the weir performance (see Chapters 8 and 9) and no attempt has been made therefore to verify Schlag's formula.

10.2 Nimmo

Nimmo (Reference 19) published in 1928 one of the first papers on a theoretical approach to the flow over side channel spillways.

The completely general case of a sloping channel, with the width of the channel and slope of the side walls varying from section to section, was considered. Transverse sections separated by a small distance dL, were taken across the flow (Figure 70) and the change in momentum across the section per unit time, less the momentum per unit time lost in overflow, was equated to the sum of the external forces.

An unwieldy differential equation for the slope of the water surface resulted (see Chapter 11 for further discussion).

Nimmo solved this equation, by finite difference methods, to calculate the flow and surface profile for a practical case. Close agreement was obtained between the practical and theoretical results.

Two main assumptions made in developing the analysis:-

1. Uniform steady flow existed.
2. The normal discharge equation for weirs applied also to the case of side weir flow.

10.3. De Marchi

In 1934, de Marchi (Reference 20) published a theoretical analysis for side weir flow. The analysis was developed from the

basic assumption of constant total energy along the length of the side weir.

The following assumptions were also made:-

1. Steady flow conditions existed.
2. The weir was situated in an infinitely long channel of uniform cross section.
3. The sill of the weir was parallel to the channel bed.
4. The flow in the channel was uniform at certain distances upstream and downstream of the weir.
5. The discharge over any given length of side weir could be calculated from standard weir formulae.
6. The total energy line remained parallel to the weir sill and the bed of the channel.

From these assumptions an equation for the slope of the water surface was derived, the equation being found to be identical (for similar channel conditions) to that obtained by Nimmo, (10.2), viz:-

$$\frac{dd}{dL} = \frac{A\,Q}{wQ^2 - gA^3} \cdot \frac{dQ}{dL} \qquad \ldots (8)$$

where at any section, A is the area of the section, Q the flow through the section, d the depth of water and L a measure of distance parallel to the channel, Figure 72.

De Marchi showed that an exact solution of this differential equation could be obtained for the case of a prismatic channel.

The two analyses by Nimmo (10.2) and de Marchi were the first to provide a satisfactory explanation of the two distinct modes of flow encountered in practice. It was found, experimentally, that the flow surface profile either rose or fell in the flow direction, the theoretical explanation being:-

For a falling profile (Figure 71) the slope of the water surface must be negative i.e. $\frac{dd}{dL} < 0$ and so from de Marchi's equation, (noting $dQ/dL < 0$) then:-

$$gA^3 < w\,Q^2$$

and so $$\frac{wQ^2}{gA^3} > 1$$

As the Froude No. F is given by:-

$$F = \sqrt{\frac{wQ^2}{gA^3}} \qquad \ldots (9)$$

hence a falling profile exists when the Froude number of the flow is greater than 1 i.e. when the flow is supercritical.

In a converse manner to the arguments applied above for a falling profile, it can be shown that a rising profile occurs in a prismatic channel when the flow is subcritical. ($F < 1$).

A combination of both types of flow is possible if a hydraulic jump occurs within the length of the weir.

In the particular case of labyrinth weirs, as the total flow must be restricted by the weir, the supercritical flow can

only occur under special circumstances and is therefore of secondary importance.

10.4. Ackers

A modified form of de Marchi's equation was derived by Ackers, Reference 21, by writing the total energy referred to the sill, E_w, in the more general form:-

$$E_w = \frac{\alpha v^2}{2g} + \beta h \qquad \ldots (10)$$

where α = velocity coefficient

β = pressure head coefficient

The resulting equation, for a prismatic channel was:-

$$l_2 = \frac{w}{c}\sqrt{\frac{2g}{\alpha}}\left\{\left(2 - \frac{\beta c}{E_w}\right)\left(\sqrt{\frac{E_w - \beta h_2}{h_2}} - \sqrt{\frac{E_w - \beta}{h_1}}\right)\right.$$
$$\left. - 3\sqrt{\beta}\left(\cos^{-1}\left(\sqrt{\beta h_2/E_w}\right) - \cos^{-1}\left(\sqrt{\beta h_1/E_w}\right)\right)\right\} \ldots (11)$$

using the notation as indicated in Figure 71 and w = channel width, c = weir crest coefficient.

Ackers then used experimental results obtained by Coleman and Smith (Reference 22) in this equation and arrived at the following conclusions:--

1. The normal weir discharge equation is applicable to side weirs.
2. The velocity coefficient, α, varies between 1.15 and 1.40.
3. The pressure head coefficient, β, is 0.80.

Unfortunately the experimental results used were for the case of supercritical flow only and so the conclusions are of limited importance to the labyrinth weir case.

10.5. Collinge

Collinge (Reference 23) attempted to confirm experimentally the de Marchi theory, for both subcritical and supercritical flow in prismatic channels.

From a series of experiments with low velocity flow - all the flow passing over the side weir - he obtained weir coefficients which he assumed were characteristic of the weir and not of the nature of the flow.

Using these experimental coefficients and de Marchi's theory, Collinge obtained a reasonable correlation between the experimental and theoretical discharges for the case of subcritical flow. A reduction in the weir coefficient of the order of a few percent was found with increase in the velocity of the flow parallel to the weir.

10.6. Other Work on Side Weirs

A large number of empirical formulae have been proposed as a result of experimental work on side weirs. A synopsis of these together with full references has been given by Ackers, (10.4),

Collinge, (10.5), Allen, and Frazer in a symposium of four papers presented to the Institution of Civil Engineers (References 21, 23, 24, 25, 26) entitled "A theoretical consideration of side weirs as storm-water overflows".

Further discussion and references may also be found in the Ph.D. thesis presented by Frazer (Reference 27) to the University of Glasgow, entitled "The behaviour of side weirs in prismatic rectangular channels".

10.7. Discussion of Work related to the Theory

The work by Schlag (10.1) although directly related to Labyrinth weir performance is empirical and only applicable to the limited experimental results by Kozák and Sváb (Chapter 1).

The theoretical analyses by Nimmo and de Marchi have been shown to describe the behaviour of side weir flow and are therefore of importance to the analysis of labyrinth weir performance. It is apparent however that these analyses contain inaccuracies introduced by the approximations and assumptions made in their derivation and therefore require some refinement.

Ackers and Collinge have separately shown that various refinements can be made to the theory by the use of experimentally determined coefficients which enable good prediction of the performance of side weirs for the particular case of storm water

overflows. Both used different experimental coefficients and these cannot be assumed applicable to the case of the side flow encountered in the labyrinth weir.

No previous experimental work on tapered channels has been found by the author, and here again the coefficients used by Ackers and Collinge would not be expected to apply in this case.

CHAPTER 11

APPLICATION OF NIMMO'S ANALYSIS TO SIDE WEIR FLOW

Although Nimmo (10.2) and de Marchi (10.3) obtained the same results using different methods of approach, Nimmo's solution was for the entirely general case of side weir flow and has therefore been used in preference to de Marchi's solution.

By a consideration of momentum principles Nimmo arrived at the following equation for the general case of side weir flow, (refer to Figure 70).

$$\frac{Q^2}{g \cdot A} + \frac{Q \cdot \Delta Q}{g \cdot A} - \frac{(Q + \Delta Q)^2}{g \cdot (A + \Delta A)} = \frac{(w + \Delta w) \cdot (d^2 + 2d \cdot \Delta d)}{2}$$

$$+ (n + \Delta n) \cdot \frac{(d^3 + 3 \cdot d^2 \cdot \Delta d)}{3} - \frac{w \cdot d^2}{2} - \frac{n \cdot d^3}{3} - \frac{\Delta w \cdot d^2 \cdot}{2}$$

$$- \frac{\Delta n \cdot d^3}{3} - \Delta x \cdot (f - s) \cdot (w \cdot d - n \cdot d^2) \qquad \ldots (12)$$

The equation applies to transverse sections of channel separated by a small distance Δx.

where: Q = flow past a section across the channel.

$+\Delta Q$ = flow lost over the weir between the sections.

A = area of flow.

g = acceleration due to gravity.

w = width of channel bed.

n = slope of side walls.

f = friction loss/unit length of channel.

s = slope of channel bed.

The main assumptions made in deriving Equation (12) were:-

1. Uniform flow conditions existed - it then followed that pressure distributions could be taken as hydrostatic and momentum coefficients as unity.

2. The water surface across the sections was horizontal - allowing a simple expression for pressure forces to be obtained in terms of w, n and d.

3. The component of velocity of the discharge over the weir, parallel to the channel, remained equal to the channel velocity at the overflow section - an assumption necessary for determination of the momentum lost by the overflow.

Small approximations were also made, e.g. retardation due to friction = $\Delta x \,.\, f \,.\, A \,.$ and the average velocity between the sections was taken as $V + 1/2\ \Delta V$.

In the initial application of Equation (12) to the experimental results then:-

$n = 0$, ($\Delta n = 0$) - vertical channel walls.

$f = 0$ - assume zero friction losses.

$s = 0$ - channel bed horizontal.

Substituting in and simplifying Equation (12) gives:-

$$\frac{Q}{g \cdot A} \cdot \frac{(Q \cdot \Delta A - A \cdot \Delta Q)}{(A + \Delta A)} = w.d. \Delta d.$$

eliminating products of Δ quantities

$$\frac{Q^{\$}}{gA^2} \cdot (Q.\Delta A - A.\Delta Q) = w.d. \Delta d.$$

Dividing through by Δx

$$\frac{\Delta d}{\Delta x} = \frac{Q}{w.d.g.A^2} \left\{ Q. \frac{\Delta A}{\Delta x}. - A . \frac{\Delta Q}{\Delta x}. \right\} \quad \ldots (13)$$

but as $n = 0$ then $A = w.d.$ (approximately) and so

$$\frac{dA}{dx} = d . \frac{dw}{dx} + w.\frac{dd}{dx}$$

i.e. in finite difference form

$$\frac{\Delta A}{\Delta x} = d . \frac{\Delta w}{\Delta x} + w.\frac{\Delta d}{\Delta x}$$

and so substitution in (13) results in:-

$$\frac{\Delta d}{\Delta x} = \frac{Q.d}{w} \cdot \frac{\left(Q.\frac{\Delta w}{\Delta x} - w.\frac{\Delta Q}{\Delta x}. \right)}{(w^2.d^3.g - Q^2).} \quad \ldots (14)$$

In the case of a tapered channel (included angle of taper = 2α)

then:-

$$\tan \alpha = \frac{\Delta w}{2. \Delta x .} \quad \ldots (15)$$

and also

$$\Delta L = \frac{\Delta x}{\cos \alpha} \quad \ldots (16)$$

where ΔL = increment of crest length (one sided weir) contained between the two transverse channel sections Δx apart.

If the standard weir formulae are assumed to apply to the case of side weir flow then:-

$$\Delta Q = c. \Delta L . h^{3/2}$$

where h = average head between sections.

c = crest coefficient.

and so $$\frac{\Delta Q}{\Delta X} = \frac{2.c.h^{3/2}}{\cos \alpha} \quad \ldots (17)$$

for a double sided flow as encountered in labyrinth weirs.

Substitution of Equations (15), (16) and (17) in Equation (14) then gives:-

$$\frac{\Delta h}{\Delta X} = \frac{2.Q.(h+p)}{w} \cdot \frac{(Q.\tan \alpha - w.c.h^{3/2} / \cos \alpha)}{(w^2 .(h+p)^3 , g - Q^2).} \quad \ldots (18)$$

being an expression for the slope of the water surface at a section of a channel, with flow from both sides.

11.1. Method of Solution

Equation (18) may be used to determine the surface profile, and the flow for a side weir spillway, providing the depth and quantity of flow are known at one section.

Solution has been obtained by a marching method using finite differences in the following manner:-

Consider the general case shown in Figure 73 where the channel is divided into a large number of sections distance Δx apart - (Δx small but finite).

Assume that the flow conditions at section O are known, then, h_O and Q_O are known together with the geometrical parameters at every section.

The slope of the water surface at section O can be calculated from Equation (18) so allowing Δh_{O1} to be determined from the defined value of Δx .

Note that, contrary to the analysis, the direction of x increasing has been taken in the reverse direction to the channel flow and so the slope $\Delta h/\Delta x$ assumes the opposite sign to that given by Equation (18).

hence $h_1 = h_O + \Delta h_{O1}$ (approx.)

the average head between the sections

$$= \frac{(h_O + h_1)}{2}$$

and so

$$\Delta Q_{O1} = \frac{2 \cdot c \cdot \Delta x}{\cos \alpha} \left(\frac{h_O + h_1}{2} \right)^{3/2} \quad \ldots (19)$$

which is the overflow between sections O and 1.

therefore $Q_1 = Q_O + \Delta Q_{O1}$

From geometrical considerations

$$\frac{\Delta w}{\Delta x} = \frac{w_1 - w_O}{\Delta x} = 2.\tan \alpha$$

$$\therefore \quad w_1 = w_0 + 2.\ \Delta x\ .\ \tan\alpha \qquad \ldots (20)$$

The flow conditions are therefore known at section 1 and the procedure may be repeated in a similar manner to determine the flow and depth at section 2, so proceeding for the length of the weir.

11.2 Application to Experimental Work

It has been shown (11.1) that Equation (18) may be used to determine the flow and surface profiles for side weir flow - providing the depth and flow are known at one section. The flow conditions are not known at any section in the flow over a labyrinth weir and so to compare Equation (18) to a practical case it was necessary to devise special experimental side weir tests. These are described in Chapter 9, (9.5.2) where a section of rectangular weir was used with the end flow restricted by a vertical board at the downstream tip section.

Pure side flow, with known (stagnation) conditions at the end sections, was achieved and therefore allowed direct evaluation of Equation (18).

A solution was obtained on a digital computer for conditions corresponding to those obtained in the practical tests.

The theoretical surface profiles are shown in Figures 67, 68 and 69, together with the experimental results.

Of the two theoretical profiles shown for each test, one was calculated using the standard Rehbock formula (applied to the side flow) and the other was obtained iteratively by successive adjustment of the Rehbock coefficient until the conditions at entry to the weir were identical to the practical case. The flow for both theoretical profiles corresponds to the experimental flow and also to the profiles obtained from an assumption of constant specific energy.

The analysis indicated that for subcritical flow a definite maximum depth occurred at the weir entry section. If the flow was increased beyond that giving the maximum inlet depth, then the inlet depth decreased with a corresponding increase in flow velocity, until critical conditions were reached. The experimental difficulties in achieving the inlet conditions predicted by the analysis, are described in (9.5.2.) and these resulted in the waves on the experimental surface profiles.

The theoretical curves demonstrate the rising profile obtained for subcritical flow and effectively confirm the constant specific energy assumption made by de Marchi.

For the particular case of prismatic channels, however, the assumption of uniform flow conditions is seen to be in error, owing to the sudden rise in depth encountered at the downstream end - caused by the momentum of the flow which should have been ideally zero at this point.

In the case of a tapered channel the surface profile would be more horizontal and the flow velocity more nearly constant along the weir length so that the flow conditions should be much closer to those assumed in the analysis.

The mean head over the weir was found at 2" intervals from the experimental curves, and from this the 2/3 root mean of $h^{3/2}$ value calculated, allowing an experimental weir coefficient to be determined. The coefficients have been indicated in the figures, although no great importance has been attached to these due to the non ideal nature of the flow.

It was concluded that the method of analysis derived by Nimmo was generally representative of side weir flow but that to obtain a high degree of accuracy, refinement would have to be made to allow for non uniform flow conditions.

It was also apparent that the crest coefficient would need slight modification in order for it to be applicable to side weirs. An effect was noticed, however, in the experimental tests, which would tend to invalidate the weir coefficients obtained by experiments of the type considered here. The channel walls ~~en~~ constraining the flow, produced at the weir entry section, a flow more representative of a jet than that of an established weir flow. Consequently the flow over the initial lengths of the weir was not fully established and was dependent on the mainstream velocity, decreasing (for constant

head) with increase in velocity. This source of error is somewhat offset in the case of the labyrinth weir as the flow is guided by the weir itself, without any interference from the channel walls.

CHAPTER 12

THEORETICAL REPRESENTATION OF LABYRINTH WEIR FLOW

Labyrinth weir flow, being relatively complex, was not expected to yield to a theoretical solution of high accuracy without the inclusion of empirical or experimentally determined coefficients. A mathematical model was designed therefore, to represent the flow as closely as possible but allowing for the effect of various coefficients and parameters on the solution to be determined.

12.1. Method of Solution

Reference has been made throughout to Figure 74, and the method of solution is summarised on pages 128 and 129.

12.1.1. Ventilated Flow (Upstream Analysis)

It was shown (Chapter 11) that the method of analysis derived by Nimmo adequately represented the spacially varied flow encountered in side weir spillways, subject to certain limitations.

The analysis depends on the knowledge of the flow conditions at some section and therefore to apply it to the labyrinth weir it was necessary to assume the flow conditions at some point.

Flow Chart Illustrating Method of Solution

Reference is made throughout to Figure 74.

1. Define the head of section O.

2. Calculate the flow through section O using the crest length downstream of O and standard weir formulae.

3. Use marching procedure to determine flow conditions at sections in the upstream channels including section 3.

4. Satisfy energy conditions between sections 3 and 4 with due allowance for the flow over the upstream tips. Hence determine the flow conditions at section 4. (The discharge thus determined is that obtained for fully ventilated flow conditions.

5. Assume depth at section 5 is equal to the crest height, and using the flow as determined in step 4 with due allowance for the flow over the downstream tips then satisfy energy conditions between sections 5 and 6 and hence determine the flow conditions at section 6.

6. Use marching procedure to define the surface profile in the downstream channels.

7. Recalculate the upstream channel flow conditions with due allowance for drowning at the sections where this occurs.

8. Repeat steps 5, 6 and 7 until a stable solution is achieved for the flow conditions at section 4. Print results.

Assuming that the labyrinth weir flow is subcritical throughout the upstream sections, then control must exist at the downstream ends of the upstream channels. Further, the flow at the downstream tips is small and so an error in flow assumption in this region represents only a very small proportion of the total flow.

The position of section O (Figure 74) is defined as being through a point on the channel centre line, equidistant from the side walls and the downstream tip.

The experimental work in Chapter 7 (7.2.1.) clearly indicated that weirs of small length magnifications ($l/w \leqslant 2$) operated ideally. Considering section O as being the entry section for a labyrinth weir - formed by the crest downstream of section O - then the length magnification downstream of O is small and consequently the flow can be assumed to be given by normal weir discharge formulae using the corresponding developed length.

As a starting point for the analysis therefore the head at section O is defined and from this the flow through O is determined.

The approach channel is then divided into a large number of equispaced sections, the distance between the sections being small - so allowing a marching solution to be obtained in the manner described in Chapter 11 (11.1).

The flow conditions at section 3 (channel entry section) are thus calculated.

The flow over the upstream weir tips, q, is assumed to be dependent on the head upstream of the weir. It is necessary therefore, to use an iterative procedure to determine the flow conditions at section 4, as the flow at this point is the total flow over the weir and includes the tip flow, q. Newton's method of successive approximation is used to satisfy the energy conditions between sections 3 and 4, i.e. specific energy at section 4 = specific energy at section 3 + energy loss due to sudden contraction.

The flow obtained in the manner described is the fully ventilated weir flow as no allowance is made for downstream interference.

12.1.2. Interference Flow (Downstream Analysis)

The experimental work showed that localised drowning occurred on sections of the weir side walls, due to choking of the offtake channels and a downstream surface profile similar to that shown in Figure 74.

If the downstream surface profile were known, it was considered a simple matter to modify the upstream analysis to allow for interference, by calculating the overflow at each section from Villemonte's Equation (Equation 5) for weir submergence.

The downstream profile, is, however, dependent on the weir flow - determined by the upstream analysis - which is in turn dependent on the downstream conditions. Thus any solution involving downstream interference must be determined by successive correction of the upstream analysis for the downstream profiles obtained.

A similar method to the upstream analysis is used forthe offtake channels. Transverse sections of the downstream channel are taken - corresponding to those used on the upstream sides of the crest. Then, by applying momentum principles to the flow elements, a marching solution can be obtained which defines the surface profile in the downstream channel.

The analysis differed slightly from that of the upstream channels in that between successive sections, an inflow instead of an outflow occurs. The inflow is determined primarily by the conditions in the upstream channels and the momentum/lb of inflow is not therefore equal to the momentum/lb of the main downstream flow.

To effect an analysis in the manner described, it is again necessary that the flow conditions should be known at one section. Subcritical flow has been assumed throughout the upstream analysis but this assumption cannot be made for the downstream flow. There are three possible means of control of the downstream flow:-

1. Control effected by flow conditions downstream of the weir - subcritical flow throughout.
2. For the case of a horizontal channel bed in the offtake channels, control (critical flow) can occur at the exit sections.
3. For the case of a sloping channel bed in the offtake channels, control points can exist at any point in the channel, in fact more than one critical section can exist in this case with hydraulic jumps in between.

Methods for the determination of the control points in case 3 have been published by Smith, (Reference 28), and Hinds, (Reference 29), but both methods depend on the knowledge of the flow profile of the normal flow. Frictional effects have been neglected throughout the analysis and it is therefore desirable to avoid, if possible, calculation of the surface profiles involving control points within the offtake channels.

Furthermore, referring back to de Marchi's analysis (10.3), the equation for the slope of the water surface is:-

$$\frac{dd}{dL} = \frac{A.Q}{w.Q^2 - g.A^3} \cdot \frac{dQ}{dL}$$

clearly if $w.Q^2 = g.A^3$

then $F = \sqrt{\frac{w.Q^2}{g.A^3}} =$ Froude No. $= 1$

and $\frac{dd}{dL} = \infty$

Thus the analysis indicates that at critical flow conditions the surface gradient is infinite, as ideally obtained in a hydraulic jump.

Because of the inability of the analysis to pass through critical flow conditions it is desirable to avoid these conditions wherever possible in the calculations.

The experimental results indicate a method of solution which would to a large extent avoid the problems encountered by critical flow conditions. It has been shown that the labyrinth weir performance is independent of the depth downstream of the weir provided this does not exceed the height of the crest. As it is essential, to the analysis, to know the flow conditions at some point it is assumed that the flow depth downstream of the weir at (section 5) is equal to the crest height.

This assumption allows the analysis to be conducted for subcritical flow conditions for the greater part of the flow range. Development of the analysis and the nature of the downstream surface profiles (Chapter 14) justify the assumption.

The flow at section 5 is already determined by the upstream analysis and so setting the depth at this point equal to the crest height, provides the known flow conditions required for the downstream analysis.

An iterative procedure is used to satisfy energy conditions between sections 5 and 6, i.e. specific energy at section 6 = specific

energy at section 5 + energy lost in the sudden expansion. Note also that the flow at section 5 is equal to the flow at section 6 plus the flow over the downstream tips.

In determining the flow conditions at section 6, if the depth is found to be less than the critical depth then the depth at this point is set equal to the critical depth, i.e. if the analysis indicates that the flow is not controlled by conditions downstream of the weir then it is assumed that a control exists at the channel exit sections (section 6).

The surface profile in the offtake channels is then determined using a finite difference marching procedure similar to that used in the upstream analysis.

If the depth in the downstream channel is found to exceed the crest height at any point then downstream interference is confirmed and information concerning the surface profile is stored. The cycle of analysis is repeated, due allowance being made in the upstream analysis for the downstream interference - at the sections where this occurs.

The new flow conditions obtained from the upstream analysis (modified to correct for interference) are used to recalculate the surface profile in the offtake channels, the cycle being repeated until the difference between the flow obtained from two successive cycles is within a small specified limit.

It will be noticed that until the analysis is complete the head and flow over the weir are unknown and so the flow obtained for a given upstream head cannot be found directly. The method does however allow calculation of the performance curves from which the required data can be obtained.

12.2. Theoretical Analysis Details

In the earlier stage of development of the mathematical model, Equation (18), (Chapter 11), was used to represent the labyrinth weir side flow. However, this equation was insufficiently accurate to cover all aspects of weir design and modifications were made accordingly.

The following analysis details are those which were finally adopted in the mathematical model.

12.2.1. Momentum of the Overflow

Nimmo assumed in his analysis that the velocity of the overflow, in the longitudinal direction, remained equal to the mainflow velocity in the upstream channel. This assumption is justified for channels of small taper but in the case of labyrinth weirs where the angle of taper can be large it is necessary to make some allowance for the acceleration of the flow normal to the crest.

The following approximations and assumptions have been made:-

1. The horizontal velocity component normal to the crest remains constant after overflow. This is justified if the pressure within the nappe is atmospheric throughout.
2. Velocity and pressure distributions within the nappe are similar for all head to crest height ratios.
3. The fluid pressure in the nappe and in the vertical plane of the weir crest is atmospheric. Although strictly incorrect this approximation was made to simplify the analysis and because any errors incurred could be simply corrected from a consideration of assumption 2.

Conditions 2 and 3 result from a consideration of the work by Hay and Markland on the determination of the discharge over weirs by the electrolytic tank. (Reference 30).

Considering the normal weir overflow as shown in Figure 75, with notation as indicated then:-

$$dq = v.dl \qquad \ldots (21)$$

(q = flow/unit length of crest.)

but $$q = c.g^{1/2}.h^{3/2} \qquad \ldots (22)$$

from standard weir formulae where c is a non-dimensional constant.

The momentum flux of the flow dq in the direction shown

$$= dm = \frac{w_s \cdot v.dq}{g}$$ where w_s = specific weight of water.

and so for the total flow

$$m = \int_0^l \frac{w_s \cdot v \cdot dq}{g} \qquad \ldots (23)$$

therefore from (21) and (23)

$$m = \int_0^1 \frac{w_s}{g} \cdot \left(\frac{dq}{dl}\right) \, dq$$

$$= \int_0^1 \frac{w_s}{g} \cdot \left(\frac{dq}{dl}\right)^2 dl$$

however differentiating (22) then

$$\frac{dq}{dl} = c.g^{1/2}. \frac{3}{2} . h^{1/2}. \frac{dh}{dl}$$

and so $m = \int_0^1 \frac{9}{4} . w_s . c^2 . h \left(\frac{dh}{dl}\right)^2 dl.$

But from assumption 2 (see Hay and Markland, Reference 30)

$$l = kh \qquad \text{where } k \simeq 0.85$$

and $\frac{dh}{dl} = \frac{1}{k}$

and so $m = \frac{9}{4} \frac{c^2 . w_s}{k^2} . \int_0^h hk \, dh$

$$= \frac{9}{8} . \frac{c^2 . h^2}{k} . w_s \qquad \ldots (24)$$

Defining an effective overflow velocity as v' such that the momentum of the overflow

$$m = \frac{w_s . q . v'}{g}$$

then $\frac{w_s . q . v'}{g} = \frac{9}{8} . \frac{c^2 h^2 w_s}{k}$

Hence $v' = \frac{9}{8} \frac{g\, c^2 h^2}{qk} = \frac{9}{8} \frac{c\sqrt{gh}}{k} \qquad \ldots (25)$

Note that if the assumption of atmospheric pressure in the nappe, in the vertical plane of the crest, incurred unnacceptable errors then the value of the constant k could be simply changed. Variation of k effectively changes the position of the nappe section under consideration.

The flow velocity on the upstream sides of the labyrinth weir can be considered as the resultant of the velocity component parallel to the weir crest (due to the main flow velocity) and the velocity component normal to the weir crest (due to the crest influence).

Hence if v_u is the main flow velocity in the longitudinal direction and v' the effective velocity normal to the crest then the effective horizontal component of velocity in the longitudinal direction

$$= v_u \cdot \cos^2 \alpha + v' \sin \alpha \qquad \ldots (26)$$

and so the component of the momentum of the overflow in the same direction

$$= \frac{q \cdot w_s}{g} \cdot (v_u \cos^2 \alpha + v' \cdot \sin \alpha) \qquad \ldots (27)$$

The above analysis applies only to the free flow weir behaviour and so to allow for drowned flow conditions the following assumptions and modifications were made:-

Consider the drowned flow conditions shown in Figure 75 where suffix d has been used in the notation to denote drowned conditions.

The height of the nappe at the crest, ld, must be within the limits:-

$$k.h < l_d < h$$

and so it was assumed that

$$l_d = h_d + k\ (h - h_d) \qquad \ldots (28)$$

then if h_d = O (free flow) $l_d = l = k.h$

and if h_d = h (total drowning-zero flow) l = h

It was also assumed that the velocity distributions within the nappe were similar to the free flow case and it followed that as $q \propto v'.l$ then

$$\frac{v_d'}{v'} = \frac{q_d}{q} \cdot \frac{l}{l_d}$$

hence

$$v_d' = \frac{q_d}{q} \quad \frac{kh}{(h_d + k(h - h_d))} \quad v' \qquad \ldots (29)$$

$\frac{q_d}{q}$ being obtained from Villemontes drowning equation (Equation 5).

As a check on the representativeness of Equation (29) then when

h_d = O i.e. free flow

$$\frac{q_d}{q} = 1 \quad \text{and} \quad \frac{v_d'}{} = v' \quad \text{as required}$$

when h_d = h i.e. total drowning-zero flow

$$\frac{q_d}{q} = O \quad \text{and} \quad v_d' = O \quad \text{as required}$$

In a similar manner to the free overflow then the horizontal component of the momentum of the overflow in the longitudinal direction

$$= \frac{qd \cdot w_s}{g} \left(v_u \cos^2 \alpha + v_d' \sin \alpha\right) \quad \ldots (30)$$

These equations (27 and 30) are used to determine the momentum of the overflow between adjacent sections of the upstream channel.

12.2.2. Upstream Channel Analysis

Because of the large angles of channel taper and the steep channel bed gradients (due to aprons) likely to be encountered in labyrinth weirs, it was decided to carry out a more accurate analysis of the upstream flow than that derived by Nimmo. (Equation 18)

Reference has been made throughout to Figure 76 in which the notation used is indicated.

The following assumptions relating to the flow conditions were made:-

1. Uniform flow.
2. Horizontal flow velocities.
3. Hydrostatic pressure throughout.
4. Flow sections bounded by vertical planes through the crest of the weir.
5. Surfaces horizontal across the sections.

6. Frictional losses negligible.

7. Overflow momentum determined by Equations 27 and 30 in (12.2.1.)

8. Overflow between two sections determined by standard weir formulae using the average head between the sections.

To simplify the algebra the specific weight of water has been neglected from the equations as this is a common factor to all.

Considering Figure 76 then the following equations result from the above assumptions.

Forces:

$$F_1 = \frac{w_1 \cdot y_1^2}{2} \qquad \ldots (31)$$

$$F_2 = \frac{w_2 \cdot y_2^2}{2} \qquad \ldots (32)$$

$$\text{Side wall area} = A_s = \frac{2 \cdot \Delta x \cdot y_1}{\cos \alpha} + (y_2 - y_1) \cdot \frac{\Delta x}{\cos \alpha}$$

and so side wall force = $F_s = \frac{\Delta x \cdot y_1^2}{\cos \alpha} + (y_2 - y_1) \cdot \frac{\Delta x}{\cos \alpha} \cdot \left(y_1 + \frac{(y_2 - y_1)}{3} \right)$ ... (33)

It can be shown that the gravitational force,

$$G = \frac{\Delta x}{2} \cdot (w_1 y_2 + y_1 w_2) + (w_2 - w_1) \cdot (y_2 - y_1) \cdot \frac{\Delta x}{3} \qquad \ldots (34)$$

and so $F_B = G / \cos \phi$ ... (35)

Momentum:

$$M_1 = \frac{Q_1^2}{gA_1} \quad \ldots (36)$$

where A_1 = flow area of section 1 = $w_1 y_1$

$$M_2 = \frac{Q_2^2}{gA_2} \quad \ldots (37)$$

where A_2 = flow area of section 2 = $w_2 y_2$

$$M_3 = \frac{\Delta Q}{g} \cdot (v_u \cos^2 \alpha + v' \sin \alpha) \quad \ldots (38)$$

determined from Equations 27 and 30 in (12.2.1.)

Hence equating forces to the rate of change of momentum in the horizontal, longitudinal direction

$$F_2 - F_1 - F_s \sin \alpha - G \tan \phi = M_1 - M_2 + M_3 \quad \ldots (39)$$

The following equations also apply:-

$$Q_2 = Q_1 + \Delta Q \quad \ldots (40)$$

$$\Delta y = y_2 - y_1 \quad \ldots (41)$$

and ΔQ is determined from standard weir formulae using the head $(h_1 + \frac{\Delta y}{2})$

In a similar manner to Nimmo's analysis the flow conditions at section 1 must be known together with the geometrical parameters of the weir at both sections 1 and 2. Hence Equation 39 can be written as a function of the only unknown quantity Δy.

thus $f(\Delta y) = F_2 - F_1 - F_s \sin \alpha - G \tan \phi - M_1 - M_3 + M_2 = 0$ .. (42)

The complexity of this equation does not allow the derivation of simple expression for Δy and so a solution is obtained by Newton's method of successive approximation

i.e. $$\Delta y' = \Delta y - \frac{f(\Delta y)}{f'(\Delta y)} \quad \ldots (43)$$

where $$f'(\Delta y) = \frac{dF_2}{d\Delta y} - \frac{dF_1}{d\Delta y} - \frac{dF_s \sin\alpha}{d\Delta y} - \frac{dG \tan\phi}{d\Delta y} - \frac{dM_1}{d\Delta y} - \frac{dM_3}{d\Delta y} + \frac{dM_2}{d\Delta y} \quad \ldots (44)$$

Thus, from the assumed conditions at one section of the upstream flow Δy is determined from a consideration of momentum principles so giving the flow conditions at an adjacent section. This procedure is then repeated for the length of the upstream channel in the manner described in (12.1.).

12.2.3. Downstream Channel Analysis

Reference is made throughout to Figure 77 in which the notation is indicated.

The analysis was carried out in exactly the same manner as that used for the upstream channel except that the assumptions made in this case were:-

1. Uniform flow.
2. Flow velocities parallel to the channel bed. A consideration of the surface profiles indicated that with aprons, the downstream channel flow is more closely represented by this assumption than the assumption of horizontal flow velocities.

3. Hydrostatic pressure throughout.

4. Surfaces horizontal across the sections.

5. Frictional losses negligible.

6. Momentum of inflow determined from Equation 27 and 30 in (12.2.1.).

7. Vertical velocity component of inflow negligible. This is justified providing the inflow has not fallen through a large vertical distance in which case downstream interference to the weir discharge does not occur and the downstream analysis does not affect the solution of the weir problem.

The downstream channel analysis is not intended to provide full information regarding the downstream flow but merely to determine the effect, if any, on the flow in the upstream channels.

The specific weight of water has again been neglected and it follows that:-

Forces:

$$F_1 = \frac{w_1 y_1^2}{2} \quad \ldots (45)$$

$$F_2 = \frac{w_2 y_2^2}{2} \quad \ldots (46)$$

$$F_s = \frac{\Delta x}{\cos \alpha} (y_1^2 + (y_2 - y_1).(y_2 - \frac{1}{3}(y_2 - y_1)) \quad \ldots (47)$$

$$G = \frac{\Delta x}{2} (w_1 y_2 + y_1 w_2 + 2(w_2 - w_1)(y_2 - y_1)/3) \quad \ldots (48)$$

Momentum: $$M_1 = \frac{Q_1^2}{gA_1 \cos\phi} \quad \ldots (49)$$

where A_1 = flow area of section 1.

$$M_2 = \frac{Q_2^2}{gA_2 \cos\phi} \quad \ldots (50)$$

where A_2 = flow area of section 2.

$$M_3 = \frac{\Delta Q}{g} (v_u \cos^2\alpha + v' \sin\alpha) \quad \ldots (51)$$

which is determined from the upstream analysis.

Equating forces to the rate of momentum change in a direction parallel to the channel bed, then

$$F_1 \cos\phi - F_2 \cos\phi + G \sin\phi + F_s \sin\alpha \cos\phi = M_2 - M_3 \cos\phi - M_1 \quad \ldots (52)$$

Again this equation can be written in the form

$f(\Delta y) = 0$, Δy being the only unknown quantity. A solution can then be obtained using Newton's method of successive approximation assuming that the flow conditions are known at one section.

12.2.4. Determination of the Control Section in the Upstream Channel

Difficulty was experienced in applying the analysis to labyrinth weirs designed with aprons, due to the occurrence of critical flow conditions in the upstream channels. It was found

however that, unlike the downstream control points, the position of the control section could be readily determined.

Consider Figure 78 with the notation as indicated and with critical flow conditions at section 1.

It can be assumed that the flow in the upstream channels is constant energy flow and so at any section the total head H is given by:-

$$H = z + y + Q^2/2g.w^2.y^2 = \text{constant} \qquad \ldots(53)$$

Differentiating with respect to x, then at any section:-

$$\frac{dH}{dx} = \frac{dz}{dx} + \frac{dy}{dx} + \frac{Q}{gw^2y^2}.\frac{dQ}{dx} - \frac{Q^2}{gw^2y^3}.\frac{dy}{dx} - \frac{Q^2}{gw^3y^2}.\frac{dw}{dx} = 0 \quad \ldots(54)$$

At section 1 - the control section, $Q = \sqrt{g.w^2.y^3}$

substituting in equation 54 and simplifying then:-

$$\frac{dz}{dx} + \frac{dy}{dx}.\left\{1 - \frac{gw^2y^3}{gw^2y^3}\right\} + \frac{1}{\sqrt{gyw^2}}.\frac{dQ}{dx} - \frac{y}{w}.\frac{dw}{dx} = 0$$

$$\therefore \text{ as } \frac{dy}{dx} \neq \infty \text{ then } \frac{dz}{dx} + \frac{1}{w\sqrt{gy}}.\frac{dQ}{dx} - \frac{y}{w}.\frac{dw}{dx} = 0 \qquad \ldots(55)$$

Assuming that the rate of outflow at any section can be determined from the head at that section used in conjunction with standard weir formulae then:-

$\frac{dQ}{dx} = +\frac{2}{\cos\alpha}.\frac{2}{3}.\sqrt{2g}.c.h^{3/2}$ where c is the weir coefficient and flow occurs over both sides of the channel.

Also:- (from geometrical considerations)

$$\frac{dz}{dx} = -\tan\phi \qquad \text{and} \qquad \frac{dw}{dx} = +2\tan\alpha$$

Therefore substituting in equation 55 and simplifying

$$-w.\tan\phi + \frac{4\sqrt{2}\ c.h^{3/2}}{3\sqrt{y}\ .\cos\alpha} - 2y.\tan\alpha = 0 \qquad \ldots(56)$$

$$\therefore \quad 3\sqrt{y}\ .\cos\alpha.(2y.\tan\alpha + w.\tan\phi) = 4\sqrt{2}\ .c.h^{3/2} \ldots(57)$$

But $y = h + d = h + p(1-r) + x.\tan\phi$

and $w = w_o + 2x.\tan\alpha$ where $w = w_o$ when $x = 0$

Thus equation 57 can be written in terms of only the two unknown variables x and h and so by defining h the position of the control section can be determined and this section then used as the starting point for the upstream analysis.

12.2.5. Allowance for Nappe Interference

Experimental results obtained by Gentilini, and Tison and Fransen (Chapter 1) indicated that when the w/p ratio is small, the impingement of the nappes from facing side walls can seriously affect the labyrinth weir performance.

In the case of triangular weirs (Figure 49) nappe interference is relatively simple as only side flow exists and it was considered that this could be represented in the mathematical model in the following manner.

It was shown by the experimental tests described in Chapter 8, (8.4) that nappe interference reduces the weir coefficient by a factor f

where $f = e^{a\ (h/x - b)^n}$

and $a = -0.572$, $b = 0.923$, $n = 0.78$. x was the distance between the crest and the board used to simulate interference.

Thus at any section in the triangular labyrinth weir (Figure 49) allowance can be made by modifying the weir coefficient at that section to c'

where $c' = c.f. = c.e^{a\ (2h/w - b)^n}$ ... (58)

c being the normal weir coefficient.

Under limiting conditions where nappe interference prevents all side flow, then the performance of the labyrinth weir approaches that of the normal linear weir i.e. the flow magnification approaches unity. It was necessary therefore to modify Equation 58 to:-

$$c' = c.(\not{x} \sin\alpha. + e^{a(2h/w - b)^n}) \quad \ldots (59)$$

Flow restrictions produced by nappe interference, and by drowning, are not additive and so it was assumed that the discharge over a section of crest was determined either by the nappe interference or by the drowning conditions, whichever effect produced the greatest restriction.

Nappe interference in the case of trapezoidal or rectangular plan form weirs is extremely complex, due to interference between the flow over the upstream tips and that issuing from the side walls. It was considered beyond the scope of the investigation to make an allowance for nappe interference in these cases.

Because allowance for nappe interference could only be made for triangular weirs, and because these effects would most probably be avoided in practice(by the use of large w/p ratios) the modifications to the analysis described above are not incorporated into the mathematical model for general use.

12.3 Development of the Analysis

Due to the complexity of the labyrinth weir flow and the large number of approximations and assumptions made in the analysis it was expected that empirical coefficients would have to be included in the mathematical model in order to obtain accurate results.

The mathematical model was translated into a computer programme with the addition of a number of coefficients to enable determination of the validity of the assumptions made in the analysis.

The empirical coefficients, or k factors, were situated in the programme so that alteration of their value directly modified the assumptions made in the analysis. For instance, the

assumed flow through section O (Figure 74) was multiplied by factor k_1. Hence the effect on the solution of an inaccurate flow assumption could be assessed by adjustment of k_1.

The values of all the k factors were read into the programme together with the weir data.

It was intended, in the first instance to represent only free flow labyrinth weir behaviour with no interference from the downstream sides of the weir.

12.3.1. Free Flow (Ventilated) Performance

Results were obtained without the use of any empirical coefficients and with the assumption of zero energy losses (Figures 79 and 80). Large discrepancies between the experimental and theoretical performance curves can be seen in the figures although the general forms of the curves are similar.

In order to obtain a solution the flow at section O (Figure 74) had been assumed. To check the validity of this assumption, the flow at this point was multiplied by a coefficient k_1. Results were obtained with k_1 set equal to 1.5 as it was considered that the higher velocity head experienced in labyrinth weirs could lead to a greater flow over the weir tips than that predicted by the use of standard weir formulae.

Figures 79 and 80 indicate that the effect of k_1 on the weir performance is most significant at low flows and it can be seen to increase the discrepancy between the theoretical and experimental results.

Standard weir coefficients and formulae were used to determine the side flow at the various sections of the weir. The Rehbock formula was used in the analysis and coefficients k_2 and k_3 were included in the coefficient in the following manner:-

$$\text{weir coefficient} = (0.605 + 0.08\, k_2\, h/p + 1/(320\, h-3))\, k_3 \quad \ldots (60)$$

The term 0.08 h/p represents the effect of approach velocity which in the case of side weir flow is smaller than normal. The inclusion of k_2 allowed variation of this term and the results obtained for $k_2 = 0$ are shown in Figures 79 and 80.

Other workers on side weir flow had concluded that the weir coefficient was reduced by 10% by virtue of the side flow (see Chapter 10). The coefficient k_3 was included to represent this and theoretical curves for $k_3 = 0.9$ are shown.

The results indicate that the effect of k_2 in the analysis is negligible whereas k_3, in a similar manner to k_1, has a greater effect on the low flow behaviour of the weirs and

consequently increases the deviation of the theoretical curves from the experimental results.

Two coefficients were used to determine the contraction energy loss at the upstream sections of the weir.

In the first case an energy loss proportional to the velocity head at section 3 (Figure 74) and in the second the energy loss was assumed proportional to the square of the change in velocity at the contraction, i.e.

Case 1. Energy loss = $k_4 \cdot v_3^2/2g$ ... (61)

Case 2. Energy loss = $k_5 \cdot (v_3 - v_4)^2/2g$ ... (62)

In fact case 1 normally applies to fluid contractions and case 2 to fluid expansions.

The effects produced by variation of the energy loss coefficients are also shown in Figures 79 and 80 and it can be seen that both coefficientshad the desired effect of reducing the discrepancy between the experimental and theoretical results. Furthermore it seemed likely that these coefficients were the only ones necessary to be included to enable development of the programme to the required degree of accuracy.

Two coefficients, k_6 and k_7, were used to modify the velocity head term in the Rehbock formula in the same manner as k_2.

Coefficient k_6 was used for the determination of the flow through section O (Figure 74) and k_7 for the determination of the upstream tip flow, q.

Both coefficients had a negligible effect on the analysis and the theoretical results obtained have not been shown in the figures.

A further refinement to the analysis was an attempt to make an allowance for the velocity head in the determination of the upstream tip flow q. An effective head was defined such that the total head of a normal weir, operating under this effective head, was equal to the total head on the labyrinth weir. The upstream tip flow, q, was then determined from standard weir formulae using the effective head, as defined.

Again the effect on the analysis was negligible and the theoretical results obtained are not shown.

It was concluded that the energy loss coefficients had the most significant effect on the solutions obtained from the programme, and that these were the only ones necessary to be included in the analysis in order to achieve a representative theoretical solution for the ventilated behaviour of labyrinth weirs.

12.3.2. Evaluation of the Energy Loss Coefficient, k_4

From the one cycle model tests described in Chapter 8, (8.2.), approximate performance curves were constructed to represent the fully ventilated behaviour of triangular plan form

models - these curves, which cover the full flow range, are shown in Figure 47 together with theoretical curves for comparison.

As the energy loss occurs at a contraction only the coefficient k_4 has been used and Figure 47 indicates the close agreement obtained between the theoretical and experimental results for $k_4 = 0.2$.

i.e. contraction energy loss = $0.2\ v_3^2/2g$.

The theoretical performance curves in Figure 81 were drawn to allow comparison with the full width model test results of the trapezoidal weirs. Close agreement occurs for small h/p values where ventilated conditions existed in the experimental tests. As expected the theoretical and experimental results diverge after the onset of downstream interference.

It was concluded that the mathematical model accurately represented the fully ventilated behaviour of labyrinth weirs with the inclusion of only the one empirical coefficient, k_4, where $k_4 = 0.2$ i.e. the energy loss at contraction = $0.2\ v_3^2/2g$. The value of the coefficient is higher than the value 0.1 determined by Formica (Reference 31) in an experimental study of open channel contractions and expansions. However, the energy loss coefficient determined by Formica was for normal open channel flow and therefore might not be applicable to the flow contractions in labyrinth weirs. Also the coefficient, k_4, probably contains

some correction for the various approximations and assumptions made in the analysis.

12.3.3. Interference Flow

Only two empirical coefficients were introduced into the analysis of the offtake channels.

Coefficient k_9 was used to determine the sudden expansion energy loss at the offtake channel exit sections and k_{10} was used in the determination of the momentum of the inflow as described in this Chapter (12.2.1.).

The experimental results indicated that the weir performance is independent of the downstream flow depth and for this reason (see also Chapter 14) the energy loss coefficient was of small significance to the analysis.

From the head on the weir, coefficient k_{10} determined the vertical height of the nappe above the crest, at the crest section, see (12.2.1.). The value of 0.855 obtained from the results of the work by Hay and Markland (Reference 30) was used and accurate theoretical results were obtained.

CHAPTER 13

THEORETICAL RESULTS.

The results described below, with the exception of those obtained for nappe interference, were all obtained from the same computer programme using the same empirical coefficients (see Appendix).

In fact, apart from the use in the side flow of accepted normal linear weir coefficients and results, only one empirical coefficient has been used. The value of this coefficient, k_4, has been taken as 0.2 throughout and determines the energy loss at the flow contraction on entry to the upstream channels of the weirs.

13.1 Basic Performance Results

For the general labyrinth weir model tests described in Chapter 7, the theoretical results obtained from the programme are shown in Figures 82-87 inclusive.

Two sets of theoretical results are shown for each model, one corresponding to the free flow or fully ventilated weir behaviour and the other to the behaviour involving localised interference from the offtake channels (interference flow). Thus for each model the maximum and minimum theoretical limits of

performance are shown, corresponding to the practical situations in which the differences between the bed elevations upstream and downstream of the weir are infinite and zero, respectively.

The experimental performance curves were all obtained with equal upstream and downstream bed elevations and therefore correspond to the minimum theoretical performance results.

The theoretical results compare very favourably with the experimental curves for all the triangular and trapezoidal models except that no allowance could be made in the analysis for the increase in performance which occurred due to the loss of ventilation at the onset of downstream interference. Although the theoretical results do not therefore display the 'humped' discontinuities present in the experimental performance curves, nevertheless the point at which downstream interference first occurs is clearly defined by the divergence of the free flow and interference flow results. In every case the point of divergence of the two sets of theoretical results corresponds to the onset of interference in the experimental tests (shown by the discontinuities).

As the programme had been developed to represent the free flow weir behaviour it was concluded that the mathematical model accurately predicted the performance of triangular and trapezoidal weirs operating under both fully ventilated and interference flow conditions.

The loss of performance due to choking of the offtake channels, as indicated by the analysis, was not considered sufficiently large to warrant experimental investigation into the behaviour of weirs constructed with a change of bed elevation between the upstream and downstream sides of the weir.

The agreement between the theoretical and experimental results was not quite as good for the rectangular models (Figure 87), although the theoretical results display the same peculiarity of rectangular weir behaviour as that shown in the experimental tests i.e. the performance curves for different length magnification factors merge into a common curve with increase in the head to crest height ratios, h/p. The explanation of this mode of behaviour lies in the nature of the surface profiles.

For the free flow behaviour of rectangular weirs the upstream surface profile falls sharply towards the upstream sections of the weir (see Figures 67-69) so that the flow over the side walls in these regions is small. Due to this, and coupled with a high degree of downstream interference, the upstream sections of the crest are largely ineffective under high flowrates. Consequently increasing the length magnification of rectangular weirs merely increases the length of the ineffective crest section with no corresponding increase in performance. The mode of operation is clearly shown in Photograph 11.

It can be shown that in fluid expansions, the uniformity of the flow decreases with increase in the rate of expansion. In labyrinth weirs the greatest rate of expansion occurs in the rectangular designs. It was considered therefore that the lesser accuracy of the analysis when applied to rectangular weirs was due to non uniformity of the flow - previously demonstrated in the side weir tests described in Chapter 9 (9.5.2). The accuracy of the theoretical results is however satisfactory especially as the rectangular plan form would not be used in practice because of its very low effectiveness compared with triangular or trapezoidal designs.

13.2. Weirs with Aprons

The theoretical results corresponding to the apron tests described in Chapter 8 (8.5.) are shown in Figures 88-93 inclusive.

Again the theoretical results compare very well with the experimental curves although some difficulty was experienced in the analysis due to the occurrence of critical flow conditions in both the upstream and downstream channels.

At or near critical flow conditions the surface gradients predicted by the analysis became very large and induced large errors in the solution due to the finite difference procedure used. The problem was overcome by setting the flow depth just slightly

greater than the critical depth at the sections where critical or supercritical flow occurred. When aprons are present in the design the position of the control section is readily defined (see Chapter 12, (12.2.4.)) and so when the marching procedure reached this point the analysis became stable and the calculation proceeded for the remaining subcritical regions of the flow.

A similar procedure has been adopted for the analysis of the offtake channels. Although strictly incorrect the accuracy of the results obtained justified the methods used.

Critical conditions arose because the height of the aprons effectively reduced the crest height so that certain sections of the weir were operating under head to crest height ratios as high as 3. It is unlikely that weirs would be designed in practice to operate under conditions such as this.

The maximum discrepancy between the theoretical and experimental results is less than 5% and surprisingly this occurs in the low flow regions of the weir with the smallest length magnification factor (Figures 92, 93). It would seem however that some slight inaccuracy was present in the experimental results obtained in this region as the aprons appeared to improve the performance compared with the normal design.

It was concluded that the programme could be used to accurately predict the performance of weir designs incorporating aprons.

13.3. Semi-Circular Crest Sections

The crest coefficient appears in the computer programme as a real function (see appendix) and so only one line of the programme needs modification to allow theoretical results to be obtained for any crest design. This presupposes that Villemontes' equation for the calculation of submerged weir performance can be applied to any crest section.

It has been shown by the experimental tests on a normal semi-circular crested weir (8.6.1.) that the semi-circular crest coefficient can be obtained by multiplying the sharp crested weir coefficient by a correction factor cf where cf = (1.29 - 0.028 h) i.e. cf = (1.29 - 0.336 h) where h is the head on the weir measured in feet.

Thus the weir coefficient in the computer programme was modified accordingly and the theoretical results obtained are shown in Figure 94.

The close agreement between the theoretical and experimental results clearly shows that the analysis can be applied to weirs constructed with any crest section.

The ability of the analysis to predict the performance of labyrinth weirs, irrespective of the type of crest used, is of major importance as it has previously been concluded that the experimental results could only be used forthe design of weirs

in which the crest coefficient differs little from that of the sharp crest.

13.4. Submerged Weir Performance

Theoretical performance results corresponding to all the experimental drowning tests are shown in Figures 26-37 and 40-43 inclusive.

It was hoped to obtain a better agreement between the results than that shown although the maximum discrepancy can be seen to be in general not greater than 10%.

The diversity of the results does not allow any definite conclusions to be drawn but nevertheless the analytical results follow the same general pattern as the experimental curves.

Not too much significance is attached to the discrepancies between the results at low flows as it was considered that Villemontes equation (Equation 5) was inaccurate for values of h_d/h approaching 1 (see Chapter 6 (6.3.)).

The higher discrepancies for triangular weirs (Figures 40-43) is thought to be due to the thickness of the crest section which has been taken as zero in the analysis. The crest wall thickness reduces the width and hence the depth in the offtake channels (for subcritical flow conditions) with a consequent increase in performance. The effect of this is greatly reduced

in trapezoidal weirs due to the larger surface gradients of the downstream flow which tend to destroy the advantages gained (see Chapter 14).

An attempt was made to allow for the crest thickness in the computer programme, particularly for the triangular weir designs but although some success was achieved, in that the discrepancy between the theoretical and experimental results was reduced, the programme generally failed to converge to a solution due to instability introduced in the sections where the downstream channel width became very small.

In view of the limitations regarding the accuracy of performance formulae for normal weirs operating under drowned conditions, and also because the behaviour of labyrinth weirs under such conditions is of secondary importance, then the accuracy of the programme in predicting the submerged performance of labyrinth weirs is considered to be satisfactory. Further if the programme is used to predict the drowned performance of weirs then the results obtained would tend to underestimate the actual performance of the weir, thus ensuring the capability of the design in meeting the design requirements.

13.5 Surface Profiles

The computer programme can also be used to determine the surface profiles of the flow in the upstream channels of the weirs.

Theoretical surface profiles are shown in Figures 64, 65 and 66 for a triangular weir, a trapezoidal weir, and a trapezoidal weir with aprons, respectively.

No allowance has been made in the analysis for draw down (non uniform velocity) and consequently the theoretical and experimental surface profiles diverge at the downstream tips of the channels. It should also be noted that as previously indicated (Chapter 12) the programme could not predict the performance for a definite head upstream of the weir but instead provides a range of solutions from which performance curves can be drawn. Consequently the theoretical profiles do not correspond to the same flow conditions as the experimental surface profiles.

The flow in the weir with aprons is contracted as shown by the falling surface profiles whereas the flow velocities in the triangular model are constant (horizontal surface profile) and in the trapezoidal weir the flow is expanded (rising surface profile). Thus due to the non uniformity of the flow encountered in fluid expansions it was expected that the closest agreement between the theoretical and experimental surface profiles would occur for the model constructed with aprons. This is in fact seen to be the case (Figure 66) although it should be noted that the high flow experimental curves, displaying waves, were obtained with downstream interference and these are not therefore comparable

with the theoretical profiles which were all obtained for fully ventilated flow conditions.

The vertical scale in the figures is greatly magnified while the horizontal scale is reduced as indicated, and it can be seen therefore that the programme gives a good indication of the upstream surface profiles present in the performance of labyrinth weirs.

13.6. Nappe Interference

The loss of performance resulting from variation of the vertical scale ratio, w/p, can be explained in terms of interference to the flow caused by the impingement of the nappes issuing from opposite side walls of the weir, (see Chapter 14). No allowance was made for this effect in the programme used to obtain the results in the preceeding sections of this chapter and variation of the w/p ratio in this programme had no effect on the theoretical results obtained.

The simulated nappe interference tests described in Chapter 8, (8.4.), enabled modification of the programme to allow for nappe interference in the case of the triangular weir design as indicated in Chapter 12 (12.2.5.).

Theoretical results have been obtained for all the triangular plan form weirs tested and these are shown in Figures 95 and 96. While the theoretical results are in close agreement with the experimental results in ventilated regions of the performance curves a discrepancy can be seen when interference from the offtake channels occurs. Thus for the high w/p ratio designs (Figure 95) the accuracy of the performance predicted by the analysis appears less than that previously obtained with the unmodified computer programme (Figures 82 and 83).

It had been observed in the experimental tests (Chapter 8 (8.3.1)) however, that the increase in performance resulting from the loss of ventilation at the onset of downstream interference was maintained for h/p values far in excess of those expected. Repeat tests on the models concerned, confirmed the experimental results and it was concluded that the downstream interference was beneficial in the performance of these particular triangular designs. This conclusion is supported by the results of the drowning tests on triangular weirs (Figures 40-43) which show that these designs are far less seriously affected by drowning than are normal weirs. It was concluded therefore that the discrepancy between the theoretical and experimental results in the interference flow regions is due to an increase in the experimentally determined performance as a result of loss of ventilation of the nappe.

More significant in evaluating the representativeness of the modified computer programme are the results shown in Figure 54 which indicates the theoretical and experimental changes in performance due to variation of the w/p ratio. The close agreement that can be seen between the results, clearly demonstrates the validity of the methods used to represent nappe interference in the mathematical model.

As a further check on the analysis, theoretical results were obtained corresponding to Gentilini's experimental work involving very small w/p ratios and these are shown in Figures 97 and 98. Figure 98 indicates the performance curves plotted in the normal manner for various w/p ratios whereas in Figure 97 the results have been plotted against h/w instead of h/p. It can be seen from Figure 97 that when w/p becomes small the flow magnification becomes a function of h/w and not h/p as in the case of high w/p ratios.

A discrepancy of the order of 15% can be seen between the theoretical results and the experimental results obtained by Gentilini (Figure 97), For small w/p ratios the head over the crest is very large in comparison with the size of the weir cycles and consequently draw down must seriously affect the experimental results obtained. In view of the highly complex nature of the flow resulting from the very small w/p ratios used in Gentilini's

tests the accuracy of the theoretical results is as high as can be expected.

Although a general analysis, including an allowance for nappe interference, could not be developed for all designs of weirs, the effect of nappe interference and its relation to the w/p ratio has been adequately demonstrated and sufficient results have been obtained to enable design recommendations to be made, such that the loss of performance due to this factor is negligible.

SECTION III

DISCUSSION, CONCLUSIONS AND DESIGN RECOMMENDATIONS

CHAPTER 14

GENERAL DISCUSSION OF LABYRINTH WEIR BEHAVIOUR

The flow over any weir is primarily determined by the piezometric head under which the weir is operating, consequently as the head on the labyrinth weir varies from section to section it follows that for optimum performance the head at all sections of the labyrinth weir should be as large as possible. This condition can only be achieved with minimum flow velocities, i.e. when the velocity head is a minimum.

Considering the special case of the parallel sided or rectangular plan form weir then surface profiles similar to those shown in Figures 67 - 69 occur in the upstream channels. As water flows over the side walls of the weir, the flow remaining in the upstream channel decreases and consequently undergoes an effective expansion. For the subcritical flow conditions encountered in labyrinth weirs, this expansion leads to a rising surface profile. Increased flowrates result in steeper profiles so that large proportions of the crest operate under a head greatly reduced from that available. This, together with a reduced head due to nonuniform velocities, results in the very low effectiveness of rectangular plan form weirs.

Reduction of the degree of inlet contraction would greatly benefit the performance of these designs for two reasons:-

1. Flow velocities would be reduced which would increase the operating head on the weir for the same total head.
2. Contraction energy losses would be reduced, again increasing the operating head on the weir for the same total head.

If the case of the triangular weir is now considered then the contraction at the entry section is a minimum, energy losses are also a minimum and the maximum operating head occurs at the entry sections to the upstream channels. Furthermore, if the weir behaves ideally along the whole of the crest length then the rate of overflow corresponds exactly to the rate of channel contraction and the flow velocity therefore remains constant throughout the upstream sections of the weir. Under the conditions described a horizontal surface profile exists along the length of the upstream channel. Thus the absence of a decrease in operating head in the triangular designs results in a considerably higher performance than that obtained with the rectangular plan forms.

Further increase in performance could ideally be obtained by increasing the length of the downstream tips of

the triangular plan form weirs. This would result in expansion of the flow and hence a greater head over the weir in the downstream sections of the approach channels. However, the gain in performance achieved would be offset by increased downstream interference to the flow and the overall performance would be less than that obtained with the triangular weir.

An interesting point, concerning trapezoidal and rectangular designs in particular, is that due to the nature of the surface profiles the performance is not so dependent on the crest coefficient of the side weir as would be expected. If a crest with a small coefficient were used then although the outflow over certain sections of the weir would be reduced (when compared with a weir with a high crest coefficient), a more horizontal surface profile would result in the remaining weir sections operating under an increased head. The net effect would be a decrease in flow but much smaller than anticipated. This explains the results obtained during development of the analysis in that variation of the side weir coefficient and also the assumed flow at section O (Figure 74) had little effect on the weir performance at high flows (Chapter 12 (12.3.1)).

The above discussion also explains the non applicability of the experimental results to weirs constructed with different crest sections. Note also that when different crest sections are used

the change in flow results in a different contraction energy loss due to the change in flow velocity. Consequently the experimental results for triangular weir designs are not applicable to different crest sections, even though the surface profiles are horizontal.

In a similar manner and as previously indicated in Chapter 13 (13.1) the large surface gradients encountered in the rectangular weirs result in largely ineffective lengths of crest immediately following the upstream channel entry sections. Thus for high flowrates no increase in performance is obtained by increasing the length magnification of the weir as this merely increases the length of the ineffective crest.

The magnitude of the surface gradients in the offtake channels is dependent on the difference between the inflow velocity and the velocity of the flow in the offtake channels.

In the downstream channels of triangular plan form weirs the rate of inflow and the rate of change of channel width are equal. Unlike the upstream channels however, the surface profile cannot be horizontal as a surface gradient must exist in order to accelerate the inflow up to the main downstream velocity.

For the designs considered it can be assumed that critical or near critical flow conditions exist at the exit sections of

the offtake channels (Section 6 i.e. Figure 74) and therefore for a minimum depth at this point the flow per unit width should also be a minimum. To satisfy this condition the width of the exit section should be a maximum and it follows that from consideration of the downstream flow also, triangular plan form weirs should give the optimum performance.

Note that, due to the nature of the downstream surface profiles the performance of the weir predicted by the analysis is not seriously affected, even though the depth at the downstream channel exit section may be incorrectly assumed. If, for the purposes of the analysis, the exit depth were assumed too high, smaller flow velocities would occur at this section and the surface gradients determined by the analysis would be smaller than those which actually occur, so, although greater downstream interference would result this would be very much smaller than anticipated. This explains the experimental results which indicate that variation of the depth downstream of the weir, up to but not exceeding crest height, does not affect the performance of the weir. For the same reasons the energy loss at the sudden expansion on exit from the offtake channels is insignificant in the analysis, and it was not therefore necessary to assume an empirical energy loss coefficient.

The surface gradient in the downstream channels is zero when the inflow velocity is equal to the main velocity downstream and therefore for the idealised triangular plan form weir, the maximum possible depth in the downstream channels must be equal to the depth in the upstream channel. This fact enables the complete elimination of downstream interference if a difference in bed level exists between the upstream and downstream channels. To eliminate the interference it is only necessary that the difference in bed elevation is as large as the maximum head at any section of the weir.

The effect of aprons on the weir performance can also be explained in terms of the surface profiles.

Aprons on the upstream sides of the weir cause contraction of the flow which results in a small operating head on the crest sections in the furthest downstream areas of the approach channels. This is clearly shown by the surface profiles in Figure 66. A loss in performance results from the reduced head.

It would seem that aprons in the offtake channels would reduce the downstream interference compared with the basic weir design by assisting the run off. In fact the increased flow velocities give rise to steeper surface gradients in the downstream channels which together with the reduced depth of the offtake channels results in greater interference to the flow.

The above discussion describes and explains the basic behaviour of labyrinth weirs although there are further factors, not mentioned above, which can seriously affect weir performance.

Initially only trapezoidal and rectangular models were tested and the effect of the w/p ratio on the performance was found to be negligible in the range considered. Subsequent tests on triangular weirs however showed that the w/p ratio can be a significant factor in determining the weir performance. The effect can be explained in terms of nappe interference produced by impingement of the nappes issuing from facing side walls of the weir (Figure 49). In the case of triangular weirs the upstream sections of the weir side walls are in such close proximity that interference between the opposing nappes is unavoidable. Loss of performance due to this effect is independent of the downstream depth which can be relatively small.

The direct reduction of flow over the upstream sections of crest results in the secondary effect that the flow remaining in the upstream channels suffers a contraction and the remaining crest length then operates under a reduced head.

Consider Figure 50 which illustrates the effect of variation of the w/p ratio on the plan forms of the weirs (the crest height is the same for each configuration). Nappe interference has been represented by ineffective regions of crest as shown. This ineffective region will be approximately the same for each weir when operating under the same head.

Clearly as the w/p ratio decreases, the ineffective areas cover a greater proportion of the crest length and furthermore the resulting loss of performance is greater than a linear function of w/p, especially if the secondary effects of flow contraction are considered.

This explains the experimental results obtained by Gentilini for weirs with small w/p ratios for which it has been shown (Chapter 13, (13.6)) that the flow magnification is a function of h/w and not h/p as used in this thesis.

Nappe interference as described above becomes a significant factor in the determination of the behaviour of weirs designed with small w/p ratios and the effect is worse on triangular plan form weirs where the side walls are in such close proximity at the upstream ends of the weirs. For weir design therefore if the value of the w/p ratio is limited to a relatively small value it will be necessary to revert from

the idealised triangular plan form to the trapezoidal plan form. If w/p is very small however the plan form of the weir becomes nothing more than a mere ripple in comparison with the head on the weir in which case zero gain in performance results from the use of the labyrinth design.

CHAPTER 15

THE DESIGN AND USE OF LABYRINTH WEIRS

15.1 Areas of Application

Labyrinth weirs are ideally suited for use in situations where it is necessary to discharge large quantities of water with only a small operating head, or alternatively, where the available site area does not allow the construction of a linear weir of sufficient length to meet the design requirements.

From structural considerations it seems unlikely that straight walled designs would be built for operation under heads greater than $2\frac{1}{2}$ feet. However the labyrinth weir principles will still apply if a modified crest section, such as a Creager profile, is used. In this latter case structural costs will be high and it will be necessary to conduct special model tests on the design in order to determine the performance.

Apart from the head limitation there seems to be no limits to the areas in which labyrinth weir designs can be used. It is envisaged that they can be incorporated as a special crest section surmounting the top of large dam structures and also the same principles can be used in shaft spillways by modification of the rim of the overflow into a "gear wheel" shape. Further

advantages would probably be gained in the latter case as the design would tend to inhibit vortex formation. In either case however the same principles of operation will apply as described in Chapter 14.

15.2 Design Considerations and Recommendations

Both the experimental and theoretical work have clearly shown that the weir performance decreases with increase in the head to crest height ratio. The design of a weir is defined non dimensionally in terms of the crest height and consequently for any design, operating under a given head, the dimensions and parameters of the weir should be in general as large as possible, in order to obtain the greatest performance.

The weir designer must therefore decide on a compromise between the performance of a design and the structural costs involved. Nevertheless there are a number of recommendations which can be made and which should greatly simplify the design of labyrinth weirs.

15.2.1 The Length Magnification Factor, l/w

If the available site area is small the length magnification will be dictated by the required discharge characteristics of the weir. There are situations however where the labyrinth

plan form would be chosen from economic rather than performance considerations.

A good example of this is the weir at Skelton Grange (Photographs 1 and 2) which because of the small head (3") behaves almost ideally. The weir is constructed on the side of a canal and it can be easily appreciated that the cost of a structure such as that shown is far smaller than that of a linear weir of equivalent discharge capacity. As in this case, where the labyrinth form is chosen purely from economic considerations there is scope for variation of the length magnification of the design.

Although increase in the length magnification factor increases the discharge capacity of the weirs it has been shown that the effectiveness of the designs decreases i.e. the gain in performance resulting from an increase in the length magnification decreases as the length magnification increases. Thus, the gain in performance achieved by the use of a higher length magnification might not justify the extra structural costs involved.

The investigation has shown that for the range of h/p considered (0 - 0.5) weirs can be designed up to length magnification of 4 with relatively high flow magnifications. The use

of higher length magnifications than 4 in the design should be justified economically unless the operating range of h/p is small ($h/p < 0.15$). Certainly if the weir is designed to operate under a head to crest height ratio greater than 0.25 then l/w ratios greater than 6 should not be considered.

Therefore where there is scope for variation of the l/w ratio then a compromise must again be reached with due regard to the economics of the problem.

15.2.2 The vertical Aspect Ratio, w/p

The effect of this factor on the weir behaviour has been described in Chapter 14. It has been shown that if the w/p ratio is small a significant loss of performance results from nappe interference. This loss of performance can be effectively eliminated however if the w/p ratio is greater than 2.

The vertical aspect ratio defines the size of the weir cycles in plan relative to the height of the crest and unfortunately increasing the w/p ratio increases the weir area and therefore the costs of the structure. Nevertheless it is recommended that unless the weir is to operate under a small head to crest height ratio then w/p ratios less than 2 should not be used and ideally the value of w/p should be

equal to or greater than 3. Providing the w/p ratio is greater than 3 this factor has little significance in determining the performance of the weirs.

It can be seen that the experimental and theoretical results do not allow interpolation to determine the performance of weirs with small vertical aspect ratios. This is because it was considered that the advantages of the use of such designs would be extremely limited and they would be restricted to operating conditions involving only very small head to crest height ratios.

Where the weir is designed for operation under very small head to crest height ratios a better parameter than w/p for determining the size of the weir cycles, is the ratio of the head to the cycle width, h/w.

In the range of h/p considered it has been shown that for w/p ratios greater than 2 then nappe interference is of small importance. It follows that satisfactory performance can be obtained from weirs with small w/p ratios provided that the range of operation does not exceed an h/w value of 0.25. The performance of a weir designed within this limit, and with a small w/p ratio, can be assessed from the performance curves for weirs with high w/p ratios in the following manner:-

Consider a weir designed with a small w/p ratio. Then without altering the plan form of the weir the channel bed could be raised to produce a w/p ratio of 2, for which the performance can be obtained from the experimental performance curves or the theoretical analysis using head to crest height ratios determined from the modified crest height. The performance obtained in this manner, will be slightly less than that obtained in the actual weir but nevertheless the errors will be small especially if the weir length magnification is not greater than 4.

15.2.3 The Side Wall Angle α.

For a given length magnification the side wall angle can be varied between 0 and the maximum value ($\alpha_{max.}$) associated with a triangular plan form.

This factor has been found to be of primary importance in determining the weir performance particularly for high length magnifications. Indeed variation of the side wall angle can have a greater effect on the weir performance even than the length magnification factor.

The results clearly show that for w/p ratios greater than 3, the side wall angle should be as large as possible for optimum performance i.e. triangular plan forms should be used

in this region.

For smaller w/p ratios nappe interference becomes a significant factor and the loss of performance resulting from this effect is increased by the use of large side wall angles due to the close proximity of the side walls in the upstream regions of the weir. It is therefore recommended that for weirs designed with w/p ratios less than 3 and operating up to h/p values of 0.5, the side wall angle, α, should be 0.75 of the maximum value.

15.2.4 Change in Channel Bed Elevation d

The drop in elevation between the channel beds upstream and downstream of the weirs determines the degree of interference to the flow produced by choking of the offtake channels. If the weirs are designed in accordance with the other recommendations contained here, then downstream interference will be of secondary importance except for the high flow performance of weirs with large length magnifications.

To reduce downstream interference the bed elevation drop, d, should be large although complete elimination will be achieved for the performance ranges considered, if d is equal to or greater than the maximum operating head.

15.2.5 Aprons

Aprons have been considered as modifications to the basic designs by "filling up" the approach and offtake channels.

Both upstream and downstream aprons have serious effects on the weir performance and consequently from performance considerations they should be as small as possible especially for weirs of high length magnification.

Where a drop in elevation of the channel bed occurs on the downstream side of the weir however, the size of the downstream aprons are not important providing the depth at all points of the offtake channels is greater than the depth of flow in the upstream channels. In this case downstream interference will be negligible.

15.2.6 Crest Sections

The increase in discharge obtained by the use of a crest section with a high weir coefficient has been found to be greatest for small flows. Under high flow conditions the crest coefficient becomes of secondary importance in determining the weir discharge.

The crest section adopted for a design is dependent therefore on the choice of the design, but it is important to note that if the coefficient of the crest used differs widely

from that of the sharp crest used in the experimental work then the weir performance cannot be determined from the experimental performance curves.

The performance in this case can however be determined either from the computer programme included in the appendix or from the performance curves in Figures 99 - 110.

15.2.7 Submergence

Because labyrinth weirs operate under a smaller upstream head than the normal linear weir discharging the same quantity of water, then in a situation which normally involves submerged flow conditions the use of the labyrinth design increases the degree of submergence. Thus although labyrinth weirs have been found to be, if anything, less seriously affected by submergence than linear weirs when operating under the same upstream and downstream heads, care must be taken in their design for operation under submerged conditions.

It is not recommended that labyrinth weirs be used in situations where they would normally operate under drowned flow conditions.

If it is necessary to use a labyrinth weir however, the drowned performance can be estimated either from the experimental results or by the use of the computer programme given in the

appendix in the manner described in Chapter 13 (13.4).

15.3 Design Charts

The close correlation between the theoretical analysis and the experimental results enabled a series of performance curves to be constructed for labyrinth weirs designed in accordance with the recommendations contained in this thesis. These curves are displayed in Figures 99 - 110 and cover the following ranges of the weir parameters and conditions:-

(a) $3 \leqslant$ length magnification $(l/w) \leqslant 8$.

(b) side wall angle, $\alpha = 0.75\ \alpha_{max.}$ (trapezoidal plan form)
or $= \alpha_{max.}$ (triangular plan form)

(c) vertical aspect ratio, $w/p \geqslant 2$ (trapezoidal plan forms)
or $\geqslant 2.5$ (triangular plan forms)

(d) $0 <$ head to crest height ratio, $h/p \leqslant 0.5$

(e) bed elevation change, $d = 0$ or ∞
i.e. performance for maximum or minimum downstream interference respectively.

(f) ratio of crest coefficient to sharp crest coefficient, f:-
$0.8 \leqslant f \leqslant 1.4$.

(g) aprons not present in the designs.

(h) depth of flow downstream of weir below the crest level.

Thus for labyrinth weirs designed within the above limits, i.e. within the recommended design ranges, the normal performance of the weir can be accurately predicted.

Briefly Figures 99 — 110 will yield by interpolation a series of curves for various length magnification factors corresponding to the coefficient of the chosen crest section and to the degree of downstream interference present. When plotted in composite form these interpolated curves then allow further interpolation to determine the performance of any labyrinth weir with a length magnification less than 8 and constructed with the chosen crest section.

Close study of the curves in Figures 99 - 110 shows however that the performance of a labyrinth weir, A, having a length magnification x_A and crest coefficient c_A is very nearly equivalent to the performance of a labyrinth weir, B, having a length magnification x_B and a crest coefficient c_B providing that:-

$$\frac{x_A}{x_B} = \frac{c_B}{c_A}$$

For example a sharp crested labyrinth weir with a length magnification of 7 is equivalent to a weir having a length magnification of 5 and a crest coefficient 7/5 times greater

than the sharp crest coefficient.

The accuracy of the above statements is within ± 4% for all the performance curves shown in Figures 99 - 110, and it follows that the information contained within the Figures can be condensed into two design charts as shown in Figures 111 and 112. One chart is for trapezoidal plan form weirs where $\alpha = 0.75\ \alpha_{max.}$ and the other for triangular plan forms ($\alpha = \alpha_{max.}$)

The design charts display the performance of sharp crested labyrinth weirs for a wide range of length magnifications and hence the performance of any sharp crested labyrinth weir can be directly interpolated.

The use of the design charts in the design and prediction of the performance of labyrinth weirs constructed with a crest section other than the sharp crest is indicated below.

Note that sharp crests are unlikely to be used in practice because of their tendency to become damaged by floating debris. The adopted crest section will probably have a rounded sill and in general its coefficient will be greater than the sharp crest coefficient (see King, Reference 10). Thus if the labyrinth weir is designed by use of the sharp crest coefficient then it may be assumed that the predicted performance will be less than that obtained in the actual weir and hence a factor of safety will be included in the design.

To design a weir outside the ranges of the design charts, due consideration should be given to the earlier sections of this chapter and the computer programme described in the Appendix may be used if necessary.

15.4 Notes on the Design of Labyrinth Weirs

The following notes indicate the steps taken during the design of a labyrinth weir and illustrate the use of the design charts (Figures 111 and 112).

1. Determine the crest height, p, and the channel width, W, from the site conditions.
2. Define the maximum allowable operating head on the weir, $h_{max.}$, such that flooding does not occur.
3. Define the maximum discharge, $(QL)_{max.}$ to be accommodated by the weir - information obtained from hydrographic surveys etc.
4. Using p and W determine the maximum discharge, $(QR)_{max.}$, that could be obtained from a corresponding sharp crested linear weir operating under the head $h_{max.}$

   i.e. $(QR)_{max.} = (3.22 + 0.40\ h/p).\ W\ .(h_{max.})^{3/2}$ cusecs

   from the fomula proposed by Kindsvater and Carter (Reference 12) where h and W are in feet.

5. From the previous notes the required flow magnification of the labyrinth weir (QL/QR) can be determined which corresponds to $(h/p)_{max.}$

6. Adopt either the triangular or the trapezoidal plan form for the weir design. Maximum performance may be obtained from the triangular plan form if the vertical aspect ratio is greater than 2.5 but designers may reject the triangular plan form from structural considerations due to the use of sharp corners.

7. Adopt the recommended design parameters i.e. vertical aspect ratio, $w/p \geqslant 2$ and no aprons in the design (see Chapter 15 - 15.2.2 and 15.2.5).

8. Determine from the site conditions whether any difference in elevation exists between the channel beds upstream and downstream of the weir. If there is a difference in bed elevation and this exceeds the maximum head on the weir then no downstream interference to the flow will occur due to choking of the offtake channels. Thus the corresponding non interference performance curves in Figures 111 and 112 will be used.

9. Plot the design point, $(h/p, QL/QR)_{max.}$ corresponding to the maximum operating conditions of the weir as determined

in note 5 on the appropriate design chart - depending on whether a trapezoidal or triangular plan form is to be used. Interpolate from the curves to determine the length magnification of a sharp crested labyrinth weir that would meet the requirements of the problem.

10. Choose a crest section for the weir and determine the relation between the crest coefficient and that of the sharp crest for the range of h/p considered.

11. Divide the length magnification of the sharp crested labyrinth weir by the ratio of the actual crest coefficient to the sharp crest coefficient corresponding to $(h/p)_{max}$. The resulting value is the length magnification of the actual labyrinth weir.

12. All the weir design parameters have thus been determined and it is a simple matter to determine the actual dimensions of the design. Note that the number of cycles of the design is W/w, and w/p should be modified such that n = integer or integer + $\frac{1}{2}$.

The following notes indicate the steps taken to determine the performance of the design over the full range of variation of h/p.

13. Select a number of values of h/p in the range $0 < h/p < (h/p)_{max}$.

14. For each value of h/p determine the ratio of the crest coefficient to the sharp crest coefficient, f, and by multiplying the length magnification of the design by each value of f hence determinethe length magnification of an equivalent sharp crested labyrinth weir corresponding to each value of h/p.

15. Determine for each value of h/p the flow magnification of the equivalent sharp crested labyrinth weirs - by interpolation from the design charts (Figures 111 and 112)

16. Multiplying the flow magnification of the equivalent sharp crested labyrinth weirs by the flow over a corresponding sharp crested linear weir then gives the discharge of the actual labyrinth weir design.

17. Dividing the flow magnifications of the equivalent sharp crested labyrinth weirs by the crest coefficient ratio, f, determines the flow magnification obtained by the actual labyrinth weir. design referred to a linear weir of the same crest shape.

15.5 Design Example

The following example has been chosen specifically to represent the calculations that would lead to the semicircular

crested labyrinth weir tested in Chapter 8 (8.6) so that the accuracy of the design method will be readily apparent.

Problem

It is required to construct a weir to discharge a maximum of 900 cusecs under a maximum head of 2 feet.

A study of the site conditions yields the following information:-

(a) The crest height should be 5 feet.

(b) The maximum channel width is 20.2 feet.

(c) No change in bed elevation exists between the channel, upstream and downstream of the weir.

The weir should be designed in accordance with recommendations contained in this thesis, i.e. $w/p \geqslant 2$, no aprons and a trapezoidal form should be adopted.

The weir should be constructed with straight side walls the crest being semicircular in section. The ratio of the semicircular crest coefficient to the sharp crest coefficient is given in Figure 113. (Note that these values should be used only in this example).

From the notes on weir design then:-

(1) $p = 5$ ft.

$W = 20.2$ ft.

(2) $h_{max.} = 2$ ft.

(3) $(QL)_{max}$ = 900 cusecs.

(4) $(QR)_{max}$ = $(3.22 + 0.4\ h/p)\ .\ W.h^{3/2}_{max}$ cusecs.

= $(3.22 + 0.16)\ .\ 20.2.\ (2)^{3/2}$

= 193 cusecs.

(5) Design requirements:-

Flow magnification, QL/QR = 4.66 at a maximum head to crest height ratio, $(h/p)_{max.}$ of 0.4.

(6) Trapezoidal plan form - design chart in Figure 112. applies.

(7) $w/p \geqslant 2$ and no aprons.

(8) No difference in bed elevation so maximum downstream interference occurs therefore use the corresponding curves in the design chart (Figure 112 - trapezoidal weirs)

(9) The design point, (0.4, 4.66) is plotted in Figure 114 which is a reproduction of Figure 112.

Interpolating between the performance curves in this Figure then a sharp crested labyrinth weir having a length magnification of 7.5 meets the design requirements.

(10) The relation between the semi-circular crest coefficient and the sharp crest coefficient is shown in Figure 113. When h/p = 0.4 then the ratio of the coefficients, f, = 1.245.

(11) The required length magnification of the design = 7.5/1.245 = 6.02.

(12) As $w/p \geq 2$ then let $w/p = 2$ and so w, the width of one cycle of weir = 10 ft.

The no of cycles of weir, $n = W/w = 20.2/w = 2.02$.

But require the number of cycles, n , to be an integer or an integer + $\frac{1}{2}$ so adopt n = 2

and hence $w = 10.1$ ft.

and $w/p = 2.05$

As $1/w = 6.02$ and $\alpha = 0.75\ \alpha_{max.}$

$$\alpha = 0.75 \sin^{-1} (1/6.02) = 0.75 \sin^{-1} (0.1662)$$

$$\therefore \quad \alpha = 7.19^{o}$$

Now if the length of the side walls = b ft. and the length of the tips = a, (see Figure 115)

then $2a + 2b = 1$

$$\therefore \quad a + b = 6.02 \times 10.1/2 = 30.45 \text{ ft.}$$

Now $w = 2a + 2b.\sin\alpha$

$$\therefore \quad 10.1 = 2(a + b\ 0.125)$$

$$\therefore \quad 10.1 = 2(30.45 - b + 0.125\ b)$$

$$\therefore \quad b = (30.45 - 5.05)/.875$$

$$= 29 \text{ ft.}$$

and $a = 1.45$ ft.

The schematic shape of the weir is shown in Figure 115.

The following table lists the values of the variables determined according to notes 13 - 17 where :-

h/p = head to crest height ratio

f = ratio of the semi-circular crest coefficient to the sharp crest coefficient.

$(l/w)_{equiv.}$ = length magnification of an equivalent sharp crested labyrinth weir = 6.02 x f.

$(QL/QR)_{equiv.}$ = flow magnification of an equivalent sharp crested labyrinth weir - interpolated from the design charts as in Figure 114.

$(QL/QR)_{corrected}$ = flow magnification of the actual labyrinth weir = $(QL/QR)_{equiv}/f$.

QR = discharge over a corresponding linear weir with a sharp crest (from Kindsvater and Carter's formula)

QR_s = discharge over a corresponding linear weir with a semi-circular crest = QR x f.

QL = discharge over the actual labyrinth weir = $(QL/QR)_{equiv.}$ x QR.

h/p	h	f	$(l/w)_{equiv.}$	$(QL/QR)_{equiv.}$	$(QL/QR)_{actr.}$	QR	QR_s	QL
0.1	0.5	1.12	6.745	6.62	5.91	23.3	26.1	154.2
0.15	0.75	1.225	7.37	6.94	5.66	43.1	52.9	298.5
0.2	1	1.26	7.59	6.65	5.28	66.6	84.0	444
0.3	1.5	1.256	7.55	5.58	4.44	124	156	692
0.4	2	1.245	7.5	4.66	3.745	193	240	900
0.5	2.5	1.226	7.38	3.89	3.175	273	334.5	1062

The performance curve for the actual labyrinth weir is shown in Figure 116 and is compared with the experimental test results obtained from the semi-circular crested model described in Chapter 8, (8.6), with which it can be seen to be in close agreement.

The discharge curve for the actual labyrinth weir is shown in Figure 117 which clearly indicates the increase in discharge which can be obtained by the use of the labyrinth weir plan form.

APPENDIXES

APPENDIX.

A1. The Computer Programme

The computer programme is considered to be an extremely useful aid in the design of labyrinth weirs and is included in this thesis on pages 214-221 together with a flow chart on pages 209-213 to describe the steps taken in the computation.

A1.1 Notes on the Use and Range of Application of the Programme

The programme was designed to be as general as possible although there are certain limitations regarding its area of application.

The effects of the fundamental design ratios, aprons, submergence, crest section, downstream interference and the number of cycles in plan have all been allowed for and without modification the programme will accurately predict the performance of any design of labyrinth weir subject to the conditions and limitations contained in the following notes:-

1. The weir plan form is restricted to a symmetrical trapezoidal shape including however triangular and rectangular plan forms. These plan forms were considered the simplest and most favoured from design considerations.

2. No allowance has been made in the programme for nappe interference because this was considered beyond the scope of the investigation and because the effects due to this factor would generally be avoided in practice. The programme should not be used therefore for weirs with w/p ratios less than 2 unless the operating range of the weir is such that h/w is less than 0.2. In this case the programme can be used with due regard to the recommendations given in Chapter 15 (15.2.2).

For triangular weir designs the programme can be modified to allow for nappe interference in the manner described in Chapter 12 (12.3.3) although this is not recommended.

3. Results can be obtained for any degree of submergence of the weirs although the accuracy of the programme is reduced under drowning conditions (see Chapter 13(13.4)). However it can be assumed that the performance predicted by the programme for these conditions, will be less than that obtained in the actual weir and so the results can be considered to contain a factor of safety.

4. The programme does not allow computation for a range of falls of the channel bed elevation downstream of the weir (d). Nevertheless the weir performance is predicted when this variable is either zero or infinite and as the effect of d is

small the performance can be interpolated with due regard to the considerations in Chapter 14.

5. The programme is particularly useful for predicting the performance of labyrinth weirs where the coefficient of the crest section differs widely from that of the normal sharp crested weir as the experimental performance curves will not apply inthese cases. However, unless the coefficient of the crest used differs by a constant factor from that of the sharp crested weir it is necessary to modify the programme to incorporate the new crest coefficient.

This can be simply done by rewriting the one line of programme (contained at the end of the programme in the real function) which determines the crest coefficient.

A1.2 Programme Input

The constants used to represent empirical coefficients in the development of the programme (see Chapter 12(12.3)) are still present although some have lost their significance during the successive modification of the programme.

It is necessary therefore to include these in the programme input but they allow variation of the computation should this be deemed necessary.

The input data should be read in therefore in the following order and as shown in the computer programme page 221

1. Length magnification factor (1/w)
2. Vertical scale ratio (w/p)
3. Number of cycles (n)
4. Side wall angle in degrees(α)
5. Ratio of the maximum apron height in the upstream channel to the crest height.
6. Ratio of the maximum apron height in the downstream channel to the crest height.
7. The degree of submergence, (h_d/h) = 0 if the weir is not drowned.
8. The width of the weir channel in feet.
9. k_1 - normally 1.
10. k_2 - normally 1. This constant has a new significance to that described in Chapter 12. The crest coefficient is multiplied by this factor.
11. k_3 = 1. This constant is now redundant.
12. k_4 - normally 0.2.
13. k_5 - normally 0.
14. k_6 = 1.. This constant is now redundant.
15. k_7 = 1. This constant is now redundant.

16. k_8 - normally O. If k_8 is set equal to 1 the upstream tip flow is determined from the effective head upstream of the weir.

17. k_9 - normally O.

18. k_{10} - normally 0.855.

19. Programme has returned to read in k_1. If set less than O then programme returns to start and so input data should then be repeated for a new weir configuration. If set greater than 90 then this ends the input. Otherwise set equal to the desired value of $k_1 (> 0)$ and read in new values of the remaining constants for a recomputation with the previously defined weir design.

A1.3 Programme Output

A sample output is shown on page 222. The output headings are self explanatory except that:-

A is the half length of the weir tips in feet.

B is the length of the weir side walls in feet.

RU is the ratio of the maximum upstream apron height to the crest height

R is the ratio of the maximum downstream apron height to the crest height.

Together with the non-dimensional performance results the actual, head, labyrinth weir discharge and the discharge that would be obtained over an alternative linear weir are given in feet and cusecs respectively.

Also the upstream surface profile is given by way of the head over the crest at ten equidistantly spaced sections in the upstream channel starting at section O in Figure 74.

It is important to note that for each operating condition the non interference flow is computed and printed, followed by the flow with allowance made for any interference from the flow in the offtake channels. Thus the results denoted by odd numbers (No) correspond to the free flow weir performance and those denoted by even numbers are the weir performance with downstream interference (if present).

PRINCIPLE SYMBOLS IN COMPUTER PROGRAMME

Section numbers are shown in Figure 74.

Ah, Ahd	- head in upstream and downstream channel respectively.
Avu	- upstream channel velocity.
ADQ	- outflow between sections of u/s channel
a	- half weir tip length
b	- length of weir side walls
c	- crest coefficient
cosa	- cos α
cos p, cos pu	- cosine of angle of slope of aprons in d/s and u/s channels respectively.
Dh	- change in head between sections of u/s channel.
Dx	- distance between sections of channels.
Dy	- change in depth between sections of d/s channel.
du	- depth in u/s channel
Dwd, Dwu, Dpu, Ddu	- change between channel sections in wd, wu, pu, du.
dif (-)	- differential coefficient of (-)
E	- specific energy of flow in u/s channel.
ET	- specific energy of flow u/s of weir.
F1, F2, FS	- forces
FF1, FF2, FFS	- differential coefficients of F1, F2, FS

g	- acceleration due to gravity.
G	- gravitational force.
GG	- differential coefficient of G
h, hd	- head in u/s and d/s channels respectively.
ho	- defined head at section O
ha	- head u/s of weir
he	- effective head u/s of weir
HD	- head d/s of weir
hdo	- d/s head at section O
k1-k10	- constant coefficients read in with data
lo	- length of crest d/s of section O
M	length magnification
M1,M2,M3	- ~~rates of change of~~ momentum flux.
MM1,MM2,MM3	- differential coefficients of M1, M2, M3.
n	- number of weir cycles in plan .
p	- crest height.
pu	- local crest height (due to aprons)
puo	- crest height at section O
Q	- flow through section of u/s channel.
Qd	- flow through section of d/s channel.
QL	- total labyrinth weir flow
QR	- total flow over a corresponding linear weir.

Qo	- flow through section O in u/s channel
Qdo	- flow through section O in d/s channel
q	- flow over u/s tip sections
rtgg	- $\sqrt{2g}$
r, ru	- ratio of maximum apron height to crest height in d/s and u/s channels respectively.
sin a	- $\sin \alpha$
sin p, sin pu	- sine of angles of slope of aprons in d/s and u/s
vu, vd	- flow velocities in u/s and d/s channels.
vuo, vdo	- flow velocities through section O in u/s and d/s channels.
vy	- flow velocity at Section 3.
vt	- flow velocity u/s of weir.
W	- vertical aspect ratio
w, wd	- width of u/s and d/s channel sections respectively.
wo, wdo	- width of u/s and d/s channels at section O.
wm	- width of one cycle of weir
x	- distance of section from section O
y	- depth at section in d/s channel.
YD	- depth of flow d/s of weir
yc	- critical depth

COMPUTER PROGRAM FLOW CHART

Numbers refer to program labels

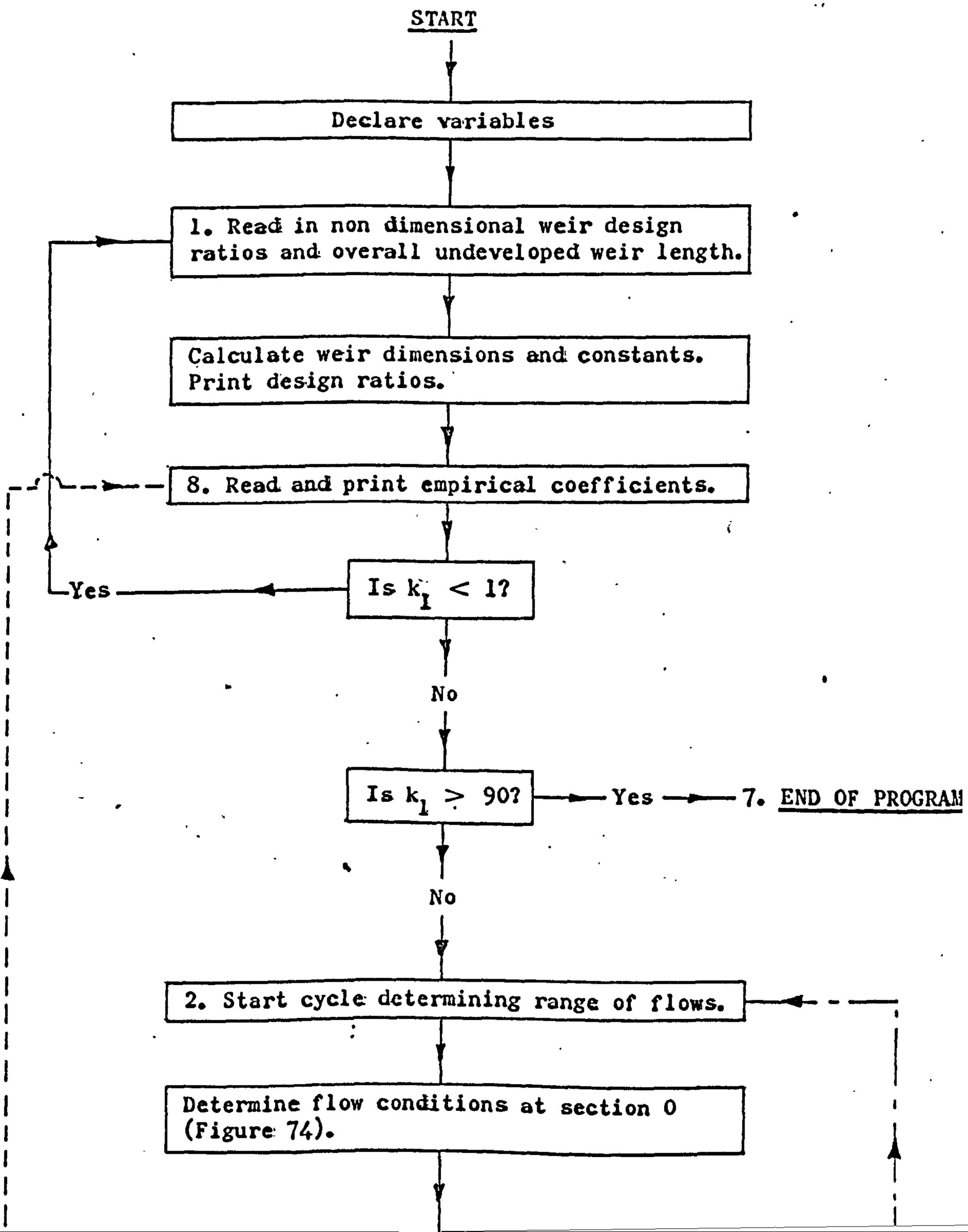

3. Set variables for start of finite difference procedure. Set depth at every section in downstream channel equal to depth downstream of weir.

24. Start cycle for finite difference procedure in upstream channel.

Estimate flow depth at adjacent section.

Calculate closer approximation for depth in adjacent section.

Is flow depth of required accuracy?

No

Yes

23. Is the upstream depth below the crest height.

Yes

No

Is the flow supercritical?

No

Yes

30. Print warning 'C'. Set depth equal to critical depth.

27. Is finite difference procedure complete?

No

Yes

12. Estimate flow conditions upstream of weir. (Effective and actual head).

Is the tip flow to be determined from the actual or effective head?

Effective head $k_8=1$

Actual head $k_8=0$

14. Counter=0

14. Counter=1

15. Counter=counter+1

15. Counter=counter+1

Determine a closer approximation for the effective head.

Set effective head equal to actual head.

Using effective head calculate the upstream tip flow and hence a better approximation for the actual head upstream of the weir.

Is counter=2?

No

Yes

19. Has the head been determined to the required accuracy?

No

Yes

Has allowance been made for downstream interference? — No

Yes

Is the difference in flow determined from the previous cycle small? — No

Yes

31. Print results.

Is $h/p \leq 0.6$ — Yes

No

Were last results for interference flow? — Yes

No

Set total flow equal to average flow determined by the last two cycles of calculation.

11. Calculate the flow conditions at the exit sections of the offtake channels.

21. Calculate the flow conditions at the section in offtake channel corresponding to section 0 in upstream channel. (Figure 74).

20. By finite difference procedure calculate and store the surface profile in the offtake channel.

Does downstream interference occur?

No

Yes

Calculate the flow conditions in the upstream channel at section 0 allowing for downstream interference.

```
***A

JOB
UNUTT.ME/TAYLOR G L/WEIR
EXECUTION 15 MINUTES
OUTPUT 0 LINE-PRINTER 3500 LINES
COMPILER AA



begin
real a,b,c,h,ho,ha,he,ht,Dh,Q,QL,QR,Qo,QT,DQ,F,x,Dx,X,e,E,ET,s,n,p,t,f,q,g,ve,vy,vt,vt2,rtgg,k10,IQ
realM,L,W,w,wo,wm,ang,lo,sina,cosa,tana,cotb,k1,k3,k4,k5,k6,k7,difET,difvt,difdh,difF,cond,hd,Dy,T
real HD,r,tanp,cosp,k9,YD,Qd,vd,difvd,cd,wd,DQo,Dwd,wdo,vdo,Qdo,y,vuo,hdo,yd,d,QZ1,QZ2,T1,T2,T3,T4
real sinp,F1,FF1,F2,FF2,G,GG,FS,FFS,M1,MM1,M2,MM2,M3,MM3,fDy,ffDy,cDy,yc,ru,tanpu,cospu,sinpu,puo
real pu,Dwu,du,vu,Dpu,Ddu,k2
integer i,j,N2,N3,N4,N5,k8,TIME,z,pj
array ADQ(1:100),Avu(1:100),Ahd(1:100),Ah(1:100)
realfnspec coeff(realname h,p)
1:   newlines(5)
caption weir$ratios$ c
..L/W.....W/P....ANGLE...CYCLES.....A.......B........RU.......R........HD/p$
read(M,W,n,ang,ru,r,HD,wm)
g=32.2;rtgg=sqrt(64.4);wm=wm/n
sina=sin(ang*π/180);cosa=cos(ang*π/180);tana=sina/cosa
cotb=cos((45-ang/2)*π/180)/sin((45-ang/2)*π/180)
a=wm*(1-M*sina)/(4*(1-sina));b=wm*(M-1)/(2*(1-sina));p=wm/W
wo=2a*cotb/cosa;lo=2a*(2+cotb*tana);X=b*cosa-a*cotb
tanp=p*r/(X+a*cotb);  cosp=(X+a*cotb)/(sqrt((X+a*cotb)^2+(r*p)^2));   sinp=tanp*cosp
tanpu=p*ru/(X+a*cotb);cospu=(X+a*cotb)/(sqrt((X+a*cotb)^2+(ru*p)^2)); sinpu=tanpu*cospu
puo=p*(1-ru)+(a*cotb*tanpu)
N2=0;N3=0;N3=0;N4=0;f=0;HD=HD*p
print(M,2,1);spaces(3);print(W,2,1);spaces(2);print(ang,3,1);spaces(3)
print(n,2,1);print(a,6,3);print(b,4,3);print(ru,4,3);print(r,4,3);print(HD/p,4,3)
8:read(k1);->1 if k1<1;->7 if k1>90
```

```
caption ##constants#are##k1.....K2.....K3.....K4.....K5.....K6.....K7.....K8.....K9.....K10#
read(k2,k3,k4,k5,k6,k7,k8,k9,k10)
spaces(11);print(k1,3,2);print(k2,3,2);print(k3,3,2);print(k4,3,2)
print(k5,3,2);print(k6,3,2);print(k7,3,2);print(k8,3,2);print(k9,3,2);print(k10,3,3)
caption ##results;spaces(60); caption surface#profiles## c
.NO...H/P.....QL/QR....H.....QR.....QL.....HD/P#


2:   cycle i=1,1,12
i=1+intpt(22HD/p) if i<(22HD/p)
ho=0.05p*i;N2=0;N3=0
pu=puo
c=coeff(ho,pu)
Qo=k1*c*lo*exp(1.5*log(ho))


3:     N2=N2+1;Dx=X/100;h=ho;Q=Qo;w=wo
Dwu=2Dx*tana
DQ=2Dx*c*exp(1.5*log(ho))/cosa
du=h+pu
vu=Q/(w*du)
Dpu=Dx*tanpu
cycle j=1,1,100
Ahd(j)=0.0000001+HD
repeat
N5=0
->24


11:
YD=HD+p
yd=YD
Qd=QL-Qo*2a/lo
10:    vd=Qd*cosp/((wm-2a)*yd)
F=yd-YD-(QL/(wm*YD))^2/(2g)+vd^2*(1-k9)/(2g)
```

```
difvd=-Qd*cosp/((wm-2a)*yd²)
difF=1+2vd*(1-kg)*difvd/(2g)
cd=-F/difF
yd=yd+cd
->10ifmod(cd)>0.0001
wd=wm-2a
yc=exp((log((Qd/wd)²/g))/3)
yd=ycifyd<yc
Dy= -0.1yd
DQo=Qo*(lo-2a)/lo
Dwd=2a*cotb*tana
c=coeff(ho,p)
T=1.105c*sina*sqrt(ho)/k10
vuo=(2Qo/((ho+p)*(4a+Dwd)))*cosa²+T

21:
F1=(wd-Dwd)*(yd-Dy)²*cosp/2
FF1= -(wd-Dwd)*(yd-Dy)*cosp
F2=wd*yd²*cosp/2
FF2=0
G=((wd-Dwd)*(yd-Dy)+wd*yd)*a*cotb*sinp/2
GG= -a*cotb*sinp*(wd-Dwd)/2
FS=(Dwd*(yd-Dy)²*cosp+Dwd*Dy*cosp*(yd-2Dy/3))/2
FFS=( -Dwd*cosp*2*(yd-Dy)+Dwd*cosp*(yd-4Dy/3))/2
M1=(Qd-DQo)²/(g*(wd-Dwd)*(yd-Dy)*cosp)
MM1=(Qd-DQo)²/(g*(wd-Dwd)*cosp*(yd-Dy)²)
M2=Qd²/(g*wd*yd*cosp)
MM2=0
M3=DQo*vuo*cosp/g
MM3=0
fDy=F1+FS+G-F2-M2+M3+M1
ffDy=FF1+FFS+GG-FF2-MM2+MM3+MM1
cDy= -fDy/ffDy
Dy=Dy+cDy
->21ifmod(cDy)>0.0001
y=yd-Dy
```

```
Qd=Qd-DQo
d=a*cotb*tanp
hd=y+d-p
hd=0.0000001if hd<0.0000001
wd=wd-Dwd
hdo=hd
Dwd=2Dx*tana

z=0
QZ1=QL
cycle j=1,1,100
Dy= -0.1y
26:  F1=(wd-Dwd)*(y-Dy)^2*cosp/2
FF1= -(wd-Dwd)*(y-Dy)*cosp
F2=wd*y^2*cosp/2
FF2=0
FS=Dwd*cosp*((y-Dy)^2+Dy*(y-2Dy/3))/2
FFS=Dwd*cosp*(-y+2Dy/3)/2
G=Dx*sinp*(2wd*y-y*Dwd-wd*Dy+2Dwd*Dy/3)/2
GG=Dx*sinp*(-wd+2Dwd/3)/2
M1=(Qd-ADQ(j))^2/(g*(y-Dy)*(wd-Dwd)*cosp)
MM1=(Qd-ADQ(j))^2/(g*(y-Dy)^2*(wd-Dwd)*cosp)
M2=Qd^2/(g*wd*y*cosp)
MM2=0
M3=ADQ(j)*Avu(j)*cosp/g
MM3=0
fDy=F1+G+FS+M1+M3-M2-F2
ffDy=FF1+GG+FFS+MM1+MM3-MM2-FF2
cDy=-fDy/ffDy
Dy=Dy+cDy
->26ifmod(cDy)>0.0001
y=y-Dy
wd=wd-Dwd
Qd=Qd-ADQ(j)
d=d+Dx*tanp
```

```
->20ify<0
->28if(Qd/(wd*y*sqrt(g*y)))<1
29:  captionC
Qd=0.001 if Qd<0.00001
y=exp(2*(log(Qd/(0.99*wd*sqrt(g))))/3)
28:
Ahd(j)=y+d-p
Ahd(j)=0.0000001ifAhd(j)<0.0000001
z=1ifAhd(j)>0
repeat
->12ifz=0
h=ho
pu=puo
c=coeff(h,pu)
HD=0.0000001 if HD<0.0000001
hdo=0.99999h if hdo>0.99999h
Qo=(c*exp(1.5*log(h)))*(2a*exp(0.385*log(1-sqrt((HD/h)↑3)))+(1o-2a)*exp(0.385*log(1-sqrt c
((hdo/h)↑3))))
Q=Qo
w=wo
DQ=2Dx*c*exp(1.5*log(h))*exp(0.385*log(1-sqrt((hdo/h)↑3)))/cosa
du=h+pu
vu=Q/(w*du)
24:  cycle j=1,1,100
x=j*Dx
Ahd(j)=0.999999hifAhd(j)>0.999999h
Ddu=0.1du
22:    F1=w*du²/2
FF1=0
F2=(w+Dwu)*(du+Ddu)²/2
FF2=(w+Dwu)*(du+Ddu)
G=Dx*tanpu*(du*(w+Dwu)+w*(du+Ddu)+2Ddu*Dwu/3)/2
GG=Dx*tanpu*(w+2Dwu/3)/2
FS=Dwu*du²/2+Dwu*Ddu*(du+Ddu/3)/2
FFS=Dwu*(du+2Ddu/3)/2
M1=Q²/(g*w*du)
```

```
MM1=0
M2=(Q+DQ)^2/(g*(w+Dwu)*(du+Ddu))
MM2=-(Q+DQ)^2/(g*(w+Dwu)*(du+Ddu)^2)
M3=DQ*vu/g
MM3=0
fDy=F1+FS+G+M1+M3-F2-M2

ffDy=FF1+FFS+GG+MM1+MM3-FF2-MM2
cDy=-fDy/ffDy
Ddu=Ddu+cDy
->22ifmod(cDy)>0.0001
Dh=Ddu-Dpu
23:  ->8if(h)<0
c=coeff(h,pu)
Ahd(j)=0.999999hifAhd(j)>0.999999h
IQ=2c*Dx*exp(1.5*log(h))/cosa
ADQ(j)=IQ*exp(0.385*log(1-sqrt((Ahd(j)/h)↑3)))
T=1.195c*ADQ(j)*sina*sqrt(h↑3)/(IQ*(Ahd(j)+k10*(h-Ahd(j))))
DQ=ADQ(j)
Avu(j)=(Q/((h+pu)*w))*cosa^2+T
h=h+Dh
Ah(j)=h
->25ifN5>0
25:  Q=Q+DQ
w=w+2Dx*tana
pu=pu+Dpu
du=du+Ddu
vu=Q/(w*du)
->30 if du<0.1
->27if(Q/(w*du*sqrt(g*du)))<1
30:captionC
du=exp(2*(log(Q/(0.99*w*sqrt(g))))/3)
vu=Q/(w*du)
h=du-pu
27:
repeat
```

```
12:
E=h+p+Q^2/(2g*(h+p)^2*(wm-2a)^2)
vy=Q/((h+p)*(wm-2a))
ha=ho;  he=ho;  vt=vy
14:   TIME=1
TIME=0ifk8>0.01


15:     N3=N3+1
TIME=TIME+1
cond=haifTIME=1
->16ifk8>0.01
cond=ha;  he=ha

16:
c=coeff(he,p)
q=0ifAhd(100)>0.9999999he
->20ifAhd(100)>0.9999999he
q=2a*c*exp(1.5*log(he))*exp(0.385*log(1-sqrt((Ahd(100)/he)↑3)))
20:  QL=Q+q
vt=QL/((ha+p)*wm)
ET=ha+p+vt^2/(2g)
F=ET-E-k4*vy^2/(2g)-k5*(vy-vt)^2/(2g)
difET=1+QL*((ha+p)*(3a*c*sqrt(ha))-QL)/(g*wm^2*(ha+p)↑3)
difvt=((ha+p)*(3a*c*sqrt(ha))-QL)/((ha+p)^2*wm)
difdh=-2k5*(vy-vt)*difvt/(2g)
difF=difET-difdh
ha=ha-F/difF
->19ifTIME=2
F=he+p+c^2*he↑3/(2g*(he+p)^2)-ET

difF=1+c^2*he^2*(he+3p)/(2g*(he+p)↑3)
he=he-F/difF
->15
19:   ->14ifmod(ha-cond)>0.00001
```

```
h=ha;c=coeff(h,p)
->31 if N5=0
QZ2=QL
QL=(QZ1+QZ2)/2
->11 if mod(QZ1-QZ2)>0.001
31;N5=N5+1;N4=N4+1
HD=0.0000001if HD<0.0000001
QR=c*wm*exp(1.5*log(h))*exp(0.385*log(1-sqrt((HD/h)↑3)))
newline
print(N4,2,0);print(h/p,3,3)
print(QL/QR,3,3);print(h,3,3);print(n*QR,3,3);print(n*QL,3,3);print(HD/p,3,3);caption ## ****
print(Ah(1),1,3);cycle pj=10,10,100;print(Ah(pj),1,3);repeat
->8if h/p>0.6
->11if N5=1
repeat
->8
realfn coeff(realname h,p)
c=((0.605+0.08h/p+1/(320h-3))*2rtgg/3)*k2
result=c
end
7:   endofprogram


6  3.5  2  7.2  0  0  0  2.9479
1  1.4  1  0.2  0  1  1  0  0  0.855
-1
6  3.5  2  7.2  0  0  0  2.9479
1  1.2  1  0.2  0  1  1  0  0  0.855
-1
6  3.5  2  7.2  0  0  0  2.9479
1  0.8  1  0.2  0  1  1  0  0  0.855
-1
6  3.5  2  7.2  0  0  0  2.9479
1  1  1  0.2  0  1  1  0  0  0.855
99


***Z
```

UNOTT.ME/TAYLOR G L/WEIR.

```
    0   BEGIN
  238       REAL FN COEFF
  241       END OF REAL FN
  242   END OF PROGRAM

PROGRAM (+PERM) OCCUPIES 4329 WORDS
PROGRAM DUMPED
COMPILING TIME   59 SEC /  46 SEC
```

WEIR RATIOS

..L/W.....	W/P....	ANGLE...	CYCLES.....	A.....	B.....	RU.....	R.....	HD/P
6.0	3.5	7.2	2.0	0.104	4.213	0.000	0.000	0.000

CONSTANTS ARE

K1.....	K2.....	K3.....	K4.....	K5.....	K6.....	K7.....	K8.....	K9.....	K10
1.00	1.40	1.00	0.20	0.00	1.00	1.00	0.00	0.00	0.855

RESULTS — SURFACE PROFILES

.NO...	H/P.....	QL/QR....	H.....	QR.....	QL.....	HD/P					
1	0.048	5.962	0.020	0.057	0.341	0.000	****	0.021	0.021	0.020	0.020	0.020
2	0.048	5.962	0.020	0.057	0.341	0.000	****	0.021	0.021	0.020	0.020	0.020
3	0.093	5.842	0.039	0.123	0.719	0.000	****	0.042	0.041	0.039	0.039	0.038
4	0.093	5.842	0.039	0.123	0.719	0.000	****	0.042	0.041	0.039	0.039	0.038
5	0.134	5.643	0.057	0.203	1.144	0.000	****	0.063	0.059	0.056	0.054	0.053
6	0.134	5.637	0.057	0.203	1.144	0.000	****	0.063	0.059	0.056	0.054	0.053
7	0.174	5.375	0.073	0.291	1.567	0.000	****	0.083	0.075	0.070	0.067	0.065
8	0.174	5.347	0.073	0.292	1.562	0.000	****	0.083	0.075	0.070	0.067	0.065
9	0.212	5.065	0.089	0.390	1.974	0.000	****	0.103	0.089	0.081	0.077	0.075
10	0.213	5.013	0.090	0.391	1.963	0.000	****	0.103	0.089	0.081	0.077	0.076
11	0.251	4.739	0.106	0.499	2.367	0.000	****	0.123	0.101	0.090	0.085	0.083
12	0.252	4.665	0.106	0.503	2.346	0.000	****	0.123	0.102	0.091	0.087	0.085
13	0.291	4.415	0.123	0.622	2.747	0.000	****	0.143	0.111	0.097	0.093	0.091
14	0.293	4.324	0.123	0.628	2.716	0.000	****	0.143	0.111	0.099	0.095	0.094
15	0.333	4.106	0.140	0.759	3.118	0.000	****	0.162	0.118	0.103	0.099	0.098
16	0.336	3.978	0.142	0.771	3.068	0.000	****	0.162	0.120	0.107	0.105	0.104
17	0.376	3.815	0.158	0.913	3.482	0.000	****	0.181	0.123	0.108	0.105	0.105
18	0.383	3.612	0.161	0.938	3.388	0.000	****	0.181	0.130	0.120	0.118	0.117
19	0.421	3.544	0.177	1.084	3.841	0.000	****	0.199	0.125	0.113	0.112	0.111
20	0.431	3.294	0.182	1.123	3.700	0.000	****	0.200	0.141	0.133	0.133	0.132
21	0.468	3.295	0.197	1.273	4.194	0.000	****	0.217	0.125	0.118	0.118	0.118
22	0.481	3.021	0.202	1.327	4.009	0.000	****	0.219	0.154	0.149	0.148	0.148
23	0.516	3.068	0.217	1.480	4.541	0.000	****	0.234	0.125	0.124	0.124	0.124
24	0.532	2.787	0.224	1.549	4.318	0.000	****	0.238	0.167	0.165	0.165	0.165

continued over

COMPUTER PROGRAM OUTPUT (continued)

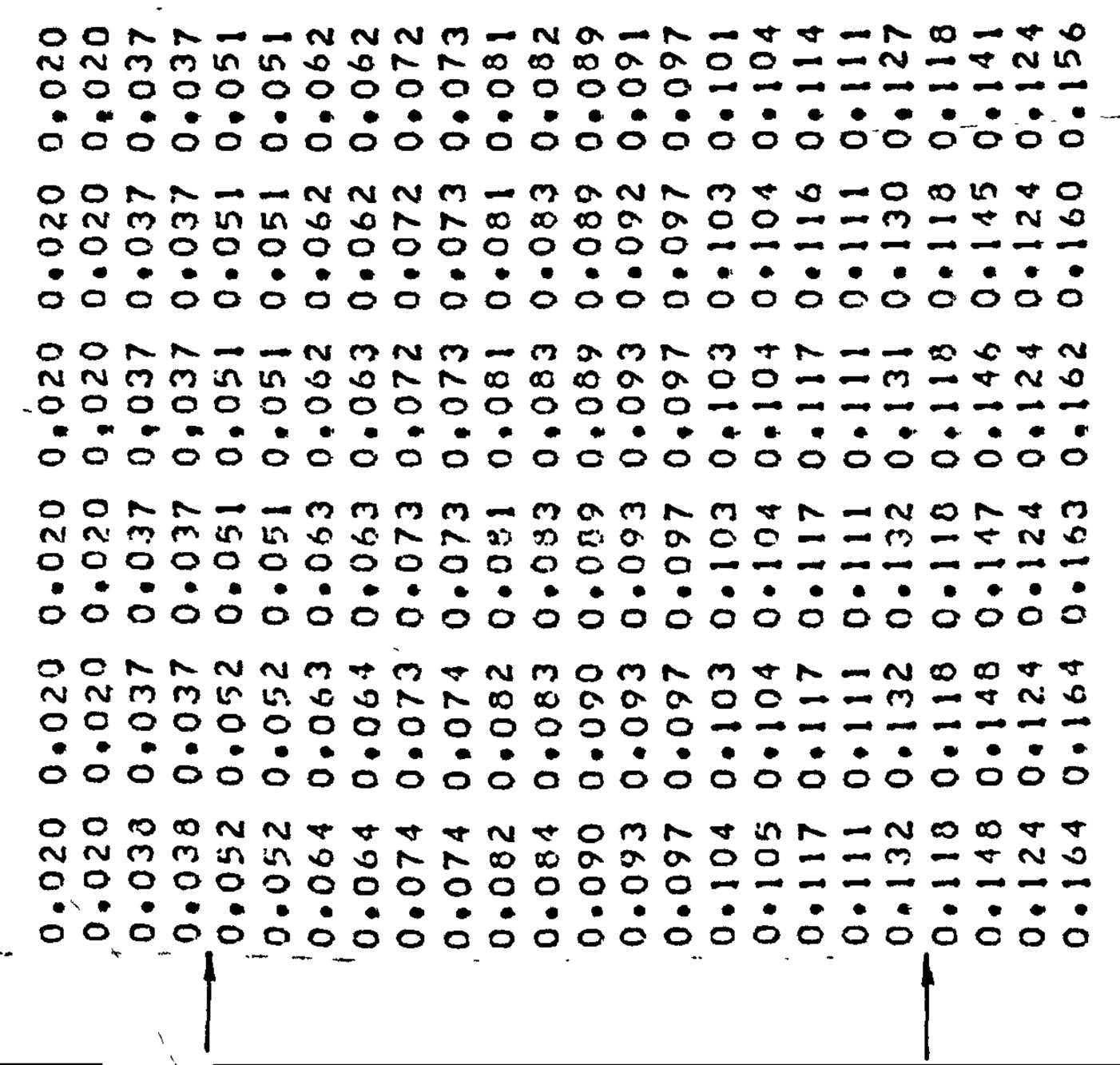

LIST OF REFERENCES

1. M. Kozák and J. Sváb. "Tort alaprojzú bukók laboratóriumi vizsgálata", Hidrológiai Közlöny, 1961, No. 5.

2. B. Gentilini. "Stramazzi con cresta a pianta obliqua e a zig-zag". Memorie e Studi dell Instituto di Idraulica e Costruzioni Idrauliche del Regio Politecnico di Milano. No. 48, 1940.

3. P. Boileau. "Traité de la mesure des eaux courantes". Mallet-Bachelier, Parigi 1854.

4. L. Escande e G. Sabathé. "Fonctionnement d'un déversoir incliné par rapport à l'axe du canal". Revue générale de l'Hydraulique, N.15, 1937.

5. S. Istomina. "L'Energia Elettrica", 1937, page 178.

6. G. Tison and T. Fransen. "Essais sur deversoirs de forme polygonale en plan". Review C. Vol. III, No. 3.

7. Guthrie Brown, J. Hydro-Electric Engineering Practice. London, Blackie, 1964.

8. "Le Barrage du Sarno" and "Le Barrage du Beni Bahdel". La diffusion du Livre Algeria.

9. R.C.S. Walters. Dam Geology. Butterworths. 1962.

10. H.W. King and E.F. Brater. Handbook of Hydraulics. McGraw-Hill.

11. Yoshinori Shimojama. "Experiments on a small rectangular weir without side contractions". Kyushu Imperial University, Memoirs of the College of Engineering 7, 185-207.

12. C.E. Kindsvater and R.W. Carter. "Discharge Characteristics of Rectangular Thin-plate Weirs", Trans. ASCE, Vol. 124, pp. 772-822, 1959.

13. J.R. Villemonte. "Submerged-weir discharge studies". Engineering News-record. Dec. 25, 1947, p.866.

14. F.T. Mavis. "How to calculate flow over submerged thin plate weirs". Engineering News-Record, July 7, 1949, p. 65.

15. British Standard Code B.S.1042, 1943, "Flow Measurement".

16. Ministry of Aviation. R and M No. 3365. "A discussion of Pitot-static tubes and their calibration factors with a description of various vertions of a new design".

17. I.O. Miner. "The Dall Tube Flow". A.S.M.E. paper 54-A-139.

18. A. Schlag. "Formule de débit de déversoirs dont le seuil est constitué par une serie de dents situées dans un plan horizontal". La Tribune du Cebedeau, Avril 1962.

19. W.H.R. Nimmo. "Side spillways for regulating diversion canals". Trans. A.S.C.E. Vol. 92, 1928, p.1561.

20. G. de Marchi. "Des formes de la surface libre de courants permanents avec debit progressivement croissant ou progressivement decroisant dans un canal de section constante". Revue Générale de L'Hydraulique. Mar/Apr. 1947.

21. P. Ackers. "A theoretical consideration of side weirs as storm water overflows" (see Reference 26).

22. G.S. Coleman and Dempster Smith. "The discharging capacity of side weirs ". Selected Engineering Paper No. 6. I.C.E. 1923.

23. V.K. Collinge. "The discharge capacity of side weirs". (see Reference 26).

24. J.W. Allen. "The discharge of water over side weirs in circular pipes". (see Reference 26).

25. W. Frazer. "The behaviour of side weirs in prismatic rectangular channels". (See Reference 26).

26. Symposium of Four Papers on Side Spillways. Proceedings I.C.E. Vol. 6, Jan/Apr. 1957, p.250-343.

27. W. Frazer. "The behaviour of side weirs in prismatic rectangular channels". Ph.D. thesis presented to the University of Glasgow. 1954.

28. K.V.H. Smith. "Control point in a lateral spillway channel". Journal of the Hydraulics Division, A.S.C.E. May 1967.

29. J. Hinds "Side channel Spillways : Hydraulic Theory, Economic Factors, and Experimental Determination of Losses". Transactions, A.S.C.E. Vol. 89, 1926, pp. 881 - 927.

30. N. Hay and E. Markland. "The determination of the discharge over weirs by the electrolytic tank". Proceedings I.C.E. Vol. 10. pp.59 - 86, May, 1958.

31. G. Formica. "Esperienze preliminari sulle perdite di carico nei canali, dovute a cambiamenti di sezione". L'Energia Elettrica, Milano, Vol. 32, No. 7, pp.554-568, July, 1955; Reprinted as Istituto di Idraulica e Construzioni Idrauliche, Milano, Memorie e Studi No. 124, 1955.

32. G. Aichel. "Experimentelle Untersuchungen über den Abfluss des Wassers bei vollkommenen Ueberfallwehren verschiedener Grunddrissanordnung". Franzcher, Lipsia 1907.

TABLES

PHOTOGRAPHS

AND

FIGURES

TABLE 1

Design parameters for the models in Model Programme No. 1.

Model Number	Series	Length Mag.l/w	Vert.Aspect Ratio w/p	α	Crest height p	Cycles n	Comment
1	A	2	2	0	5.92	3	Discarded
2	D	2	2	0	7.10	$2\frac{1}{2}$	"
3	A	2	2	7	5.92	3	"
4	D	2	2	7	7.10	$2\frac{1}{2}$	"
5	A	2	2	15	5.92	3	"
6	D	2	2	15	7.10	$2\frac{1}{2}$	"
7	A	2	2	20	5.92	3	"
8	D	2	2	20	7.10	$2\frac{1}{2}$	"
9	B	2	3.5	0	5.07	2	"
10	B	2	3.5	7	5.07	2	"
11	B	2	3.5	15	5.07	2	"
12	B	2	3.5	20	5.07	2	"
13	C	2	5	0	7.10	1	"
14	C	2	5	7	7.10	1	"
15	C	2	5	15	7.10	1	Tested
16	C	2	5	20	7.10	1	Tested
17	A	4	2	0	5.92	3	Discarded
18	D	4	2	0	7.10	$2\frac{1}{2}$	"

Model Number	Series	Length Mag.l/w	Vert.Aspect Ratio w/p	α	Crest height p	Cycles n	Comment
19	A	4	2	7	5.92	3	Tested
20	D	4	2	7	7.10	$2\frac{1}{2}$	Discarded
21	A	4	2	15	5.92	3	"
22	D	4	2	15	7.10		"
23	B	4	3.5	0	5.07	2	"
24	B	4	3.5	7	5.07	2	Tested
25	B	4	3.5	15	5.07	2	Tested
26	A	6	2	0	5.92	3	Tested
27	D	6	2	0	7.10	$2\frac{1}{2}$	Discarded
28	A	6	2	7	5.92	3	Tested
29	D	6	2	7	7.10	$2\frac{1}{2}$	Tested
30	B	6	3.5	0	5.07	2	Tested
31	B	6	3.5	7	5.07	2	Tested
32	A	8	2	0	5.92	3	Tested
33	D	8	2	0	7.10	$2\frac{1}{2}$	Tested
34	Linear weir with sharp crest						Tested

TABLE 2

Design ratios of the models in Model Programme No. 2.

Model Number	Length Mag.l/w	Vert.Aspect Ratio w/p	Side Wall Angle α °	Comment
35	8	2.5	6.6 (max)	Tested (Triangular)
36	7	3	7.7 (max)	Tested (Triangular)

Model Number	Length Mag.l/w	Vert.Aspect Ratio w/p	Side Wall Angle α °	Comment
37	6	3.5	9.1 (max)	Tested (Triangular)
38	5	4.5	11.1 (max)	Tested (")
39	8	2.5	5.4(0.75max)	Tested (Trapezoidal)
40	7	3	6.2(0.75max)	Tested (")
41	6	3.5	7.2(0.75max)	Tested (")
42	5	4.5	8.7(0.75max)	Tested (")
43	8	2.5	3.6(0.5max)	Discarded (Trapezoidal)
44	7	3	4.1(0.5max)	Discarded (")
45	6	3.5	4.8(0.5max)	Discarded (")
46	5	4.5	5.8(0.5max)	Discarded (")

TABLE 3

Design ratios of the models in Model Programme No. 4.

Model Number	Length Mag.l/w	Vert.Aspect Ratio w/p	Side Wall Angle α °	Comment
52	8	2	6.6 (max)	Tested (Triangular)
53	7	2	7.6 (max)	Tested (Triangular)
54	6	2	8.9 (max)	Tested (Triangular)
55	5	2	10.7 (max)	Tested (Triangular)

TABLE 4

Design ratios of the models in Model Programm No. 5. (Apron tests)

Model Number	Length Mag.l/w	Vert. Aspect Ratio w/p	Side Wall Angle α^{o}
56	8	2.5	5.4
57	6	3.5	7.2
58	4	3.5	7

Four arrangements of aprons were used in each model.

(a) Apron ratio = 0.5 } Aprons in upstream

(b) Apron ratio = 0.75 } channel only.

(c) Apron ratio = 0.5 } Aprons in both upstream

(d) Apron ratio = 0.75 } and downstream channels.

Photograph 1

SKELTON GRANGE LABYRINTH WEIR NR. LEEDS

Note obstruction by floating debris

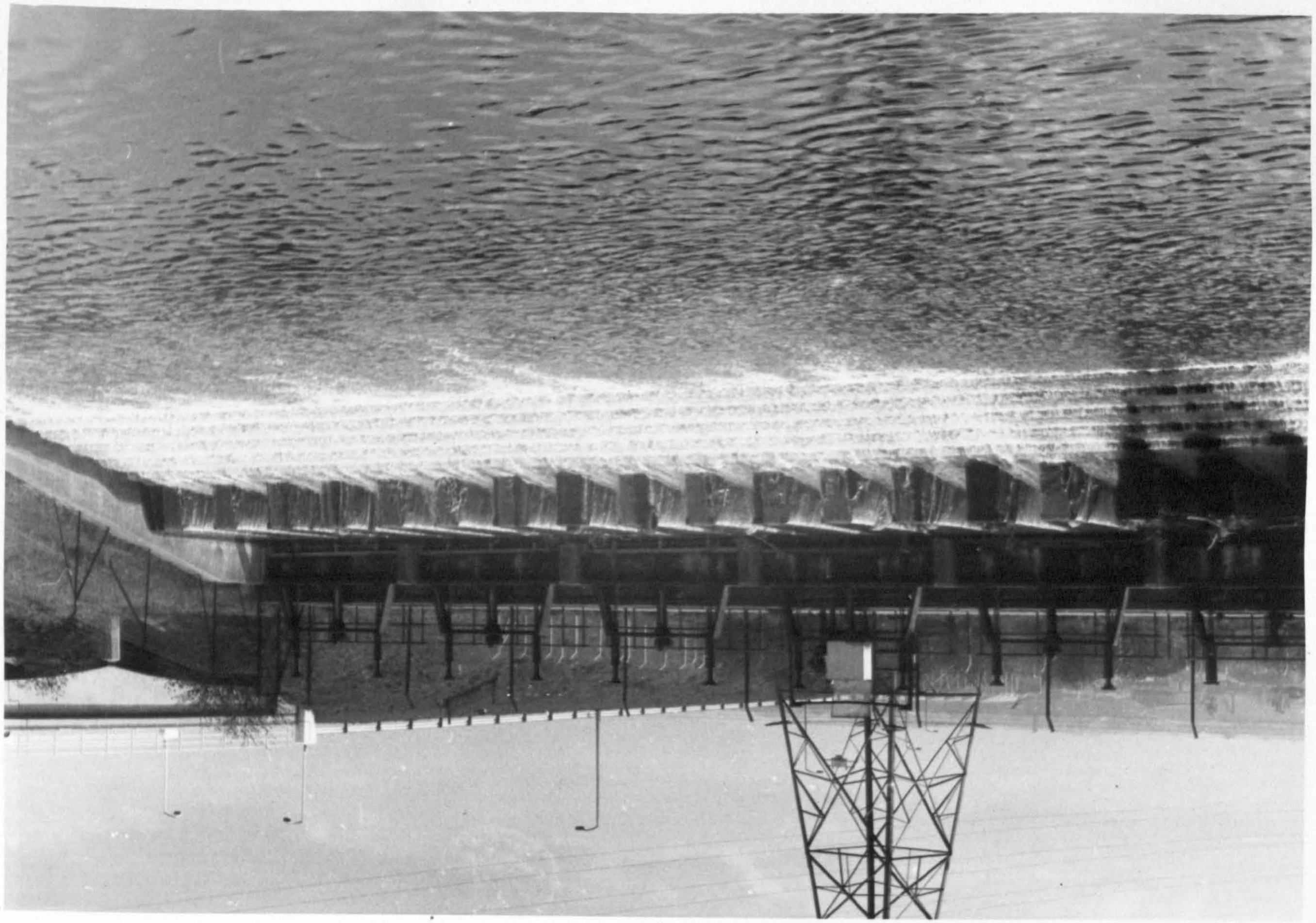

SKELTON GRANGE WEIR - CLOSE UP OF CHANNELS

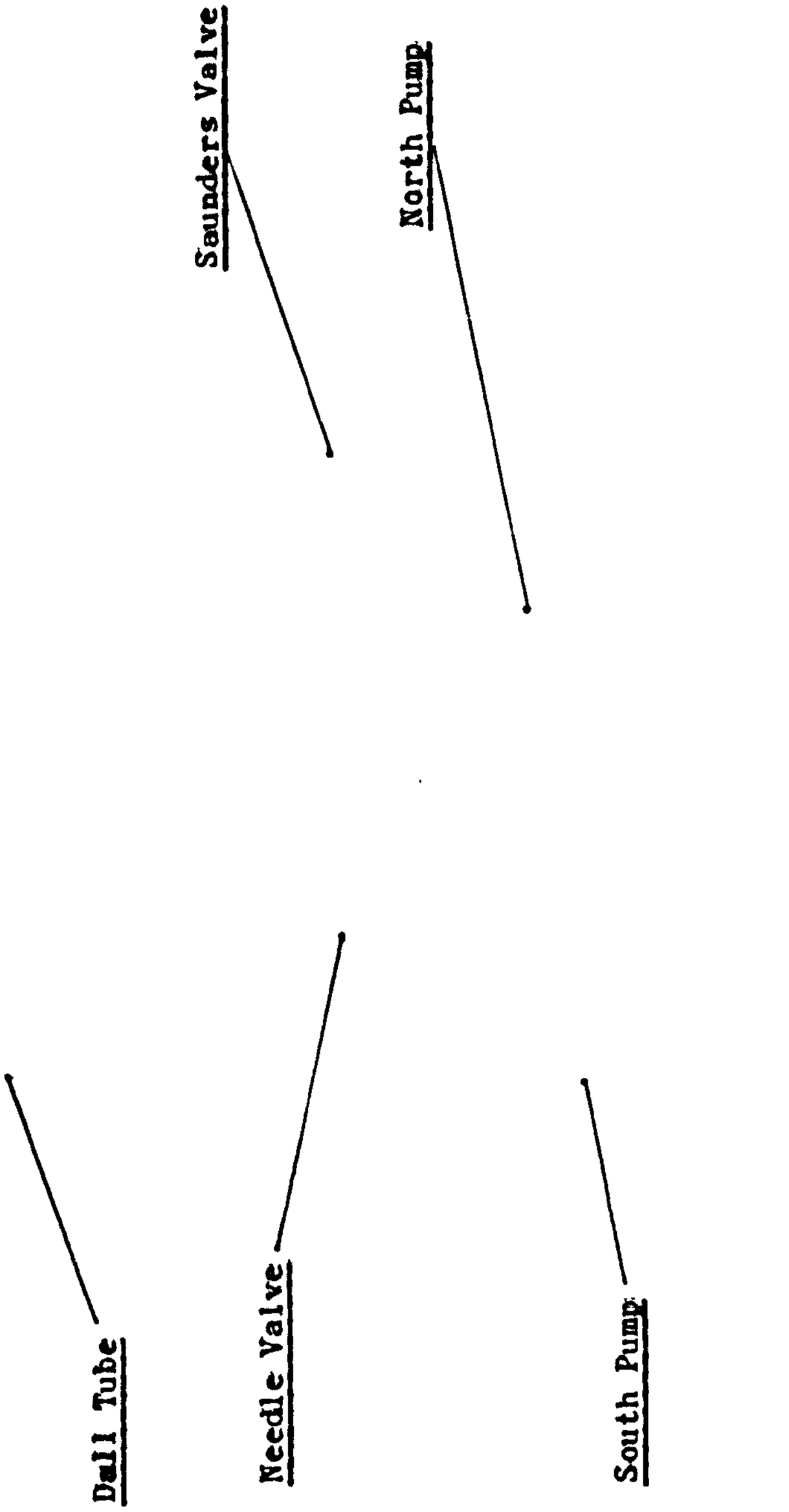

LAYOUT OF APPARATUS ON GROUND FLOOR

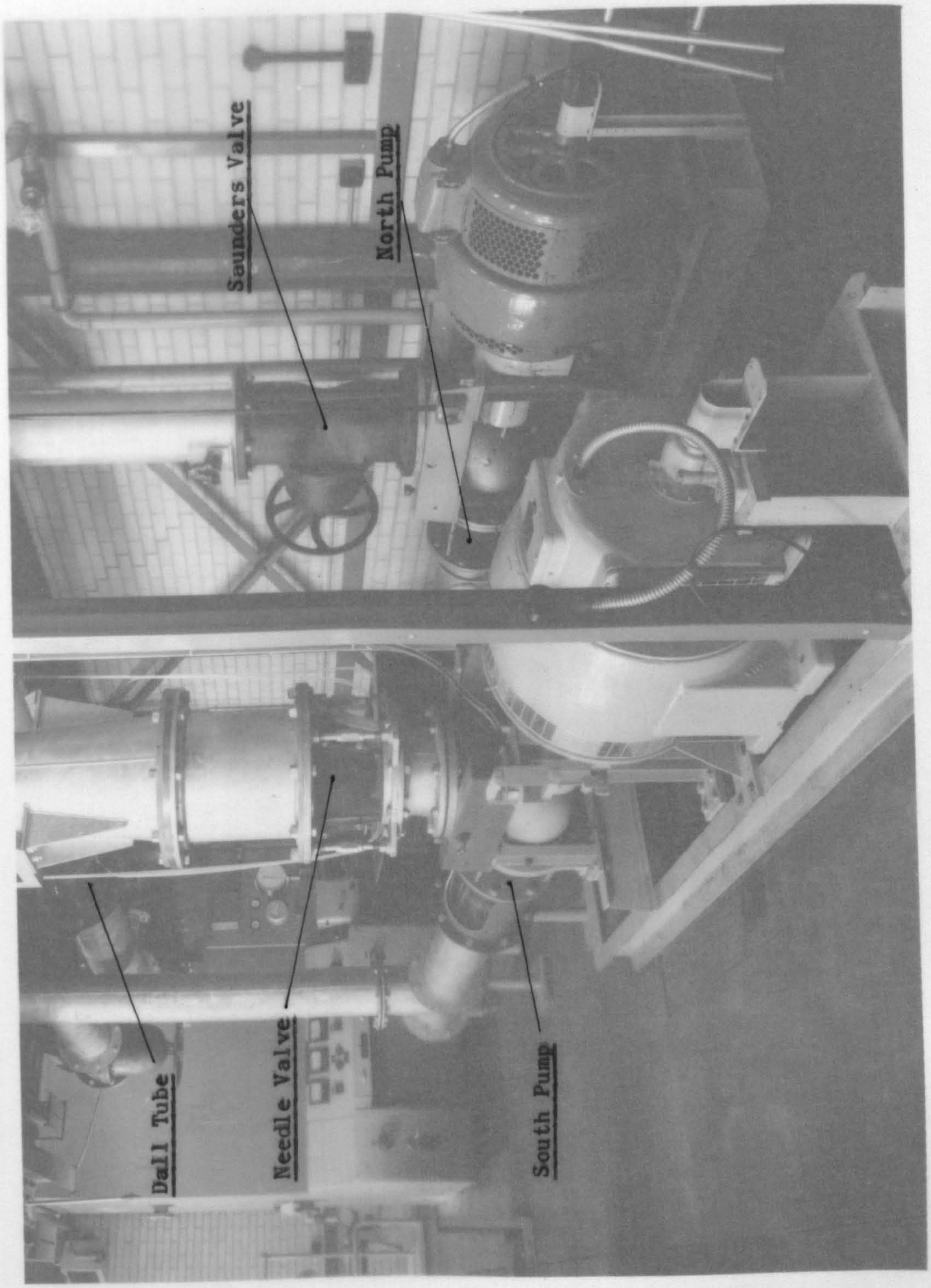

LAYOUT OF APPARATUS ON GROUND FLOOR

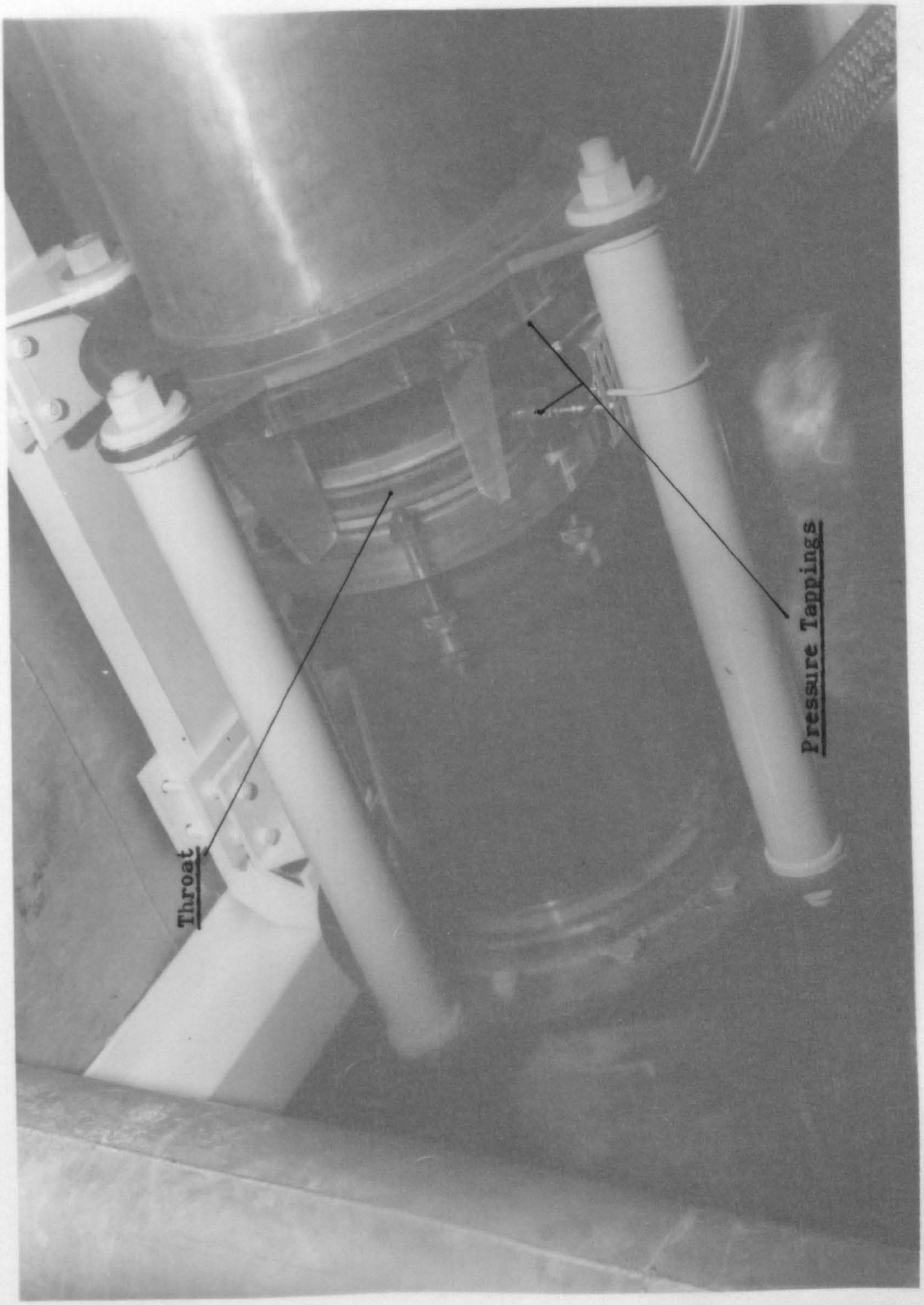

THE DALL TUBE

Photograph 5

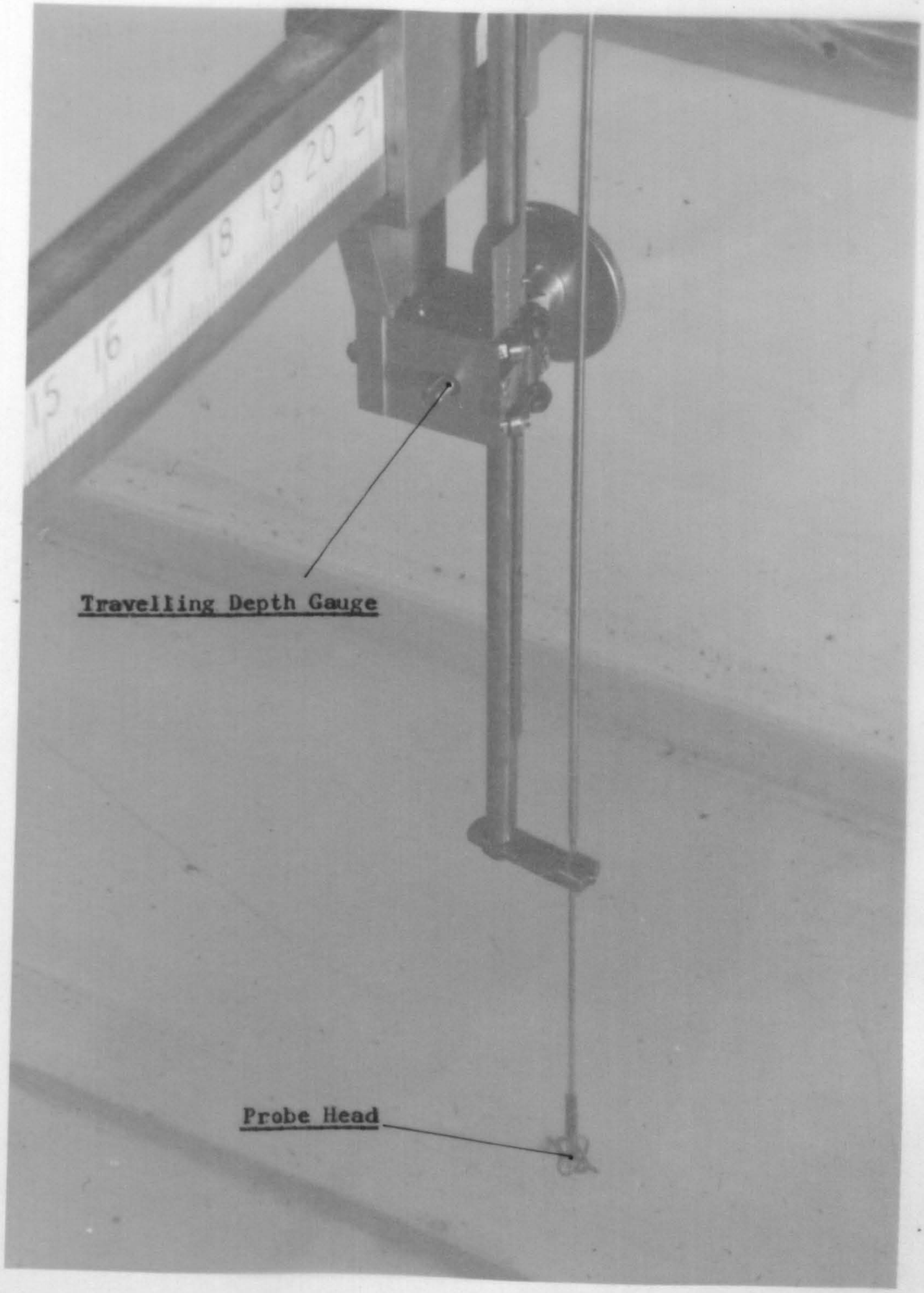

THE MINI-FLOWMETER

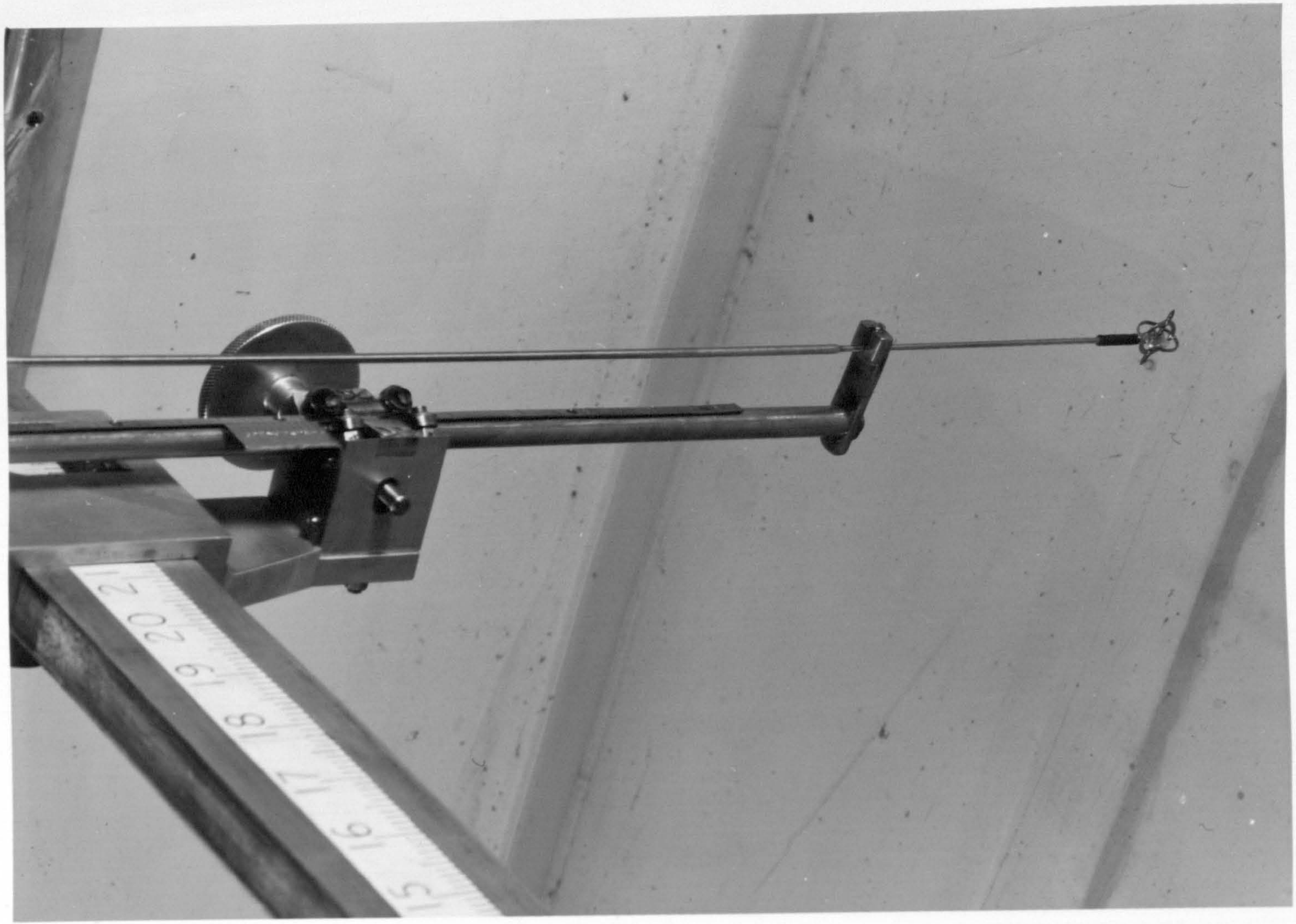

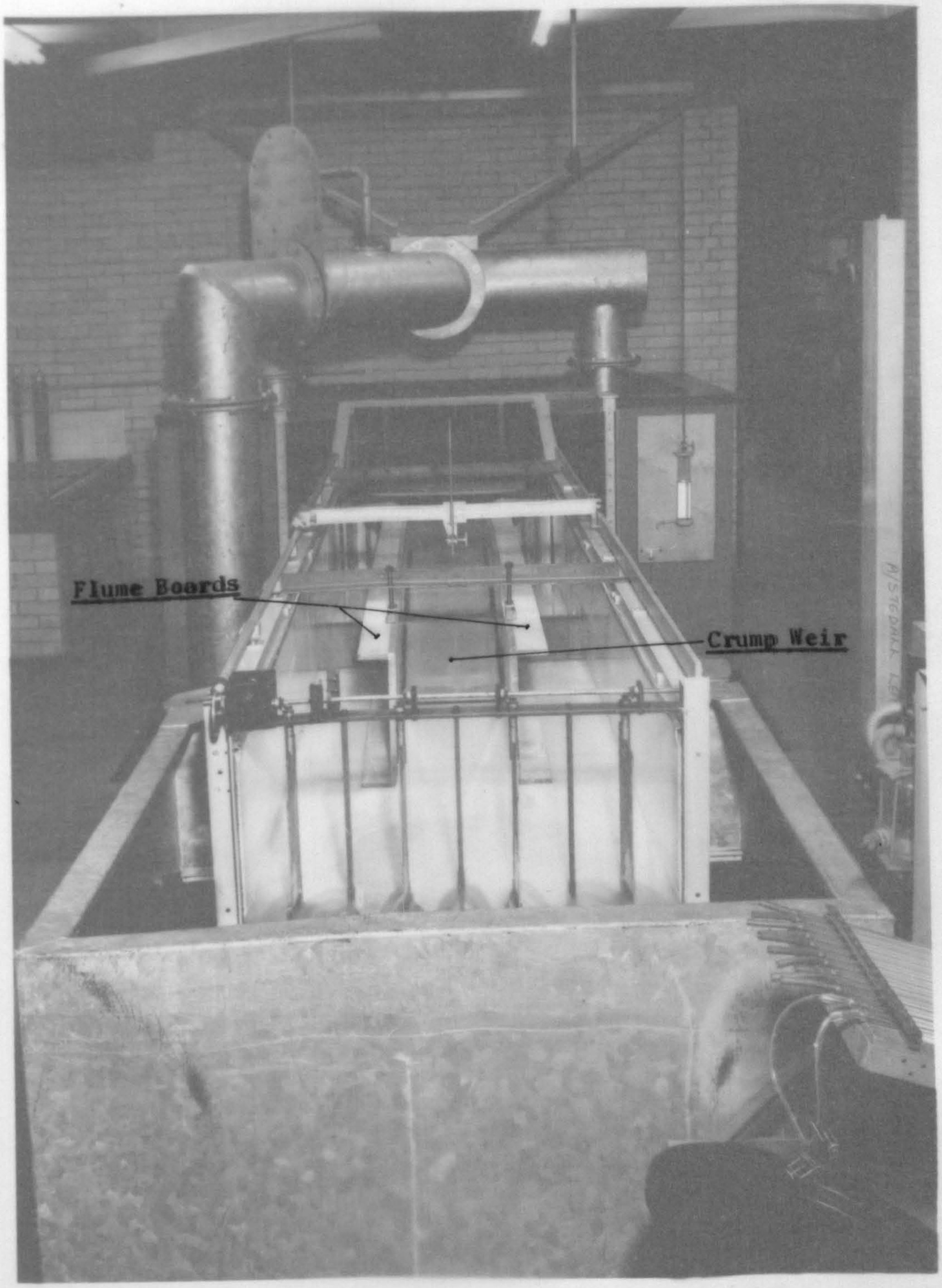

ARRANGEMENT OF APPARATUS FOR SMALL CRUMP WEIR TESTS

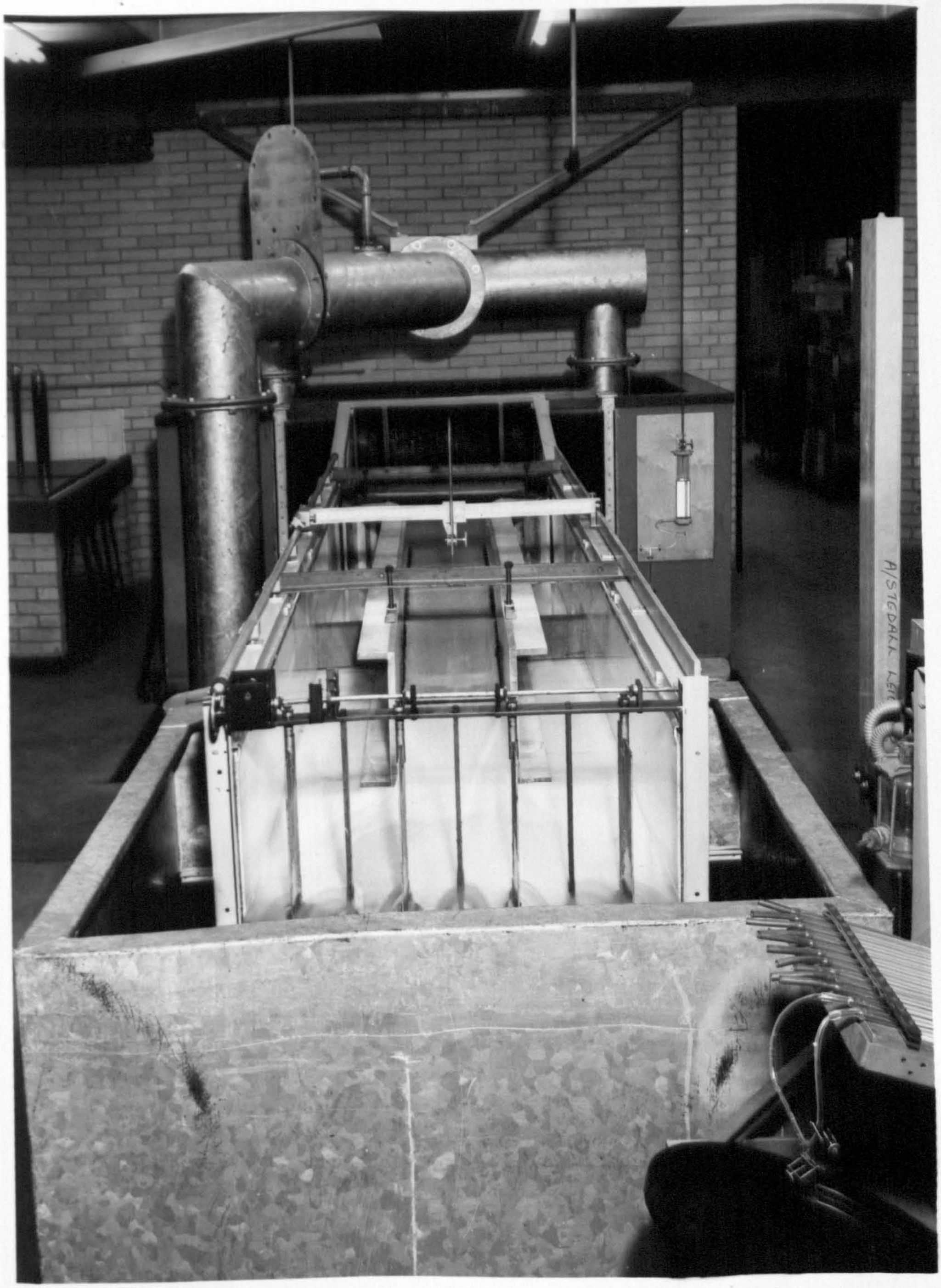

Photograph 7

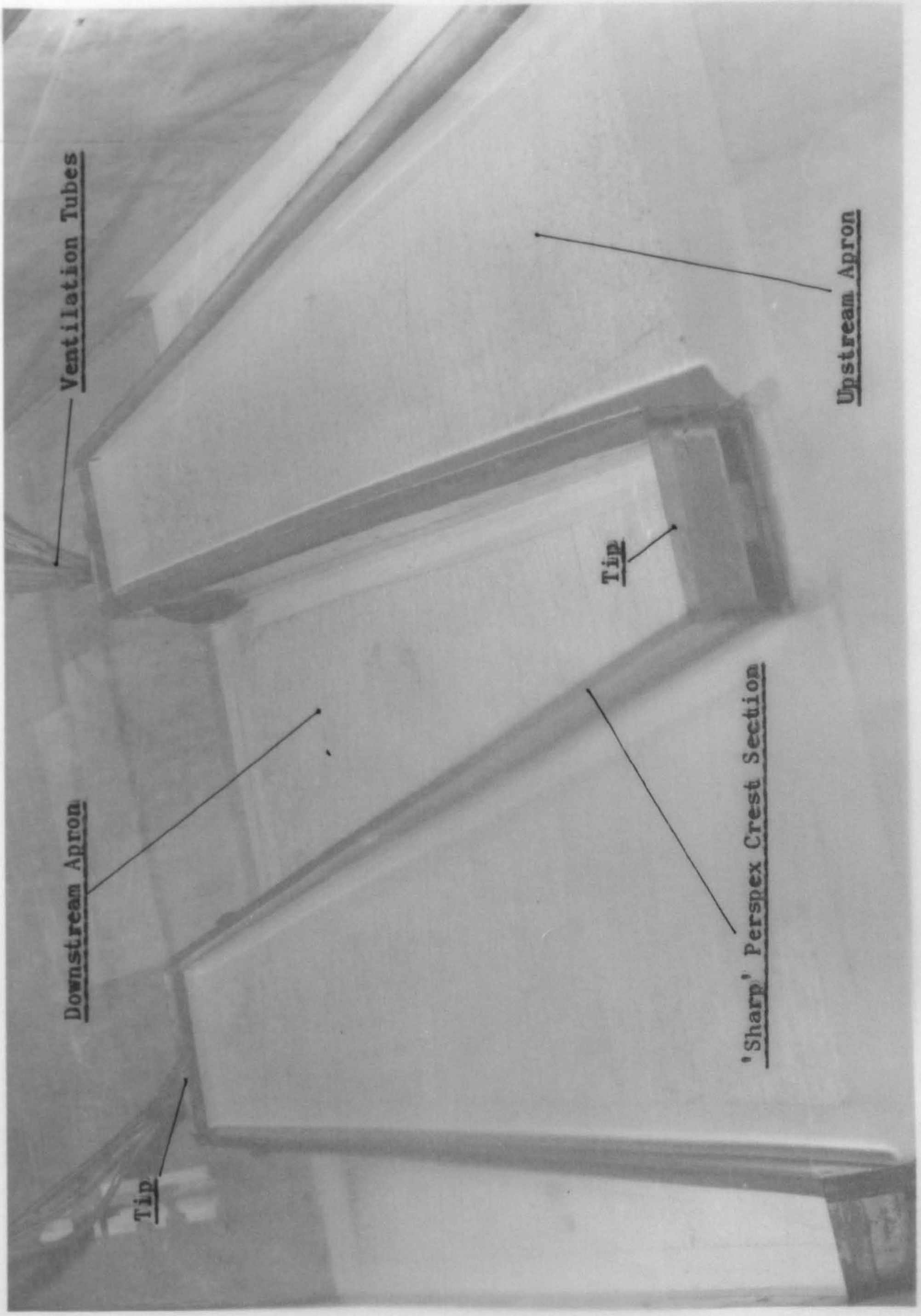

MODEL CONSTRUCTION

Photograph 8

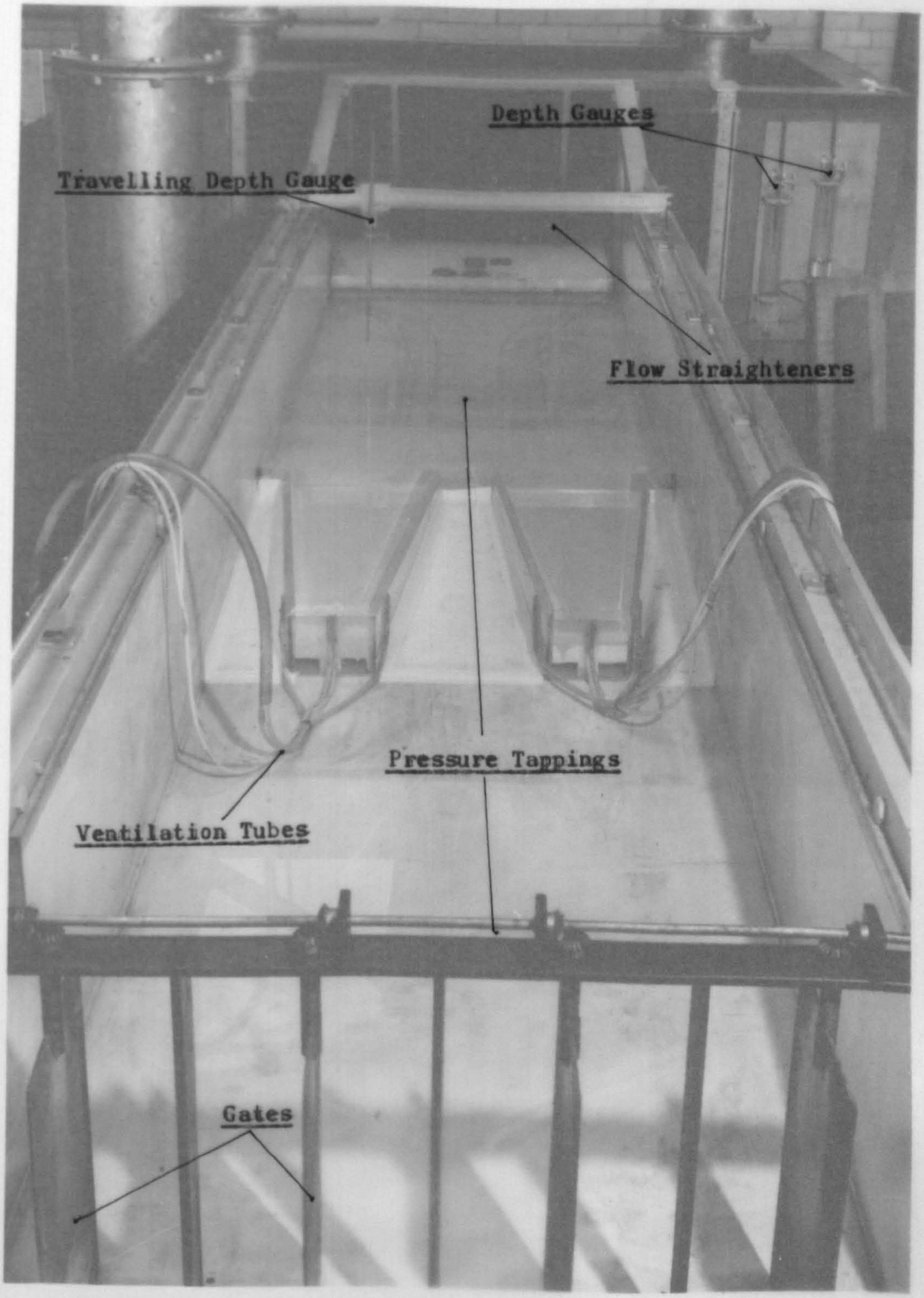

ARRANGEMENT OF APPARATUS FOR MODEL TESTS

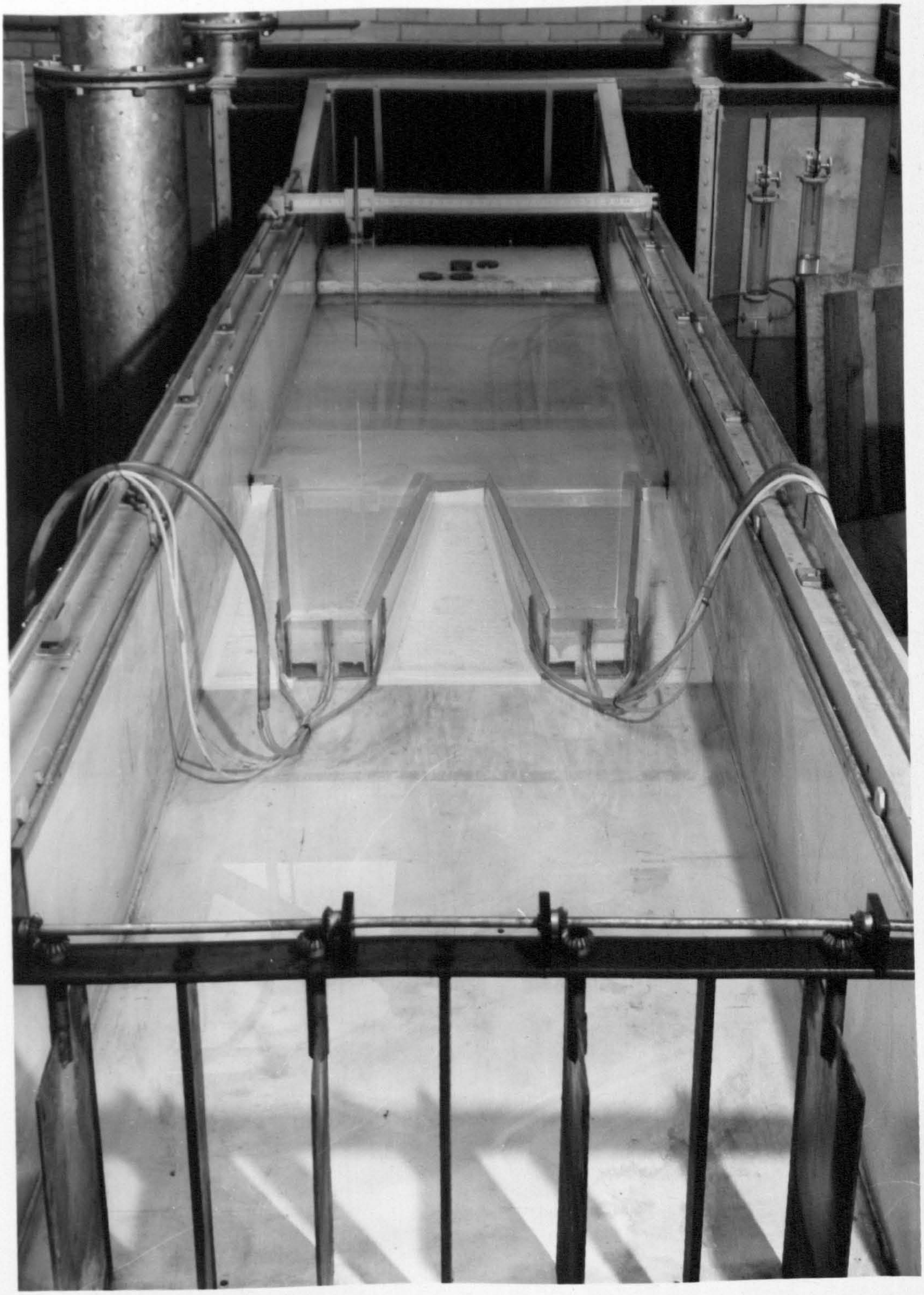

Photograph 9

VENTILATED FLOW OVER A RECTANGULAR WEIR

Photograph 10

RECTANGULAR WEIR OPERATING UNDER MEDIUM FLOW CONDITIONS

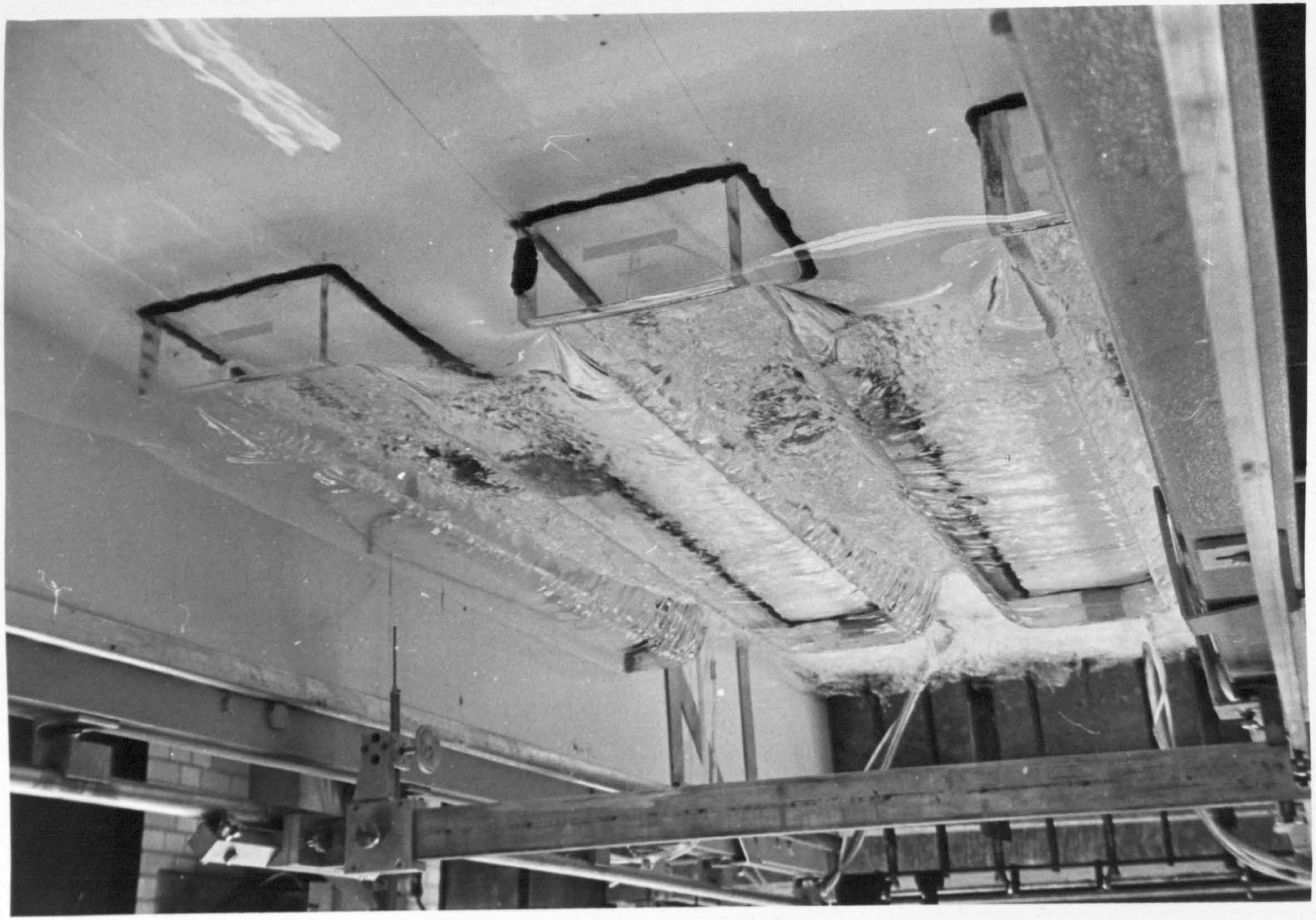

RECTANGULAR WEIR OPERATING UNDER HIGH FLOW CONDITIONS

Photograph 12

VENTILATED FLOW OVER A TRAPEZOIDAL WEIR

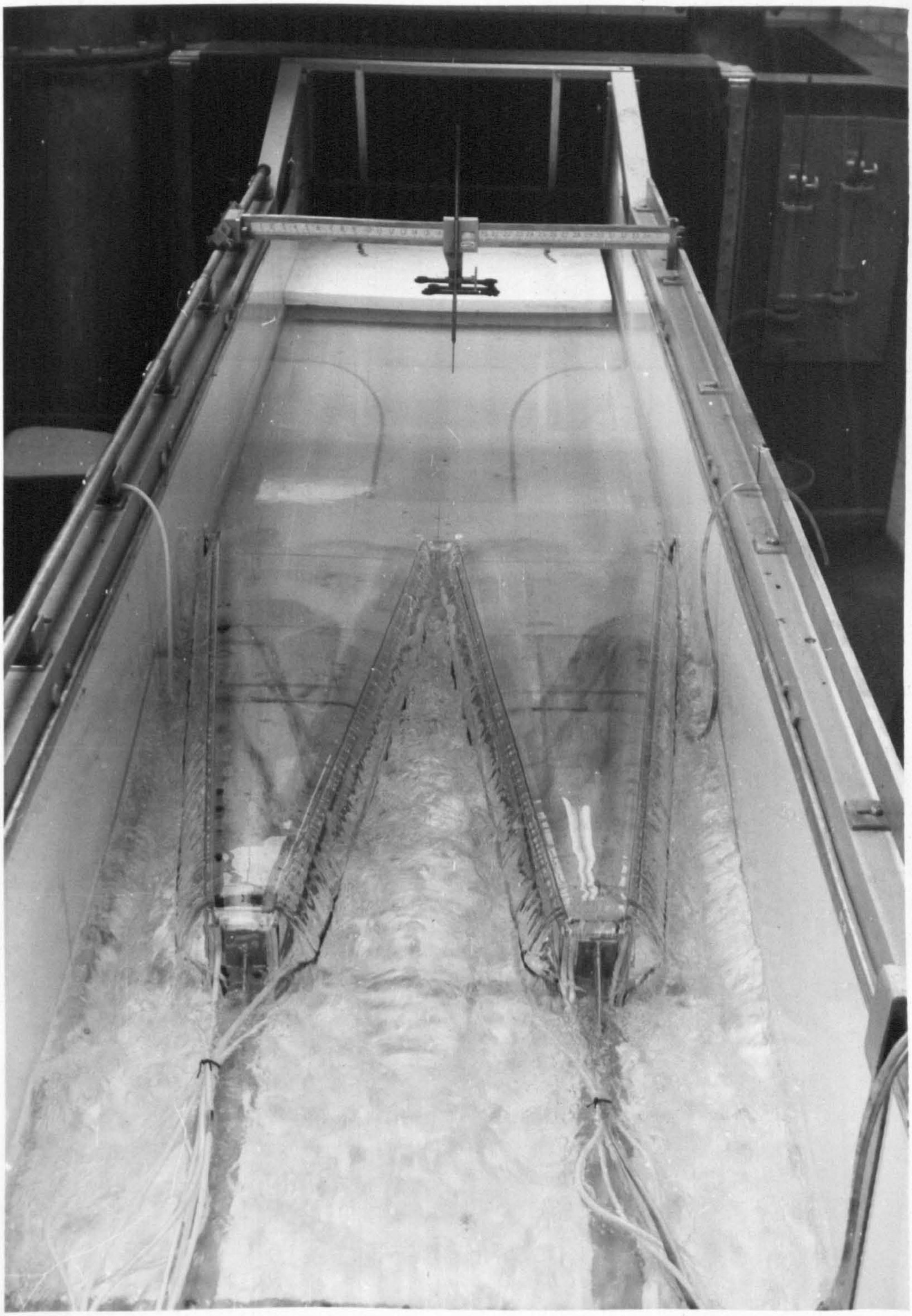

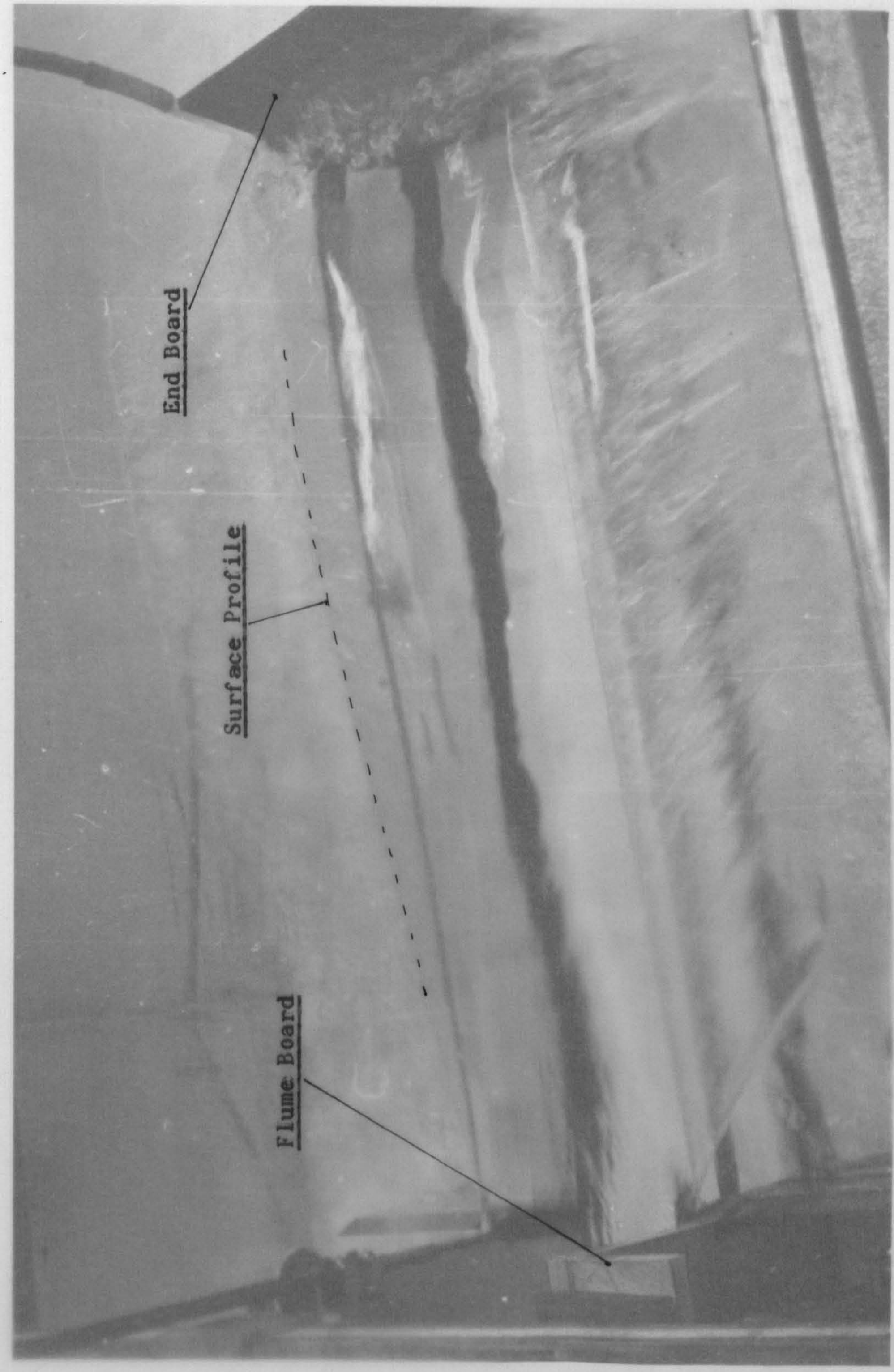

SIDE FLOW FROM A PRISMATIC CHANNEL

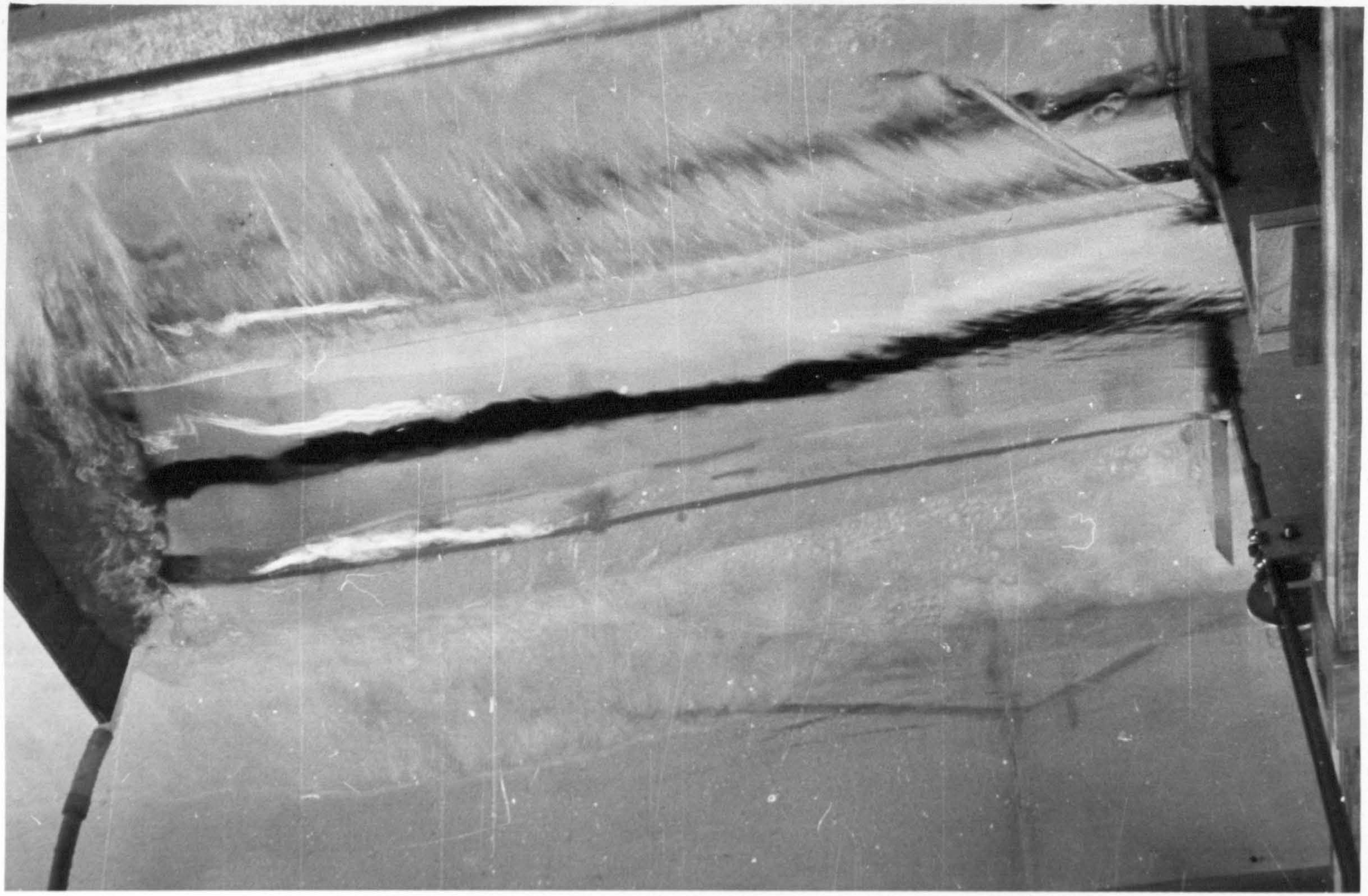

FLOW VISUALISATION BY DYE INJECTION

TRIANGULAR PLAN FORM WEIR

Photograph 15

FLOW VISUALISATION BY FLOATING PARTICLES

TRIANGULAR PLAN FORM WEIR

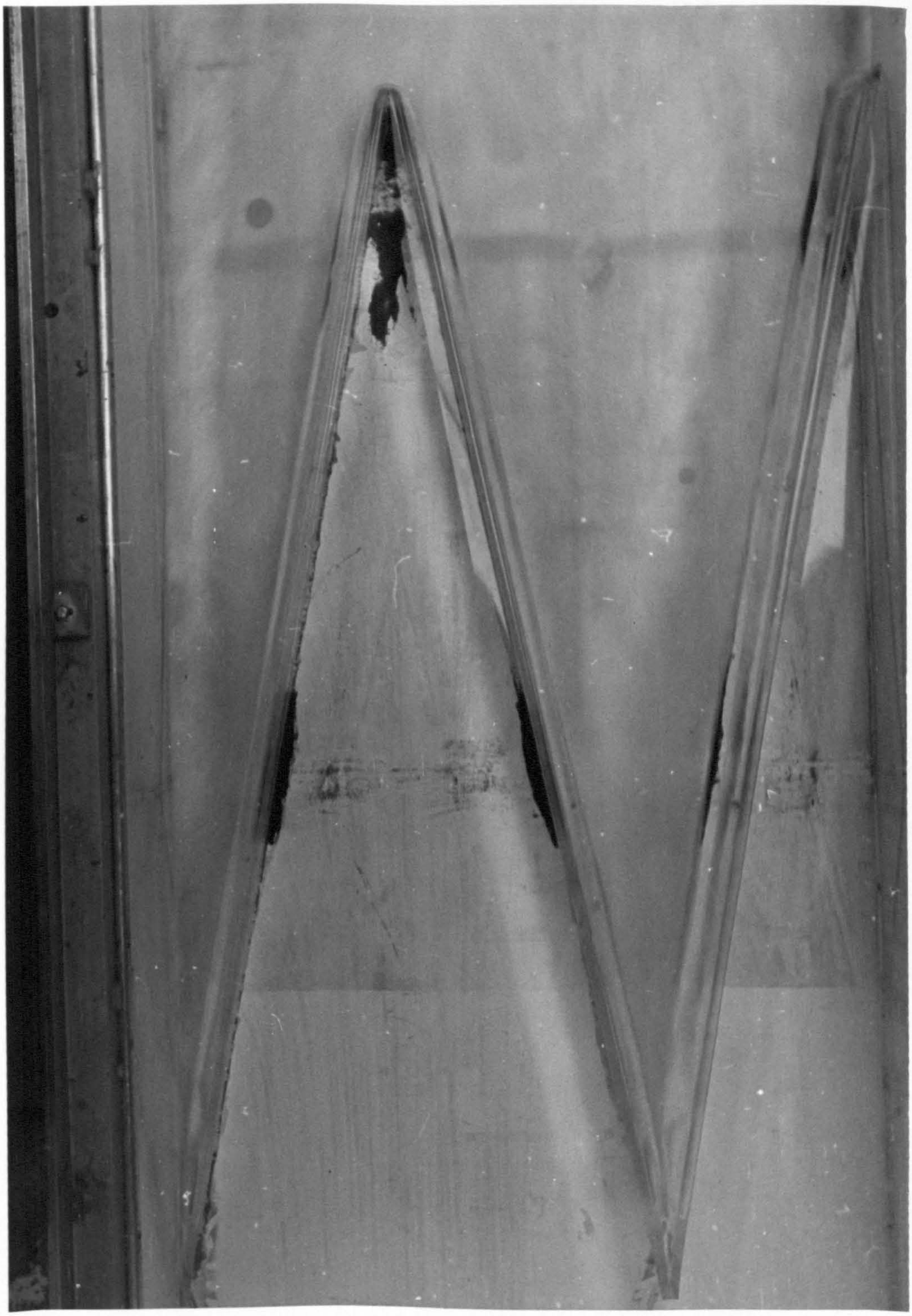

Figure I

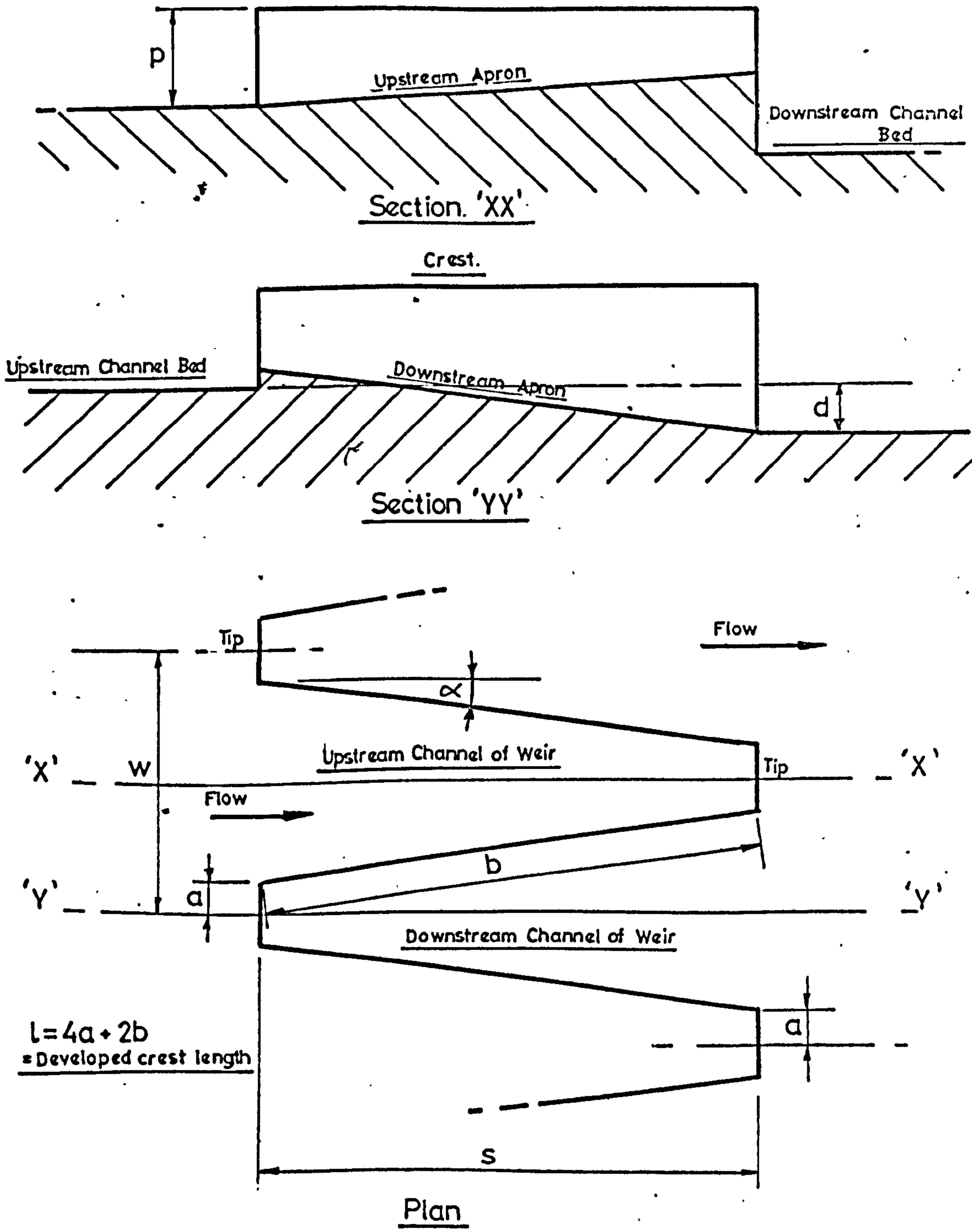

SCHEMATIC DIAGRAM OF THE LABYRINTH WEIR

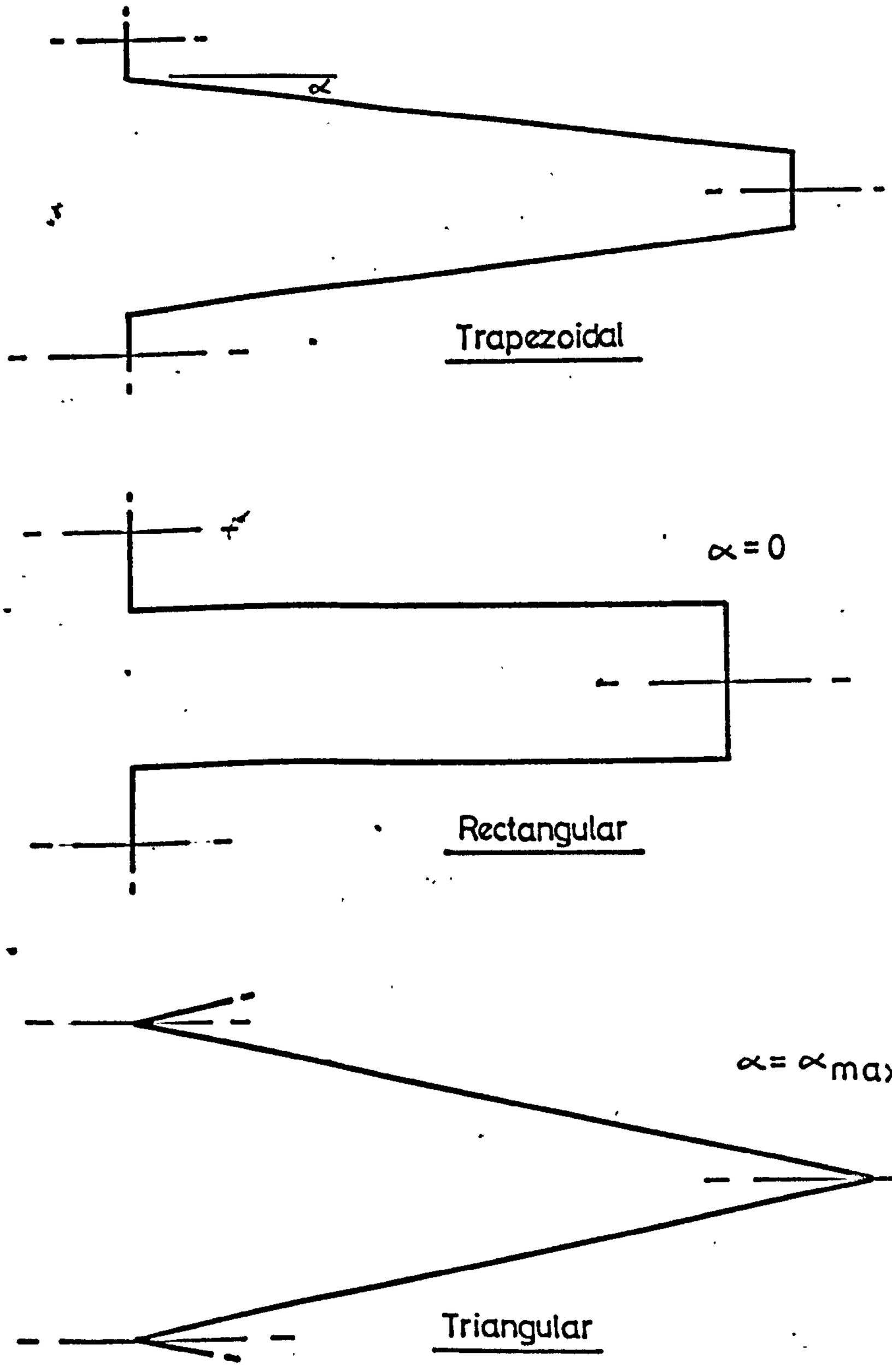

LABYRINTH WEIR PLAN FORMS

Figure 3

EXPERIMENTAL RESULTS OBTAINED BY KOZÁK AND SVÁB

Flow magnification, QL/QR, versus head to crest height ratio, h/p

Model no.	l/w	w/p	∝°
2	1.23	4.61	16.7
3	1.46	2.31	17.2
4	1.69	1.54	16.7
5	1.92	1.15	16.7
6	1.42	4.61	20.6
7	2.05	2.31	8.9
8	2.59	1.54	8.6
9	3.11	1.15	8.6
10	1.84	4.61	5.7
11	2.67	2.31	5.9
12	3.51	1.54	5.7
13	4.35	1.15	5.7

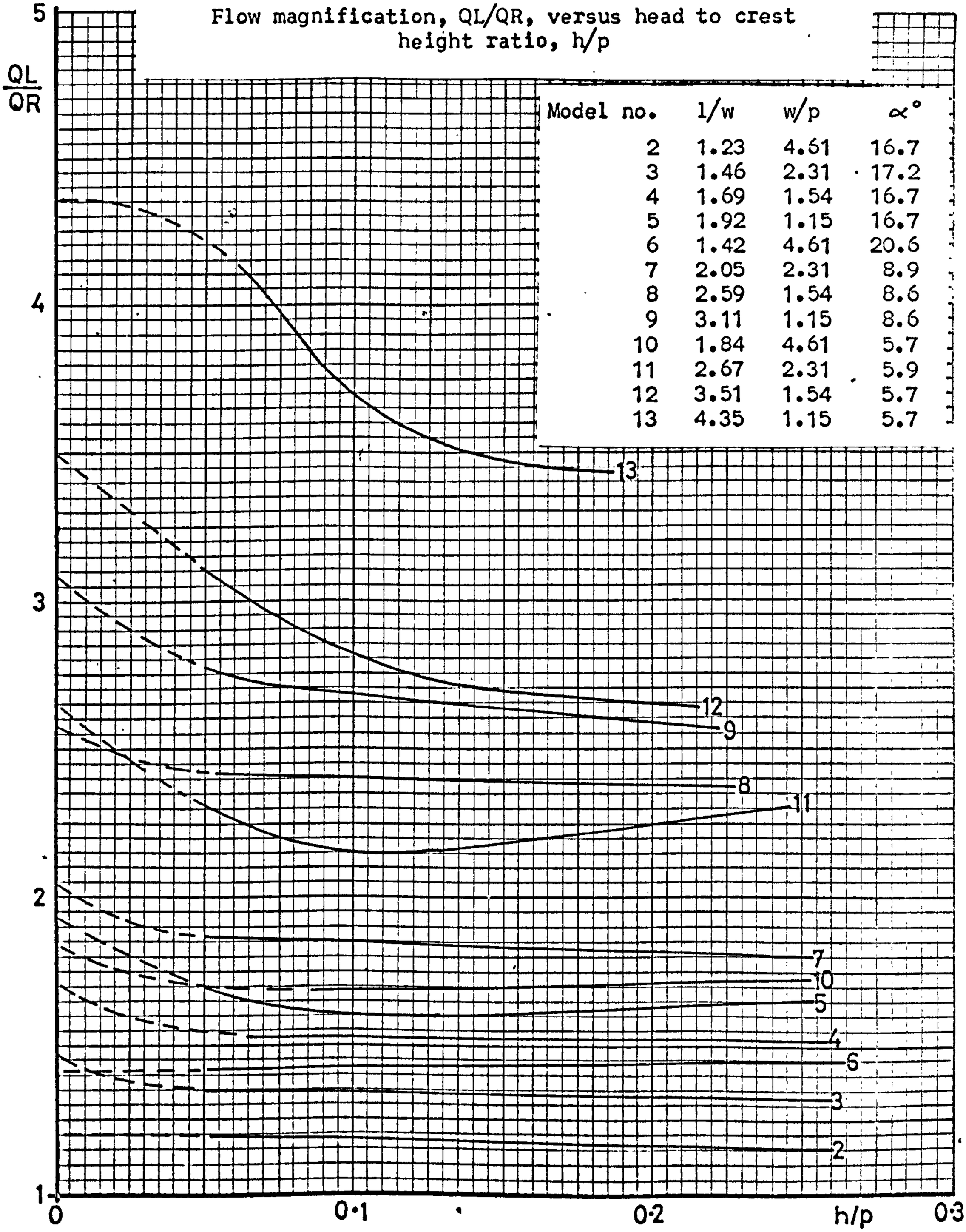

Figure 4

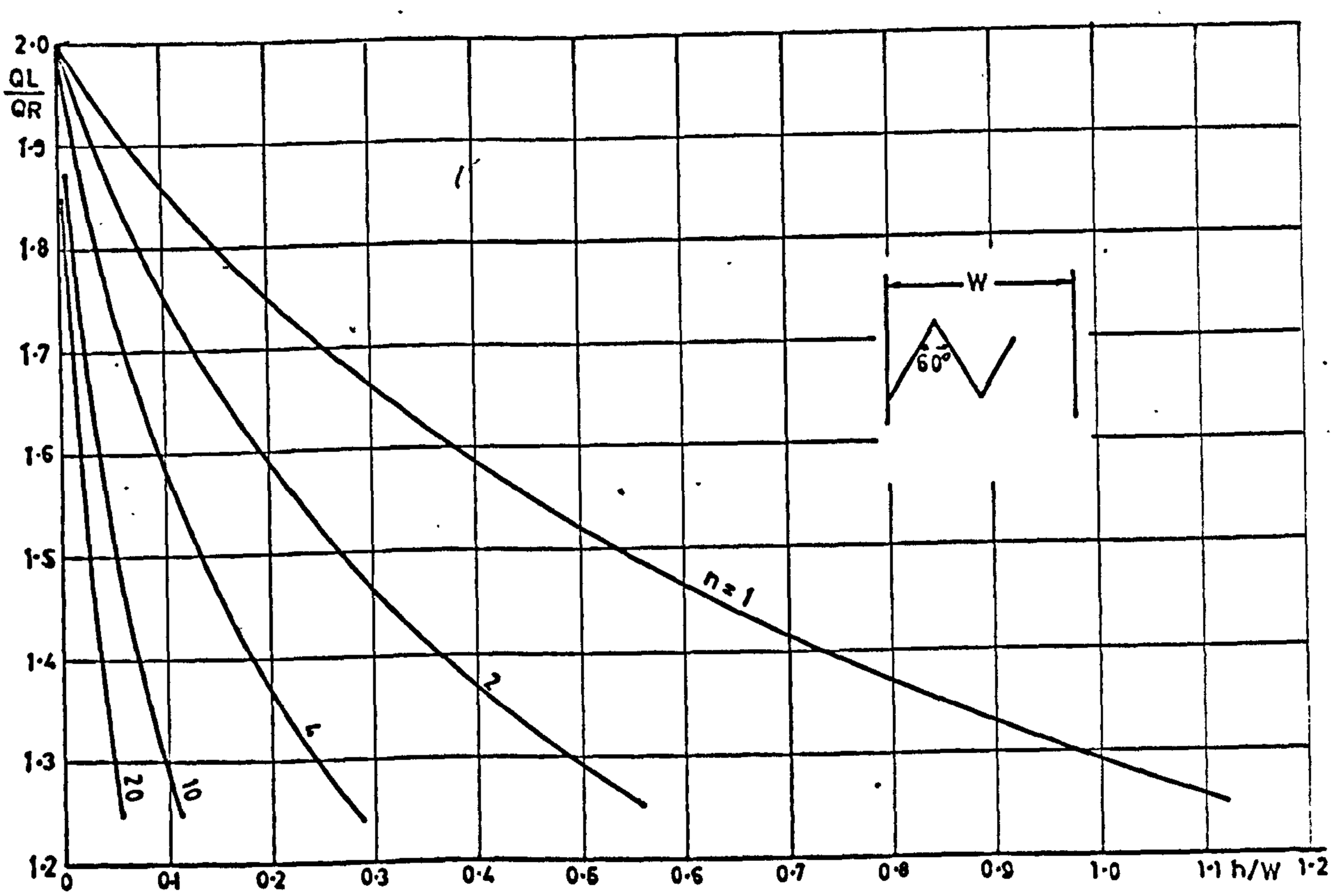

EXPERIMENTAL RESULTS OBTAINED BY GENTILINI

Flow magnification, QL/QR versus head to channel width ratio, h/W

Figure 5

EXPERIMENTAL RESULTS OBTAINED BY TISON AND FRANSEN

Flow magnification, QL/QR versus head to crest height ratio, h/p

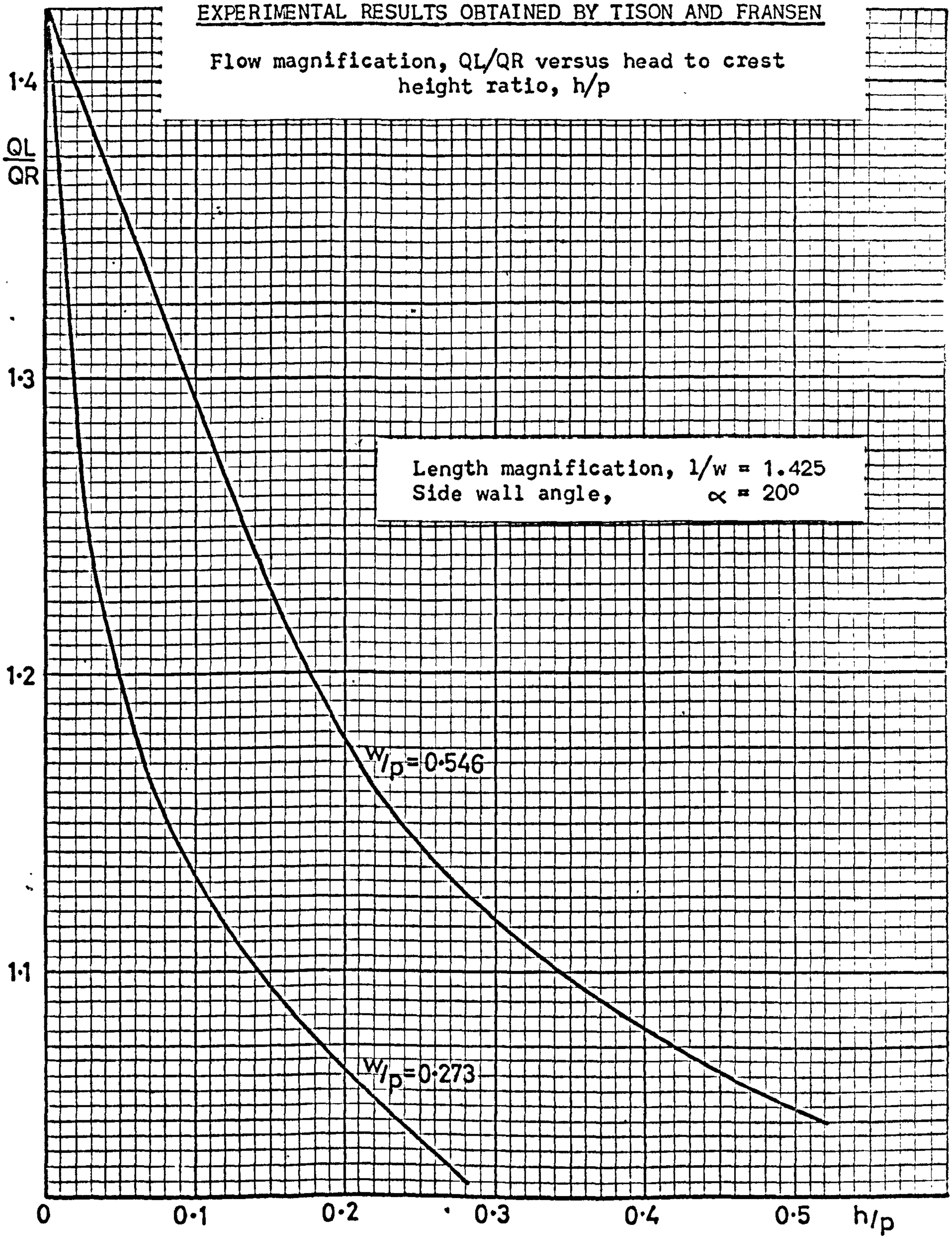

No.	PART
1	CONCRETE TANK 8ft × 4ft × 19ft DEEP
2	CHANNEL 3ft WIDE × 16ft LONG
3	HOPPER
4	FEED TANK
5	DALL TUBE
6	MOTOR OPERATED NEEDLE VALVE
7	10in SAUNDERS VALVE
8	14in FLOW STRAIGHTENER SECTION
9	CASCADED ELBOWS
10	CLEAR PERSPEX SECTION
11	ELECTRIC MOTORS 2 OFF.

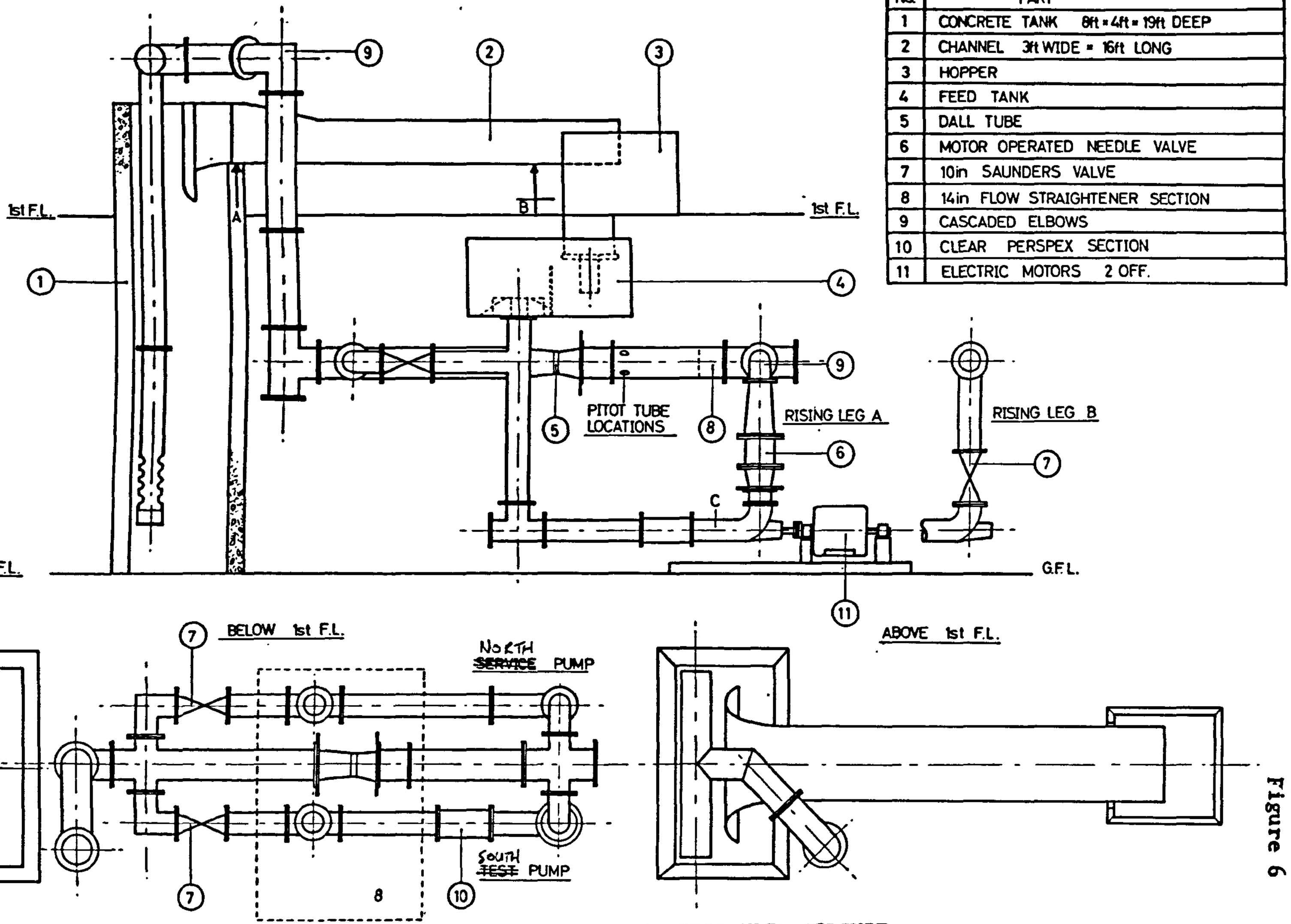

Figure 6

LAYOUT OF HYDRAULIC CIRCUIT

Figure 7

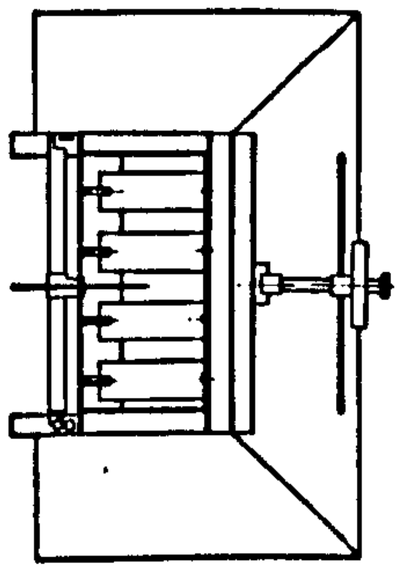

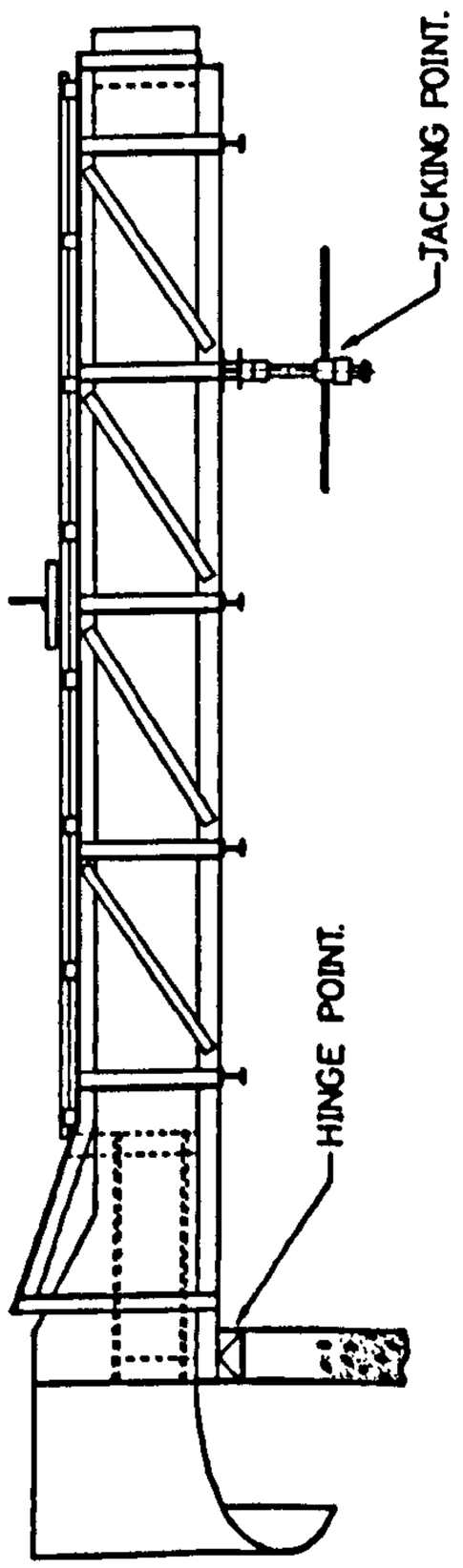

EXPERIMENTAL CHANNEL

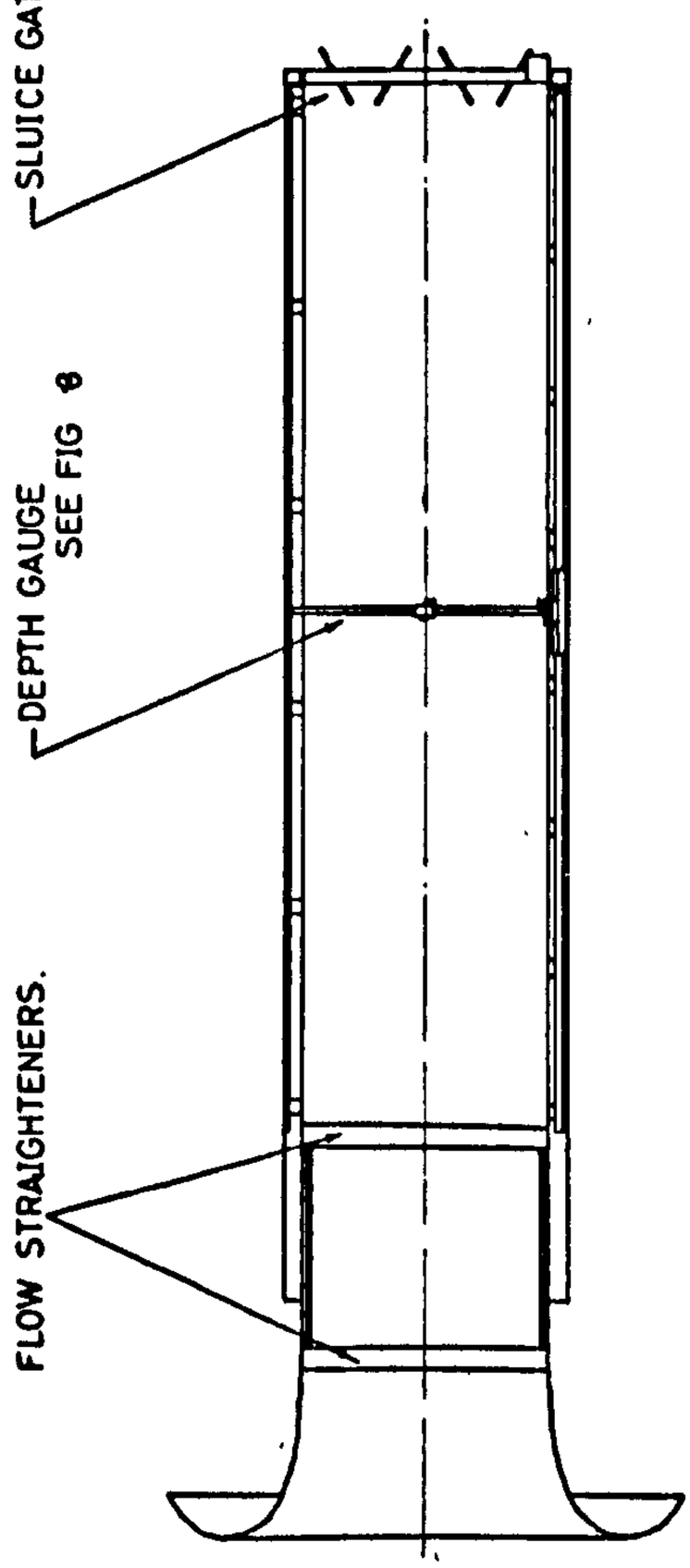

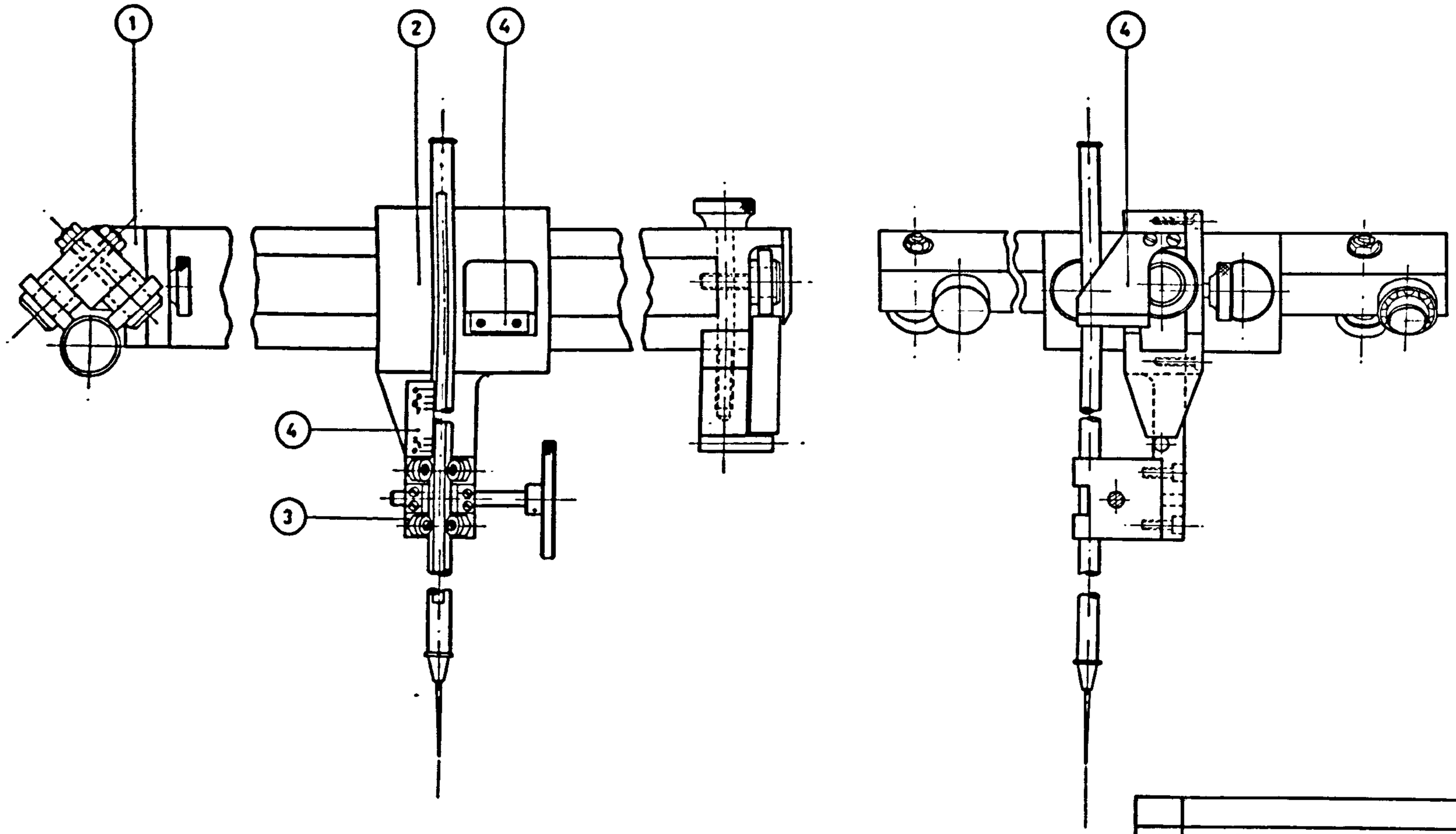

4	VERNIER SCALES.
3	GAUGING HEAD.
2	TRAVERSING BLOCK.
1	SLIDING CARRIAGE
No.	PART.

TRAVELLING DEPTH GAUGE ASSEMBLY

Figure 8

Figure 9

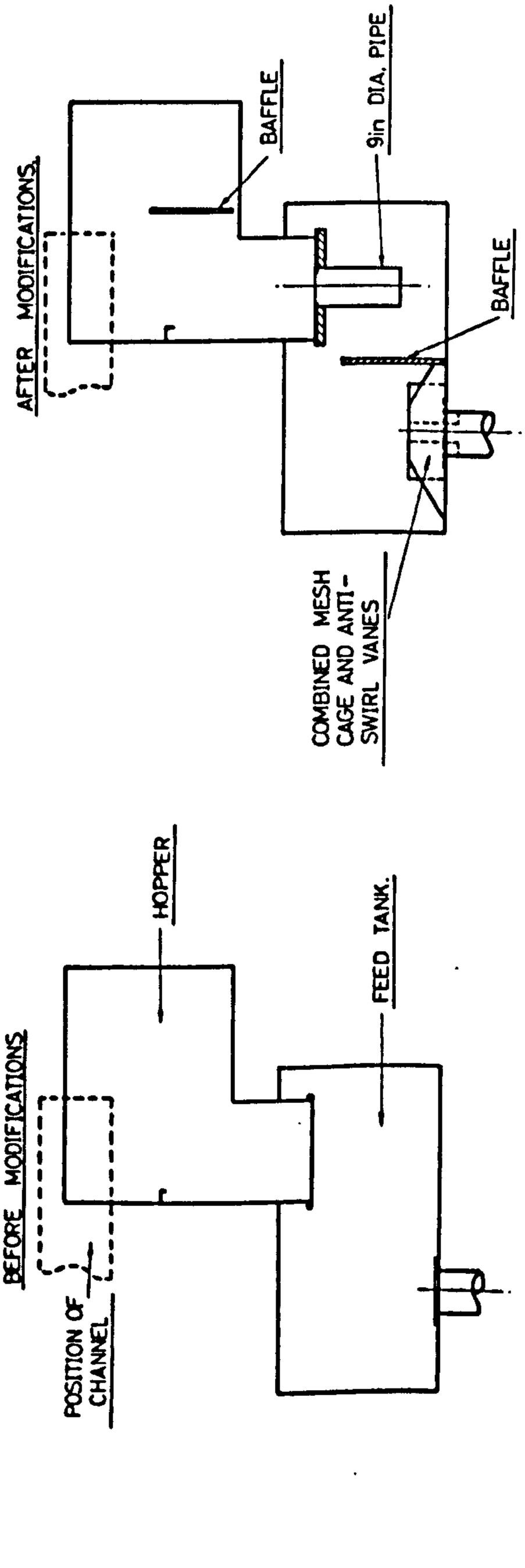

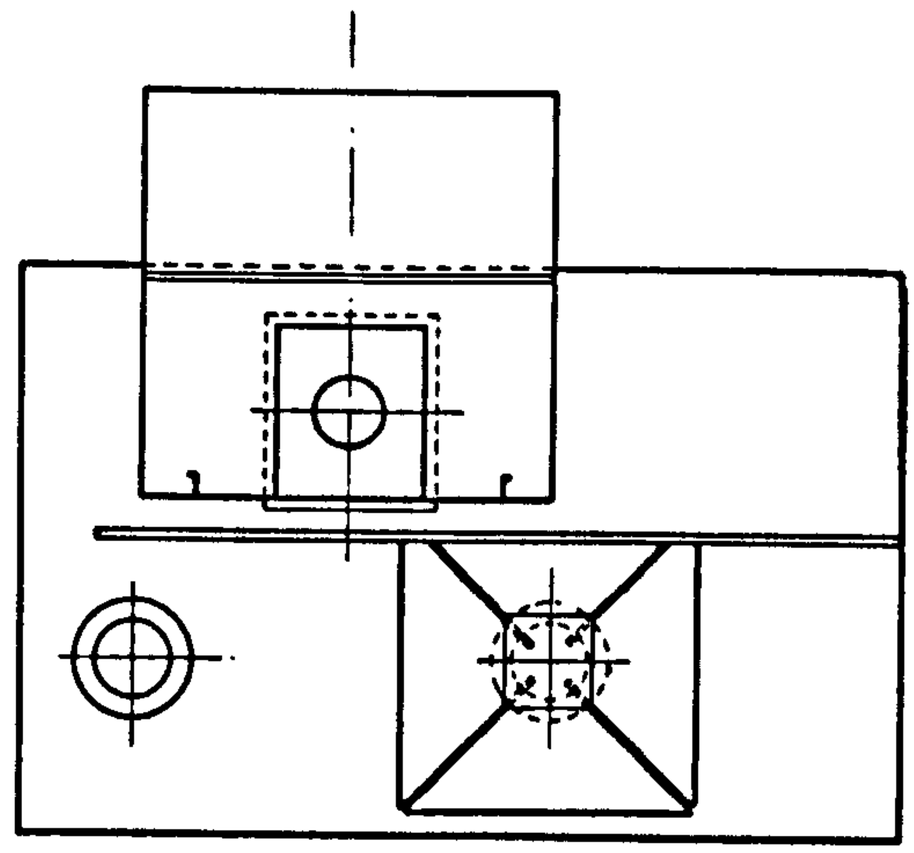

MODIFICATIONS TO ELIMINATE AIR ENTRAINMENT

Figure IO

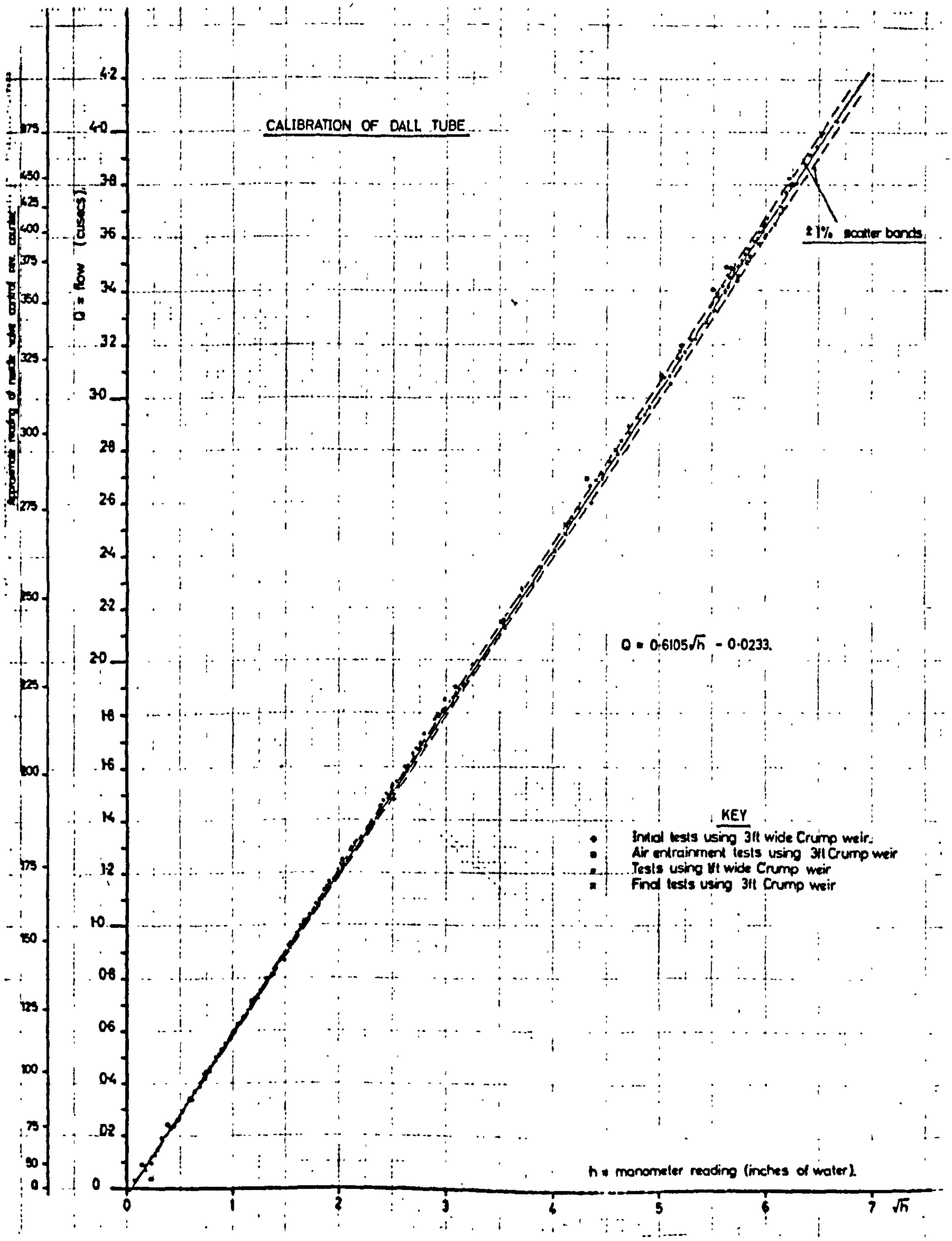

DALL TUBE CALIBRATION BY CRUMP WEIRS

Figure II

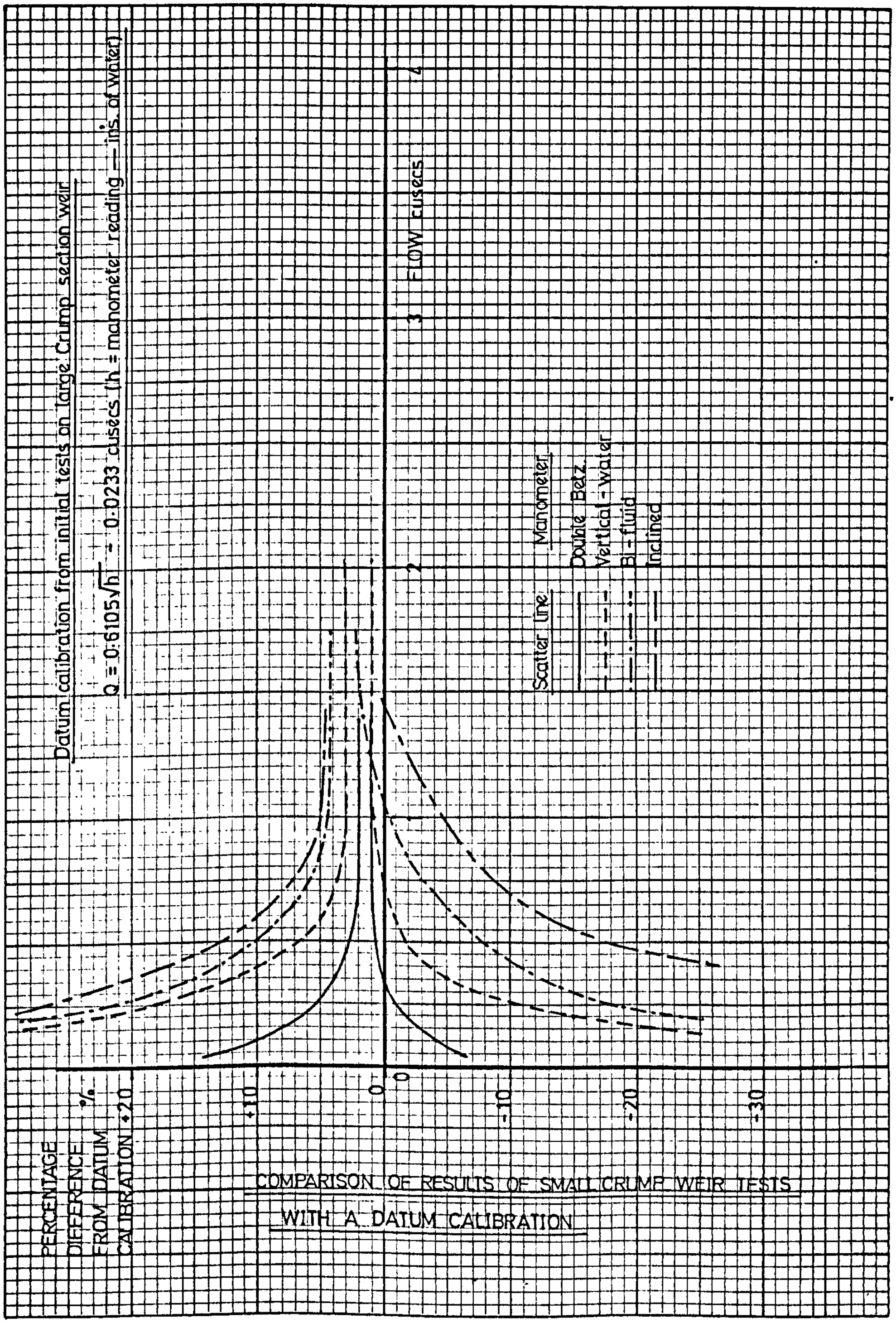
Datum calibration from initial tests on large Crump section weir
Q = 0·6105√h + 0·0233 cusecs (h = manometer reading — ins. of water)
FLOW cusecs
Scatter line
Manometer
Double Betz
Vertical - Water
Bi-fluid
Inclined
PERCENTAGE DIFFERENCE FROM DATUM CALIBRATION ±20 %
+10
0
-10
-20
-30
COMPARISON OF RESULTS OF SMALL CRUMP WEIR TESTS WITH A DATUM CALIBRATION

Figure 12

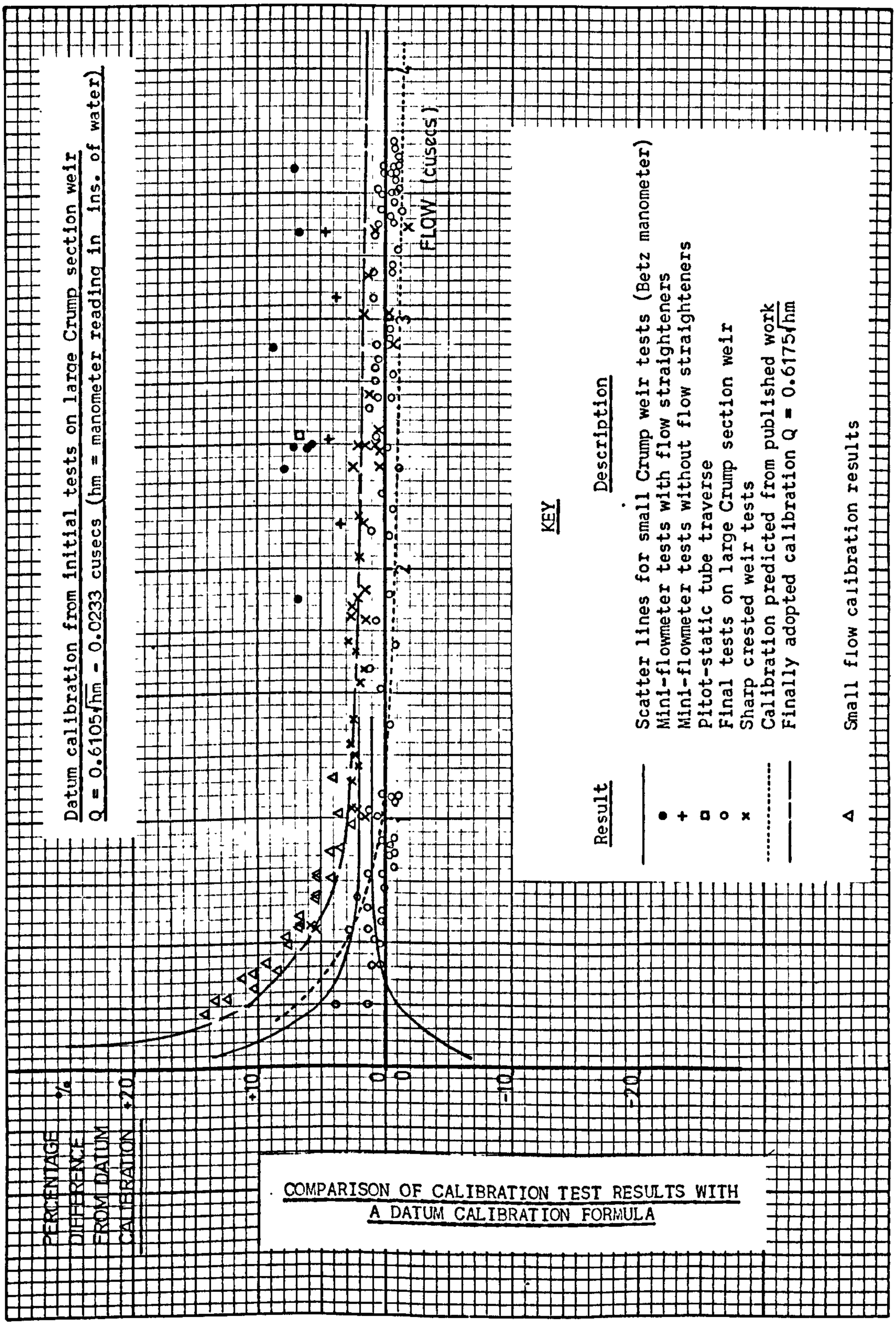
Datum calibration from initial tests on large Crump section weir
Q = 0.6105√hm - 0.0233 cusecs (hm = manometer reading in ins. of water)
FLOW (cusecs)
KEY
Result
Description
Scatter lines for small Crump weir tests
Mini-flowmeter tests with flow straighteners
Mini-flowmeter tests without flow straighteners
Pitot-static tube traverse
Final tests on large Crump section weir
Sharp crested weir tests
Calibration predicted from published work
Finally adopted calibration Q = 0.6175√hm
Small flow calibration results
PERCENTAGE % DIFFERENCE FROM DATUM CALIBRATION
+20
+10
0
-10
-20
COMPARISON OF CALIBRATION TEST RESULTS WITH A DATUM CALIBRATION FORMULA

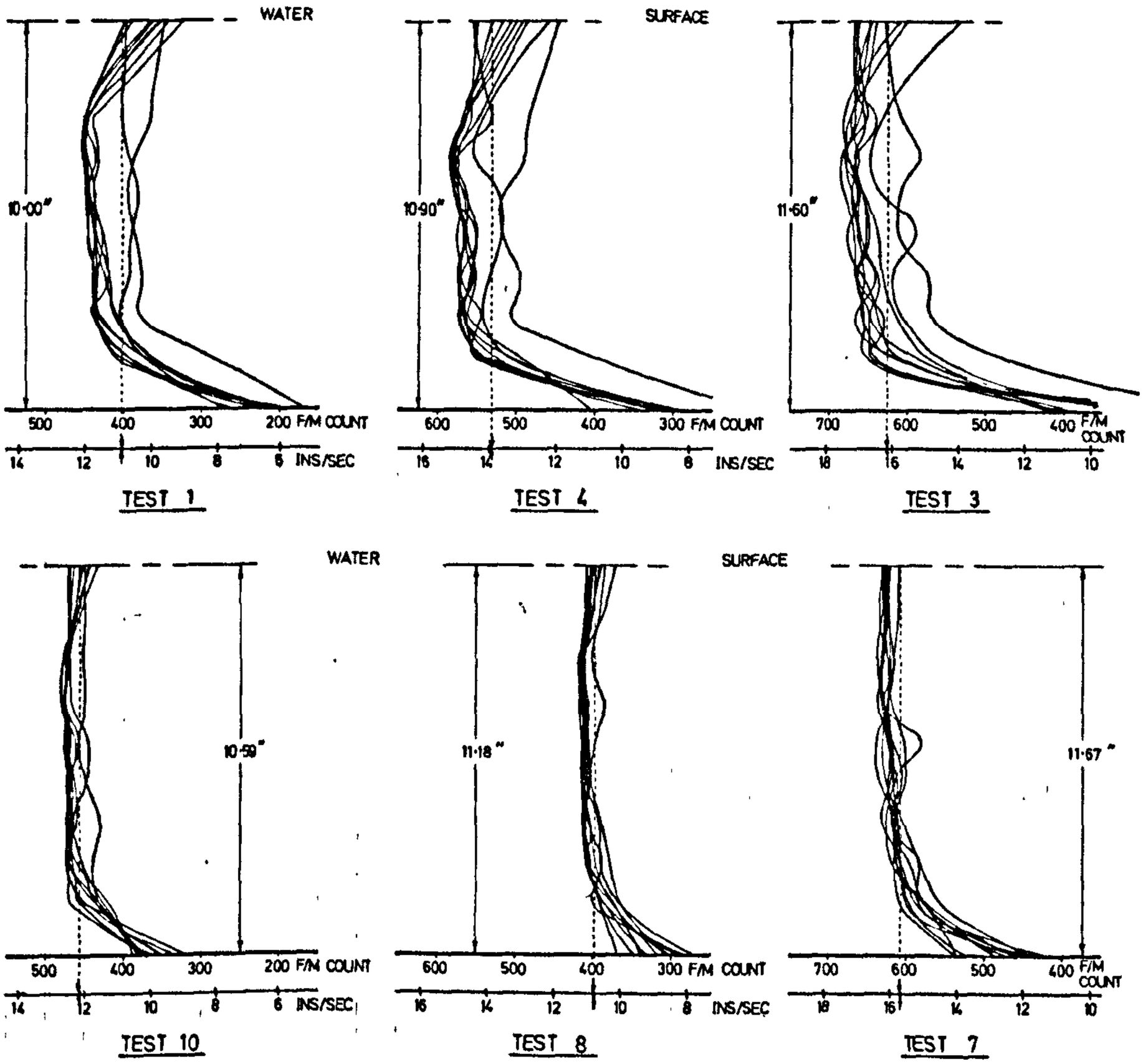

CALIBRATION OF DALL TUBE BY MINI-FLOWMETER ——— SAMPLE VELOCITY PROFILES

TESTS 1, 3 & 4 CONDUCTED WITH FLOW STRAIGHTENERS.

TESTS 2, 8 & 10 CONDUCTED WITHOUT FLOW STRAIGHTENERS.

The 10 velocity profiles shown for each test correspond to equal sections across the flow and result from 100 mini-flowmeter readings per test.

Figure 14

RELATION BETWEEN THE MAXIMUM SIDE WALL ANGLE, α

AND THE LENGTH MAGNIFICATION FACTOR, l/w

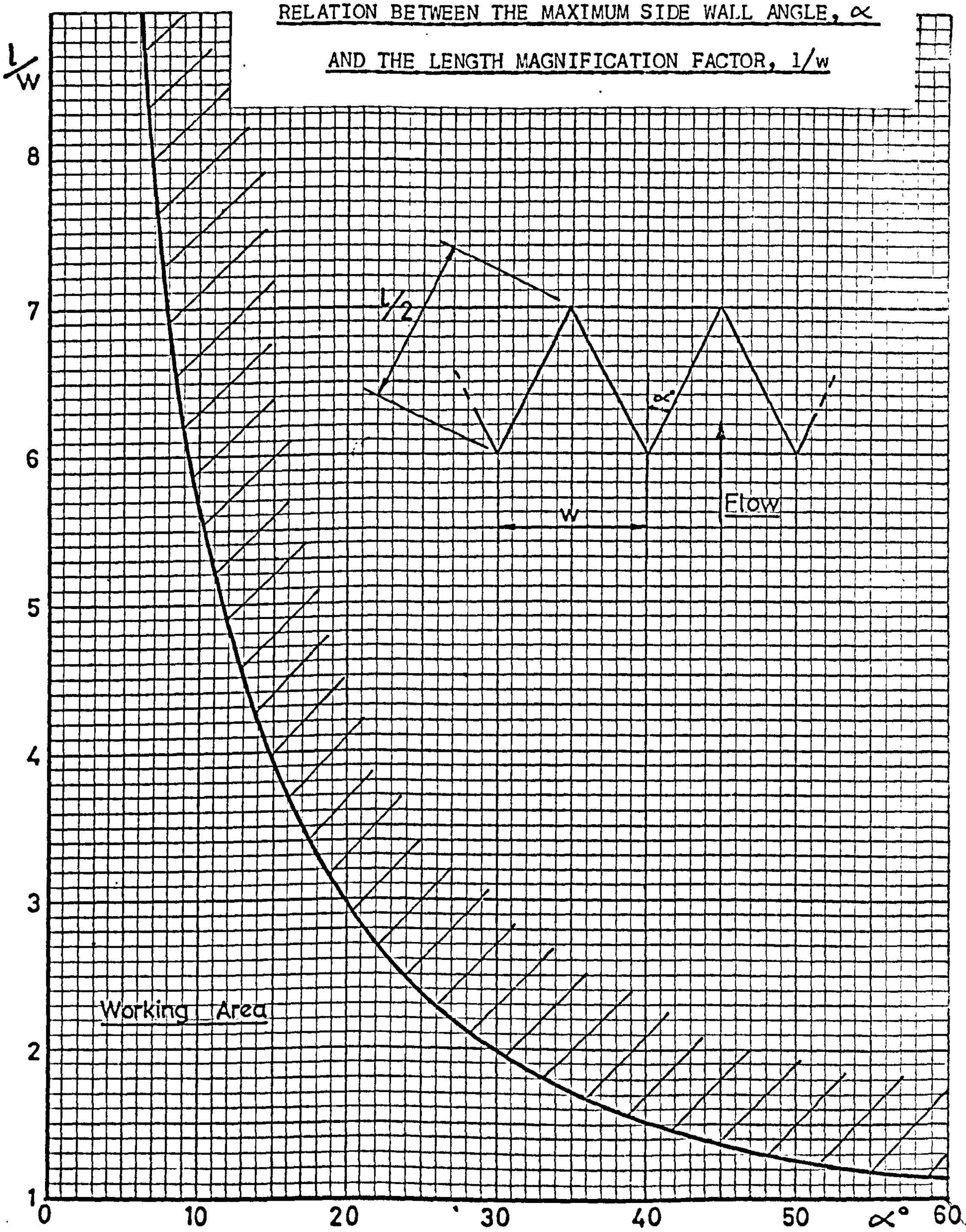

RELATION BETWEEN THE DEVELOPED CREST LENGTH OF A MODEL WEIR, l AND THE LENGTH MAGNIFICATION FACTOR, l/w, FOR VARIOUS NUMBERS OF CYCLES IN PLAN, n.

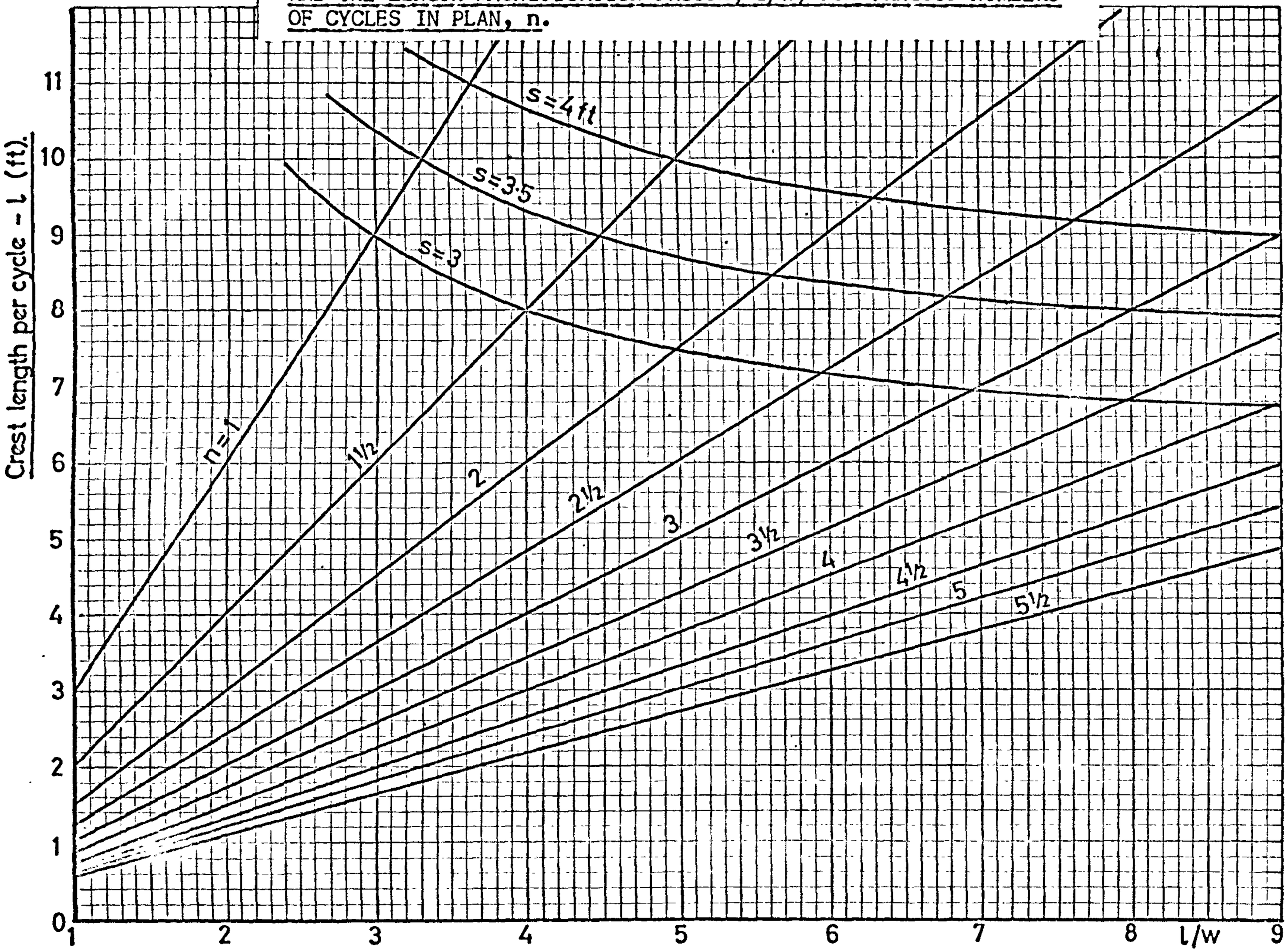

Figure 15

Figure 16

RELATION BETWEEN THE MODEL CREST HEIGHT, p, AND THE VERTICAL ASPECT RATIO, w/p, FOR VARIOUS NUMBERS OF CYCLES IN PLAN, n

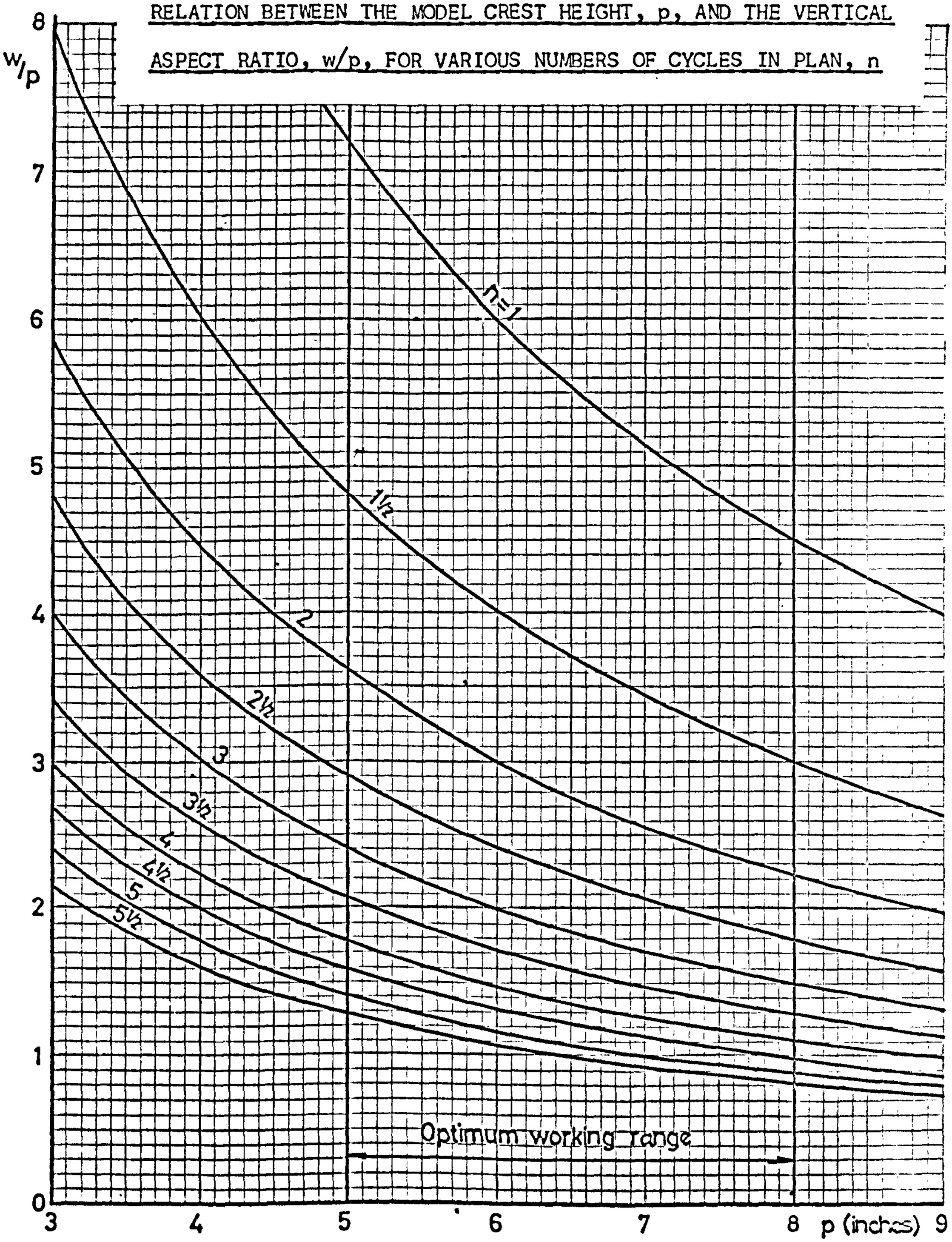

Figure 17

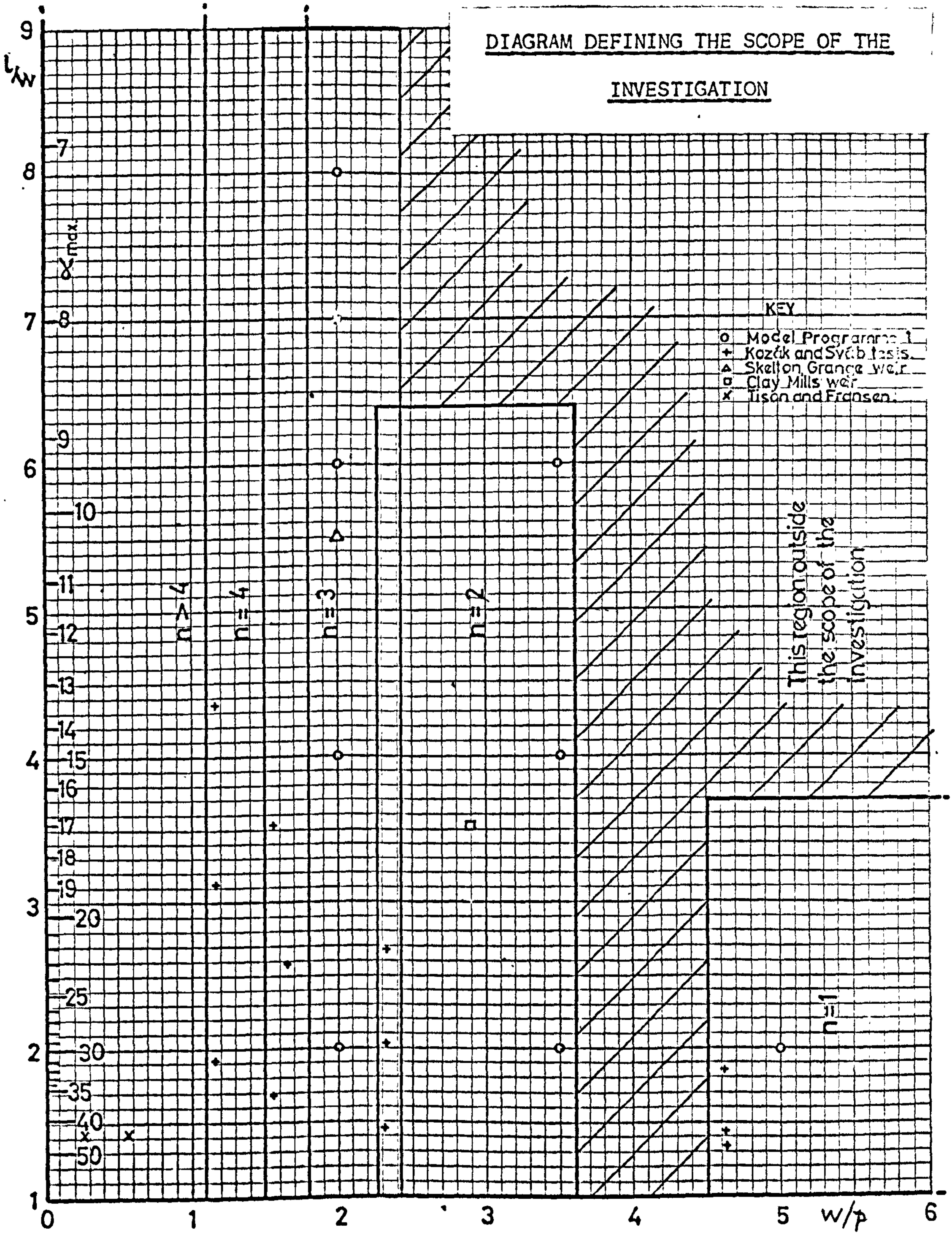
DIAGRAM DEFINING THE SCOPE OF THE INVESTIGATION
KEY
Model Programme 1
Kozák and Svab tests
Skelton Grange weir
Clay Mills weir
Tison and Fransen
This region outside the scope of the investigation
n>4
n=4
n=3
n=2
n=1
L_w
γ_{max}
w/p
9
8
7
6
5
4
3
2
1
0
1
2
3
4
5
6
7
8
9
10
11
12
13
14
15
16
17
18
19
20
25
30
35
40
50

Figure 18

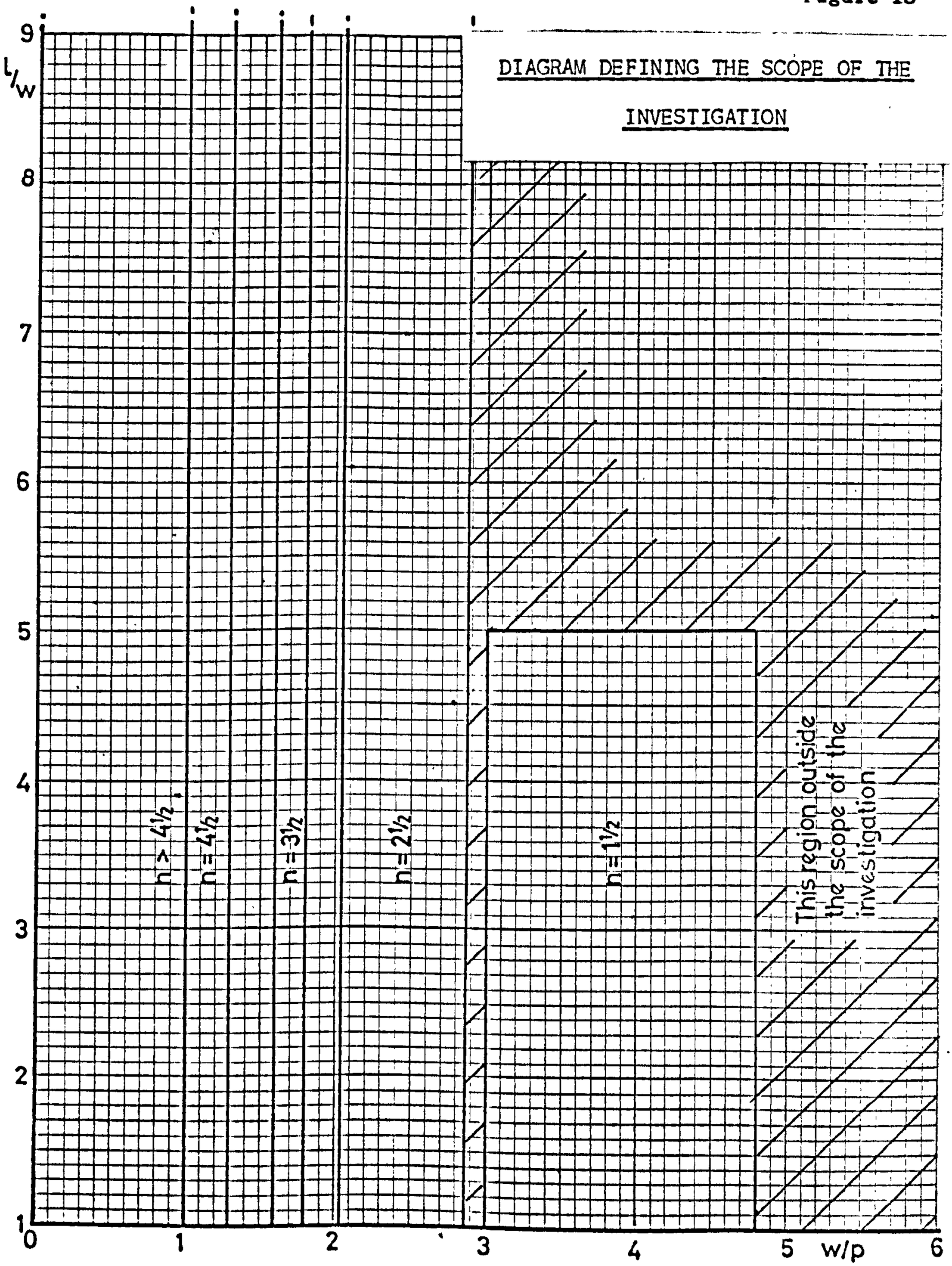
DIAGRAM DEFINING THE SCOPE OF THE INVESTIGATION
l/w
9
8
7
6
5
4
3
2
1
0
1
2
3
4
5
w/p
6
n ≥ 4½
n = 4½
n = 3½
n = 2½
n = 1½
This region outside the scope of the investigation

Figure 19

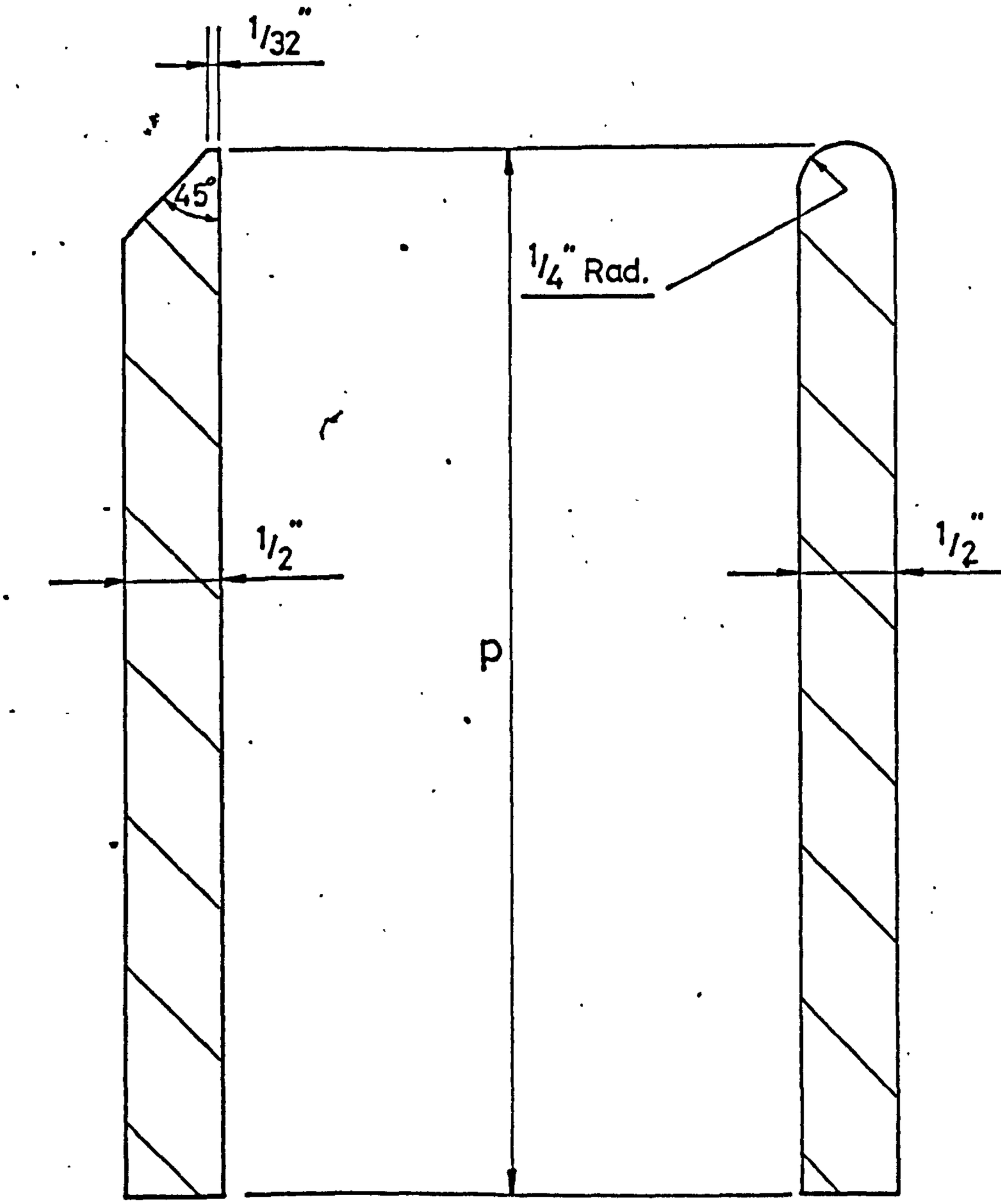

Sharp crest section

Semi-circular crest section

MODEL CREST SECTIONS

Figure 20

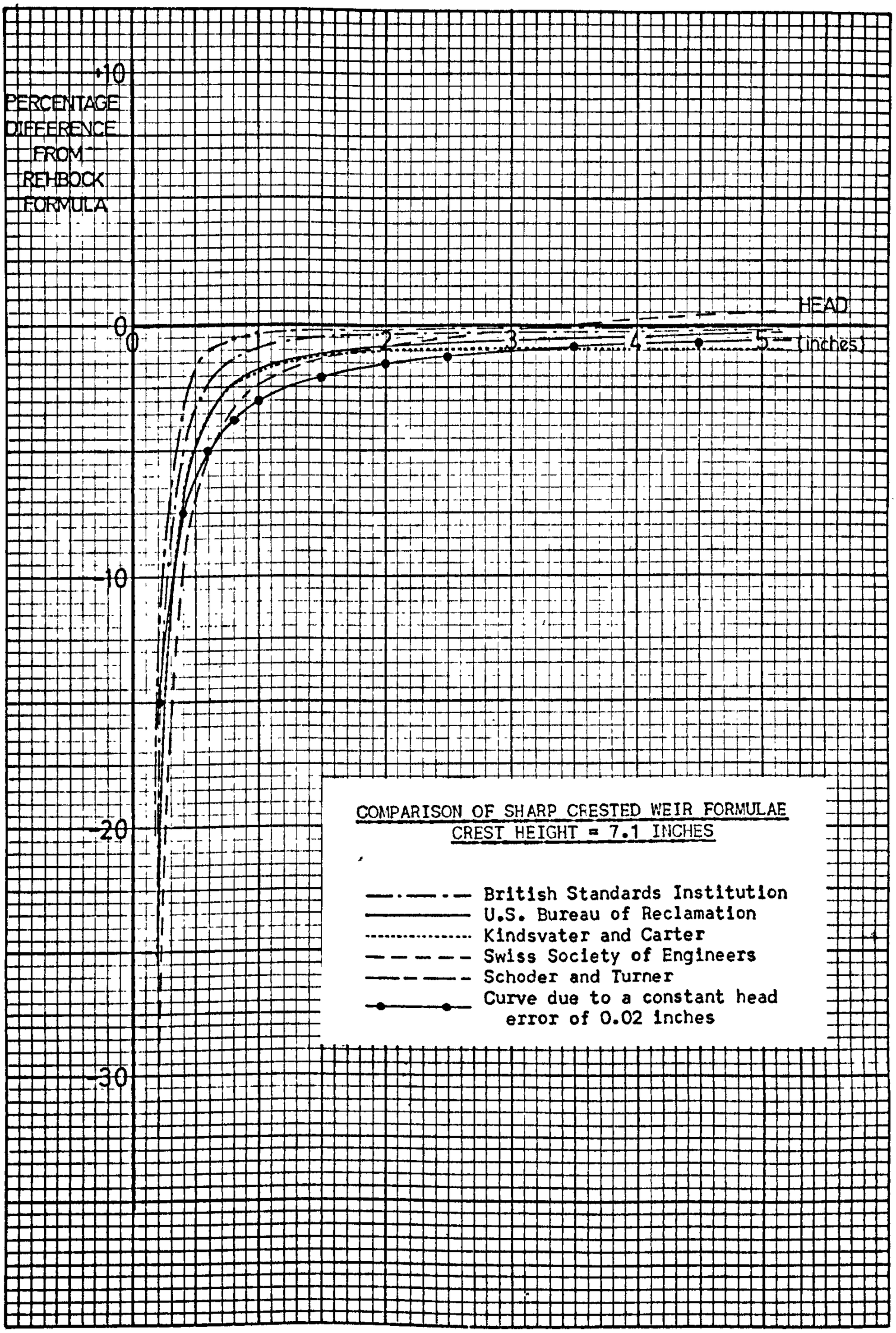
+10
PERCENTAGE DIFFERENCE FROM REHBOCK FORMULA
0
0
1
2
3
4
5
HEAD (inches)
-10
-20
-30
COMPARISON OF SHARP CRESTED WEIR FORMULAE
CREST HEIGHT = 7.1 INCHES
British Standards Institution
U.S. Bureau of Reclamation
Kindsvater and Carter
Swiss Society of Engineers
Schoder and Turner
Curve due to a constant head error of 0.02 inches

Figure 21

SCHEMATIC SHAPES OF MODELS IN MODEL PROGRAMME NO. 1

(continued over)

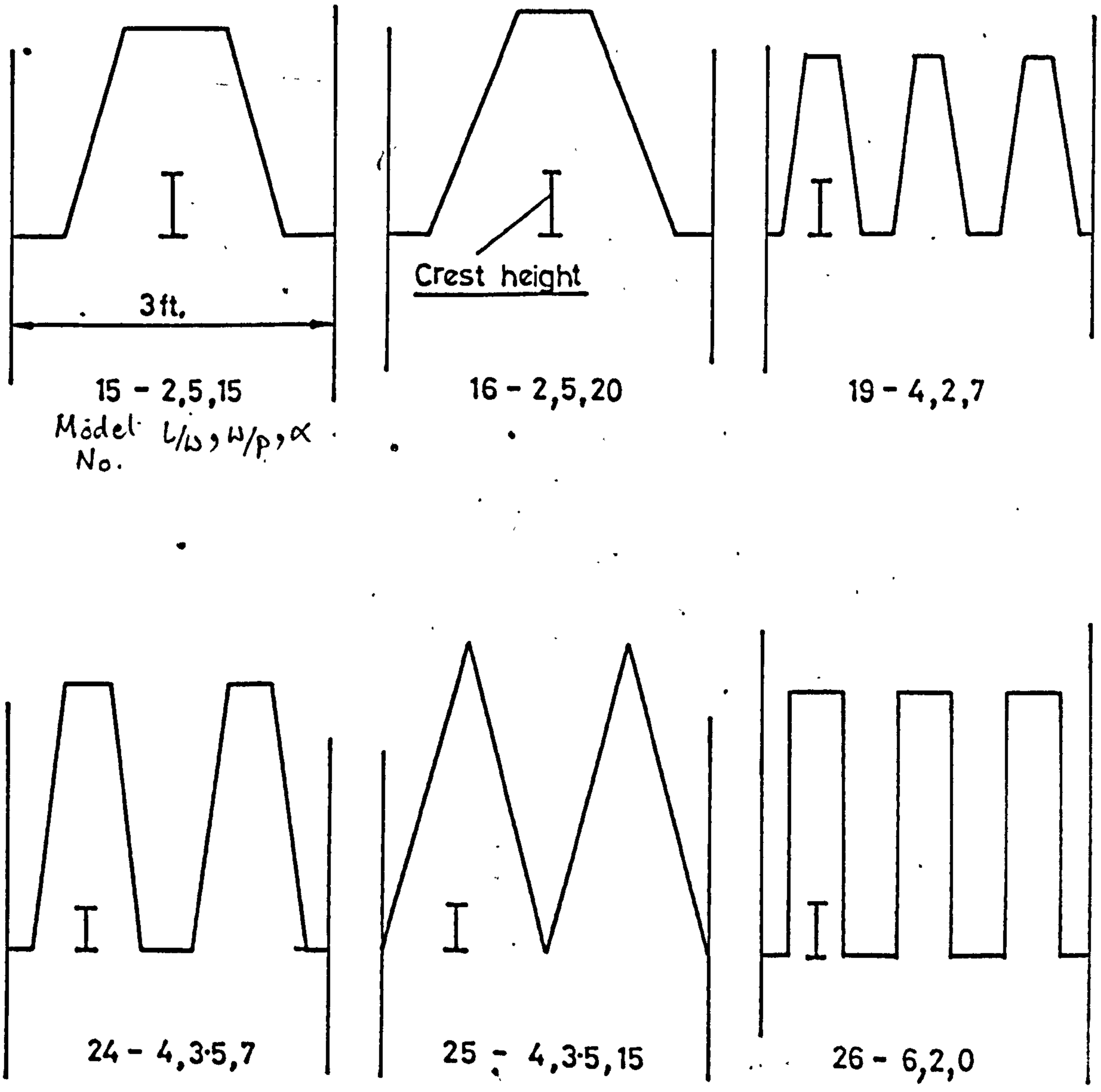

Model No. $L/\omega, \omega/p, \alpha$

Figure 21 continued

SCHEMATIC SHAPES OF MODELS IN MODEL PROGRAMME NO. 1. (CONT.)

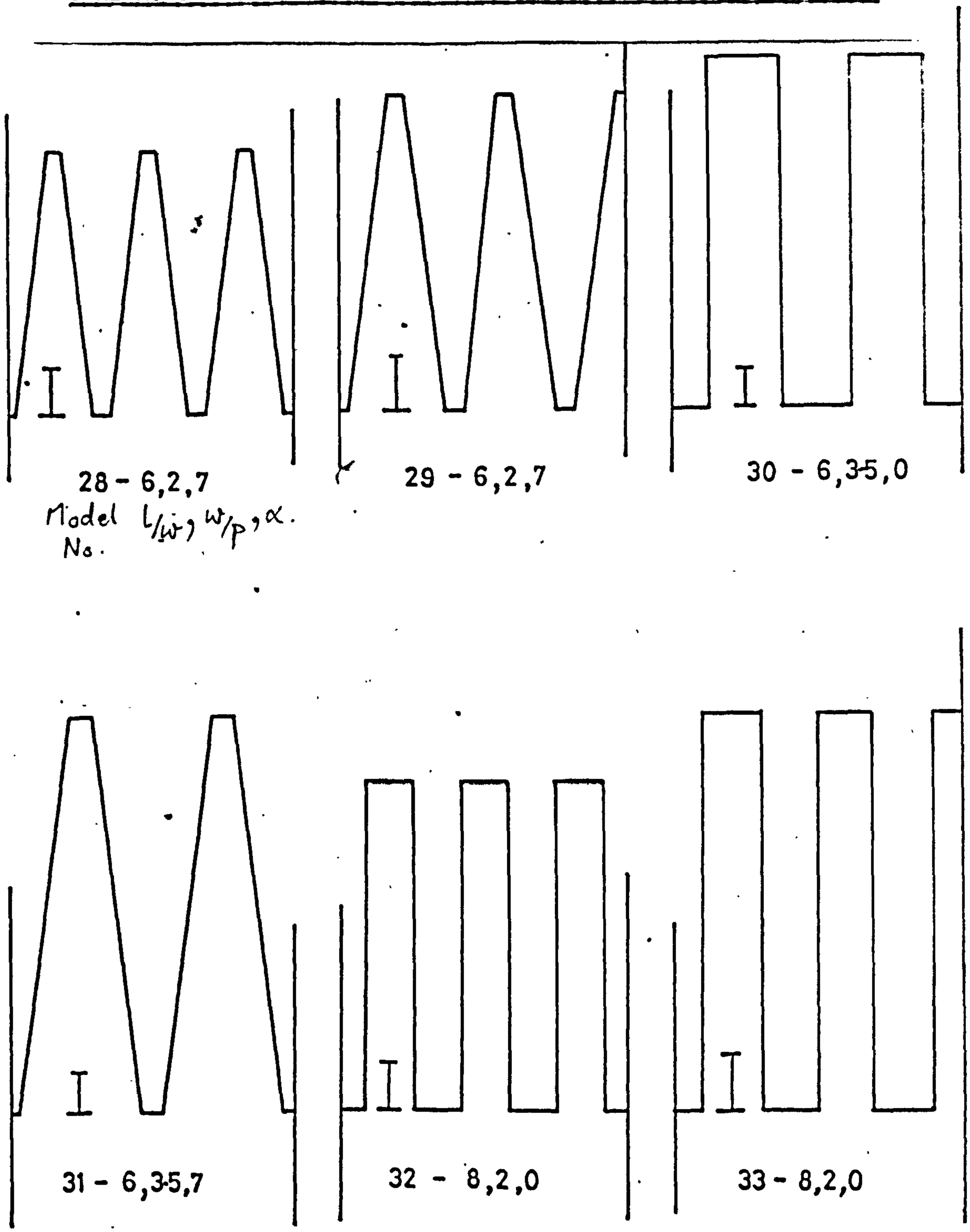

Figure 22

COMPOSITE PERFORMANCE RESULTS OBTAINED FROM MODEL PROGRAMME

No. 1 USING THE REHBOCK FORMULA FOR THE CALCULATION OF QR

IN THE FLOW MAGNIFICATION, QL/QR

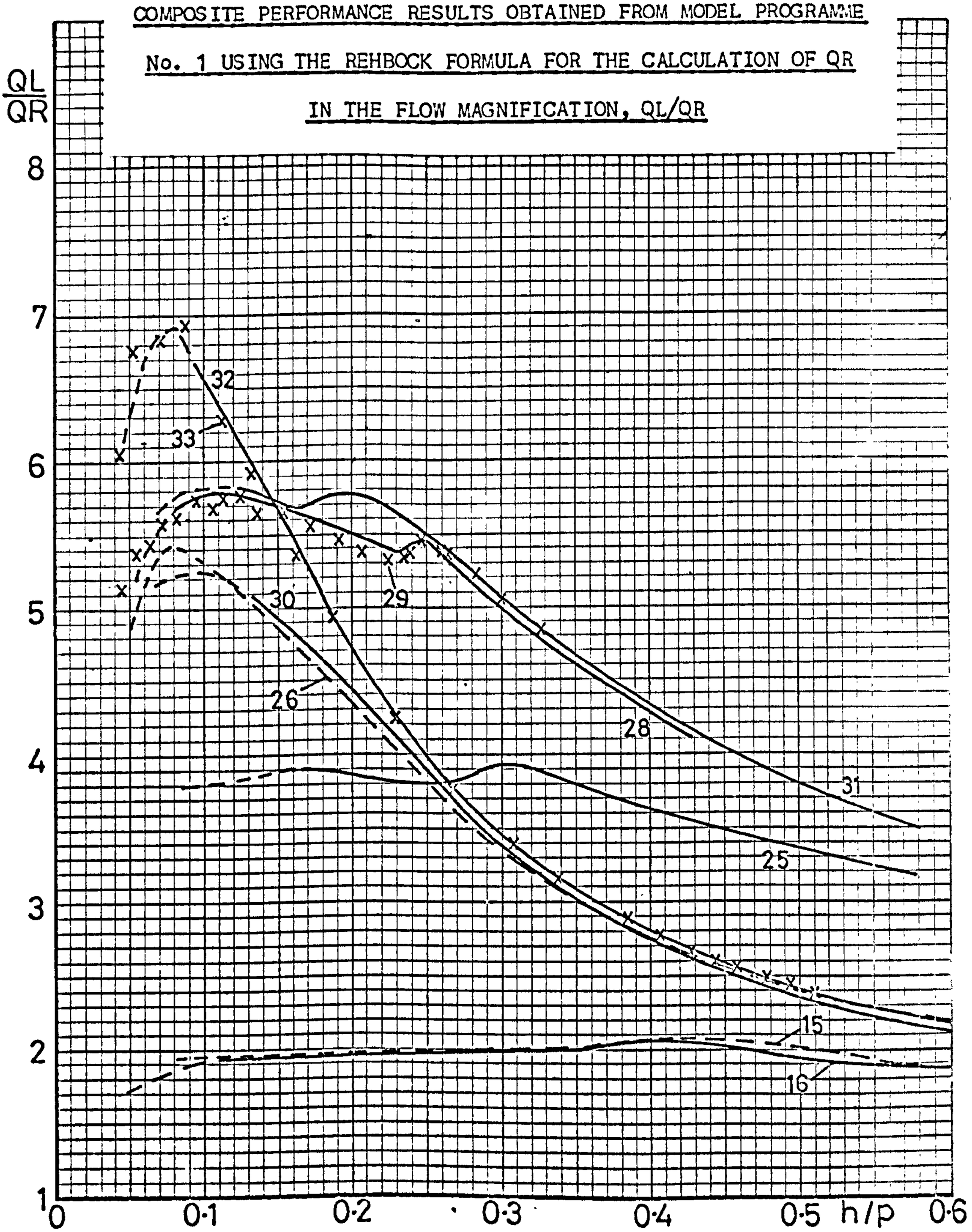

Figure 23

COMPOSITE PERFORMANCE RESULTS OBTAINED FROM MODEL PROGRAMME

No. 1 USING THE REHBOCK FORMULA FOR THE CALCULATION OF QR

IN THE EFFECTIVENESS E

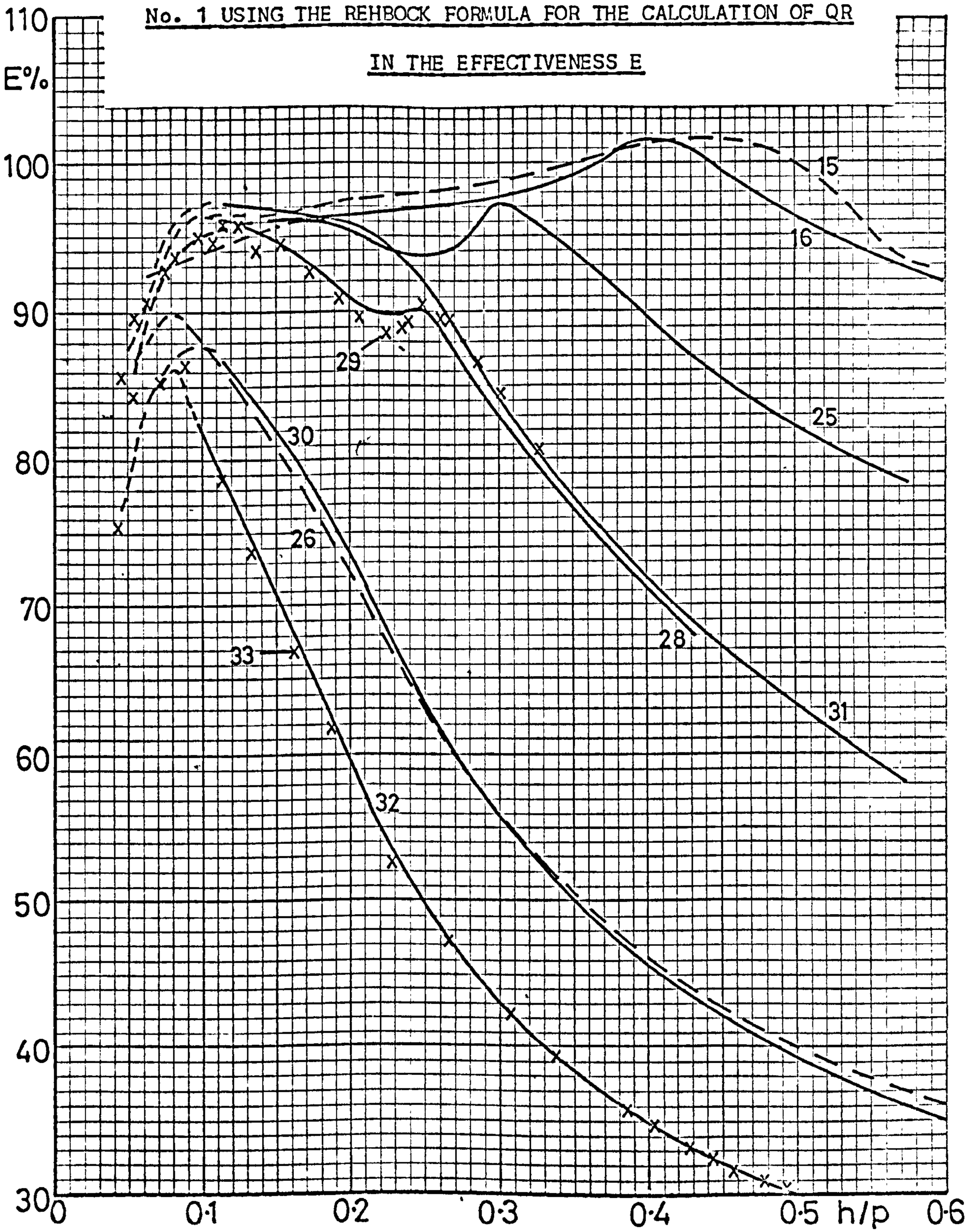

Figure 24

COMPOSITE PERFORMANCE RESULTS OBTAINED FROM MODEL PROGRAMME No. 1 WITH THE FLOW MAGNIFICATION, QL/QR, CORRECTED BY USE OF THE KINDSVATER AND CARTER WEIR FORMULA

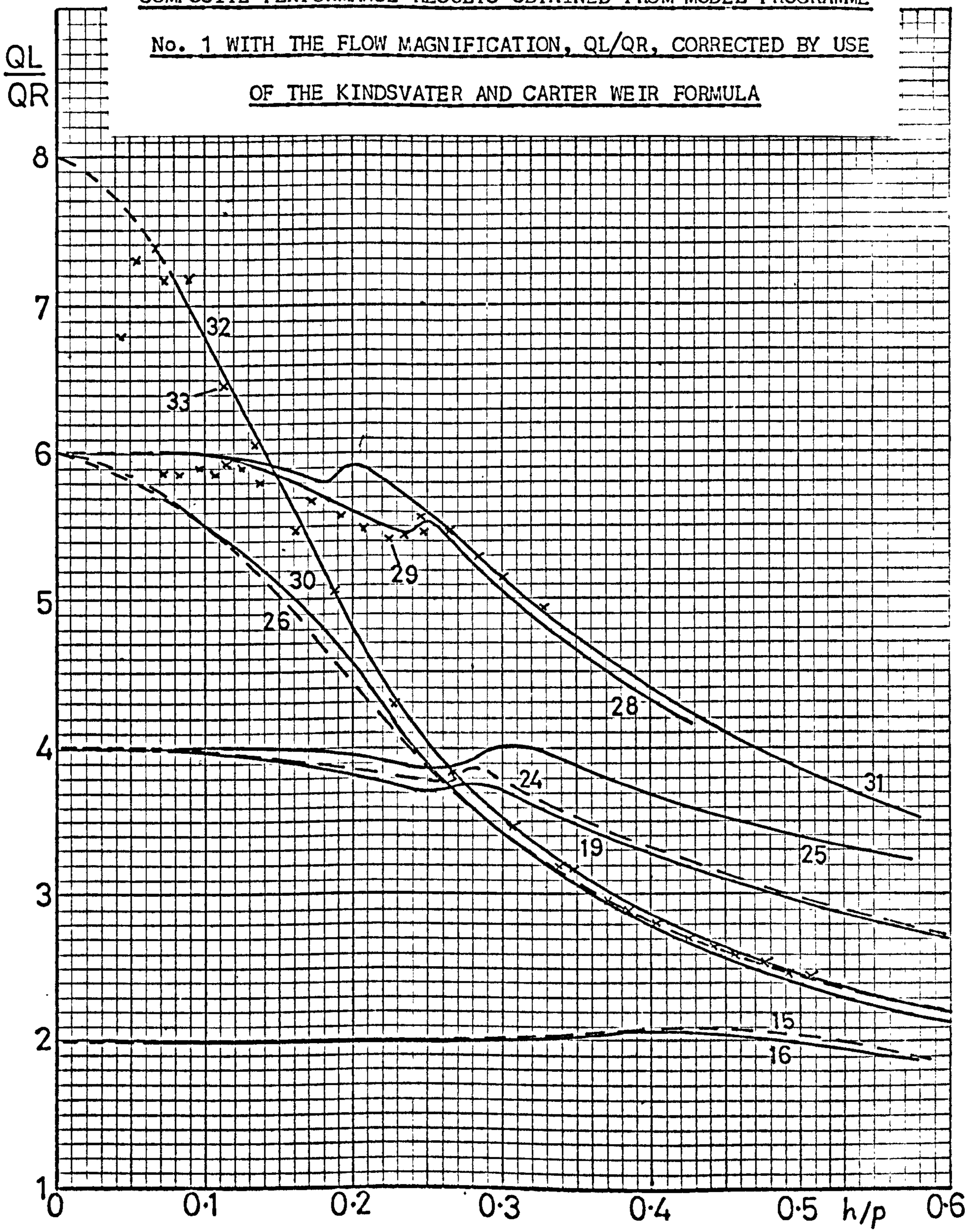

Figure 25

COMPOSITE PERFORMANCE RESULTS OBTAINED FROM MODEL PROGRAMME No. 1 WITH THE EFFECTIVENESS, E, CORRECTED BY USE OF THE KINDSVATER AND CARTER WEIR FORMULA

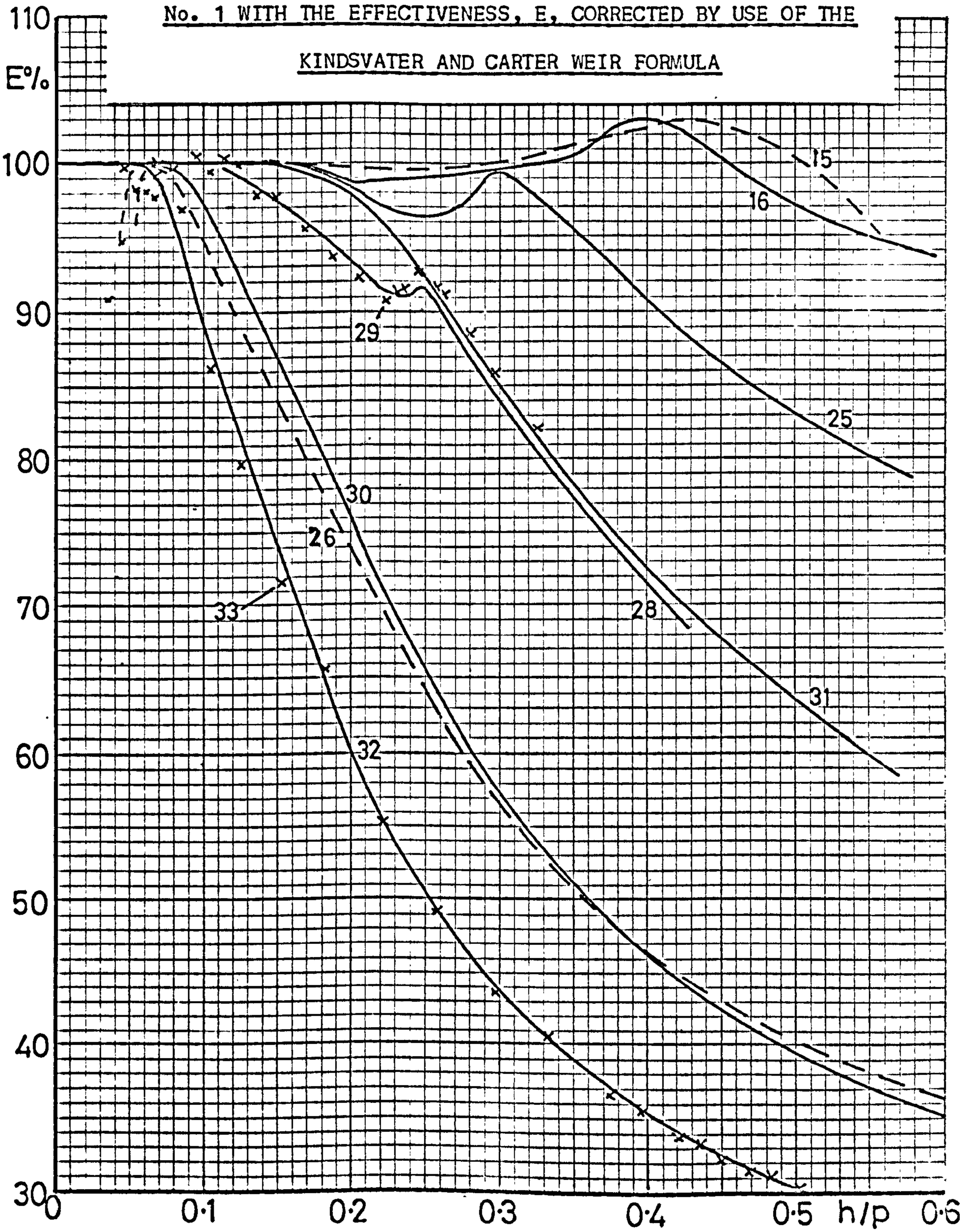

EXPERIMENTAL TEST RESULTS MODEL NO. 15

$l/w = 2$, $w/p = 5$, $\alpha = 15^{\circ}$, (trapezoidal plan)

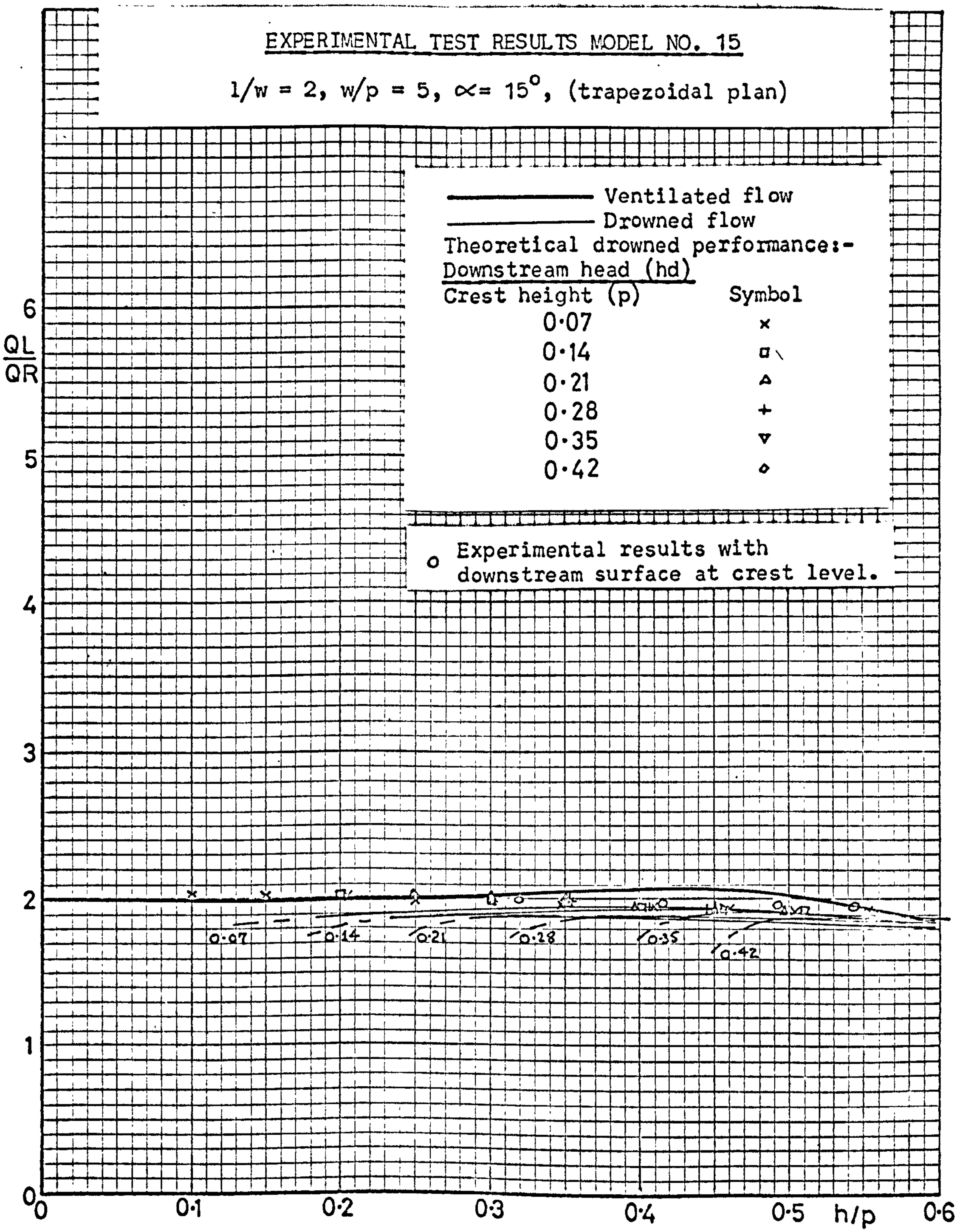

Figure 27

EXPERIMENTAL TEST RESULTS MODEL NO. 16

$l/w = 2$, $w/p = 5$, $\alpha = 20^{\circ}$ (trapezoidal plan)

——————— Ventilated flow

——————— Drowned flow

Theoretical drowned performance:-

Downstream head (hd) / Crest height (p)	Symbol
0·075	×
0·150	□
0·225	△
0·300	+
0·375	▽

o Experimental results with downstream surface at crest level.

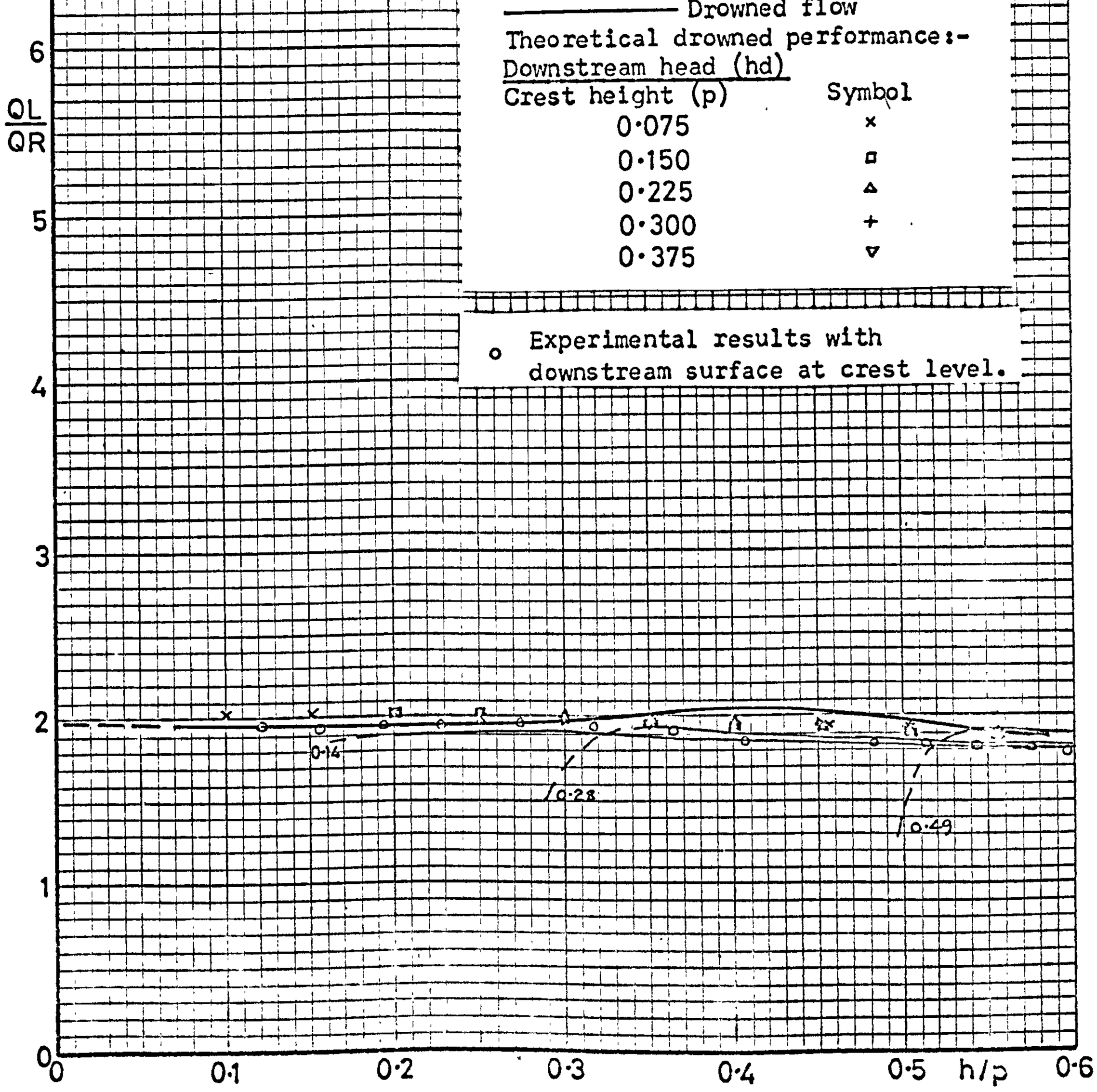

Figure 28

EXPERIMENTAL TEST RESULTS MODEL NO. 19

$l/w = 4$, $w/p = 2$, $\alpha = 7^{\circ}$ (trapezoidal plan)

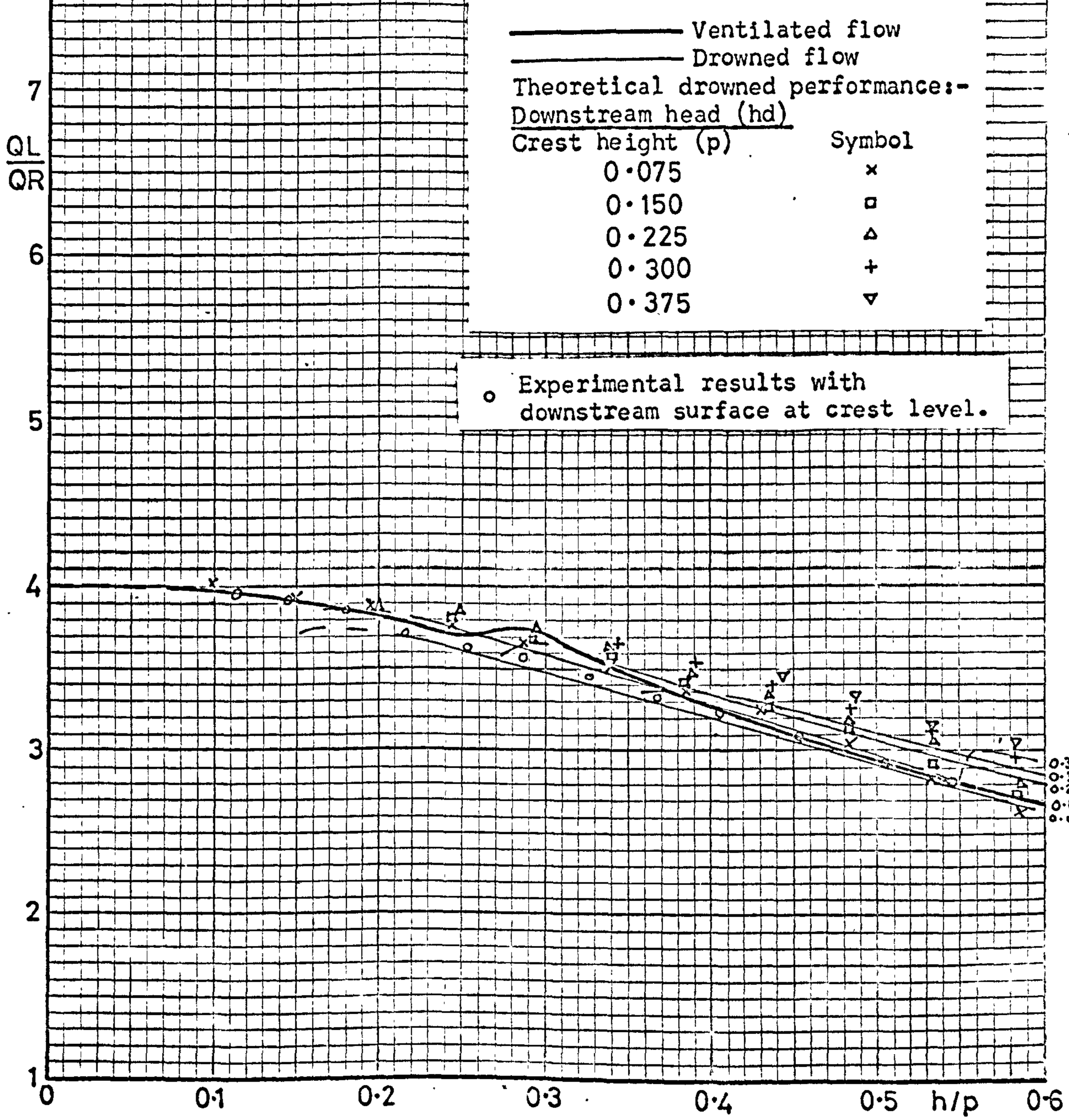

o

Figure 29

EXPERIMENTAL TEST RESULTS MODEL NO. 24

$l/w = 4$, $w/p = 3.5$, $\alpha = 7^{\circ}$ (trapezoidal plan)

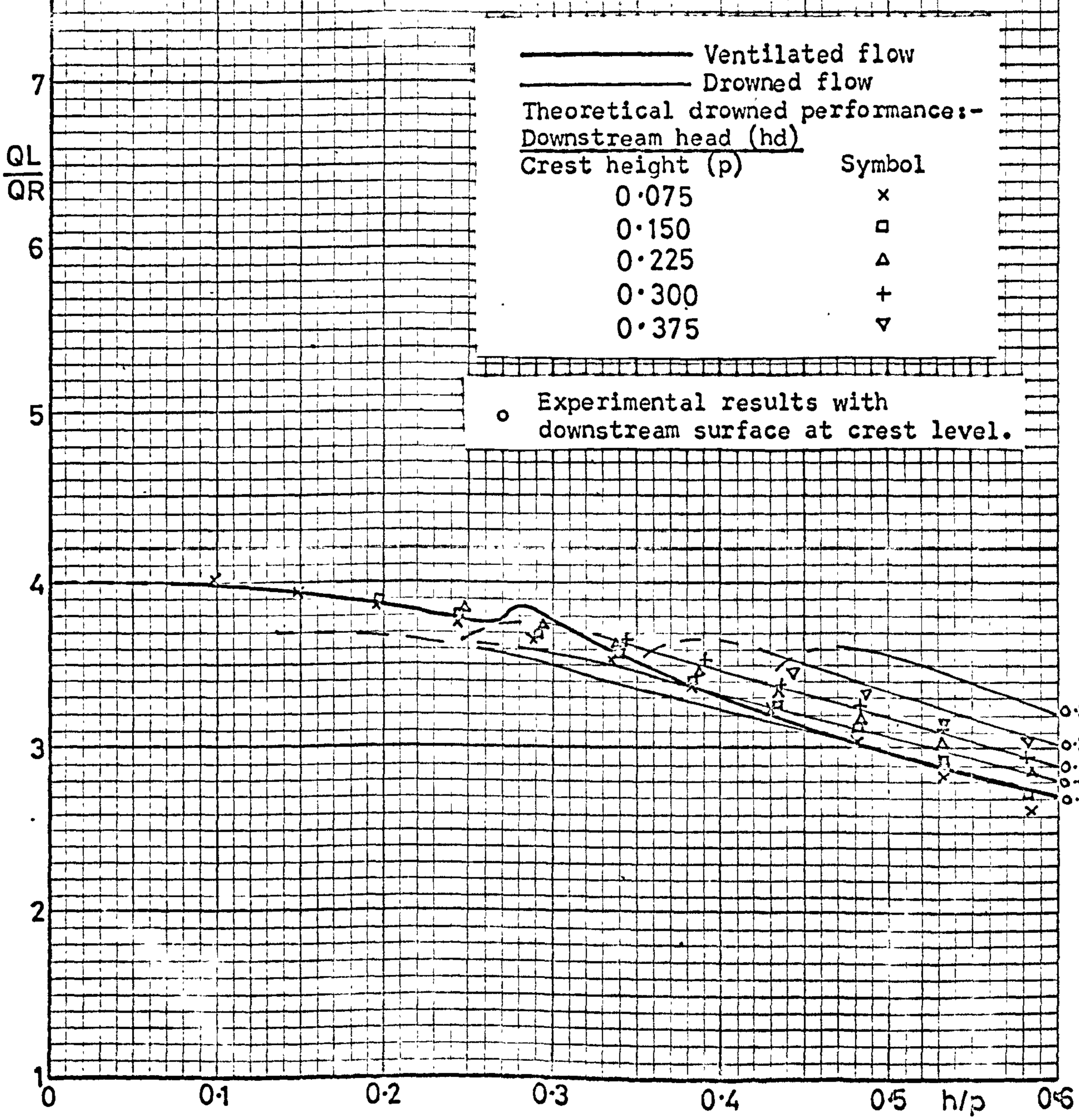

Figure 30

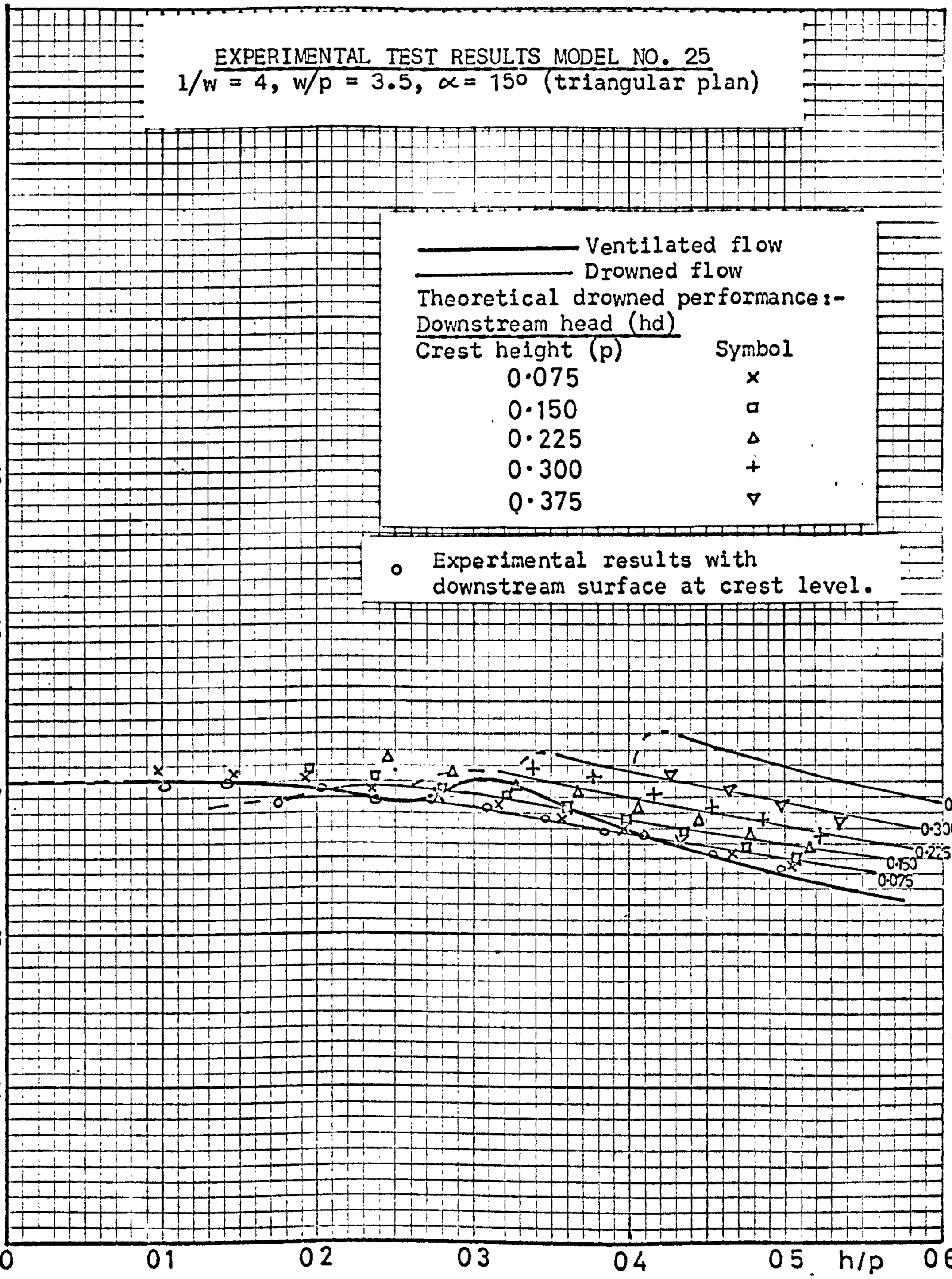
EXPERIMENTAL TEST RESULTS MODEL NO. 25
l/w = 4, w/p = 3.5, ∝ = 15° (triangular plan)
Ventilated flow
Drowned flow
Theoretical drowned performance:-
Downstream head (hd)
Crest height (p) Symbol
0·075 ×
0·150 □
0·225 △
0·300 +
0·375 ▽
o Experimental results with downstream surface at crest level.
QL/QR
7
6
5
4
3
2
1
0
01
02
03
04
05
h/p
06
0·375
0·300
0·225
0·150
0·075

Figure 31

EXPERIMENTAL TEST RESULTS MODEL NO. 26
$l/w = 6$, $w/p = 2$, $\alpha = 0^{o}$ (rectangular plan)

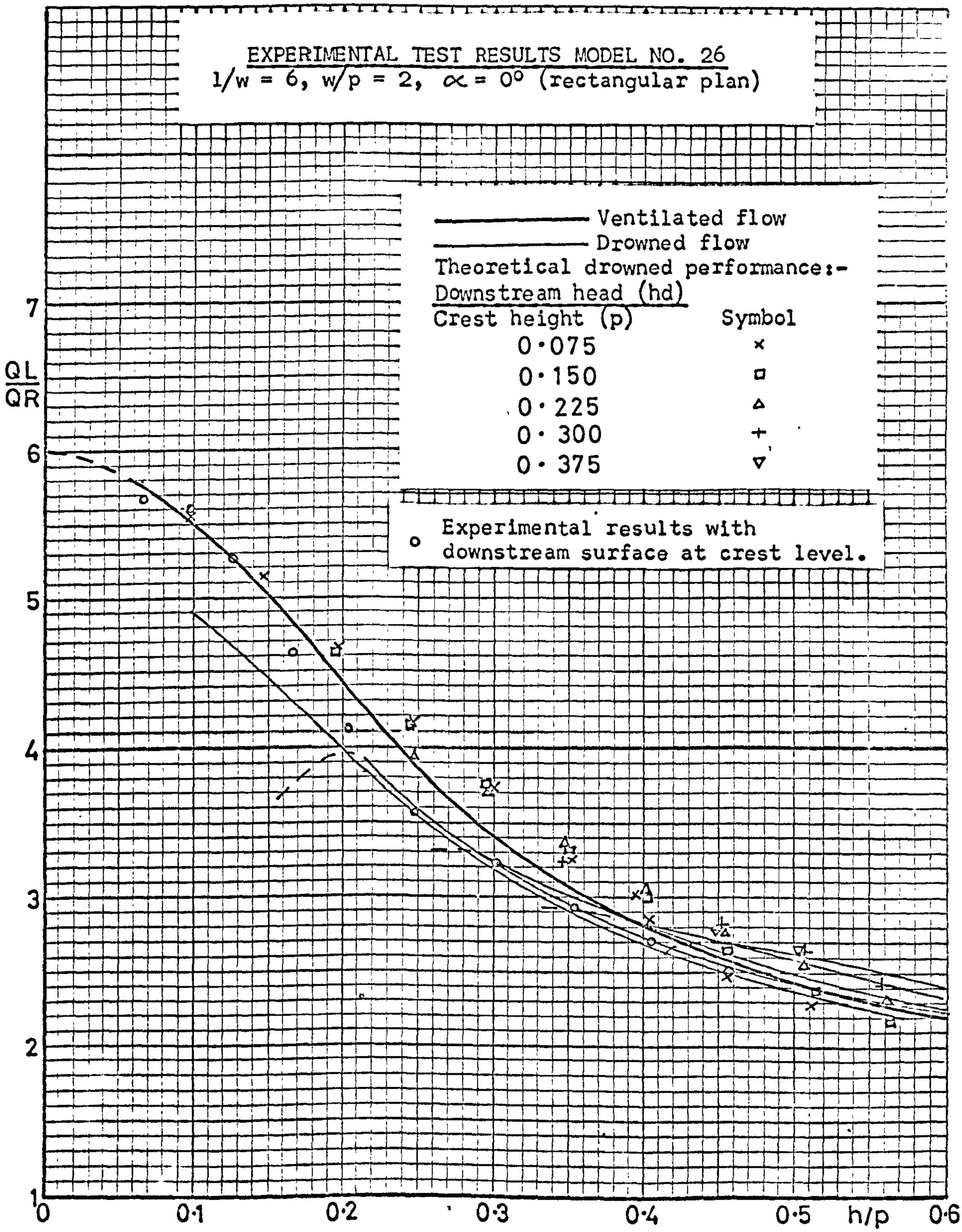

Figure 32

EXPERIMENTAL TEST RESULTS MODEL NO. 28
$l/w = 6$, $w/p = 2$, $\alpha = 7^o$ (trapezoidal plan)

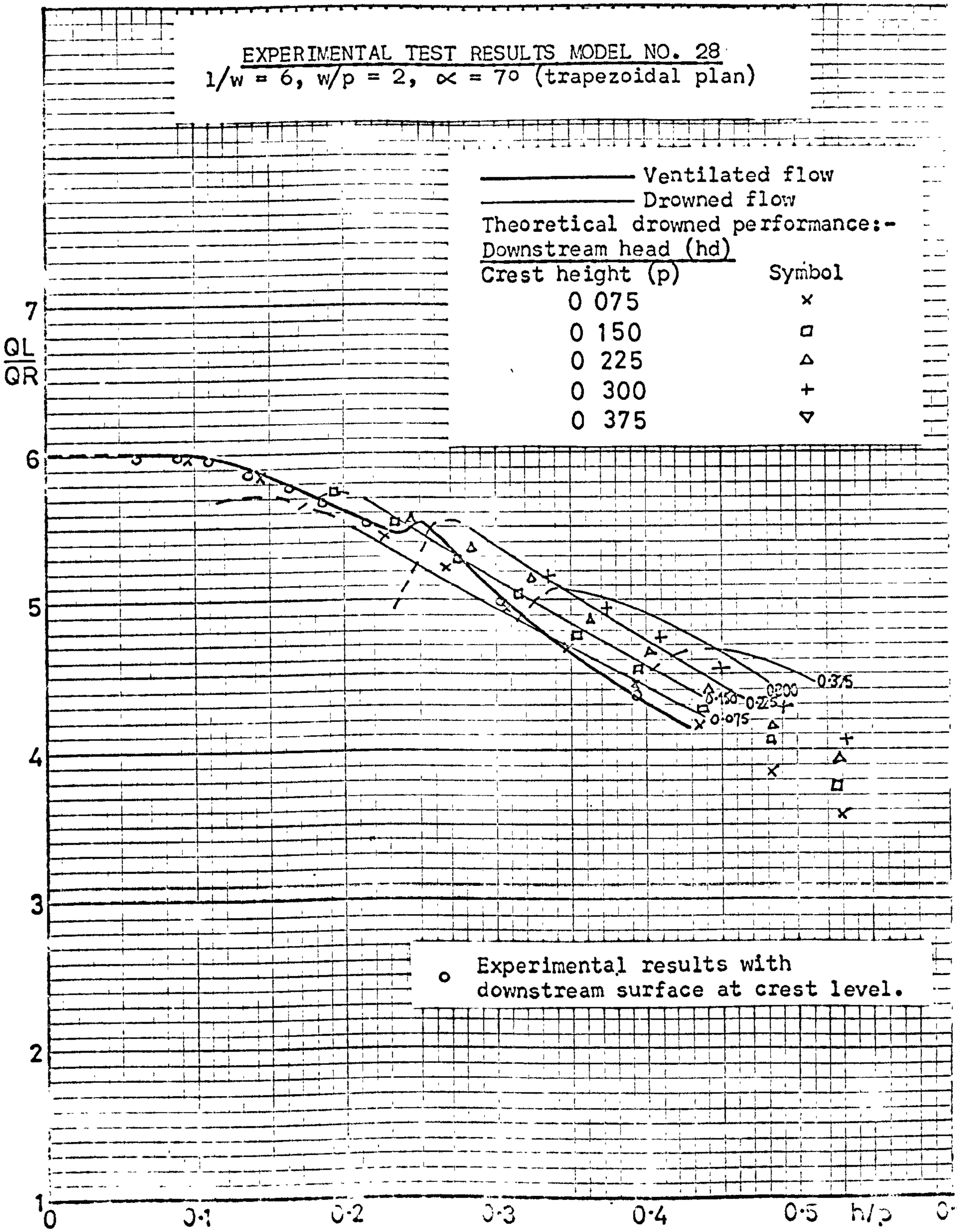

Figure 33

EXPERIMENTAL TEST RESULTS MODEL NO. 29

$l/w = 6$, $w/p = 2$, $\alpha = 7^{\circ}$, $n = 2.5$ (trapezoidal plan)

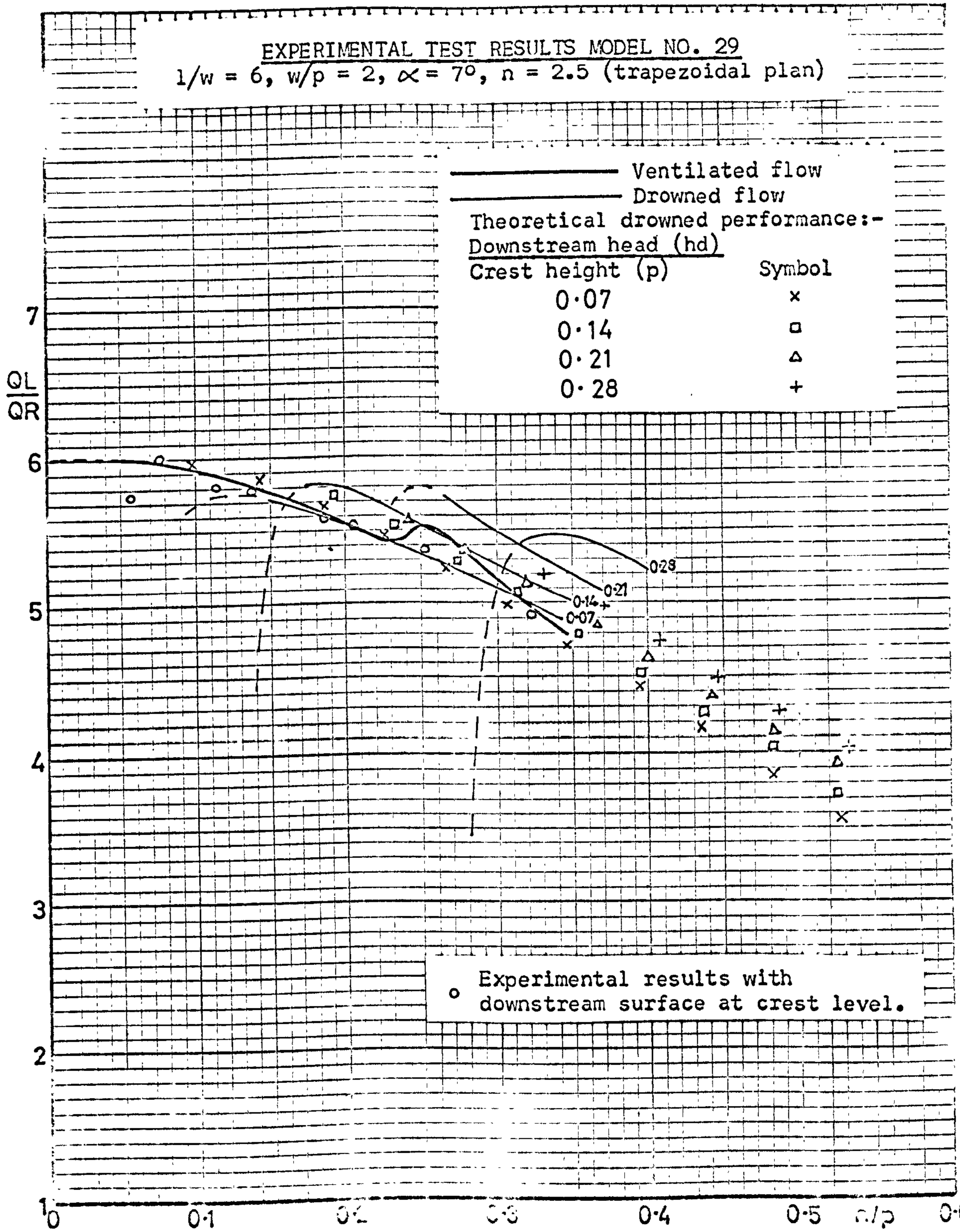

Figure 34

EXPERIMENTAL TEST RESULTS MODEL NO. 30
l/w = 6, w/p = 3.5, α = 0 (rectangular plan)

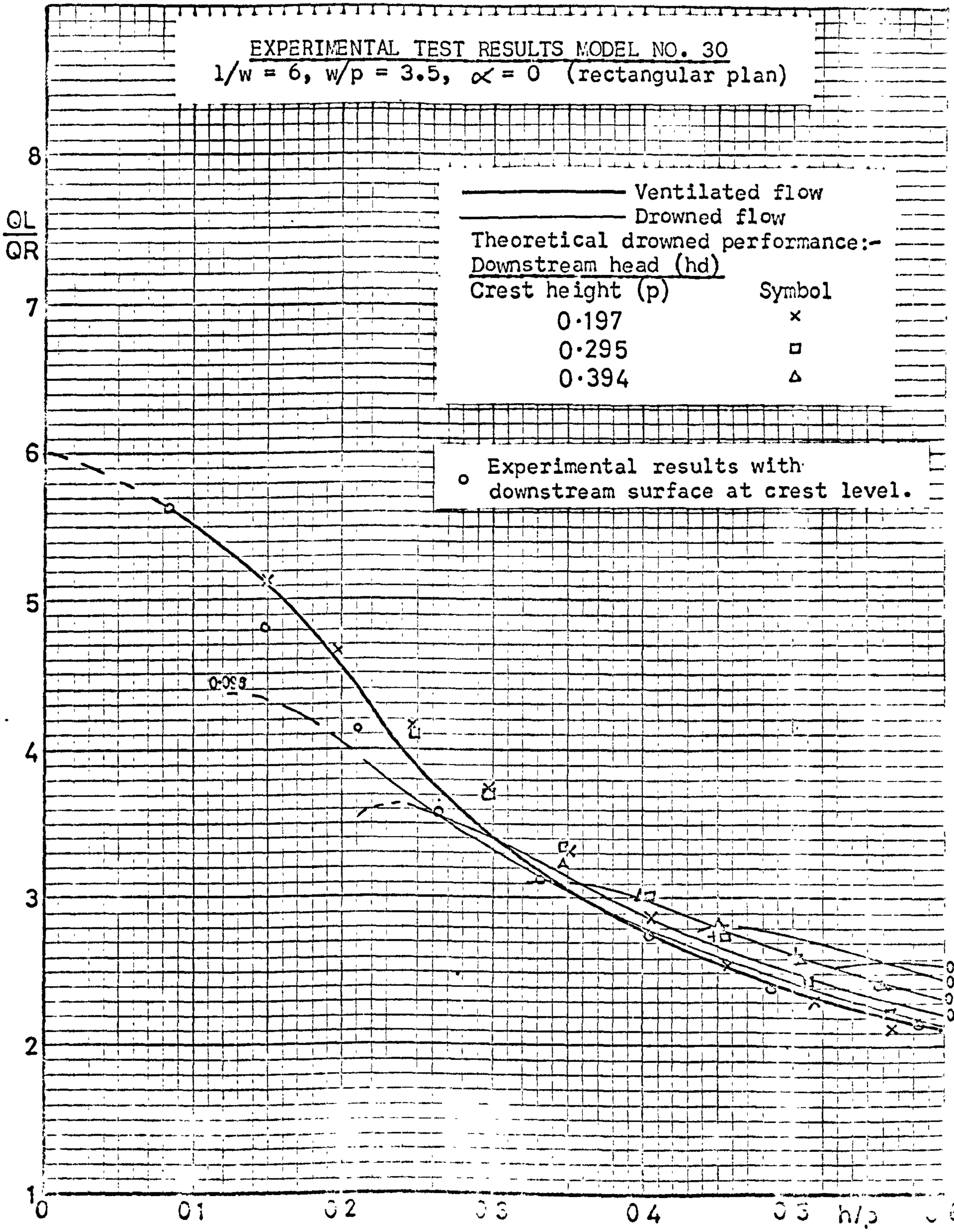

——————— Ventilated flow

——————— Drowned flow

Theoretical drowned performance:-

Downstream head (hd) / Crest height (p)	Symbol
0·197	×
0·295	□
0·394	△

o Experimental results with downstream surface at crest level.

Figure 35

EXPERIMENTAL TEST RESULTS MODEL NO. 31
1/w = 6, w/p = 3.5; ∝ = 7 (trapezoidal plan)

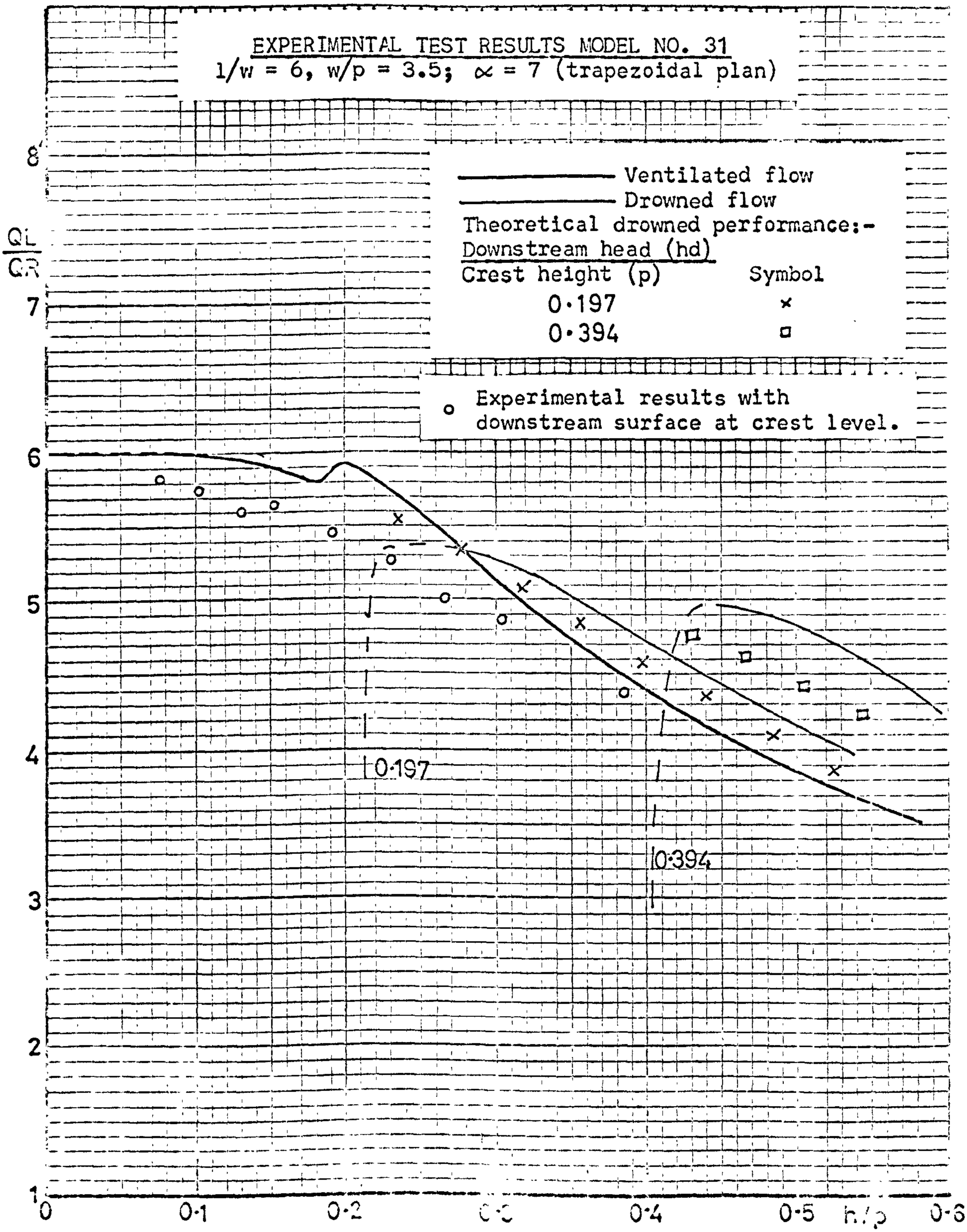

Figure 36

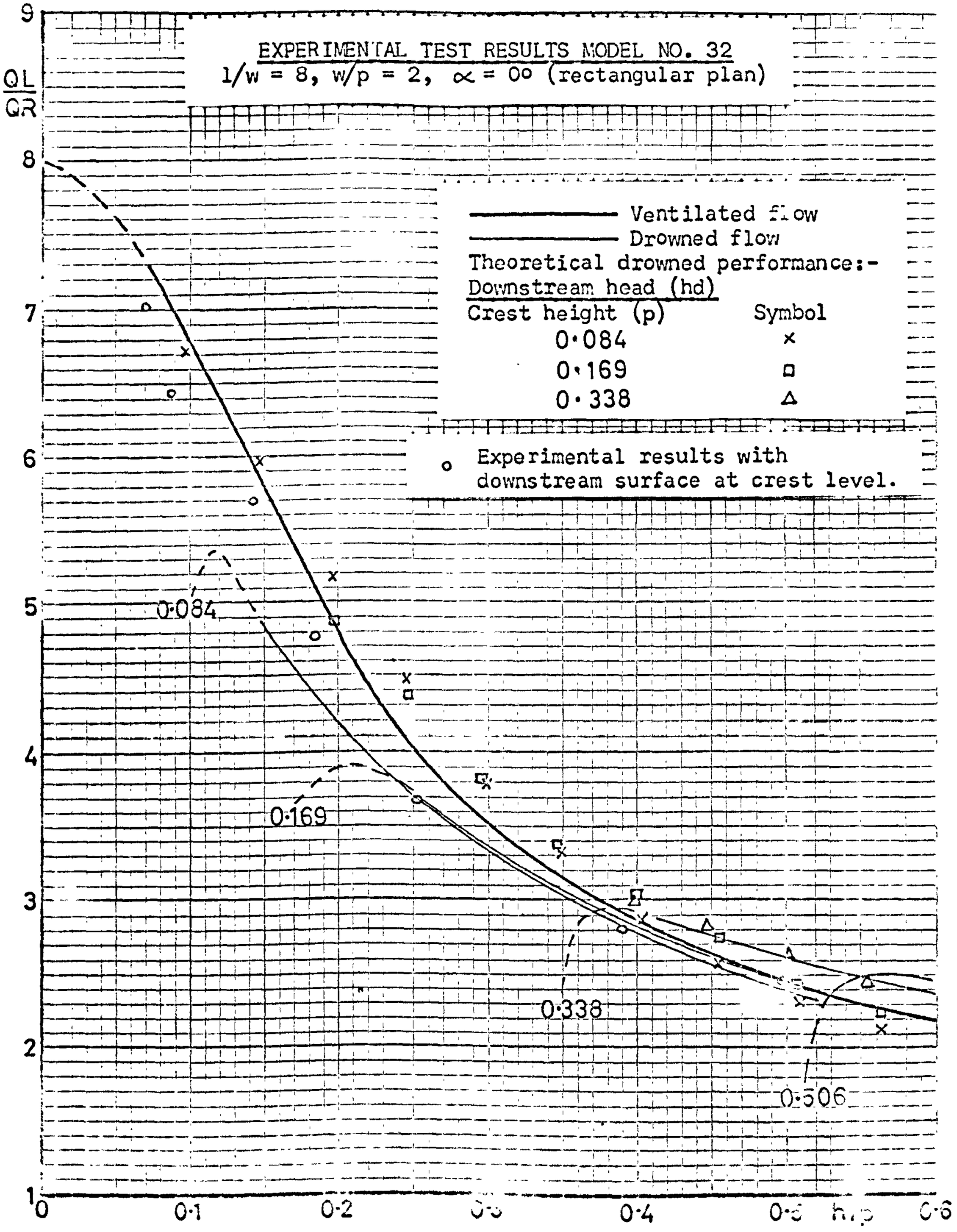
EXPERIMENTAL TEST RESULTS MODEL NO. 32
l/w = 8, w/p = 2, ∝ = 0° (rectangular plan)
QL/QR
Ventilated flow
Drowned flow
Theoretical drowned performance:-
Downstream head (hd)
Crest height (p) Symbol
0·084 ×
0·169 □
0·338 △
o Experimental results with downstream surface at crest level.
0·084
0·169
0·338
0·506
hd/p
9
8
7
6
5
4
3
2
1
0
0·1
0·2
0·4
0·6

Figure 37

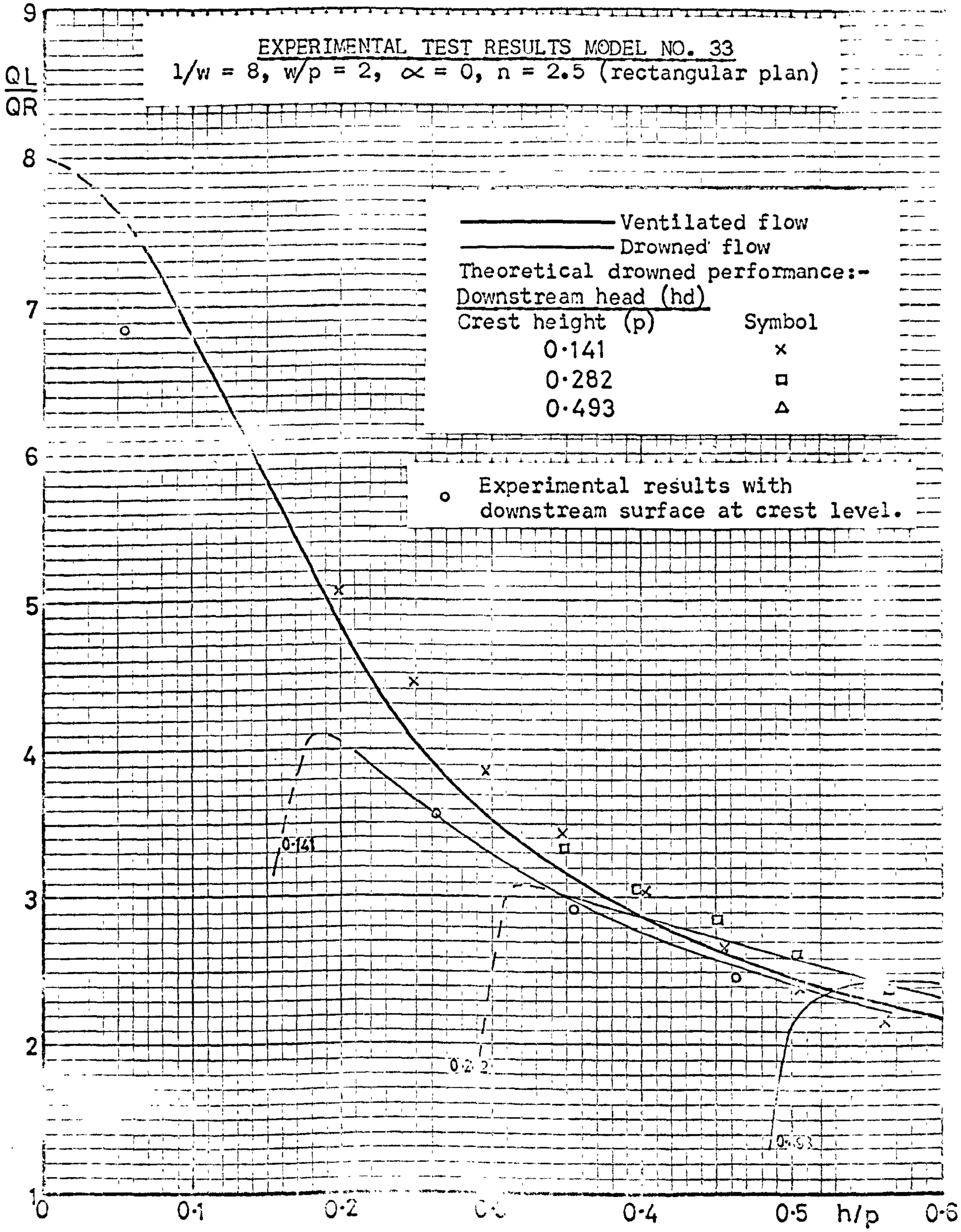
EXPERIMENTAL TEST RESULTS MODEL NO. 33
1/w = 8, w/p = 2, ∝ = 0, n = 2.5 (rectangular plan)
QL/QR
Ventilated flow
Drowned flow
Theoretical drowned performance:-
Downstream head (hd)
Crest height (p) Symbol
0·141 ×
0·282 □
0·493 △
o Experimental results with downstream surface at crest level.
0·141
0·282
0·493
h/p
9
8
7
6
5
4
3
2
1
0
0·1
0·2
0·4
0·5
0·6

Figure 38

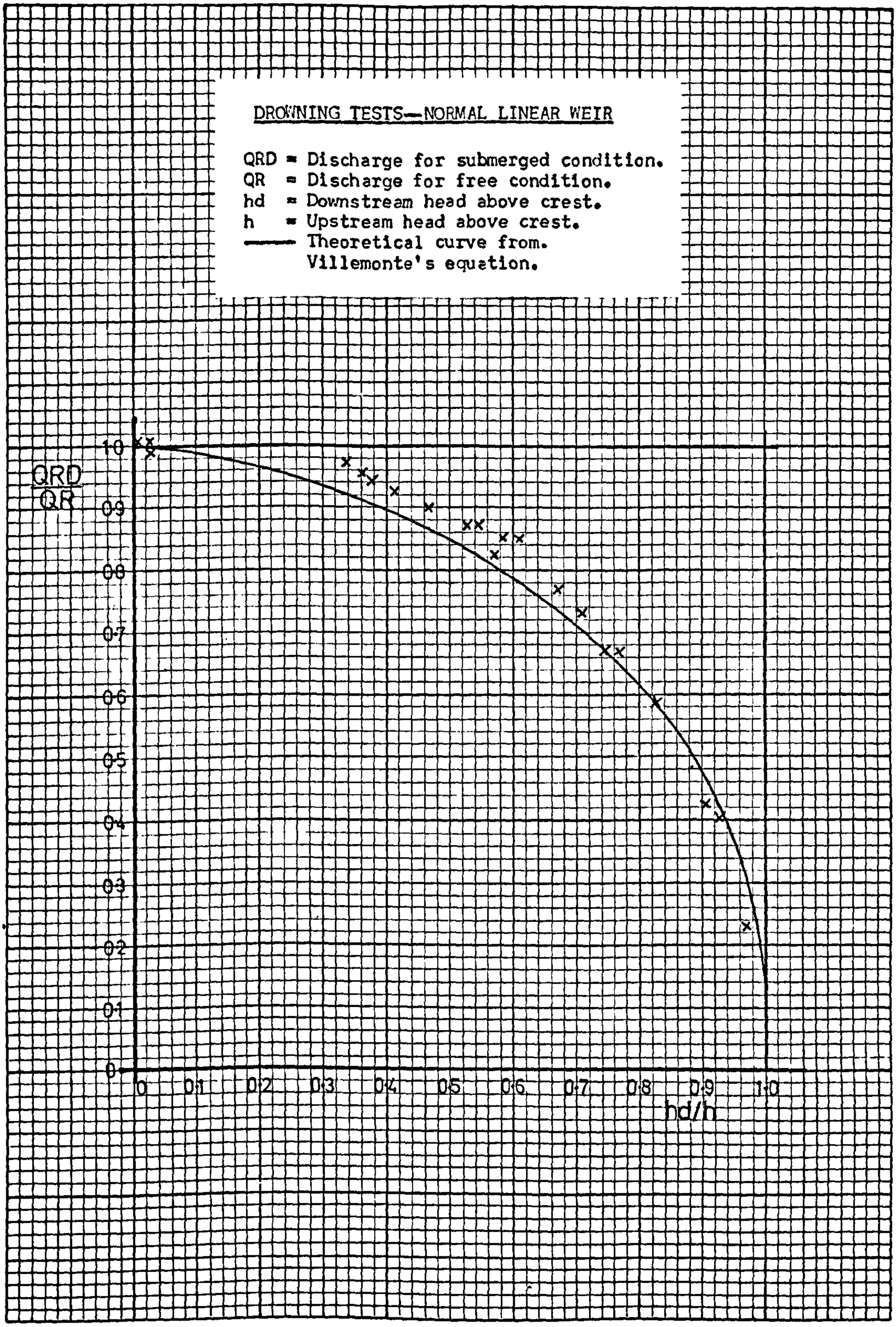
DROWNING TESTS—NORMAL LINEAR WEIR
QRD = Discharge for submerged condition.
QR = Discharge for free condition.
hd = Downstream head above crest.
h = Upstream head above crest.
—— Theoretical curve from.
Villemonte's equation.
QRD/QR
1·0
0·9
0·8
0·7
0·6
0·5
0·4
0·3
0·2
0·1
0
0
0·1
0·2
0·3
0·4
0·5
0·6
0·7
0·8
0·9
1·0
hd/h

Figure 39

SCHEMATIC SHAPES OF MODELS IN MODEL PROGRAMME NO. 2
(continued over)

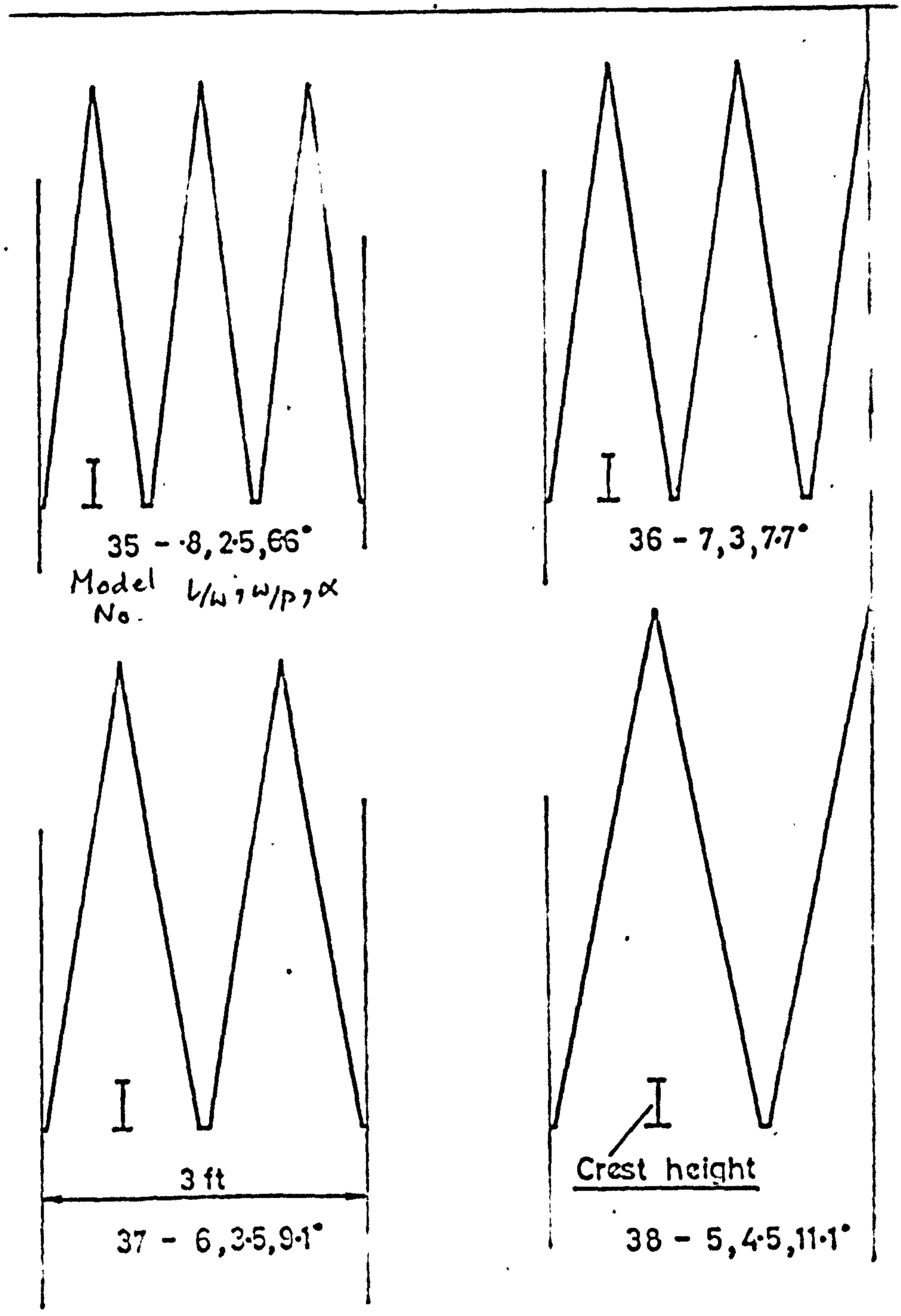

Figure 40

EXPERIMENTAL TEST RESULTS MODEL NO. 35
1/w = 8, w/p = 2.5, α = 6.6 (triangular plan)

$\frac{QL}{QR}$

9
8
7
6
5
4
3
2
1

0.075
0.150
0.225
0.300
0.375

o Experimental results with downstream surface at crest level.

——————— Ventilated flow
——————— Drowned flow

Theoretical drowned performance:-
Downstream head (hd)

Crest height (p)	Symbol
0·075	×
0·150	□
0·225	△
0·300	+
0·375	▽

0 0·1 0·2 0·3 0·4 0·5 h/p 0·6

Figure 41

EXPERIMENTAL TEST RESULTS MODEL NO. 36
l/w = 7, w/p = 3, α = 7.7 (triangular plan)

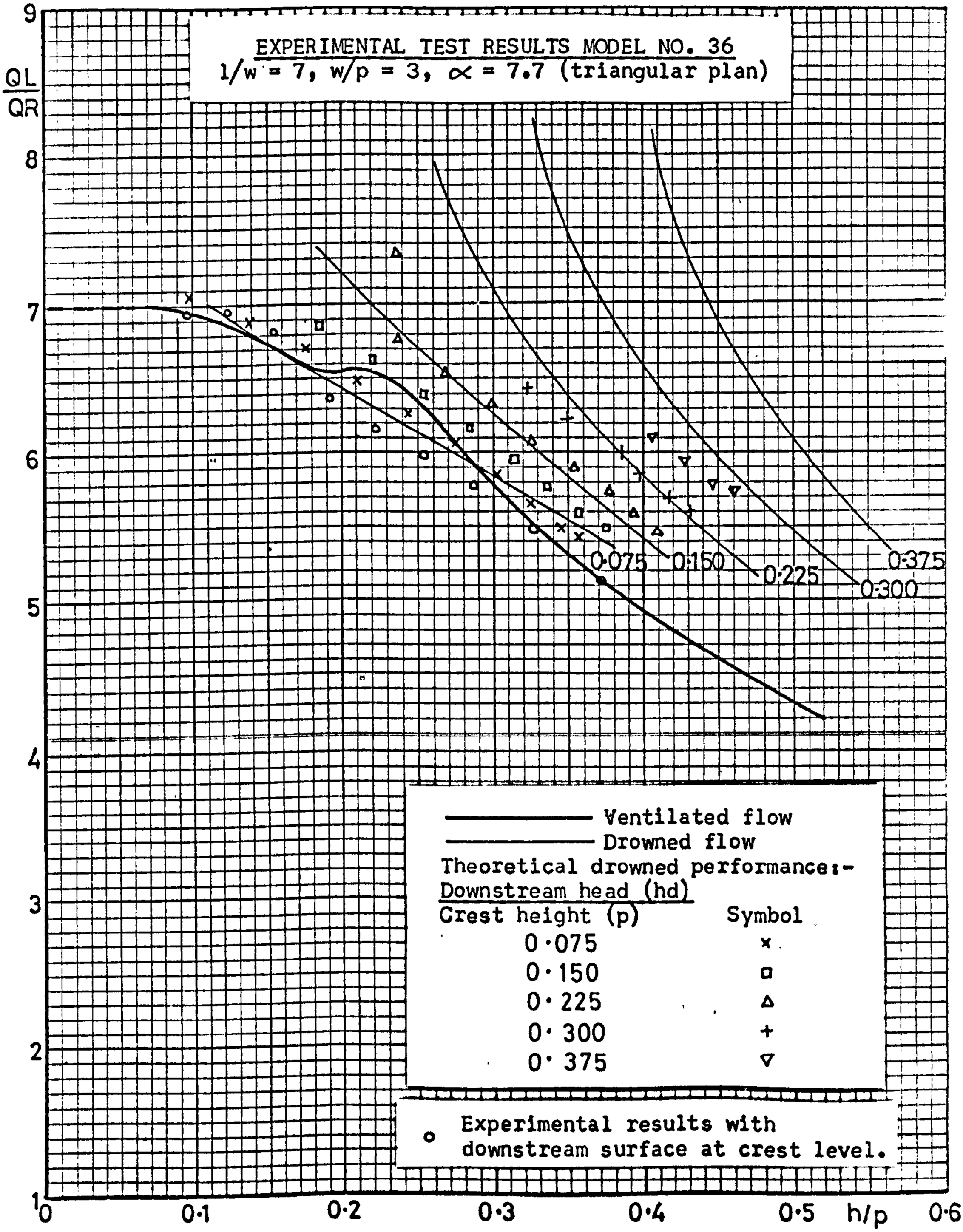

Figure 42

EXPERIMENTAL TEST RESULTS MODEL NO. 37
1/w = 6, w/p = 3.5, ∝ = 9.1 (triangular plan)

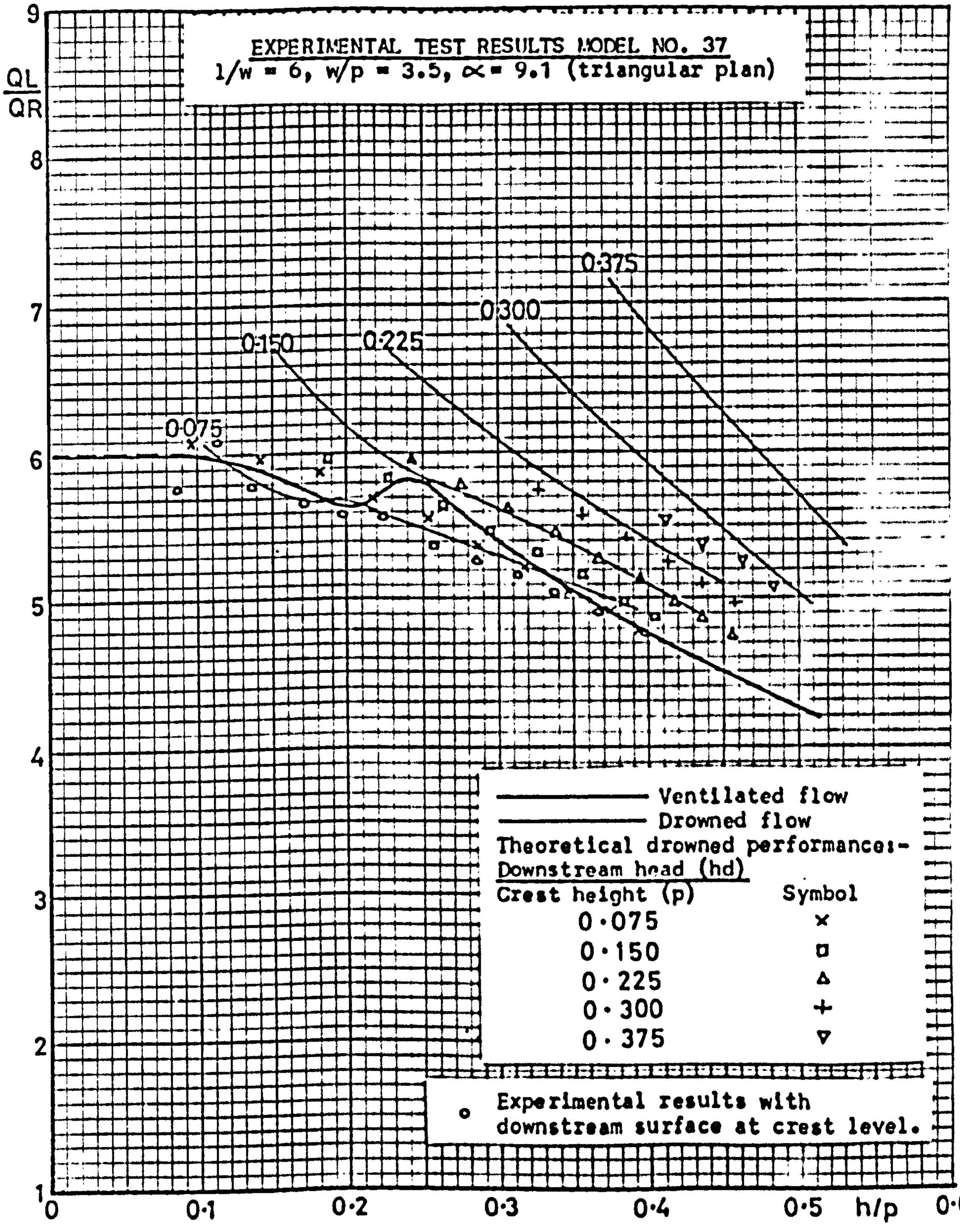

Figure 43

o

EXPERIMENTAL TEST RESULTS MODEL NO. 38
1/w = 5, w/p = 4.5, α = 11.1 (triangular plan)

o Experimental results with downstream surface at crest level.

$\frac{QL}{QR}$

0·375
0·300
0·225
0·150
0·075

——— Ventilated flow
——— Drowned flow

Theoretical drowned performance:-
Downstream head (hd)

Crest height (p)	Symbol
0·075	×
0·150	□
0·225	△
0·300	+
0·375	▽

h/p

Figure 44

EXPERIMENTAL TEST RESULTS - MODELS 39-42

Model	l/w	w/p	∝
39	8	2.5	5.4
40	7	3	6.2
41	6	3.5	7.2
42	5	4.5	8.7

All models trapezoidal in plan

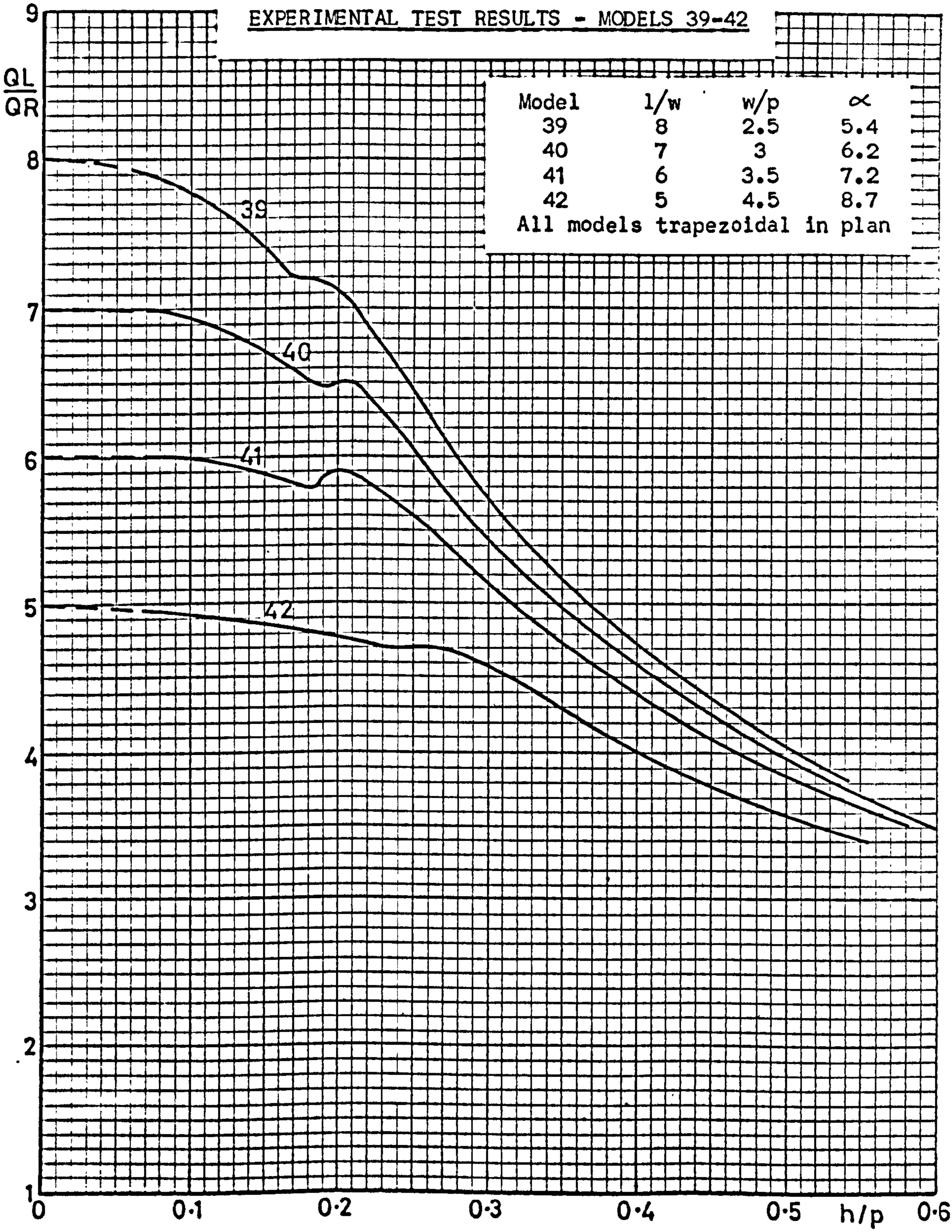

Figure 45

EXPERIMENTAL VENTILATED PERFORMANCE RESULTS FROM MODEL PROGRAMMES 1 AND 2

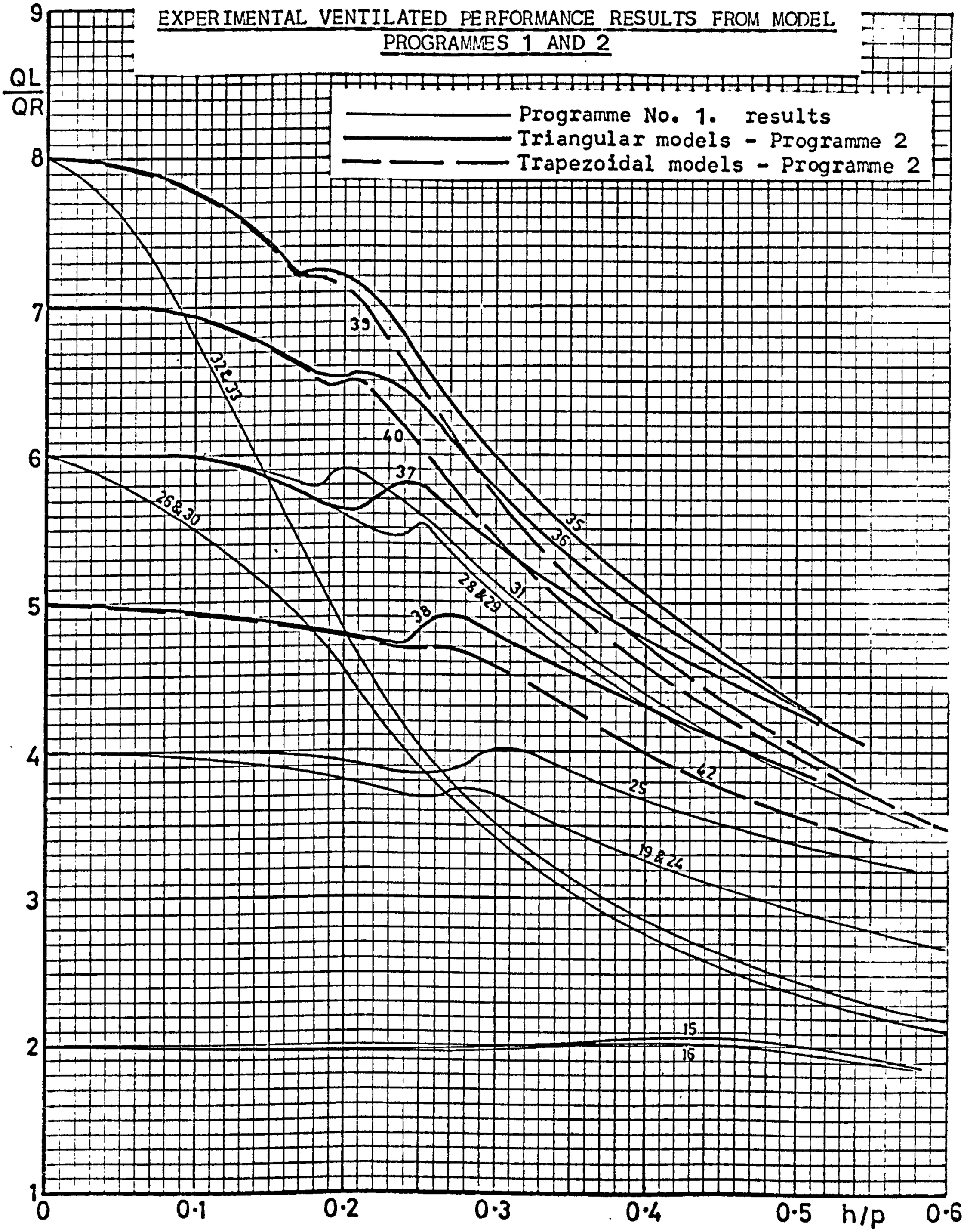

Figure 46

EXPERIMENTAL TEST RESULTS - 1 CYCLE MODEL TESTS

Model	l/w	w/p	∝
47	8	2.5	6.6
48	7	3	7.7
49	6	3.5	9.1
50	5	4.5	11.1

Plan forms triangular.

——— Unrestricted nappe expansion
— — — Restricted nappe expansion

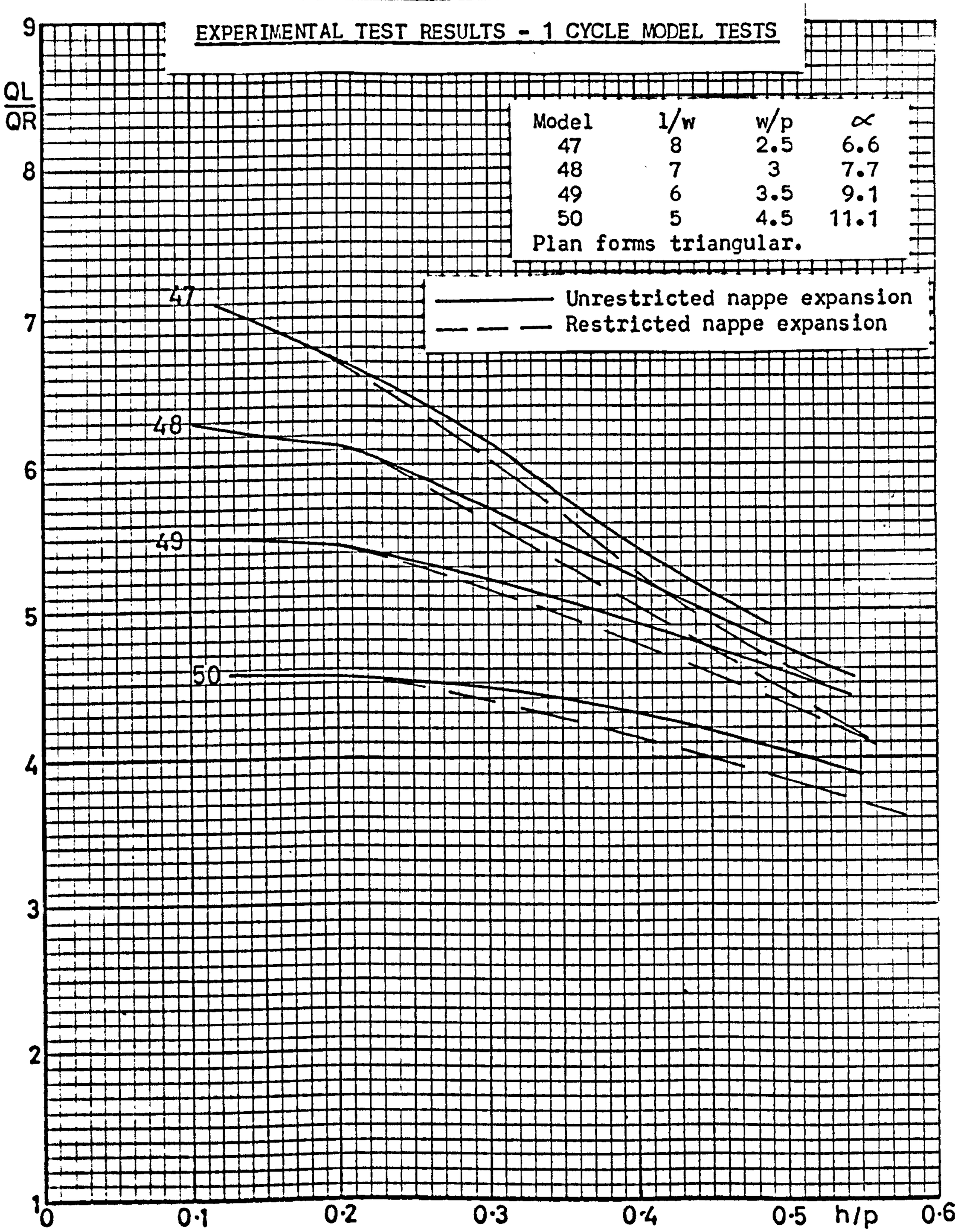

Figure 47

EFFECT OF DOWNSTREAM INTERFERENCE ON THE PERFORMANCE OF TRIANGULAR WEIRS

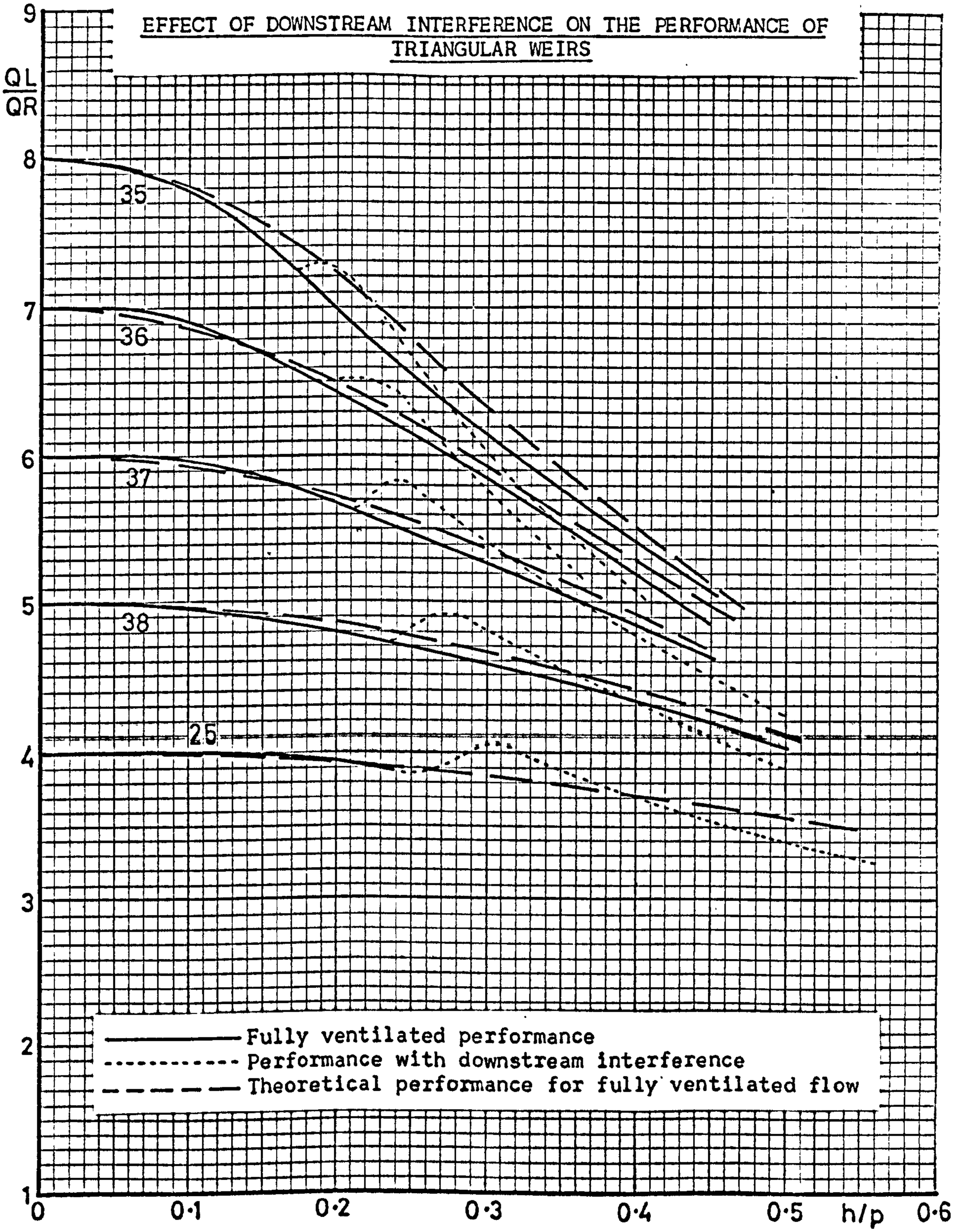

Figure 48

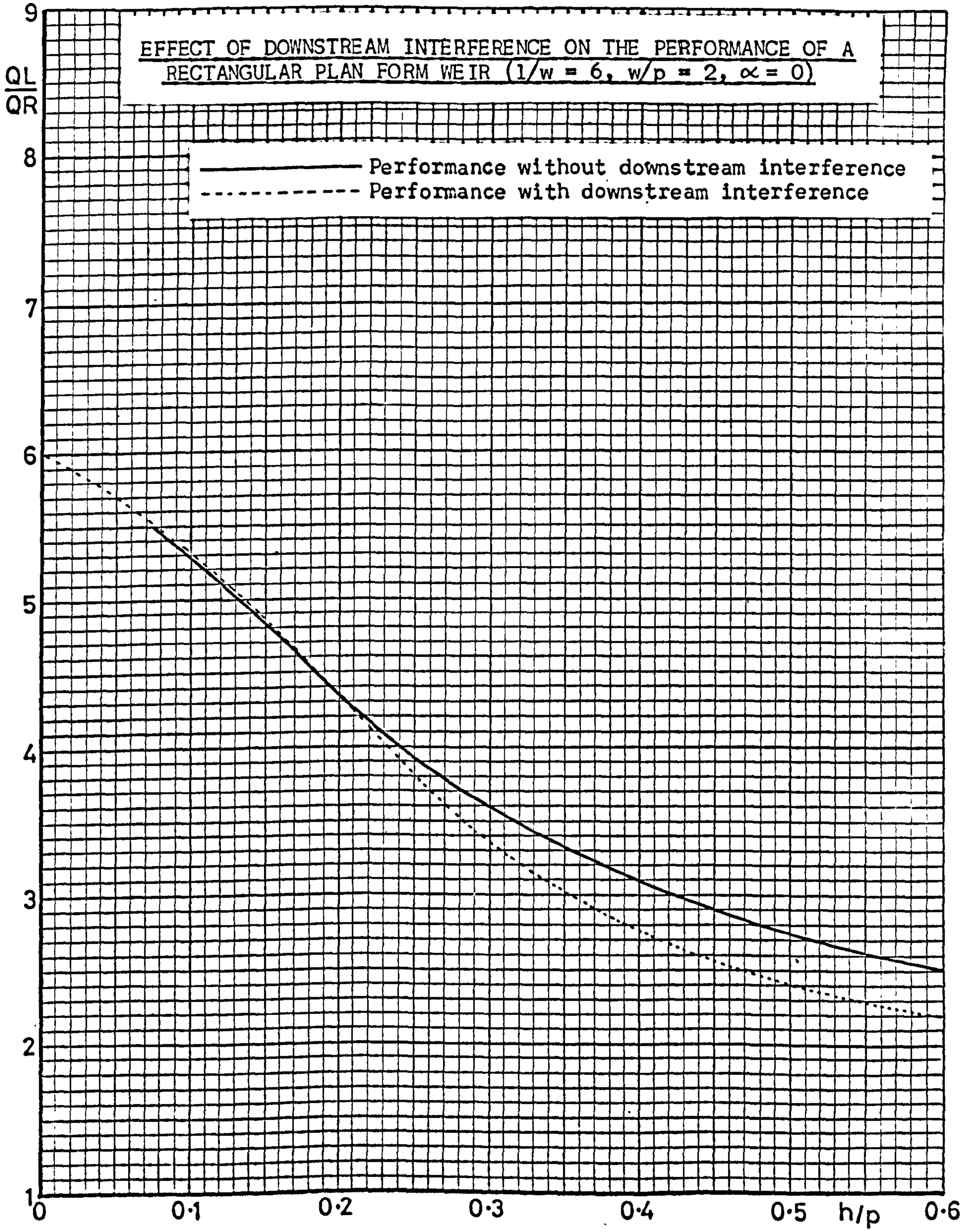
EFFECT OF DOWNSTREAM INTERFERENCE ON THE PERFORMANCE OF A RECTANGULAR PLAN FORM WEIR (1/w = 6, w/p = 2, ∝ = 0)
QL/QR
Performance without downstream interference
Performance with downstream interference
9
8
7
6
5
4
3
2
1
0
0·1
0·2
0·3
0·4
0·5
h/p
0·6

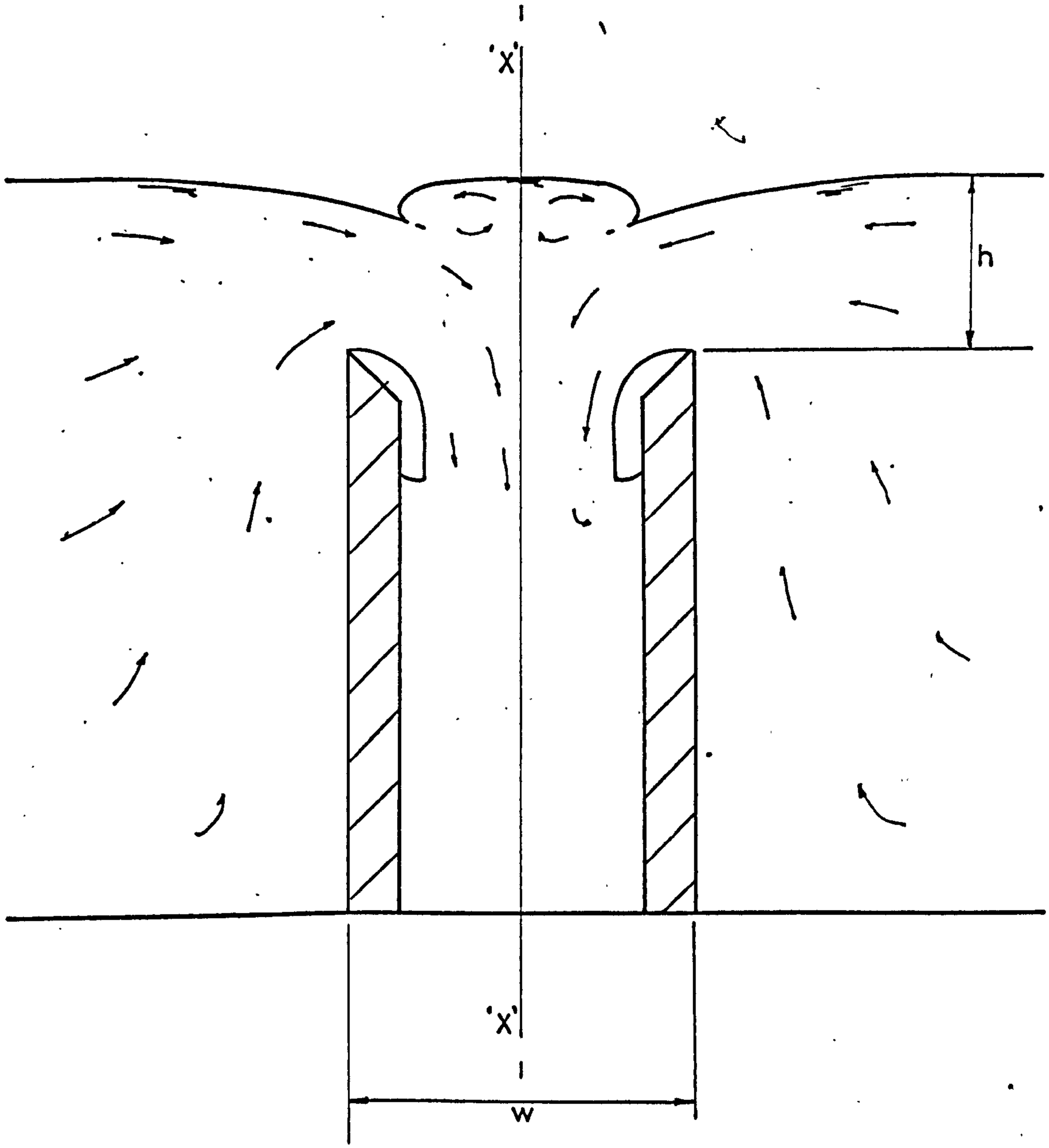

IMPINGEMENT OF NAPPES ISSUING FROM FACING SIDE WALLS OF LABYRINTH WEIRS

Figure 50

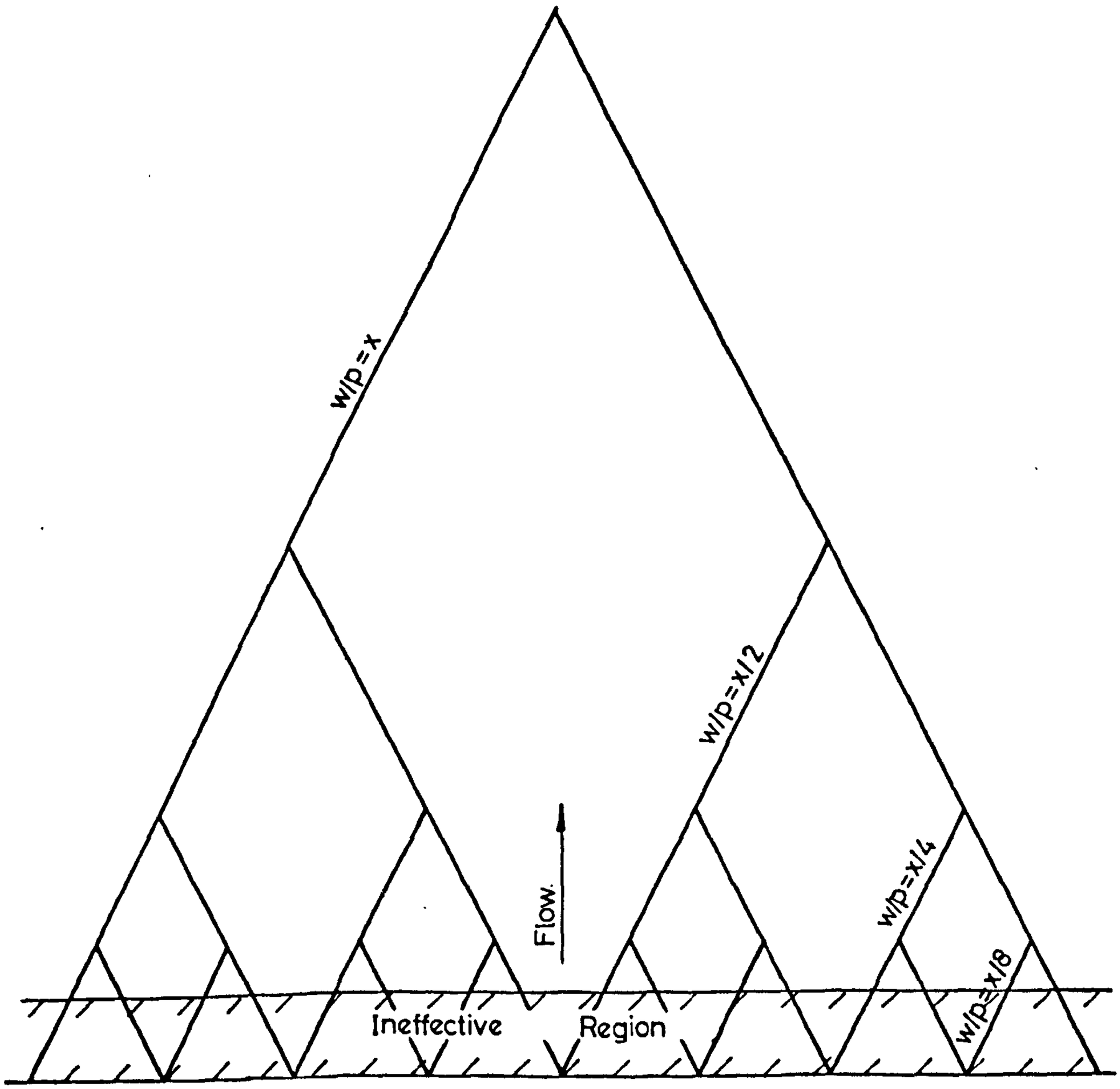

DIAGRAM ILLUSTRATING THE RELATION BETWEEN NAPPE INTERFERENCE AND THE w/p RATIO

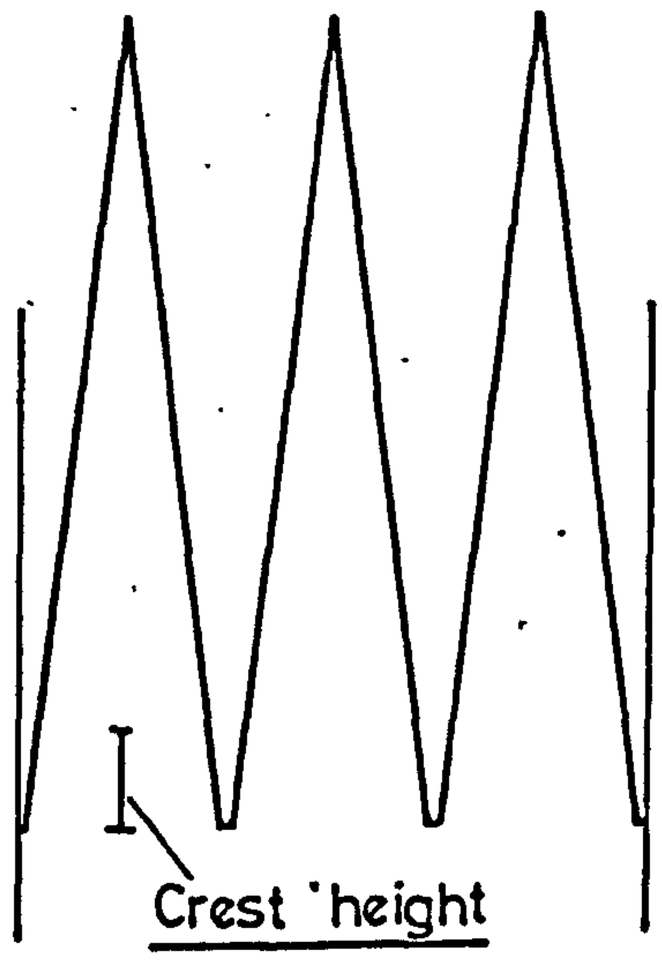

52 - 8,2,6·6

Model No. l/w, w/p, α

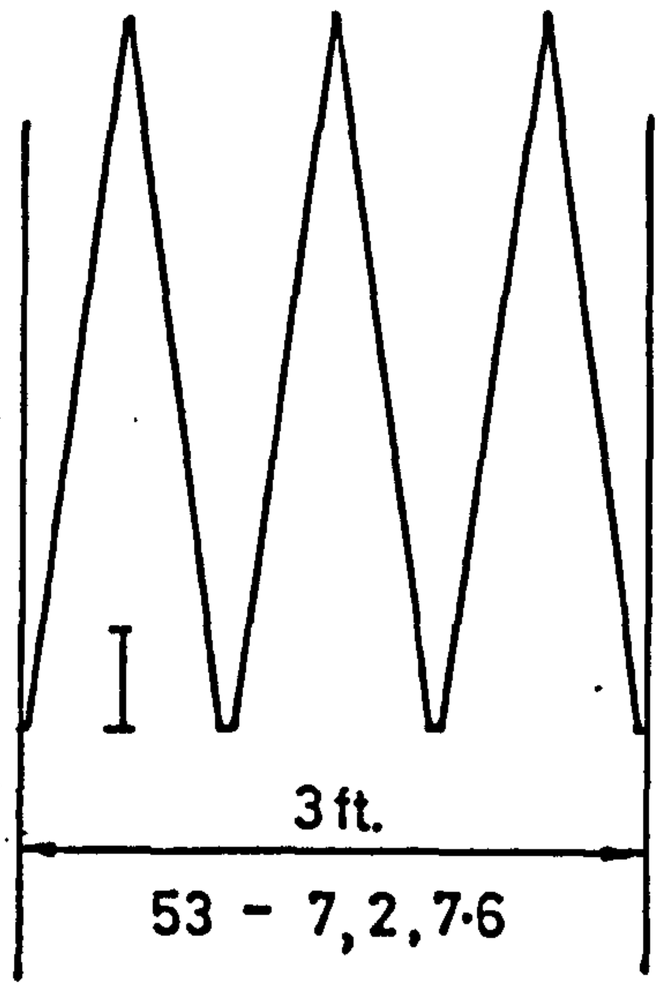

53 - 7,2,7·6

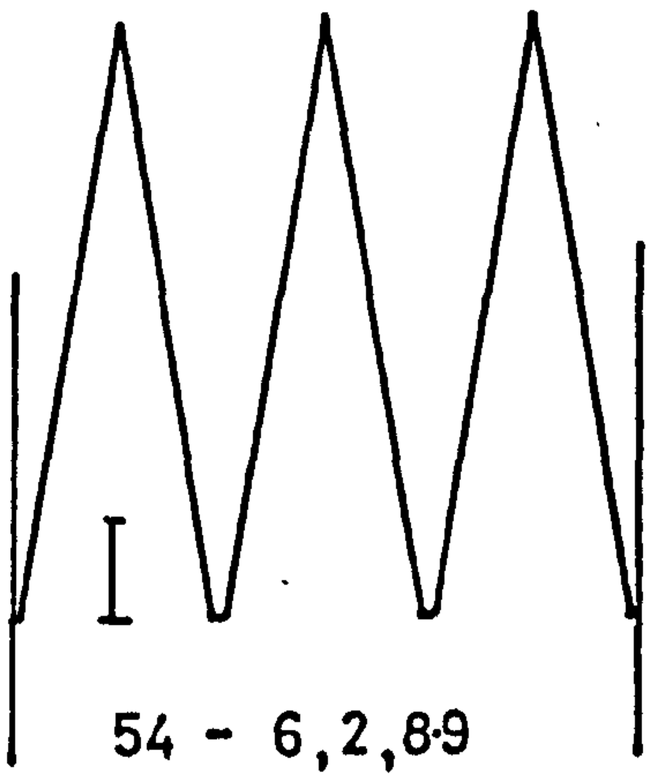

54 - 6,2,8·9

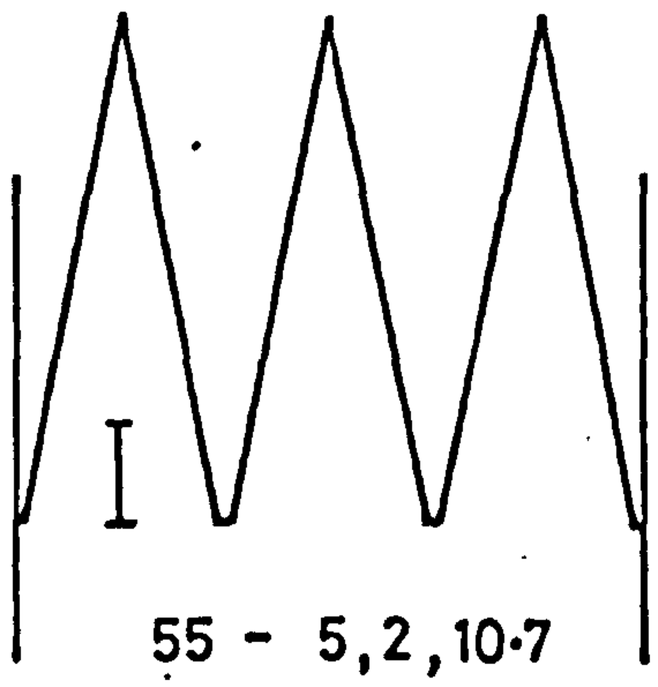

55 - 5,2,10·7

SCHEMATIC SHAPES OF MODELS IN MODEL PROGRAMME NO. 4

Figure 52

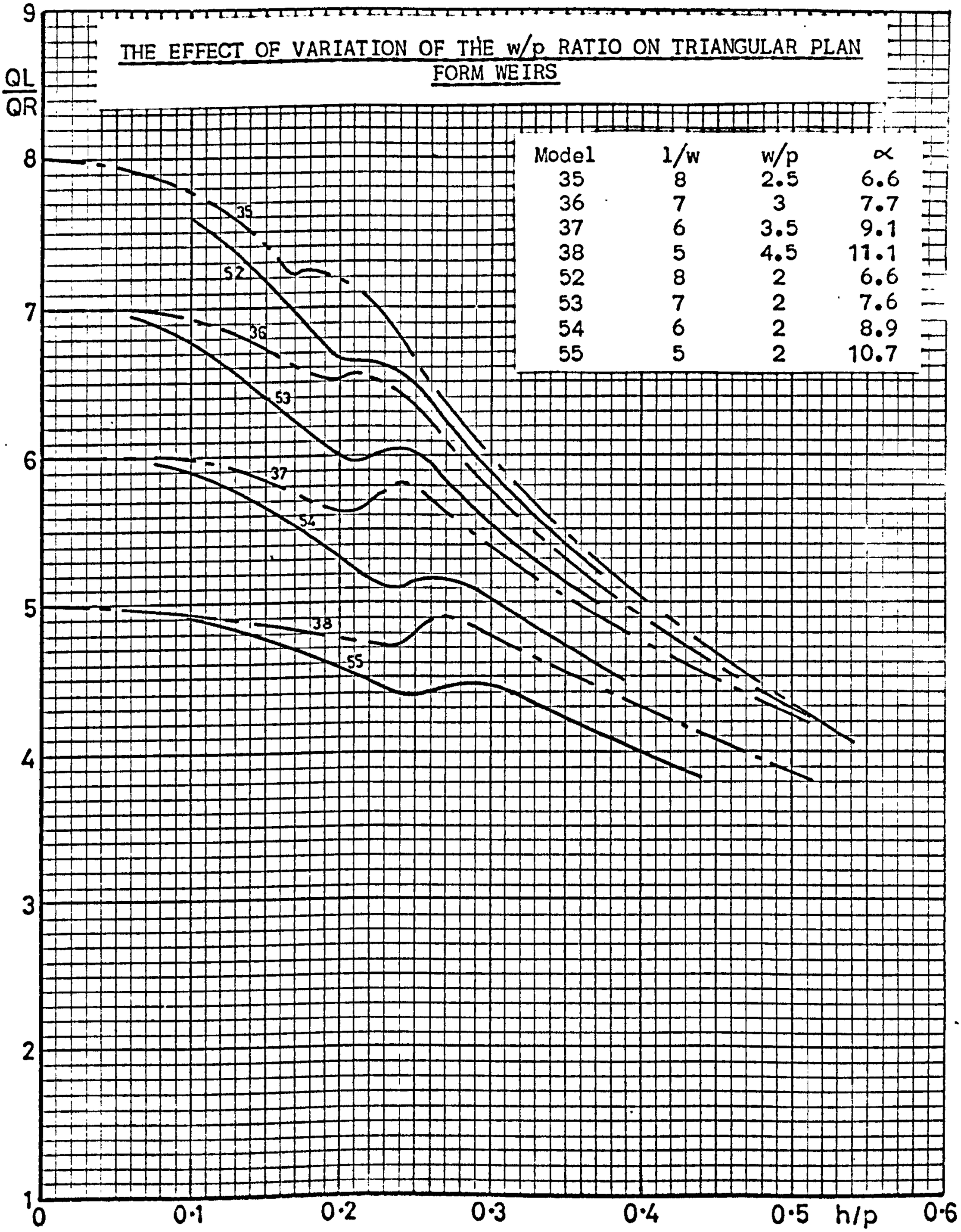

Model	l/w	w/p	∝
35	8	2.5	6.6
36	7	3	7.7
37	6	3.5	9.1
38	5	4.5	11.1
52	8	2	6.6
53	7	2	7.6
54	6	2	8.9
55	5	2	10.7

Figure 53

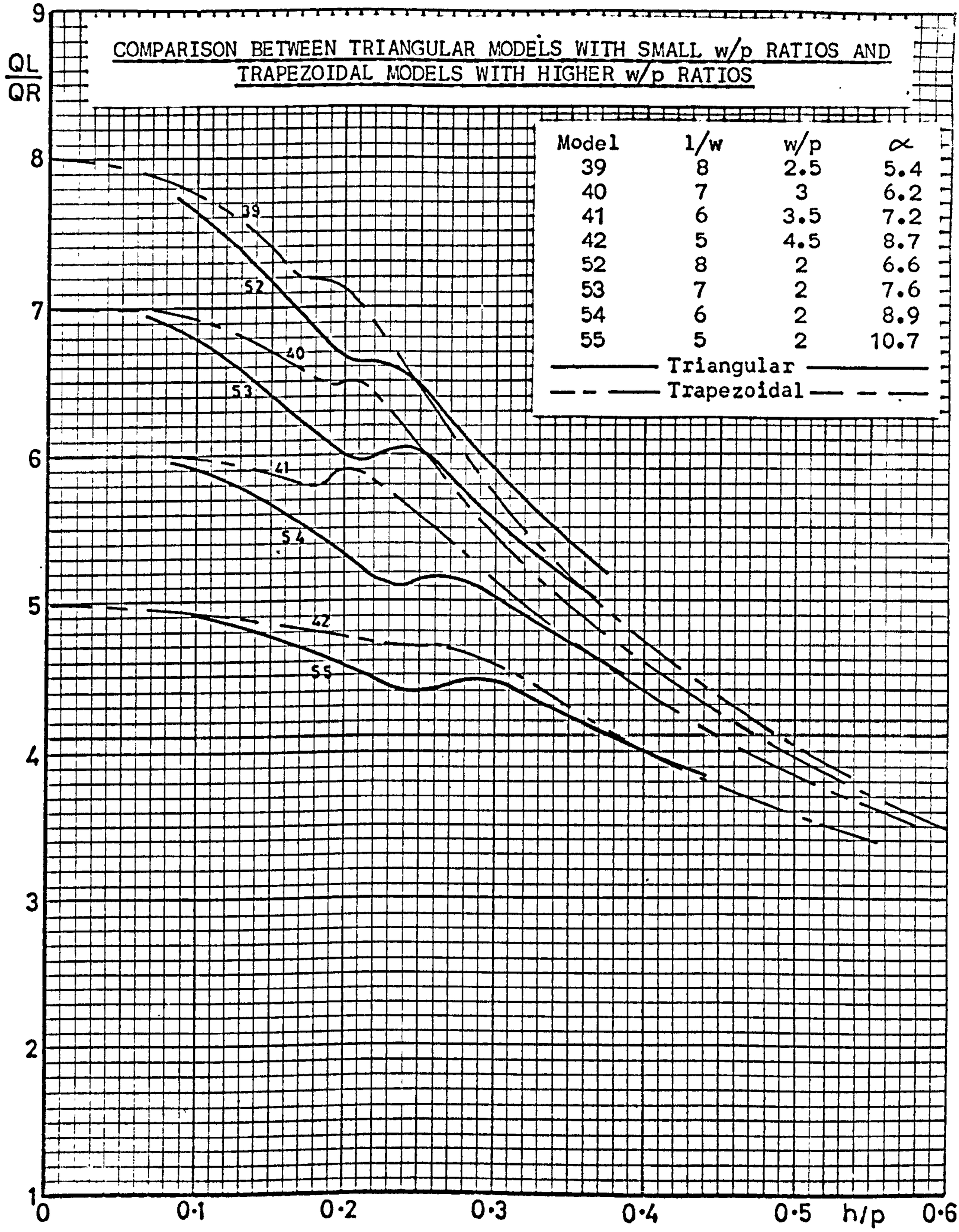
COMPARISON BETWEEN TRIANGULAR MODELS WITH SMALL w/p RATIOS AND TRAPEZOIDAL MODELS WITH HIGHER w/p RATIOS
QL/QR
Model 1/w w/p ∝
39 8 2.5 5.4
40 7 3 6.2
41 6 3.5 7.2
42 5 4.5 8.7
52 8 2 6.6
53 7 2 7.6
54 6 2 8.9
55 5 2 10.7
Triangular
Trapezoidal
h/p

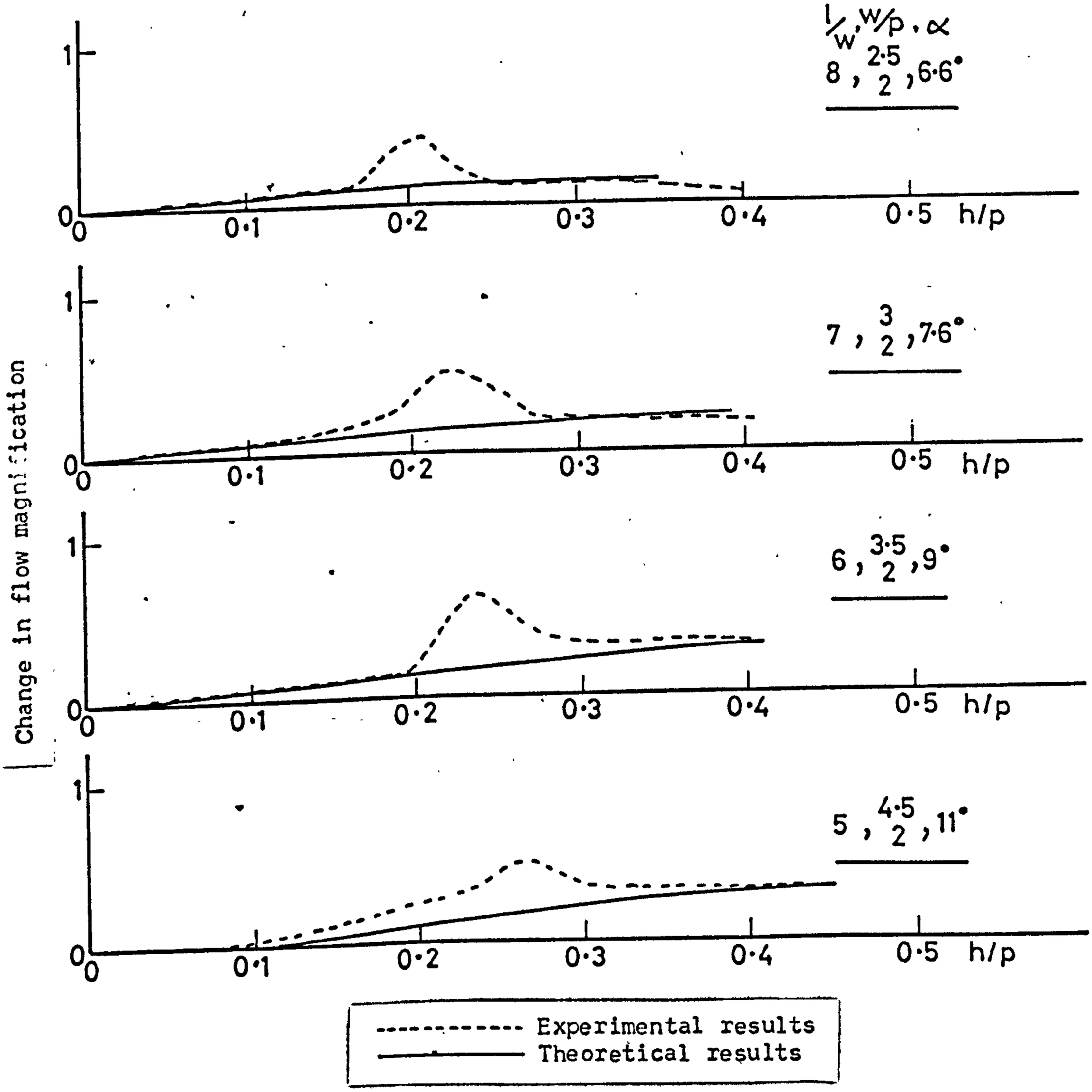

CHANGE IN FLOW MAGNIFICATION RESULTING FROM VARIATION OF THE VERTICAL ASPECT RATIO w/p

Figure 55

COMPARISON BETWEEN THE RESULTS OF THE ORIGINAL AND THE REPEATED TESTS IN MODEL PROGRAMME NO. 4

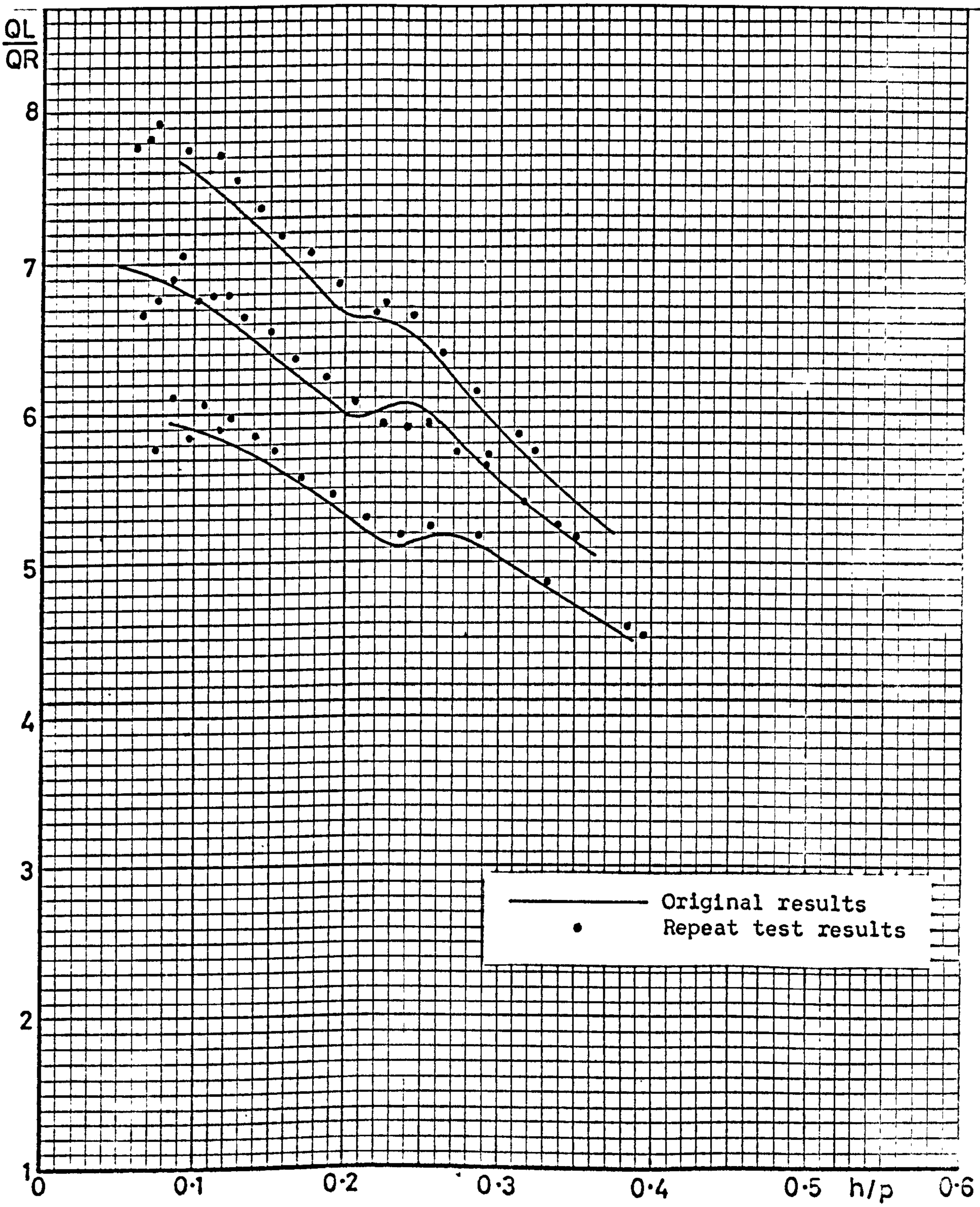

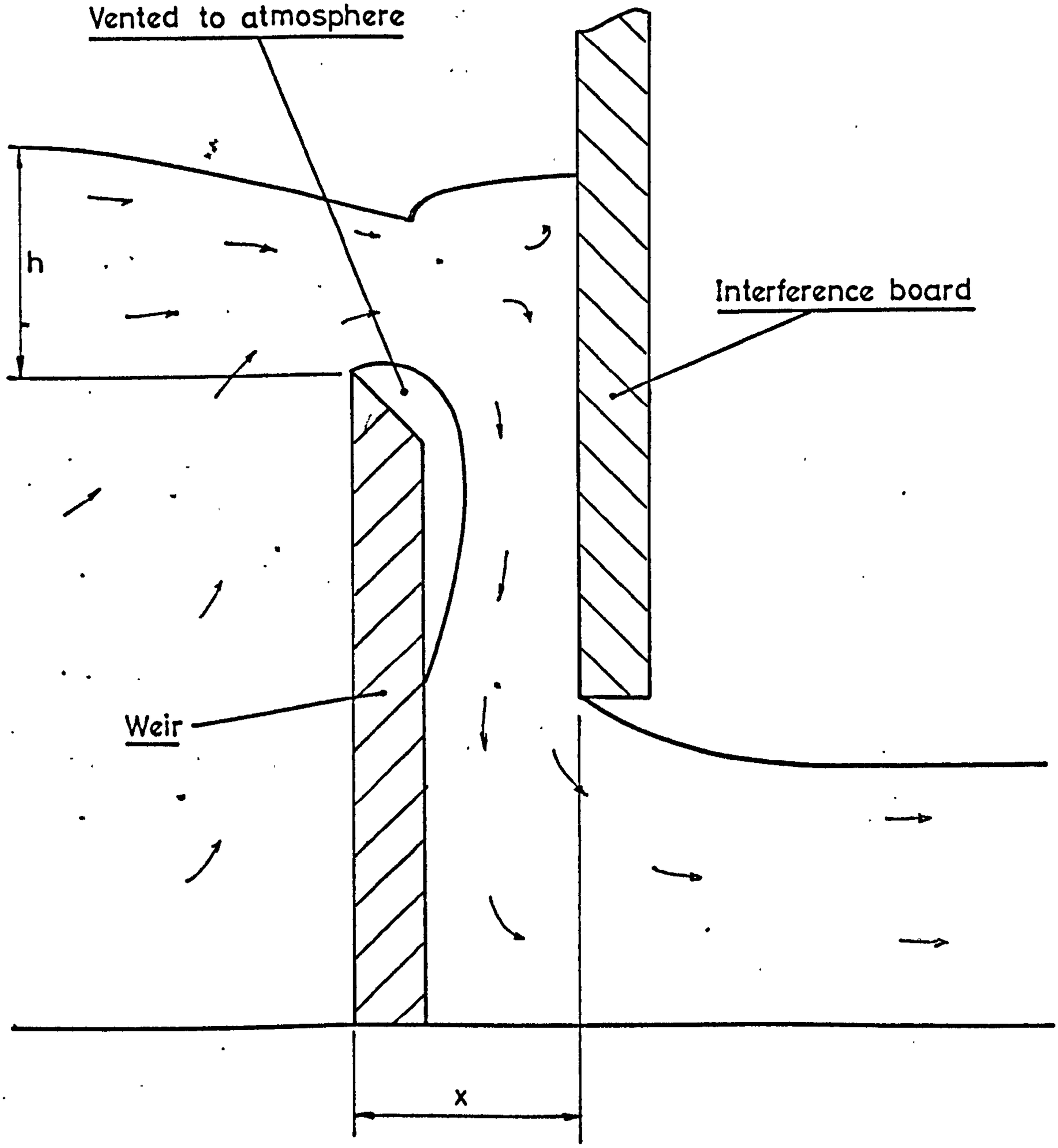

ARRANGEMENT OF APPARATUS TO SIMULATE NAPPE INTERFERENCE ON A LINEAR WEIR

Figure 57

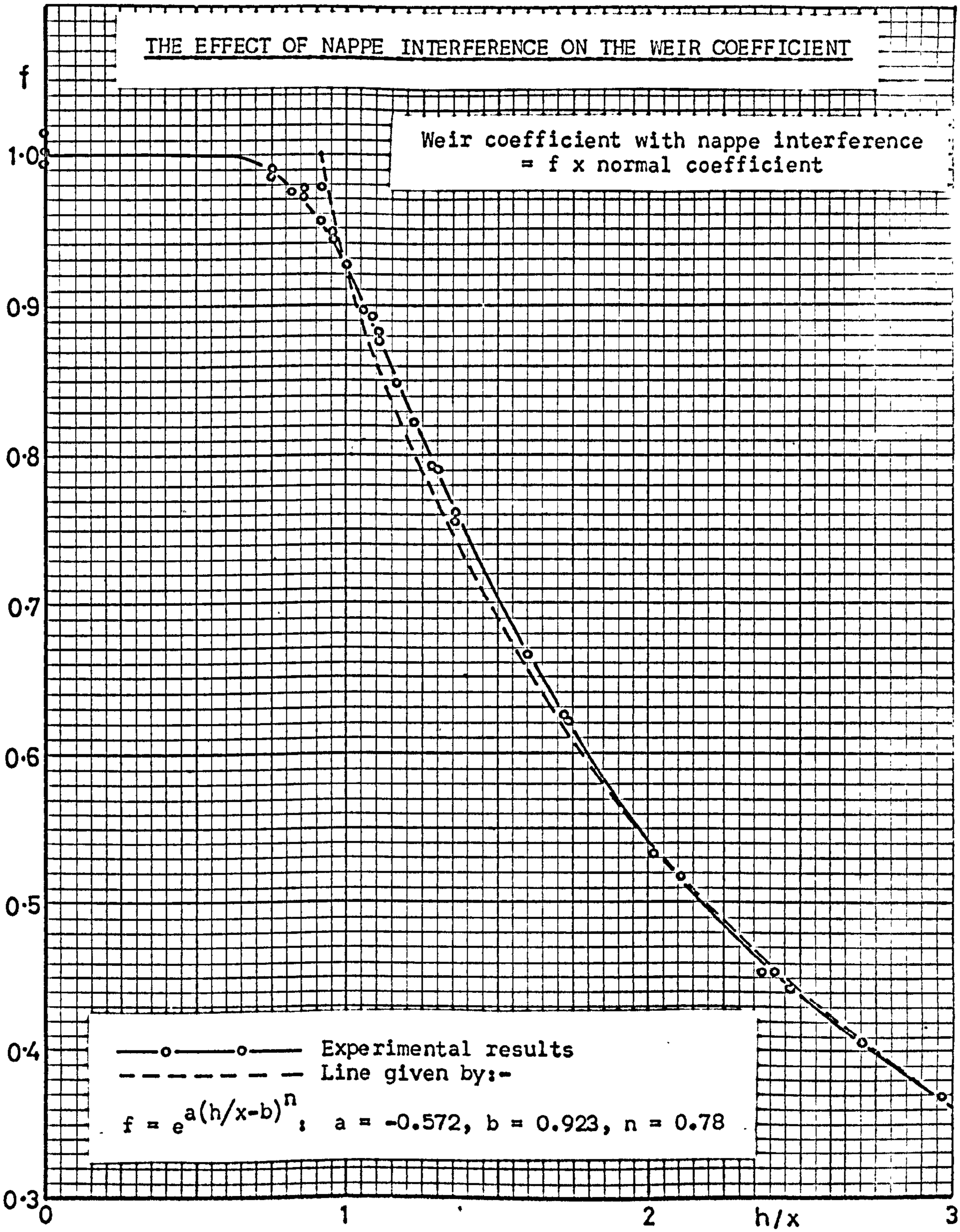
THE EFFECT OF NAPPE INTERFERENCE ON THE WEIR COEFFICIENT
f
Weir coefficient with nappe interference
= f x normal coefficient
1·0
0·9
0·8
0·7
0·6
0·5
0·4
0·3
0
1
2
h/x
3
Experimental results
Line given by:-
$f = e^{a(h/x-b)^n}$; a = -0.572, b = 0.923, n = 0.78

Figure 58

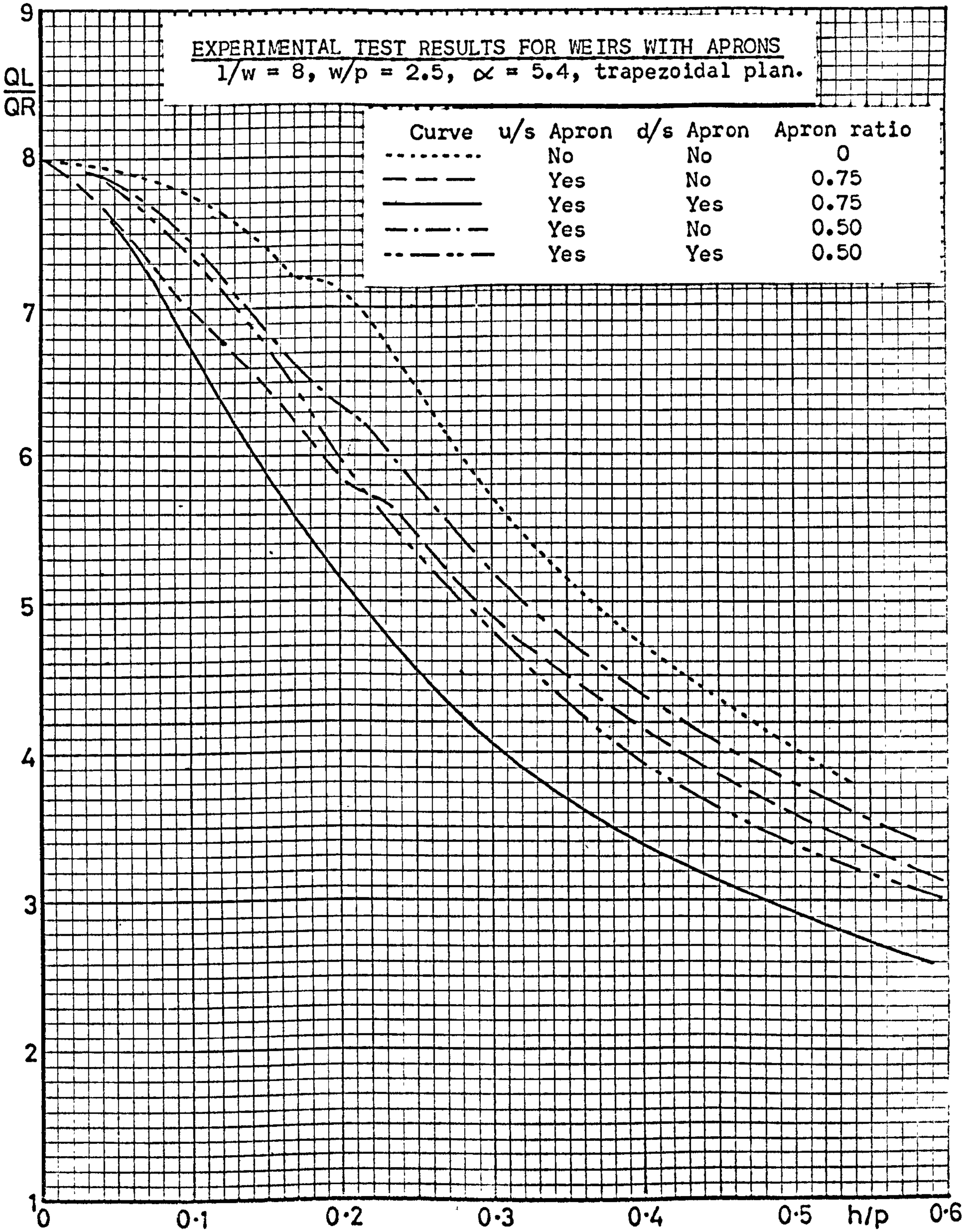
EXPERIMENTAL TEST RESULTS FOR WEIRS WITH APRONS
l/w = 8, w/p = 2.5, ∝ = 5.4, trapezoidal plan.
Curve u/s Apron d/s Apron Apron ratio
No No 0
Yes No 0.75
Yes Yes 0.75
Yes No 0.50
Yes Yes 0.50
QL/QR
9
8
7
6
5
4
3
2
1
0
0·1
0·2
0·3
0·4
0·5
h/p
0·6

Figure 59

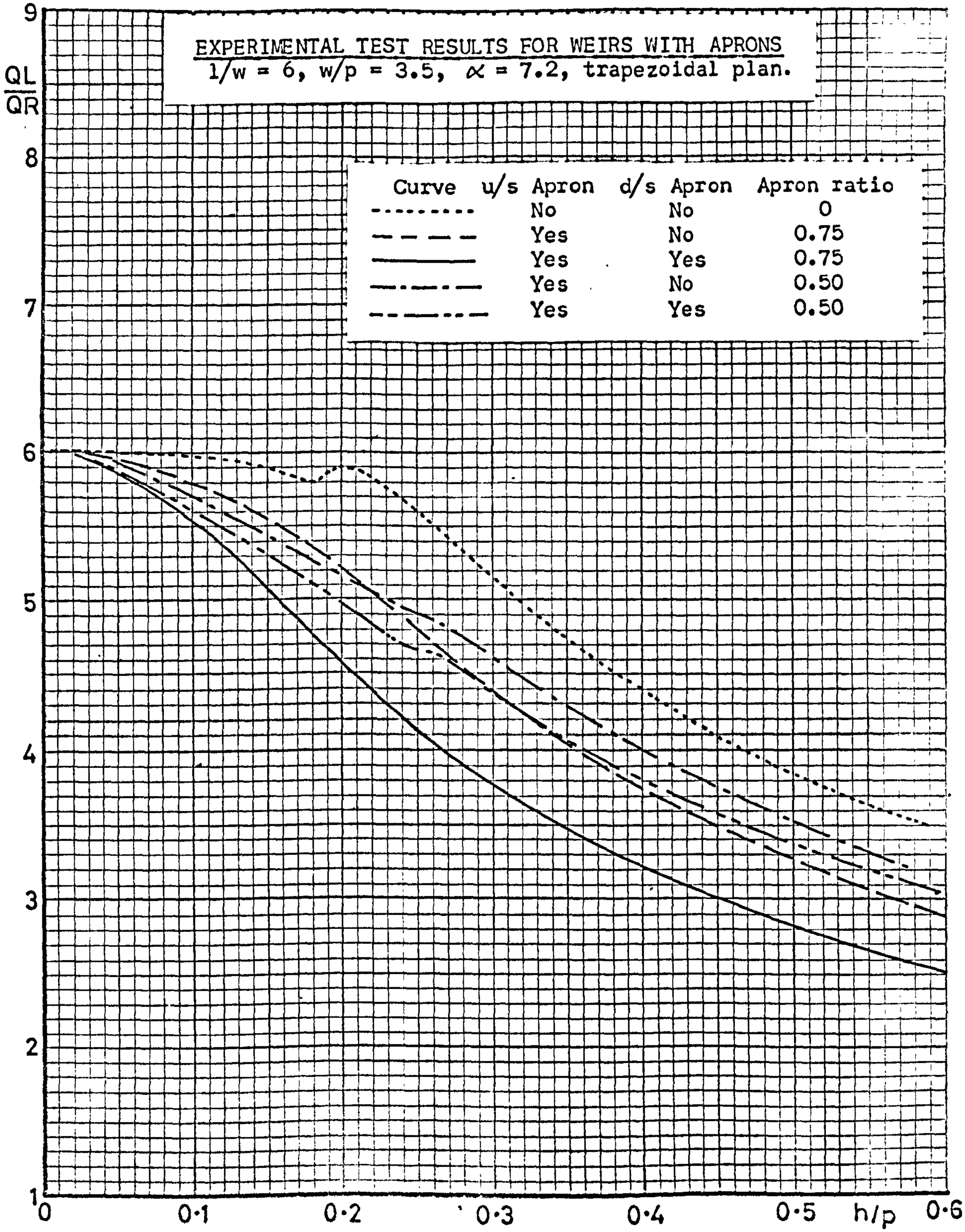
EXPERIMENTAL TEST RESULTS FOR WEIRS WITH APRONS
1/w = 6, w/p = 3.5, α = 7.2, trapezoidal plan.
Curve u/s Apron d/s Apron Apron ratio
No No 0
Yes No 0.75
Yes Yes 0.75
Yes No 0.50
Yes Yes 0.50
QL/QR
9
8
7
6
5
4
3
2
1
0
0·1
0·2
0·3
0·4
0·5
h/p
0·6

Figure 60

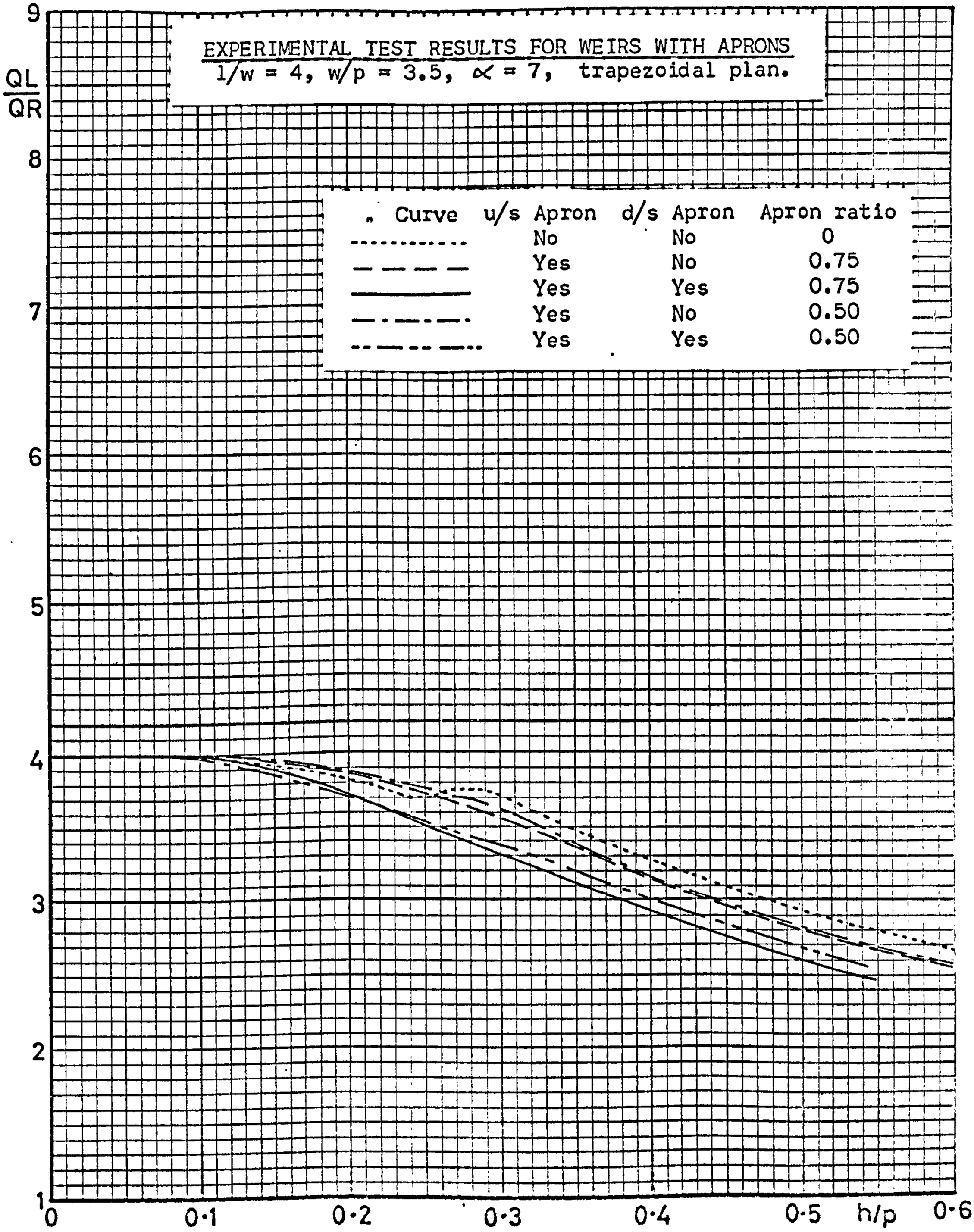
EXPERIMENTAL TEST RESULTS FOR WEIRS WITH APRONS
l/w = 4, w/p = 3.5, ∝ = 7, trapezoidal plan.
QL/QR
Curve u/s Apron d/s Apron Apron ratio
No No 0
Yes No 0.75
Yes Yes 0.75
Yes No 0.50
Yes Yes 0.50
9
8
7
6
5
4
3
2
1
0
0·1
0·2
0·3
0·4
0·5
h/p
0·6

Figure 61

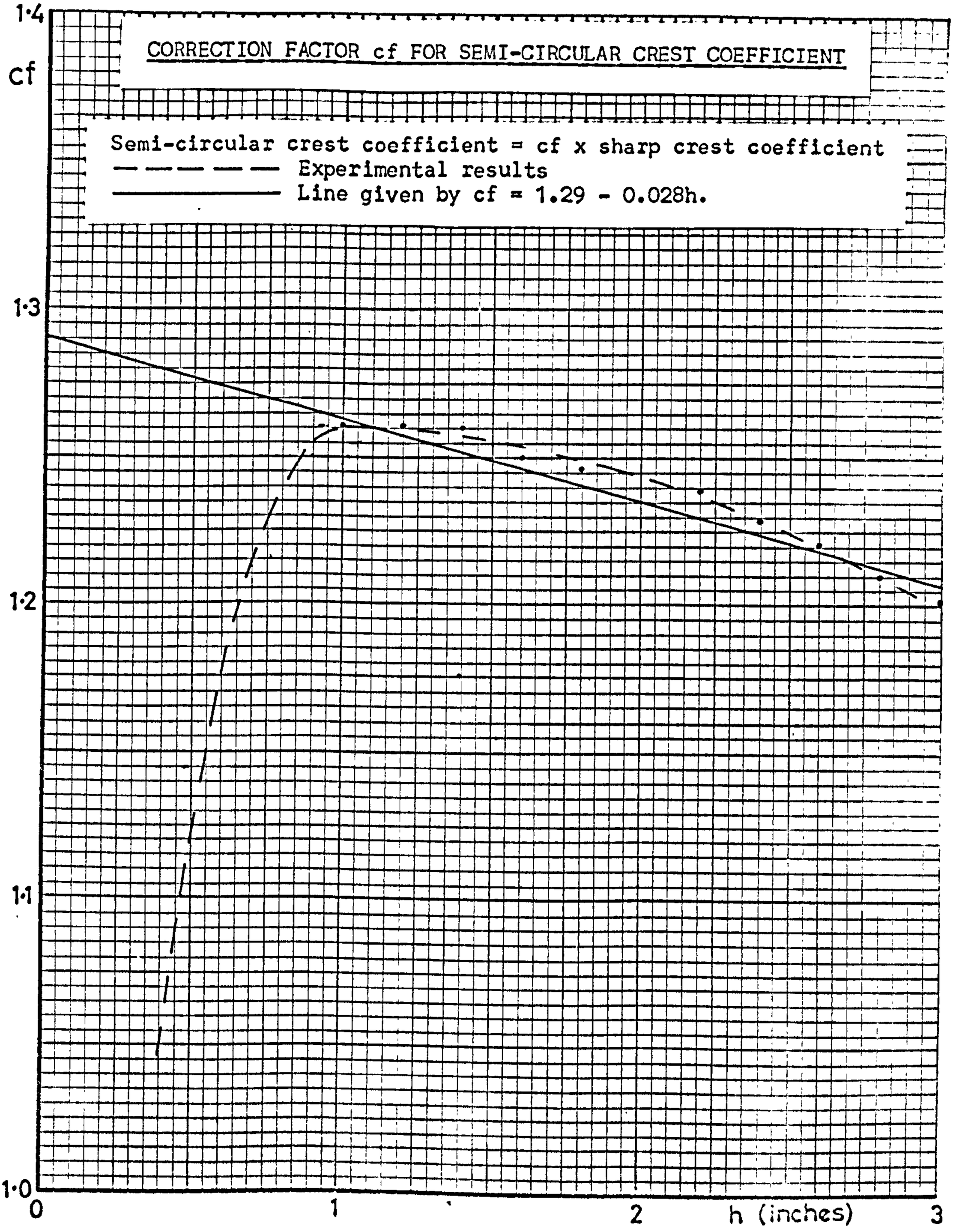
CORRECTION FACTOR cf FOR SEMI-CIRCULAR CREST COEFFICIENT
Semi-circular crest coefficient = cf x sharp crest coefficient
Experimental results
Line given by cf = 1.29 - 0.028h.
cf
1·4
1·3
1·2
1·1
1·0
0
1
2
h (inches)
3

Figure 62

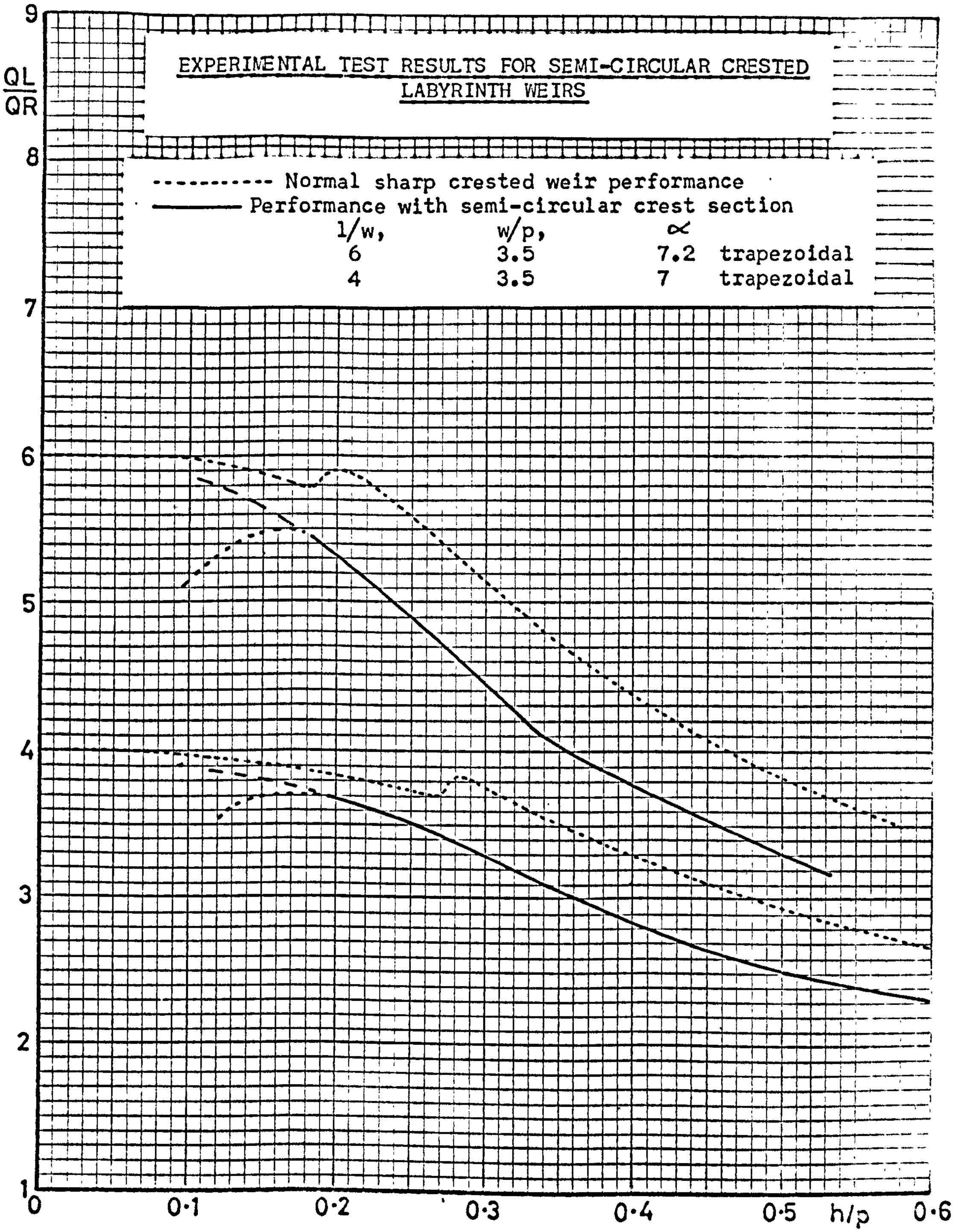
EXPERIMENTAL TEST RESULTS FOR SEMI-CIRCULAR CRESTED LABYRINTH WEIRS
QL/QR
---------- Normal sharp crested weir performance
——— Performance with semi-circular crest section
l/w, w/p, ∝
6 3.5 7.2 trapezoidal
4 3.5 7 trapezoidal
9
8
7
6
5
4
3
2
1
0
0·1
0·2
0·3
0·4
0·5
h/p
0·6

Figure 63

EXPERIMENTAL TEST RESULTS FOR SEMI-CIRCULAR CRESTED LABYRINTH WEIRS WHERE THE FLOW MAGNIFICATION REPRESENTS THE LABYRINTH WEIR DISCHARGE COMPARED WITH THE CORRESPONDING SHARP CRESTED LINEAR WEIR DISCHARGE

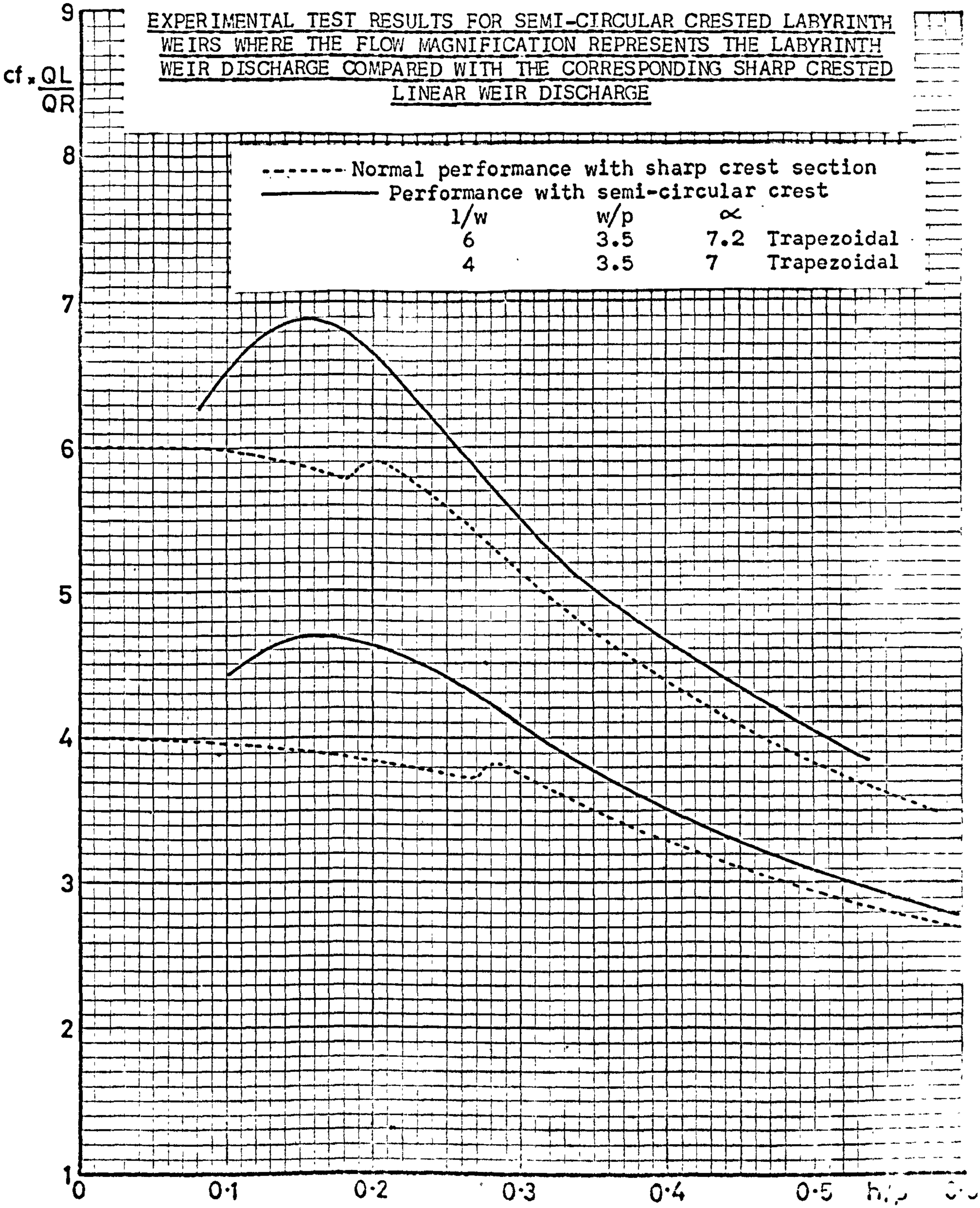

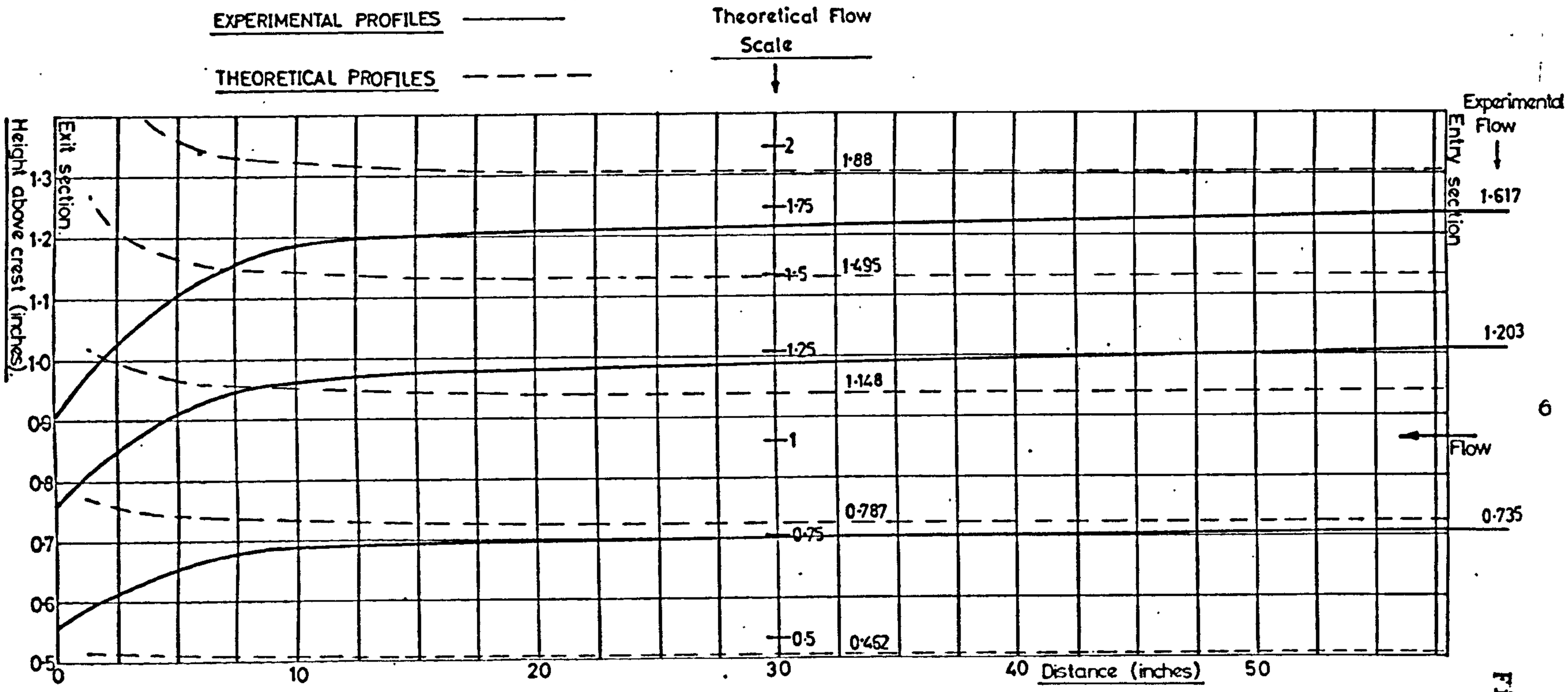

UPSTREAM CHANNEL (CENTRE LINE) SURFACE PROFILES FOR TRIANGULAR PLAN FORM WEIR (LENGTH MAGNIFICATION = 5)

Figure 64

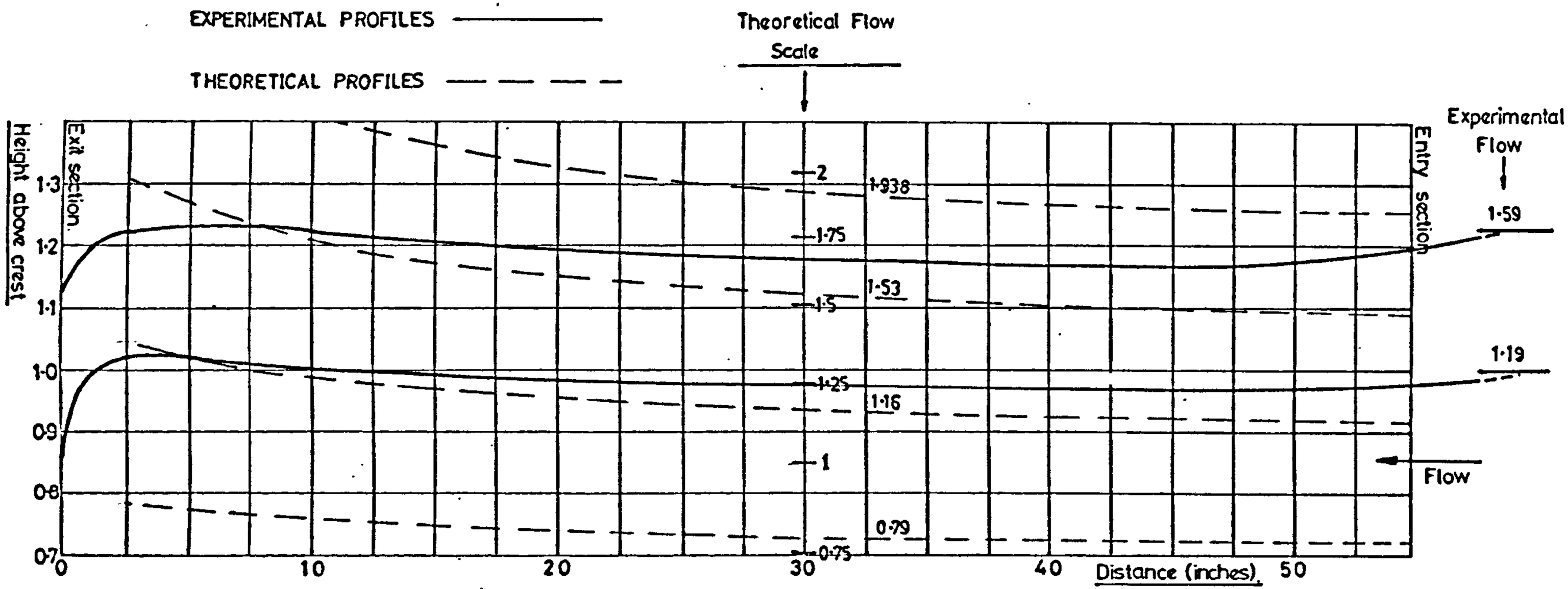

UPSTREAM CHANNEL (CENTRE LINE) SURFACE PROFILES FOR TRAPEZOIDAL PLAN FORM WEIR (LENGTH MAGNIFICATION = 5)

Figure 65

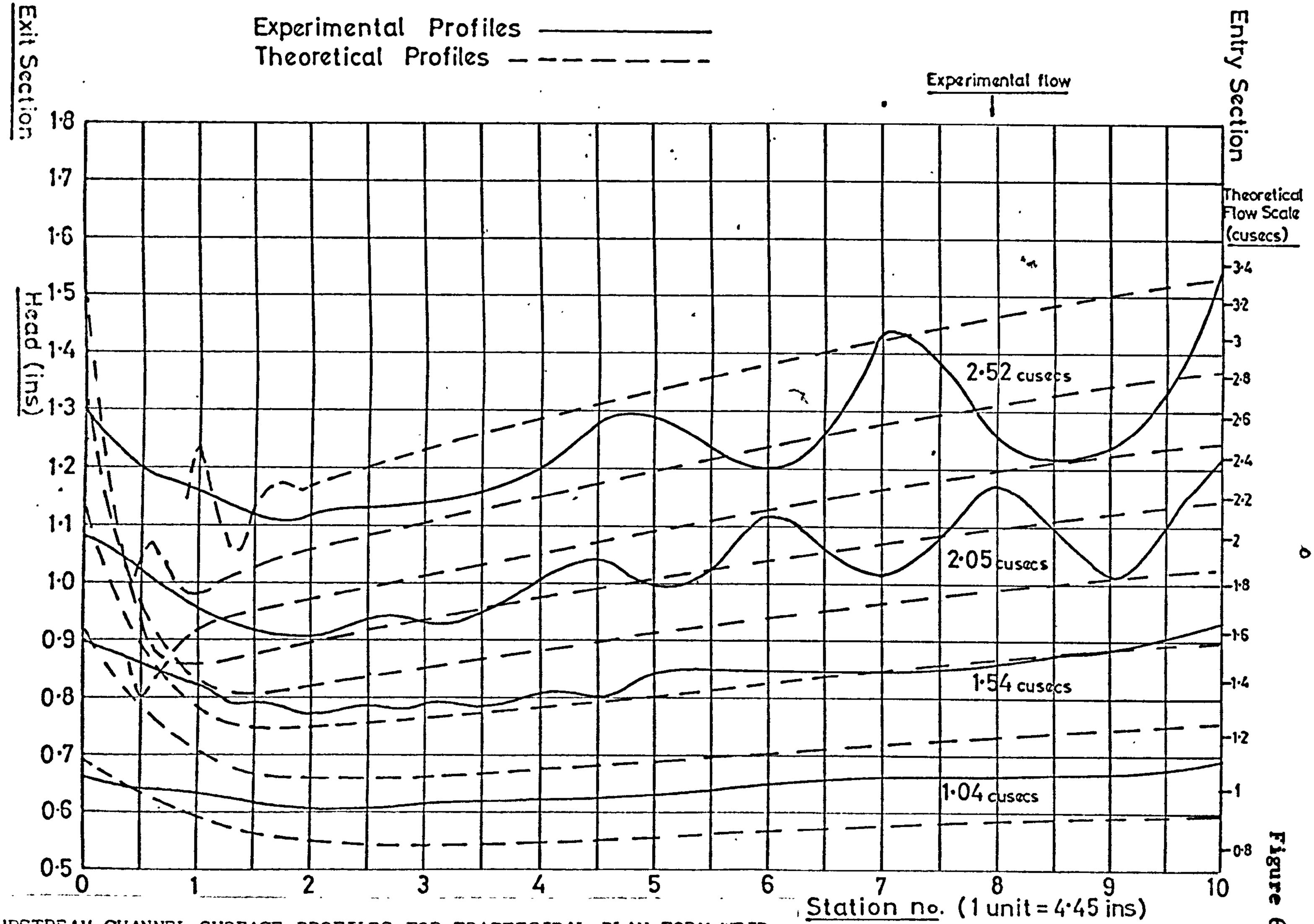

UPSTREAM CHANNEL SURFACE PROFILES FOR TRAPEZOIDAL PLAN FORM WEIR WITH APRONS $1/w = 8$, $w/p = 2.5$, $\alpha = 5.4^{\circ}$

Figure 66.

Figure 67

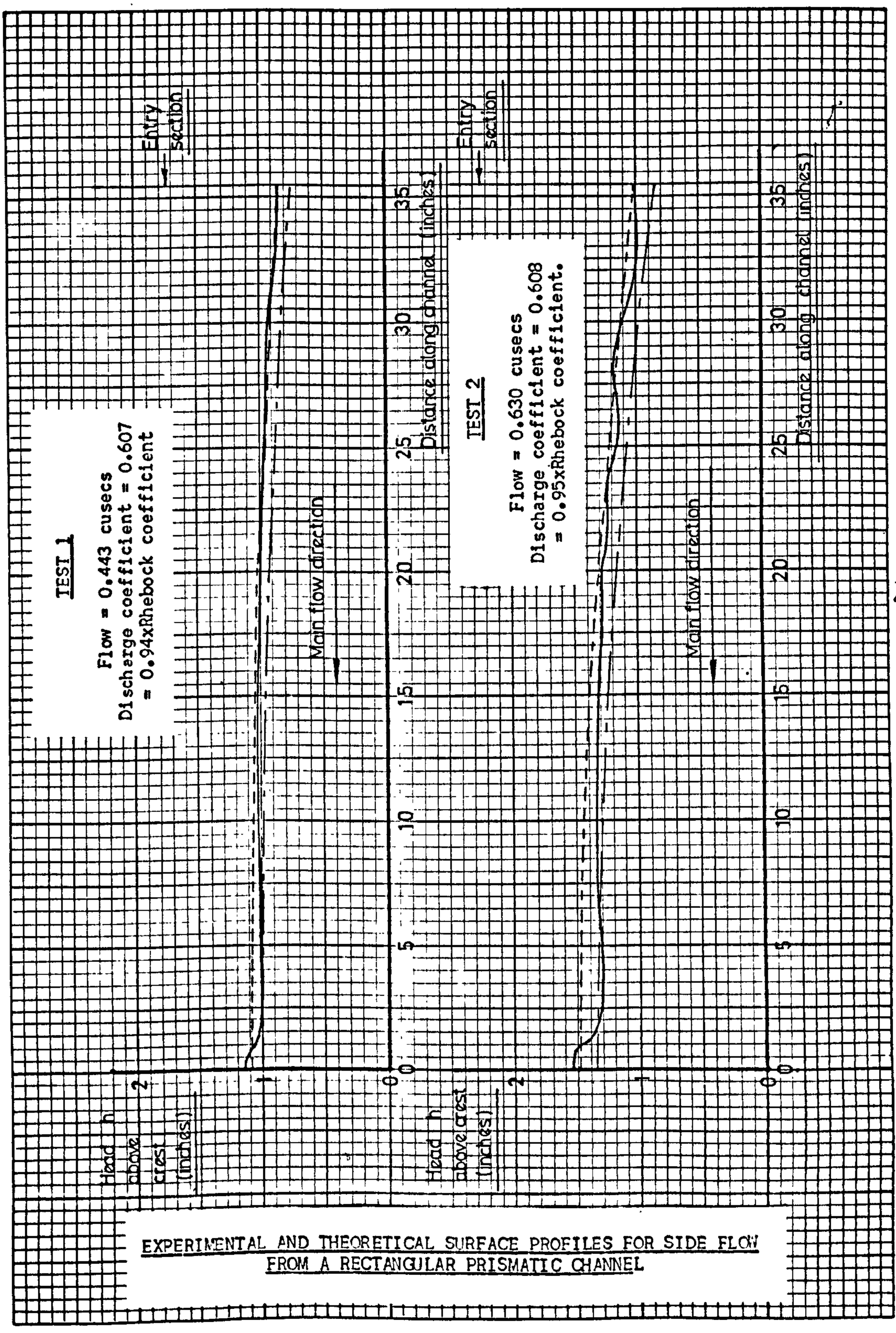

EXPERIMENTAL AND THEORETICAL SURFACE PROFILES FOR SIDE FLOW FROM A RECTANGULAR PRISMATIC CHANNEL

Figure 68

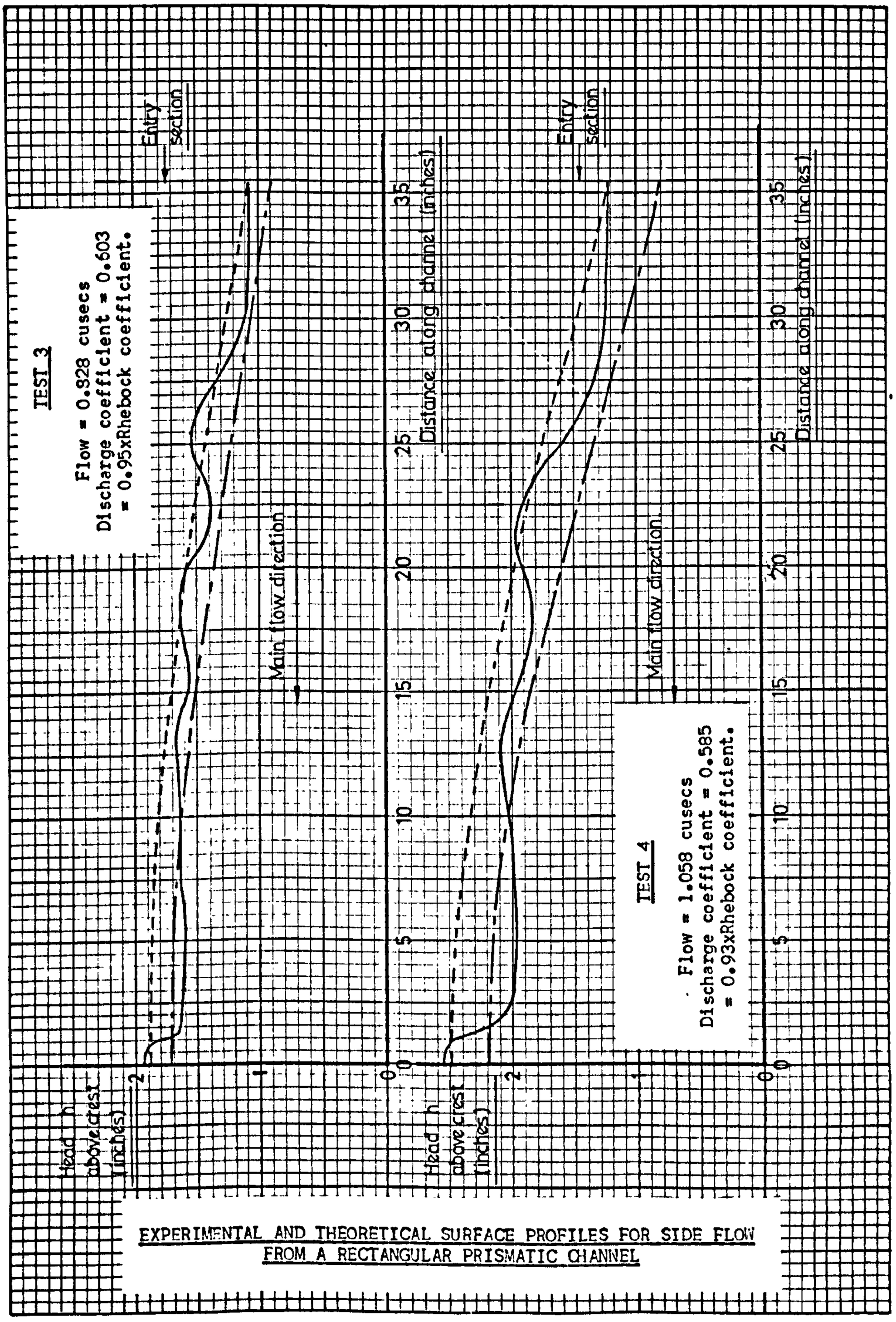

EXPERIMENTAL AND THEORETICAL SURFACE PROFILES FOR SIDE FLOW FROM A RECTANGULAR PRISMATIC CHANNEL

For key see Figure 67

Figure 69

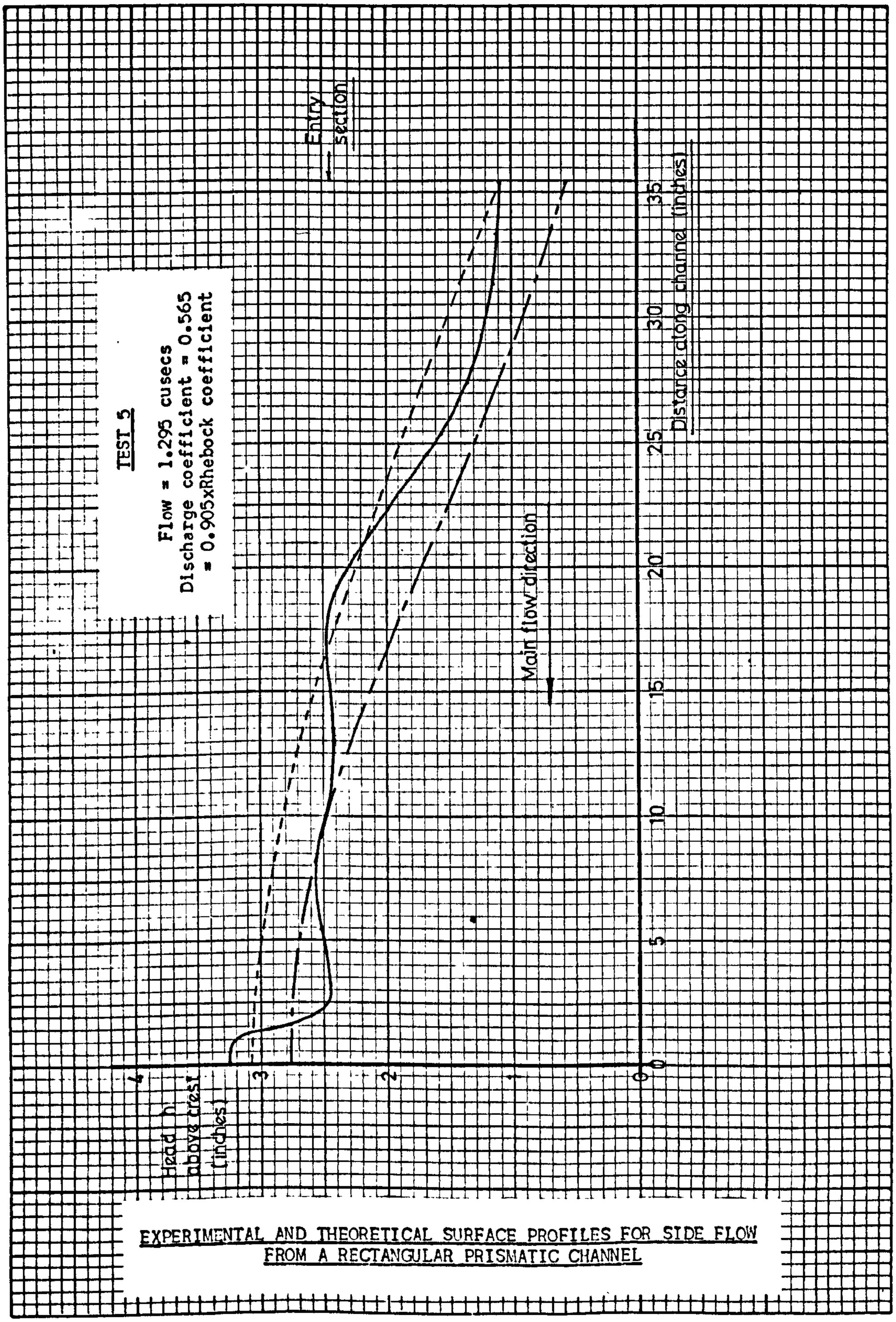

EXPERIMENTAL AND THEORETICAL SURFACE PROFILES FOR SIDE FLOW FROM A RECTANGULAR PRISMATIC CHANNEL

For key see Figure 67.

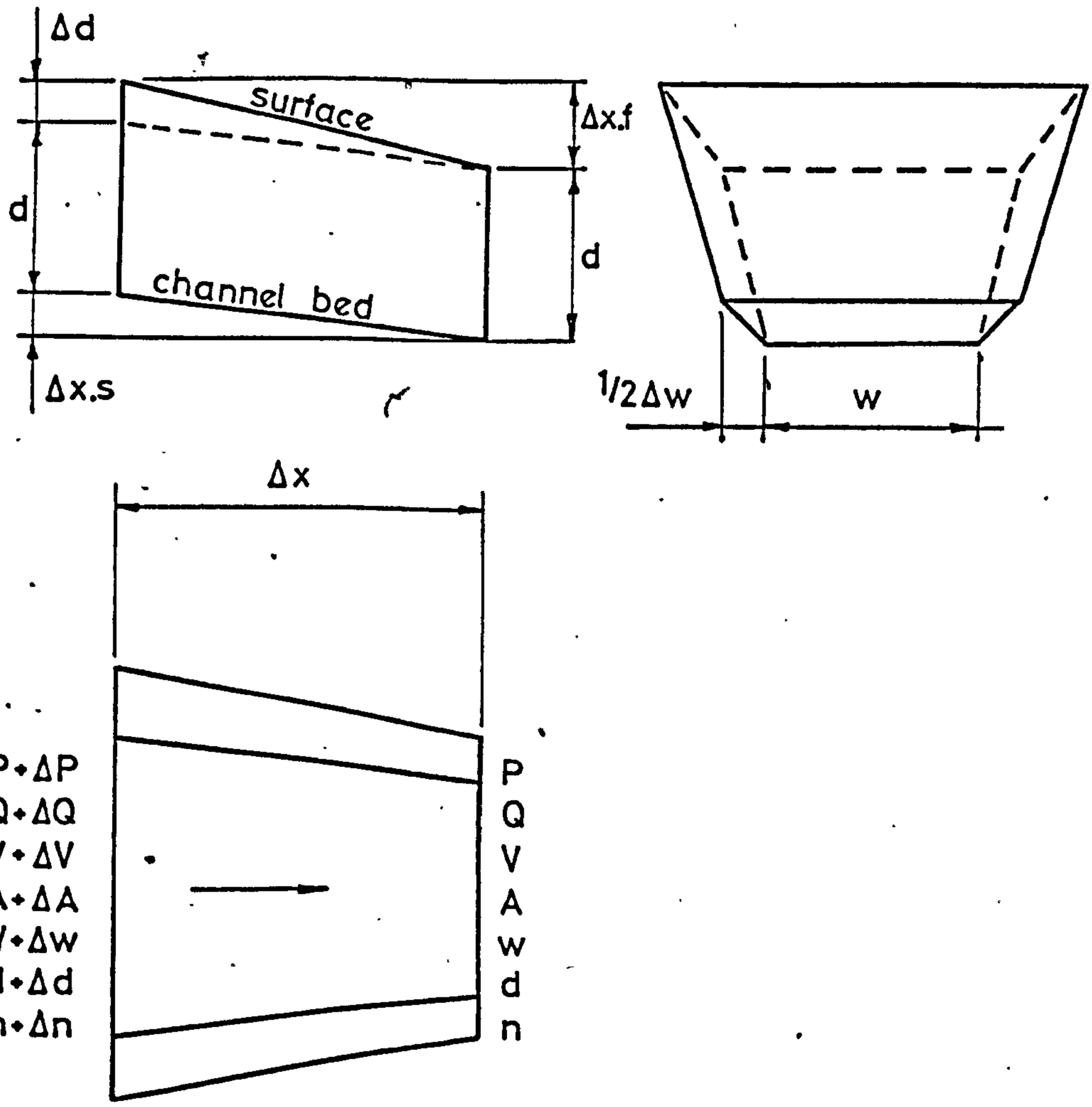

DIAGRAM AND NOTATION USED IN THE ANALYSIS DERIVED BY NIMMO

Figure 7I

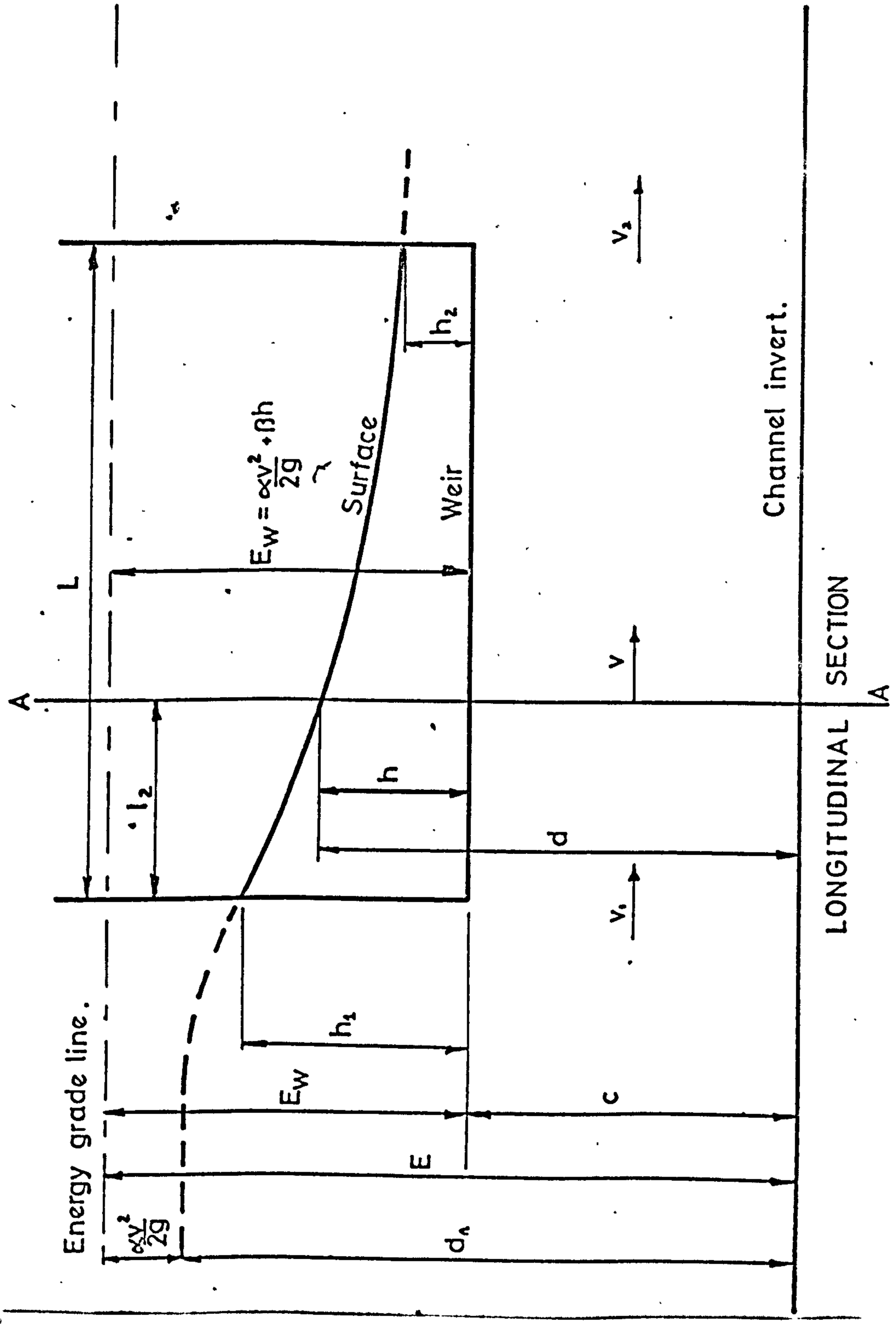

FALLING SURFACE PROFILE IN A RECTANGULAR CHANNEL INDICATING NOTATION USED BY ACKERS (FLOW SUPERCRITICAL)

Figure 72

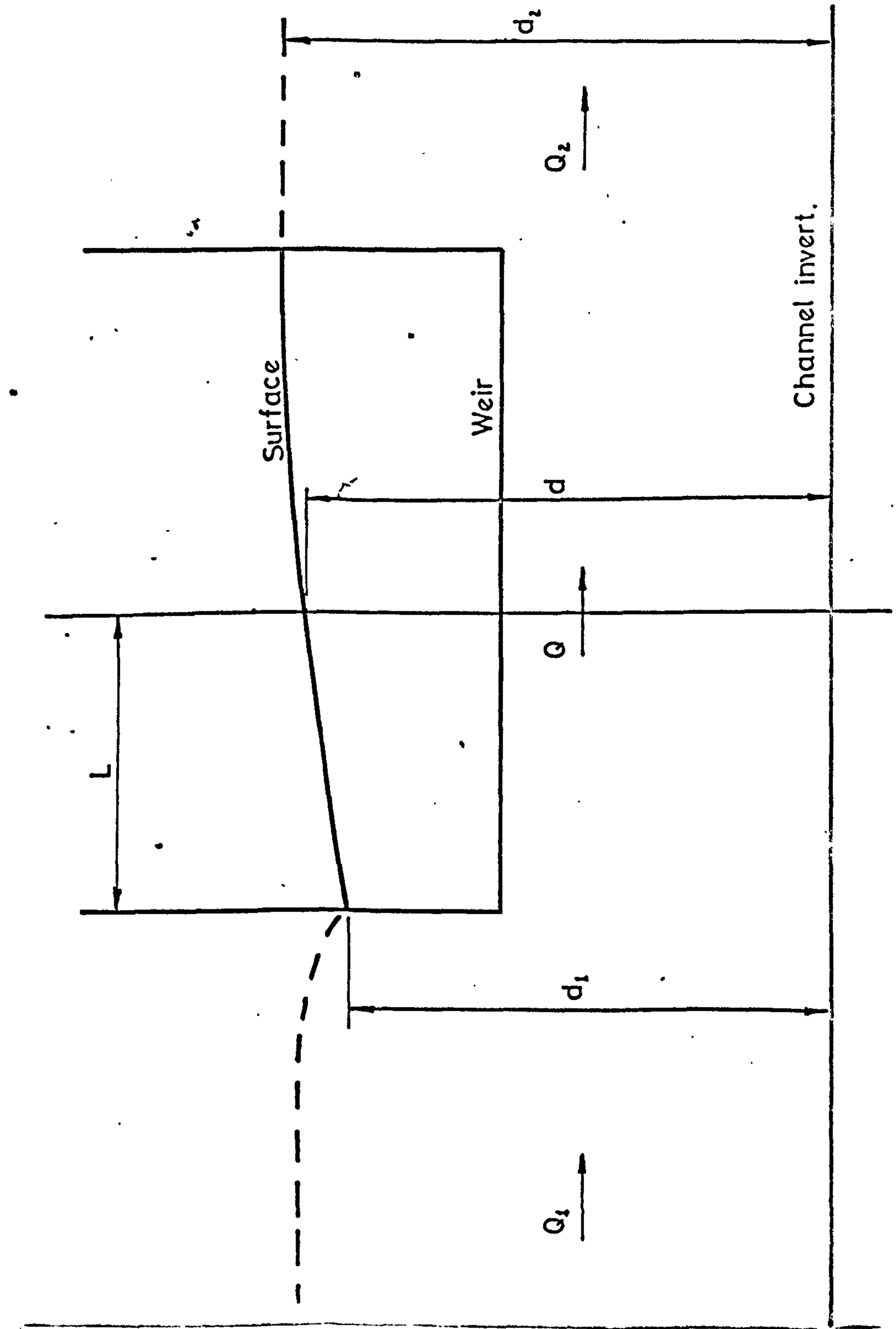

RISING SURFACE PROFILE IN A RECTANGULAR CHANNEL INDICATING NOTATION USED BY DE MARCHI (FLOW SUBSCRITICAL)

Figure 73

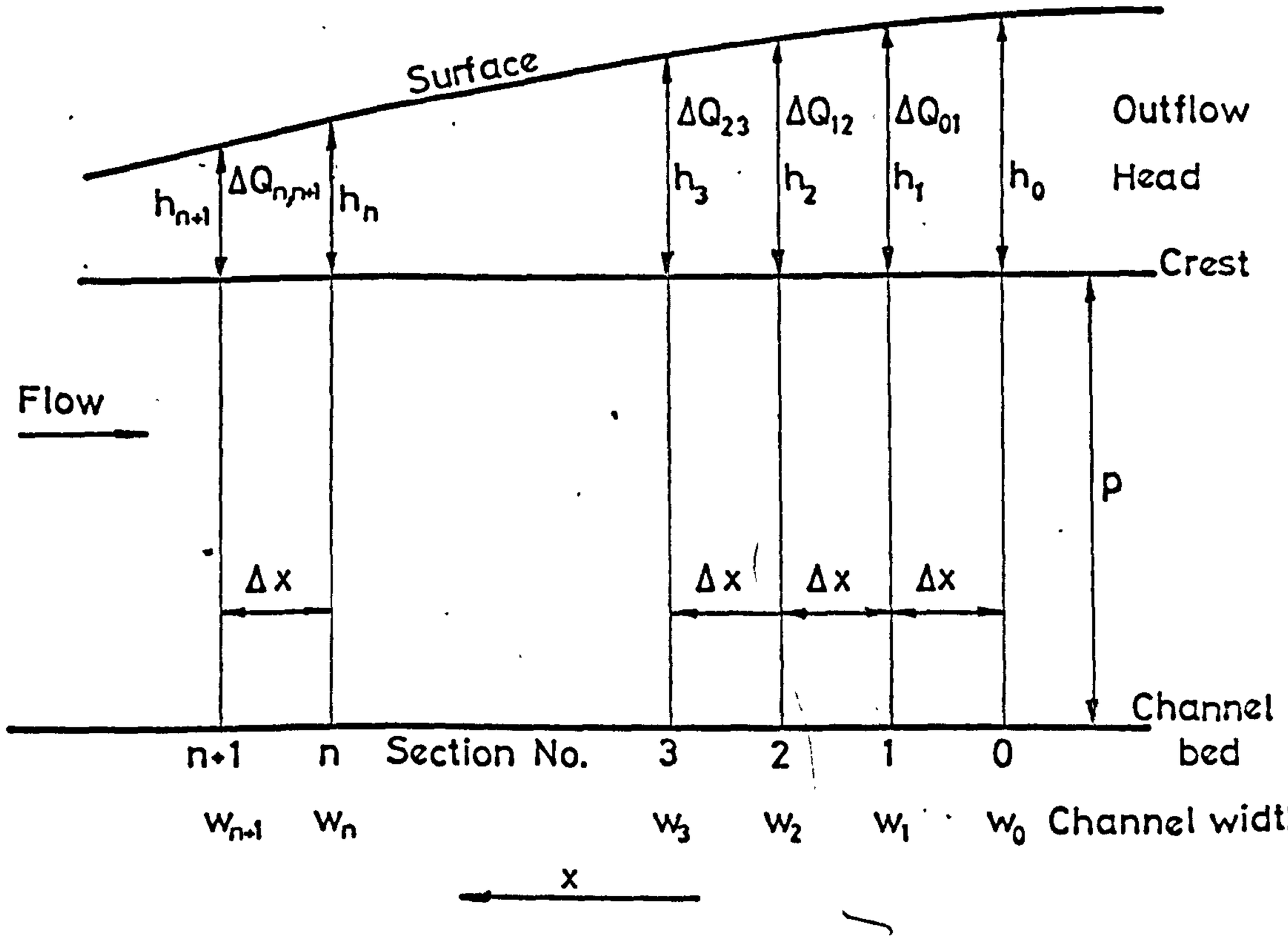

DIAGRAM ILLUSTRATING METHOD OF SOLUTION BY MARCHING PROCEDURE

Figure 74

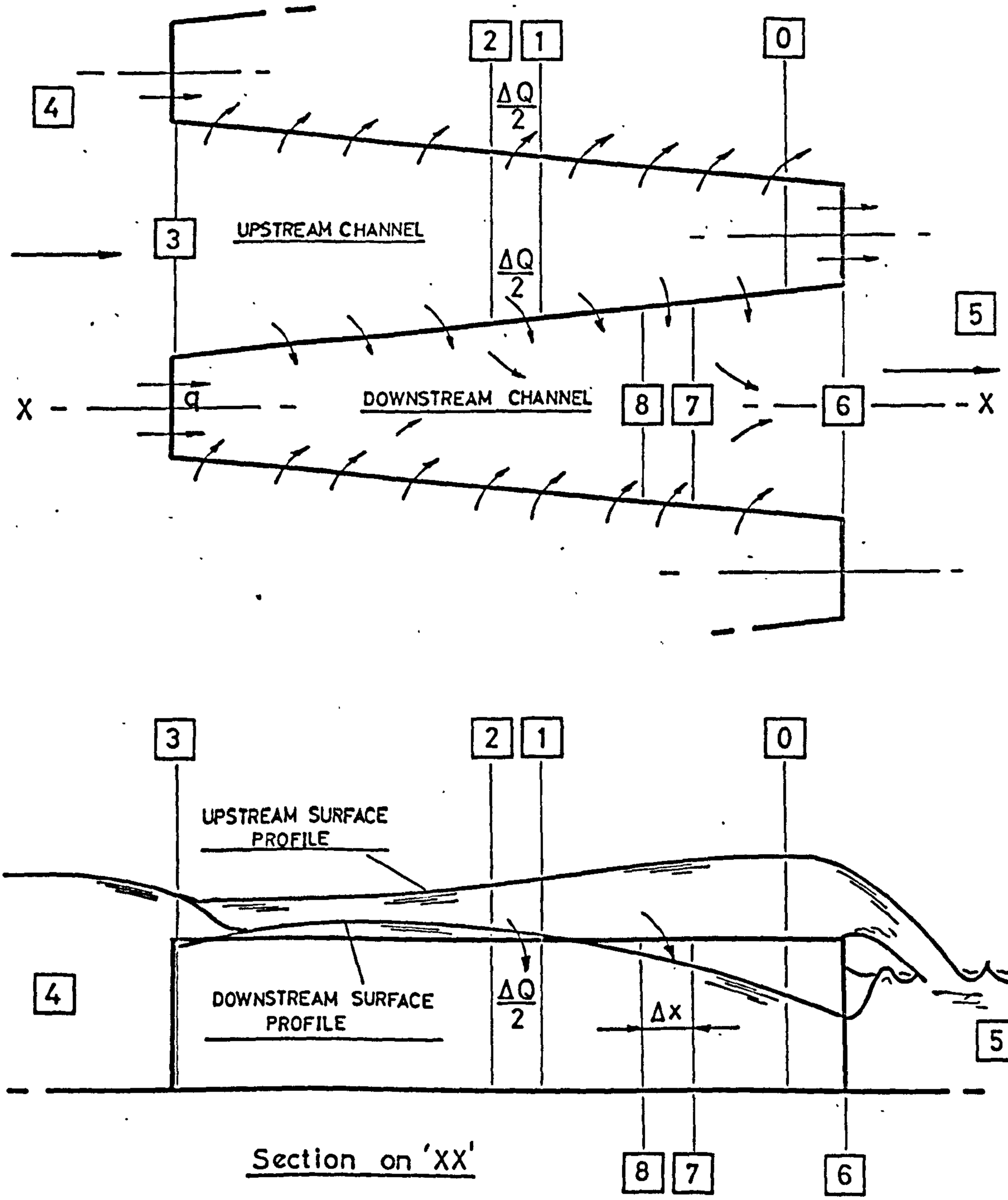

DIAGRAM USED TO DESCRIBE THE THEORETICAL ANALYSIS OF LABYRINTH WEIR FLOW

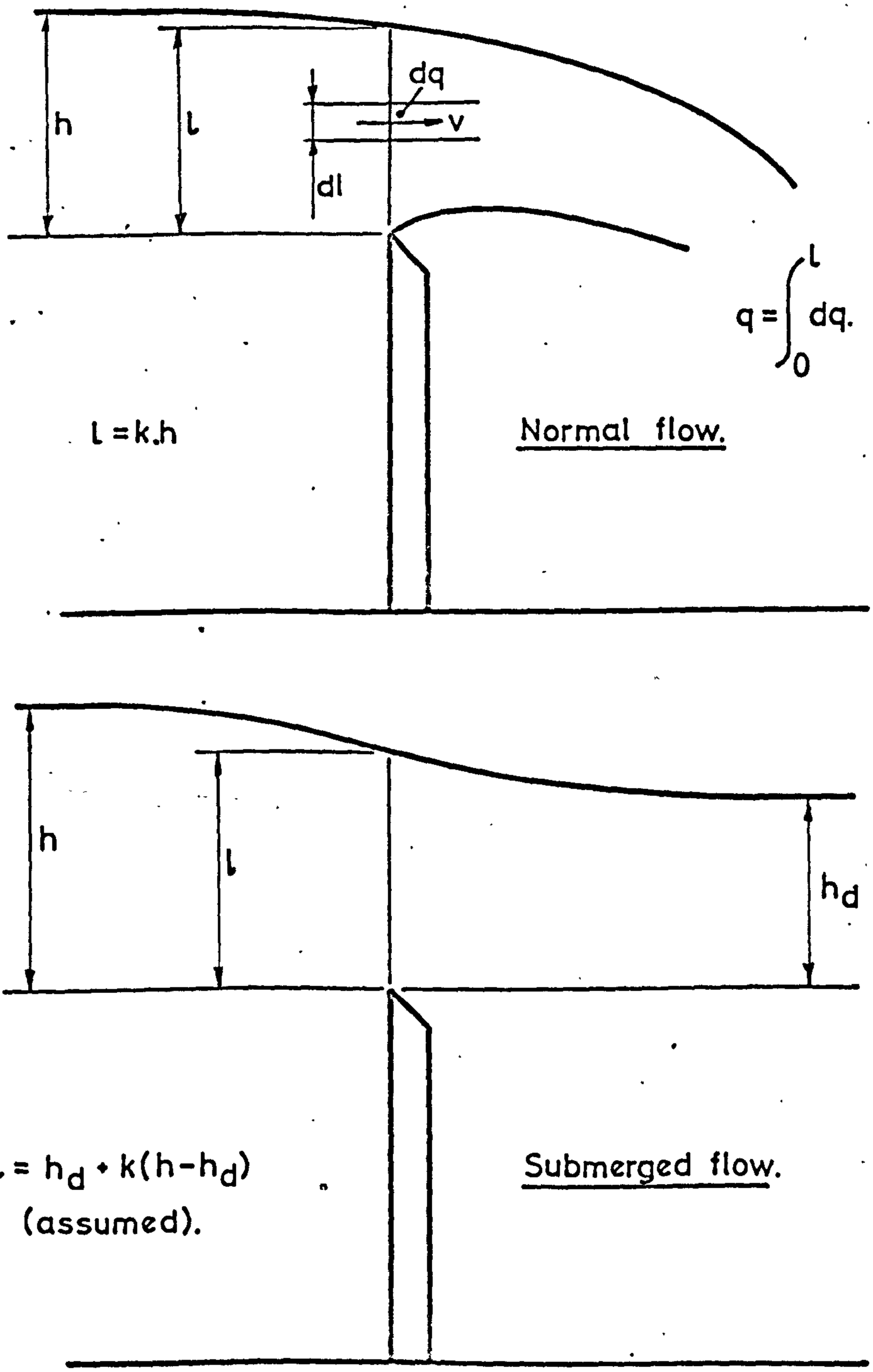

DIAGRAM INDICATING THE NOTATION USED IN DETERMINING THE MOMENTUM OF THE OVERFLOW

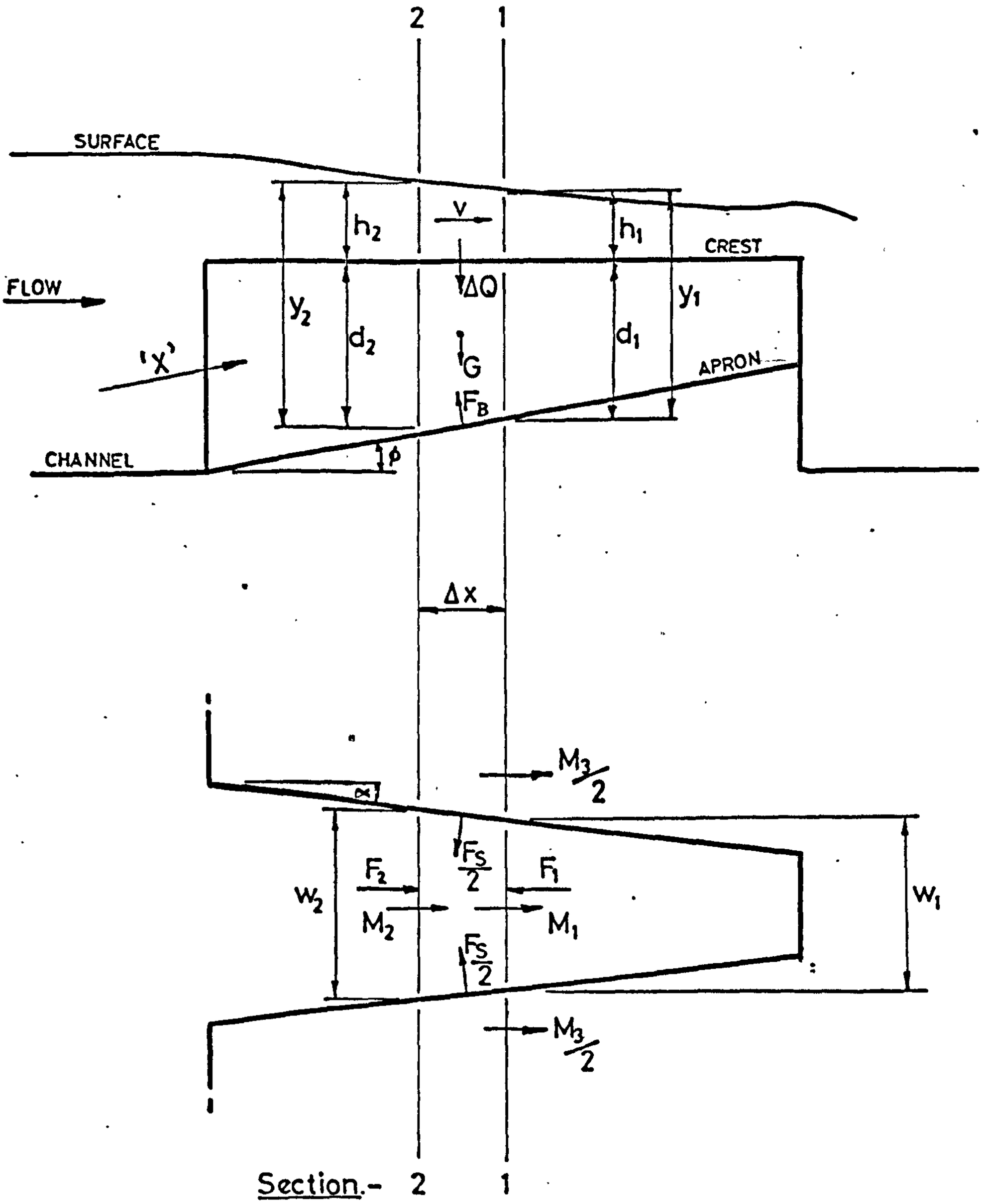

DIAGRAM INDICATING THE NOTATION USED IN THE UPSTREAM CHANNEL ANALYSIS

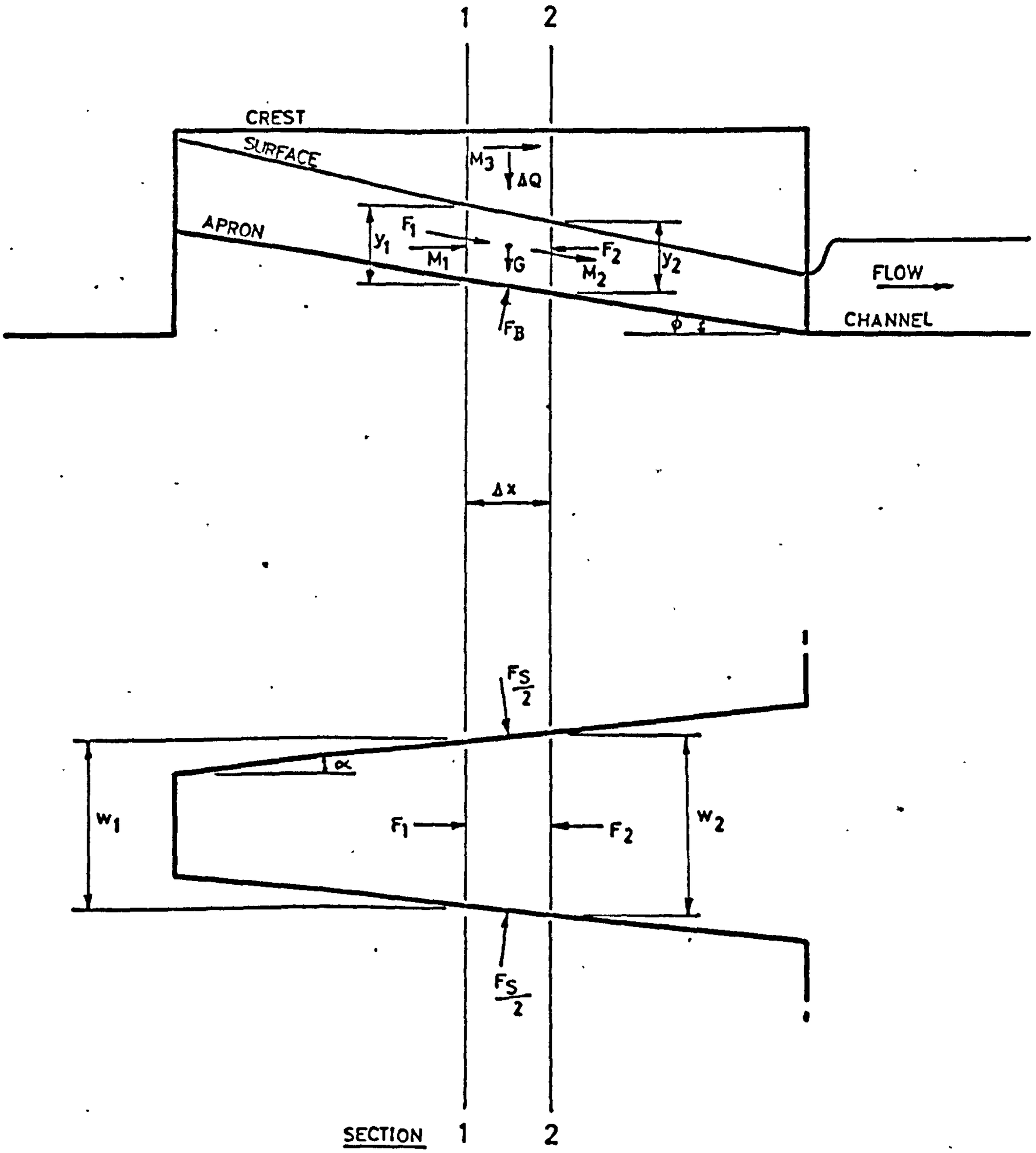

DIAGRAM INDICATING THE NOTATION USED IN THE DOWNSTREAM CHANNEL ANALYSIS

Figure 78

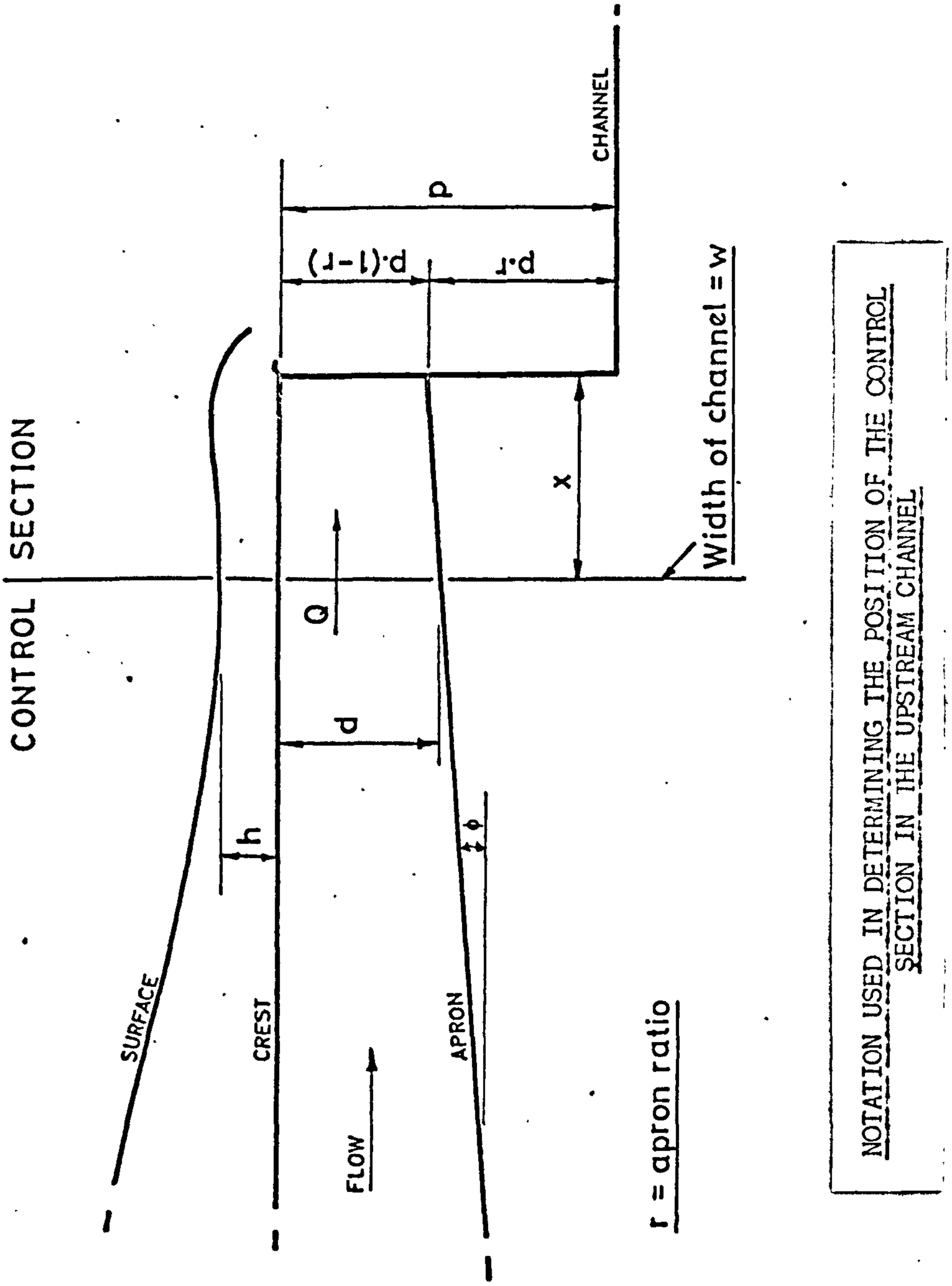
CONTROL SECTION
CHANNEL
d
p.(1-r)
p.r
SURFACE
CREST
APRON
h
d
Q
FLOW
φ
x
Width of channel = W
r = apron ratio
NOTATION USED IN DETERMINING THE POSITION OF THE CONTROL SECTION IN THE UPSTREAM CHANNEL

Figure 79

THEORETICAL RESULTS OBTAINED FROM MATHEMATICAL MODEL FOR FULLY VENTILATED FLOW - ILLUSTRATING THE EFFECT OF EMPIRICAL COEFFICIENTS

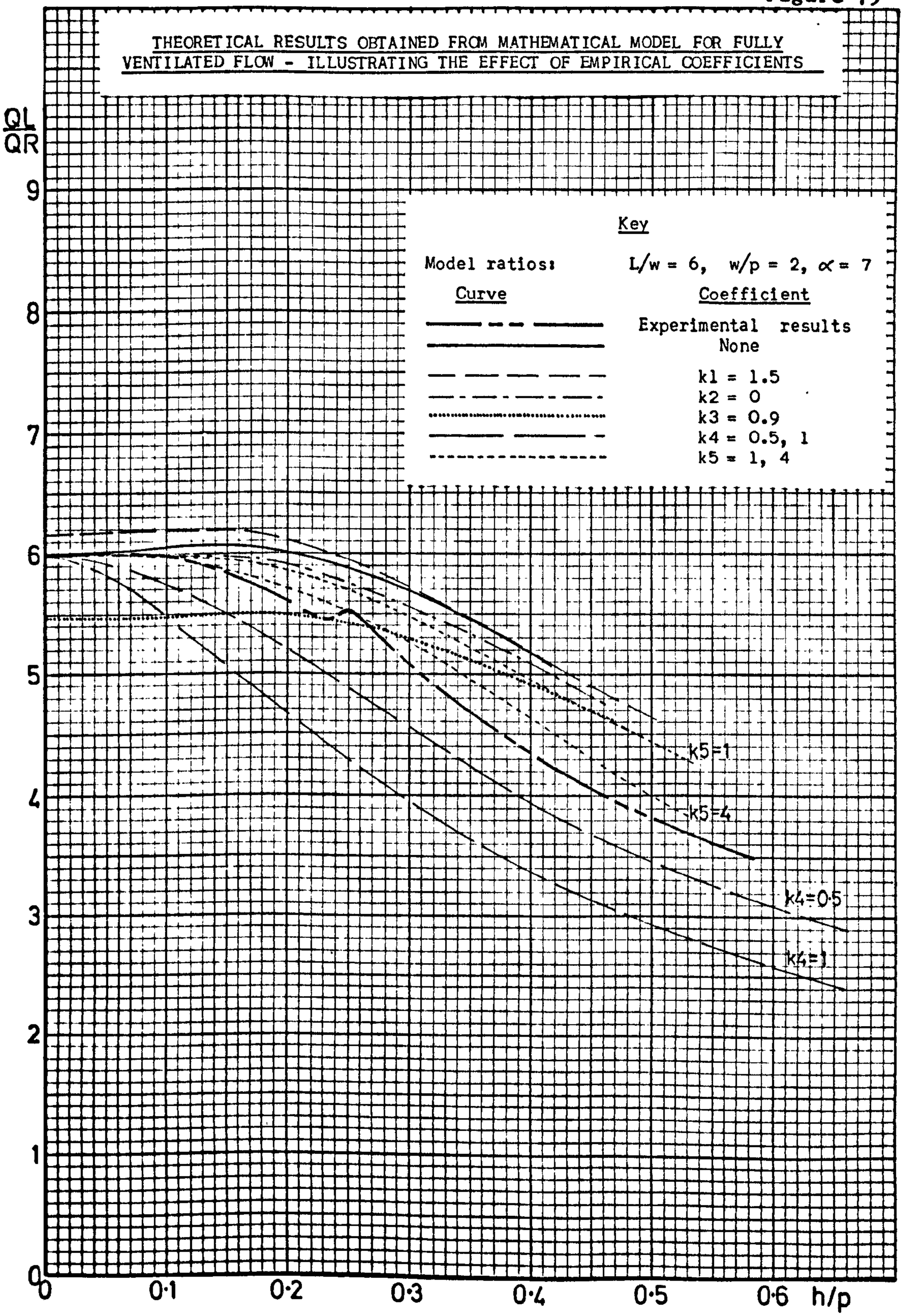

Figure 80

THEORETICAL RESULTS OBTAINED FROM MATHEMATICAL MODEL FOR FULLY VENTILATED FLOW - ILLUSTRATING THE EFFECT OF EMPIRICAL COEFFICIENTS

$\frac{QL}{QR}$

Key

Model ratios: L/w = 6, w/p = 2, α = 0

Curve	Coefficient
——— -- ——— --	Experimental results
———	None
— — — — —	k1 = 1.5
— - — - — - —	k2 = 0
.....	k3 = 0.9
——— ——— —	k4 = 0.5, 1
- - - - - - -	k5 = 1, 4

k5=1
k4=1
k4=0.5
k5=4

9
8
7
6
5
4
3
2
1
0

0 0·1 0·2 0·3 0·4 0·5 0·6 h/p

Figure 81

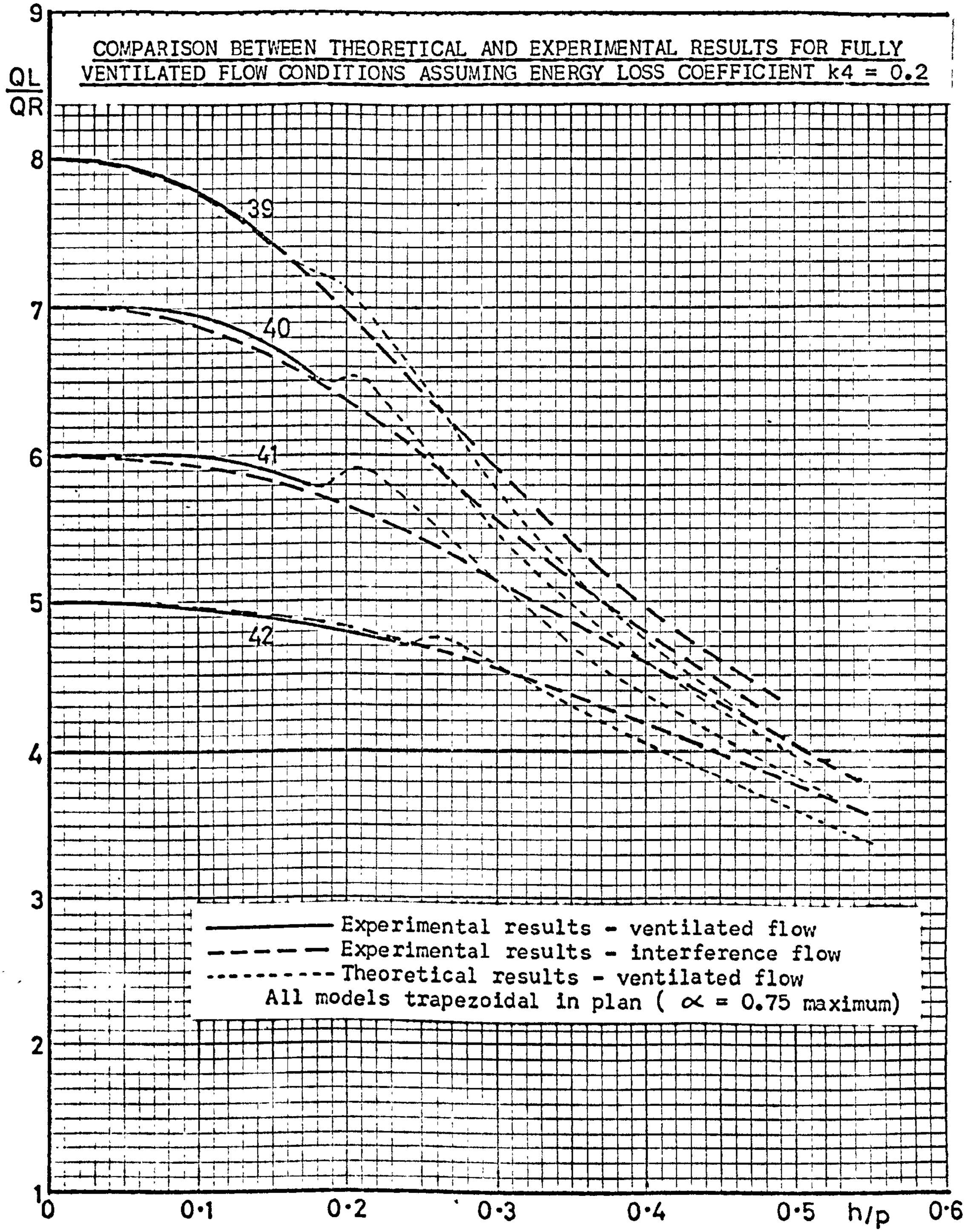
COMPARISON BETWEEN THEORETICAL AND EXPERIMENTAL RESULTS FOR FULLY VENTILATED FLOW CONDITIONS ASSUMING ENERGY LOSS COEFFICIENT k4 = 0.2
QL/QR
9
8
7
6
5
4
3
2
1
39
40
41
42
Experimental results - ventilated flow
Experimental results - interference flow
Theoretical results - ventilated flow
All models trapezoidal in plan (∝ = 0.75 maximum)
0
0·1
0·2
0·3
0·4
0·5
h/p
0·6

Figure 82

COMPARISON BETWEEN THEORETICAL AND EXPERIMENTAL RESULTS INCLUDING AN ALLOWANCE IN THE ANALYSIS FOR DOWNSTREAM INTERFERENCE

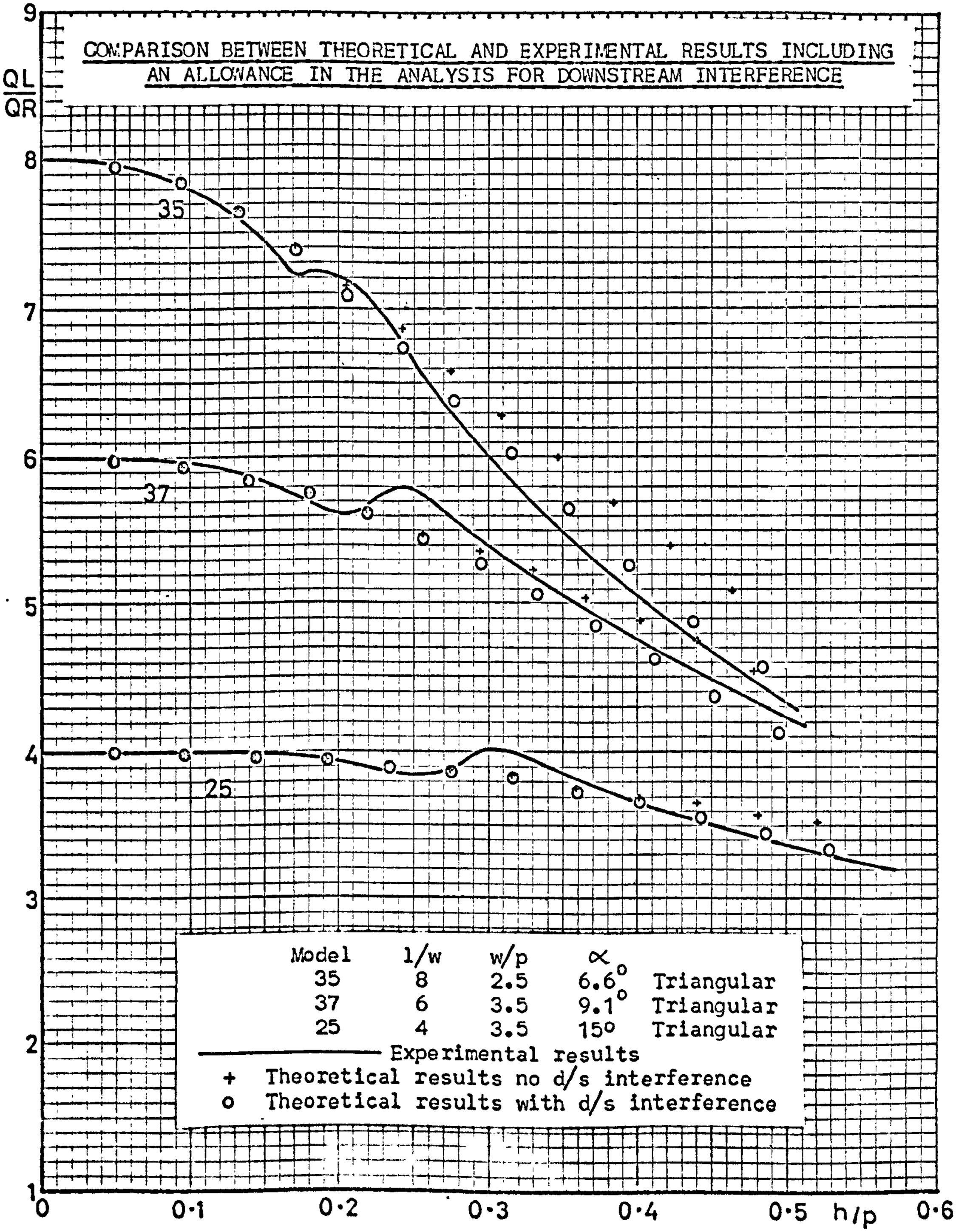

Model	l/w	w/p	∝	
35	8	2.5	6.6°	Triangular
37	6	3.5	9.1°	Triangular
25	4	3.5	15°	Triangular

——— Experimental results

\+ Theoretical results no d/s interference

o Theoretical results with d/s interference

Figure 83

COMPARISON BETWEEN THEORETICAL AND EXPERIMENTAL RESULTS INCLUDING AN ALLOWANCE IN THE ANALYSIS FOR DOWNSTREAM INTERFERENCE

Model	l/w	w/p	α	
36	7	3	7.7	Triangular
38	5	4.5	11.1	Triangular

——— Experimental results

\+ Theoretical results - no d/s interference

o Theoretical results - with d/s interference

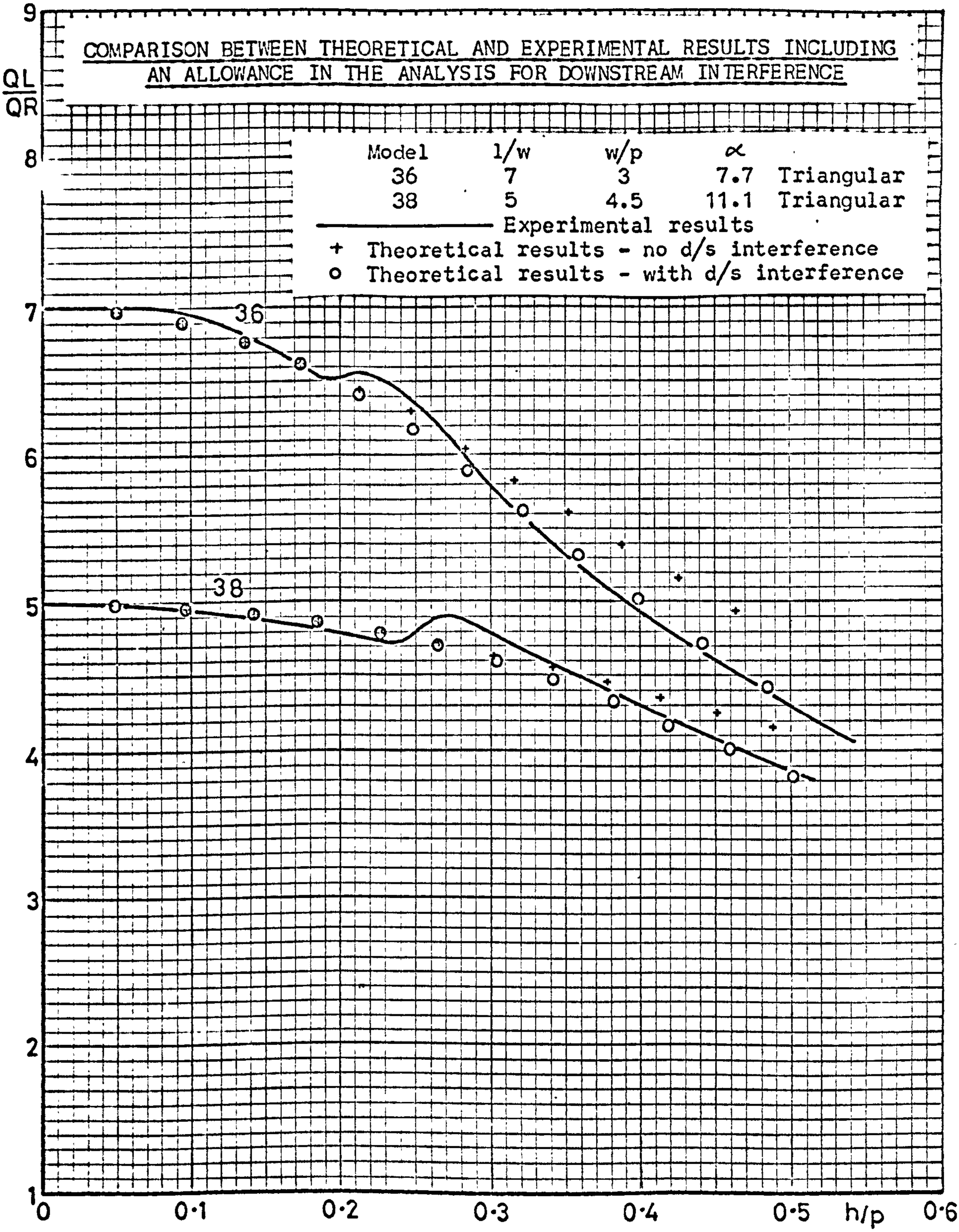

Figure 84

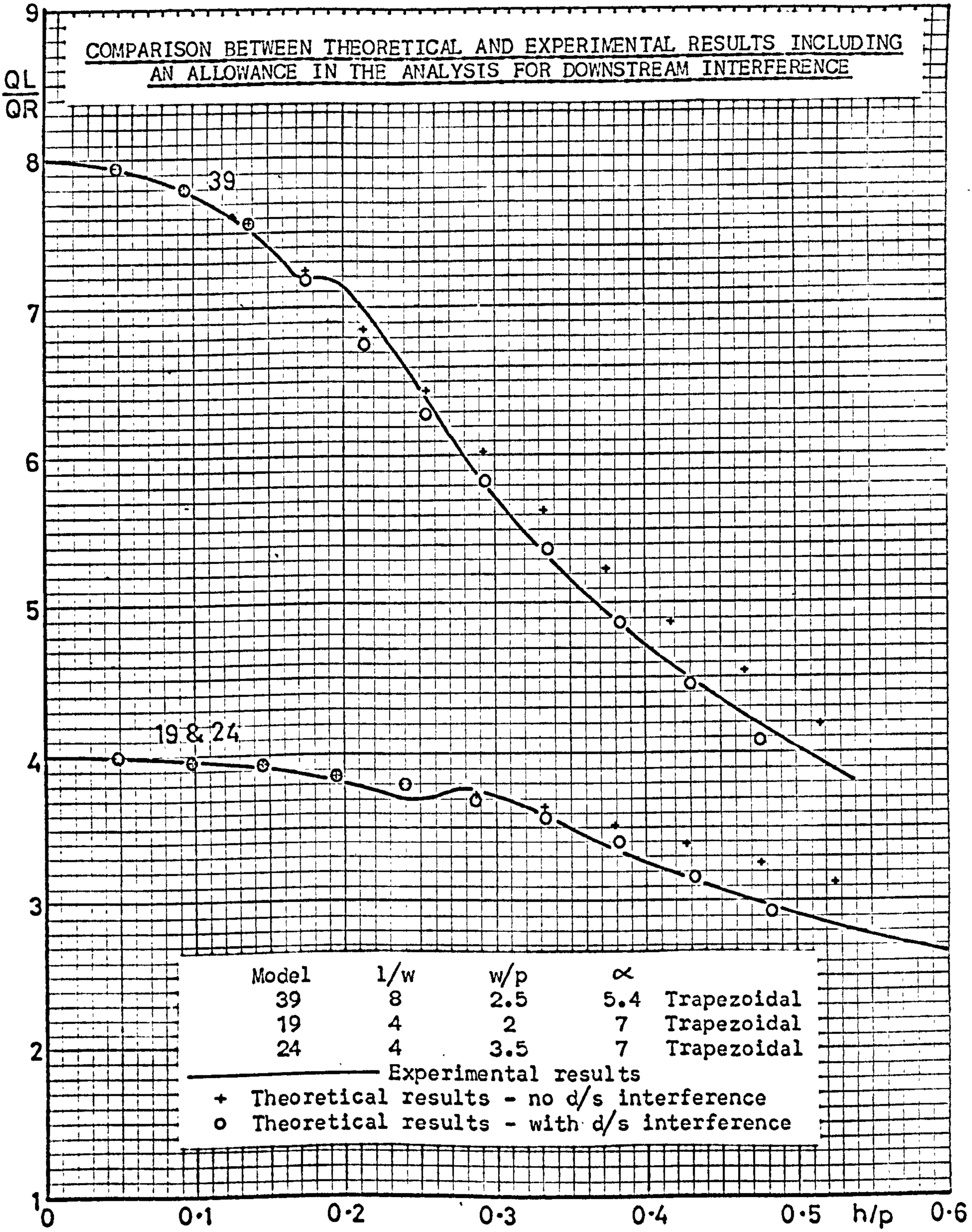
COMPARISON BETWEEN THEORETICAL AND EXPERIMENTAL RESULTS INCLUDING AN ALLOWANCE IN THE ANALYSIS FOR DOWNSTREAM INTERFERENCE
QL/QR
9
8
7
6
5
4
3
2
1
39
19 & 24
0
0·1
0·2
0·3
0·4
0·5
h/p
0·6
Model 1/w w/p ∝
39 8 2.5 5.4 Trapezoidal
19 4 2 7 Trapezoidal
24 4 3.5 7 Trapezoidal
Experimental results
+ Theoretical results - no d/s interference
o Theoretical results - with d/s interference

Figure 85

COMPARISON BETWEEN THEORETICAL AND EXPERIMENTAL RESULTS INCLUDING AN ALLOWANCE IN THE ANALYSIS FOR DOWNSTREAM INTERFERENCE

Model	l/w	w/p	∝	
28	6	2	7	Trapezoidal
31	6	3.5	7	Trapezoidal
15	2	5	15	Trapezoidal
16	2	5	20	Trapezoidal

——— Experimental results

\+ Theoretical results - no d/s interference

o Theoretical results - with d/s interference

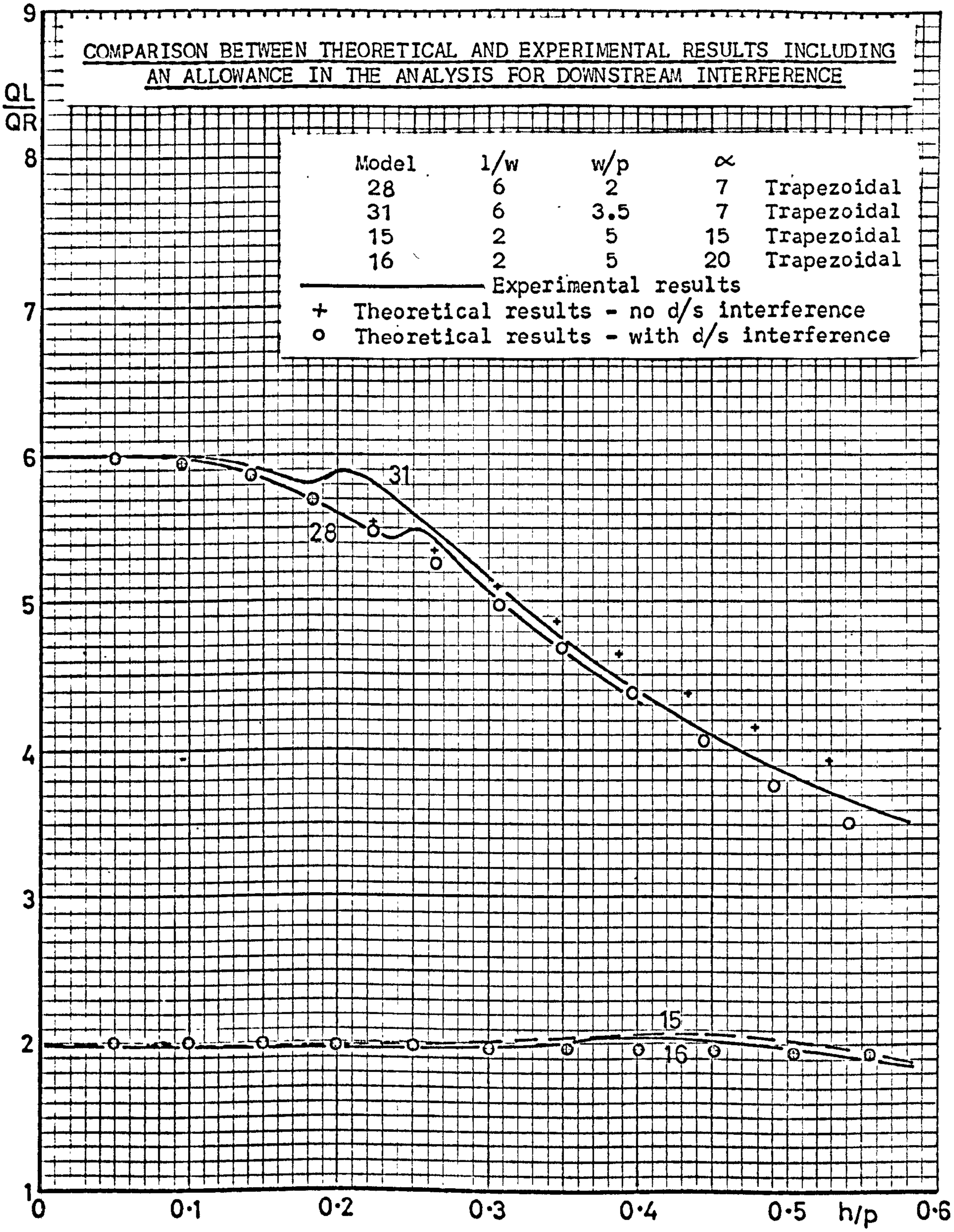

Figure 86

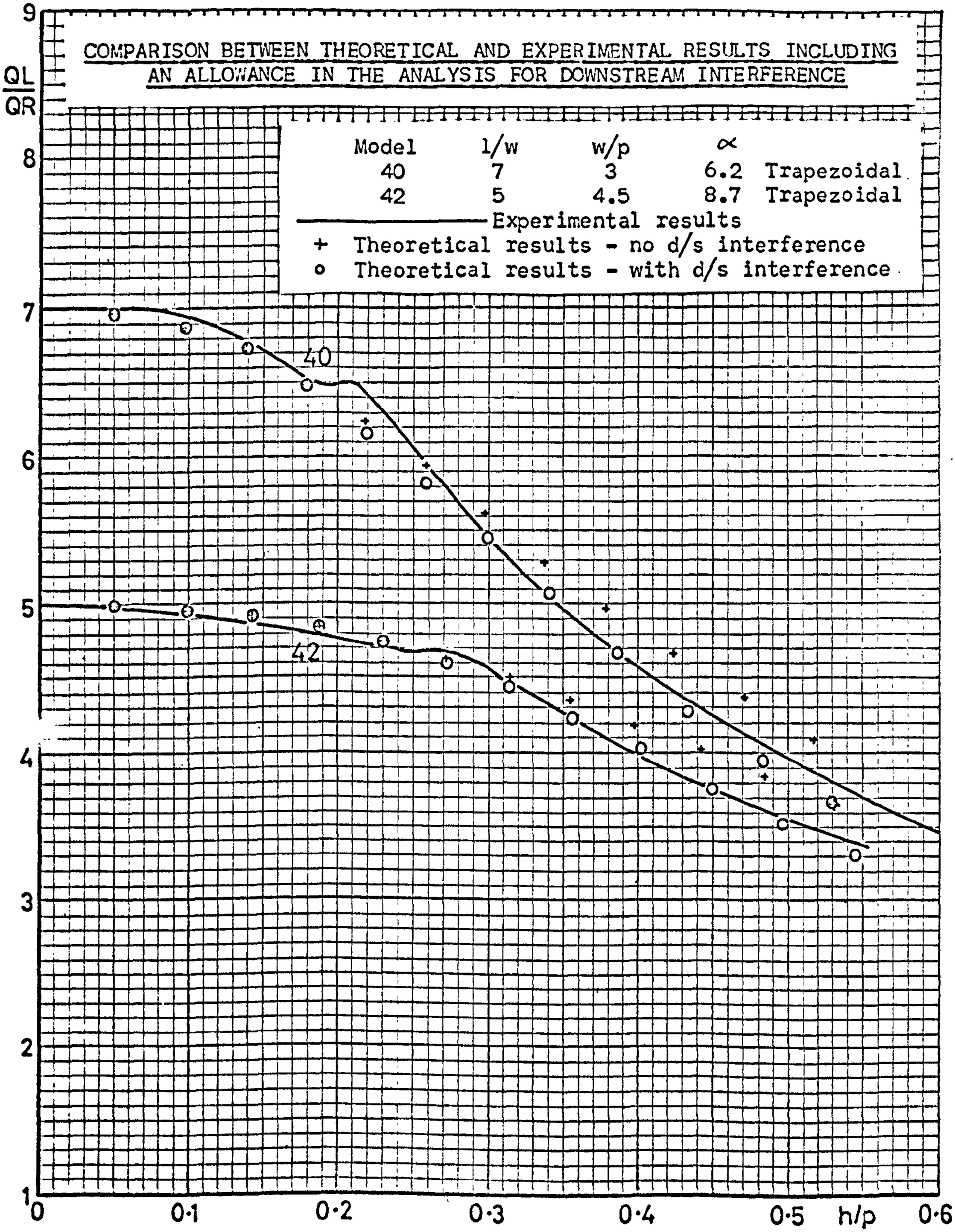
COMPARISON BETWEEN THEORETICAL AND EXPERIMENTAL RESULTS INCLUDING AN ALLOWANCE IN THE ANALYSIS FOR DOWNSTREAM INTERFERENCE
Model l/w w/p ∝
40 7 3 6.2 Trapezoidal
42 5 4.5 8.7 Trapezoidal
Experimental results
+ Theoretical results - no d/s interference
o Theoretical results - with d/s interference
QL/QR
9
8
7
6
5
4
3
2
1
40
42
0
0·1
0·2
0·3
0·4
0·5
h/p
0·6

Figure 87

COMPARISON BETWEEN THEORETICAL AND EXPERIMENTAL RESULTS INCLUDING AN ALLOWANCE IN THE ANALYSIS FOR DOWNSTREAM INTERFERENCE

Model	l/w	w/p	∝	
26	6	2	0	Rectangular
30	6	3.5	0	Rectangular
32	8	2	0	Rectangular

——— Experimental results

\+ Theoretical results - no d/s interference

o Theoretical results - with d/s interference

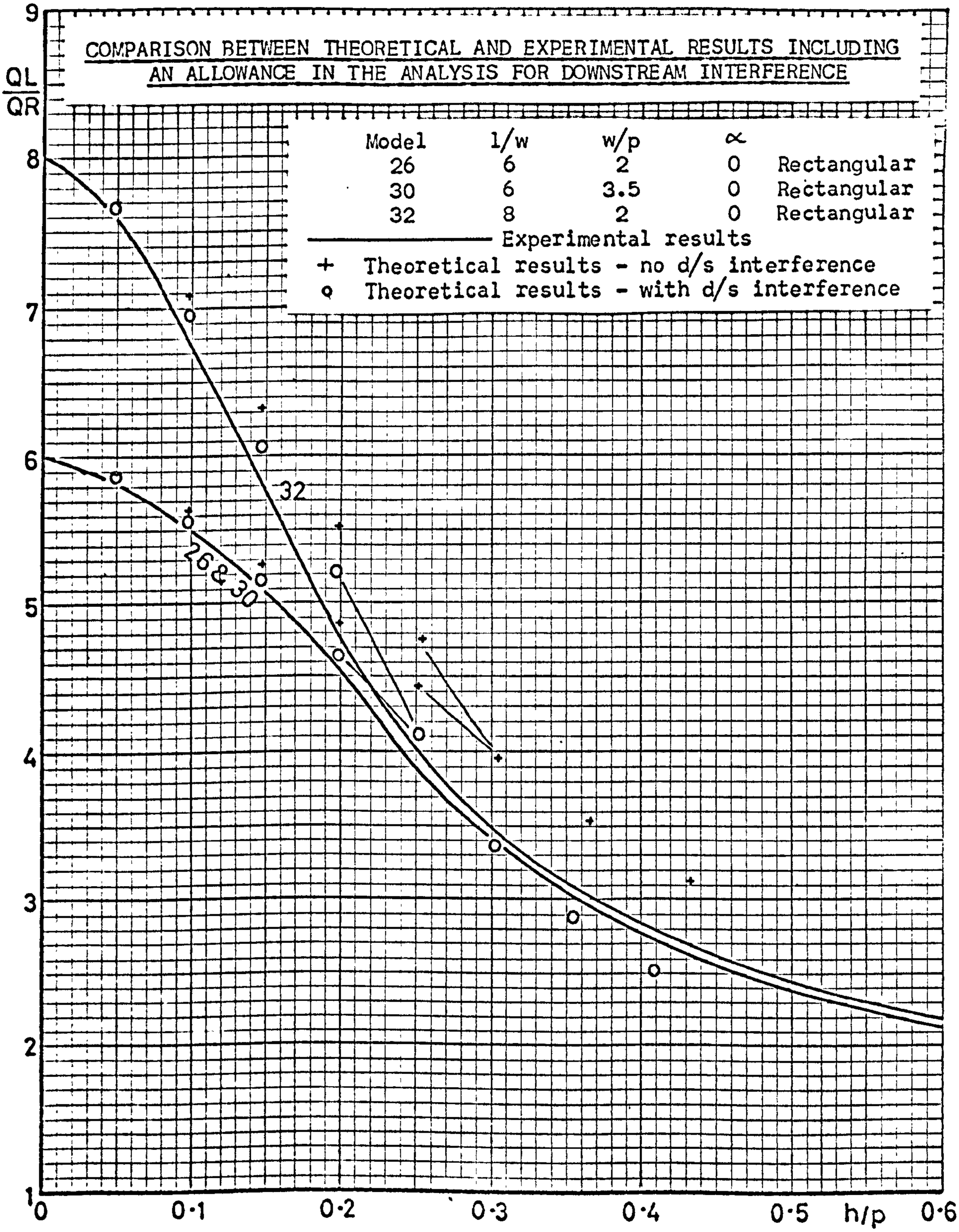

Figure 88

COMPARISON BETWEEN THEORETICAL AND EXPERIMENTAL RESULTS FOR A WEIR WITH APRONS IN THE UPSTREAM CHANNELS ONLY

Apron Ratio	Experimental results	Theoretical results
0.5	———	o
0.75	— - ——— - ———	+

l/w = 8, w/p = 2.5, α = 5.4 (trapezoidal).

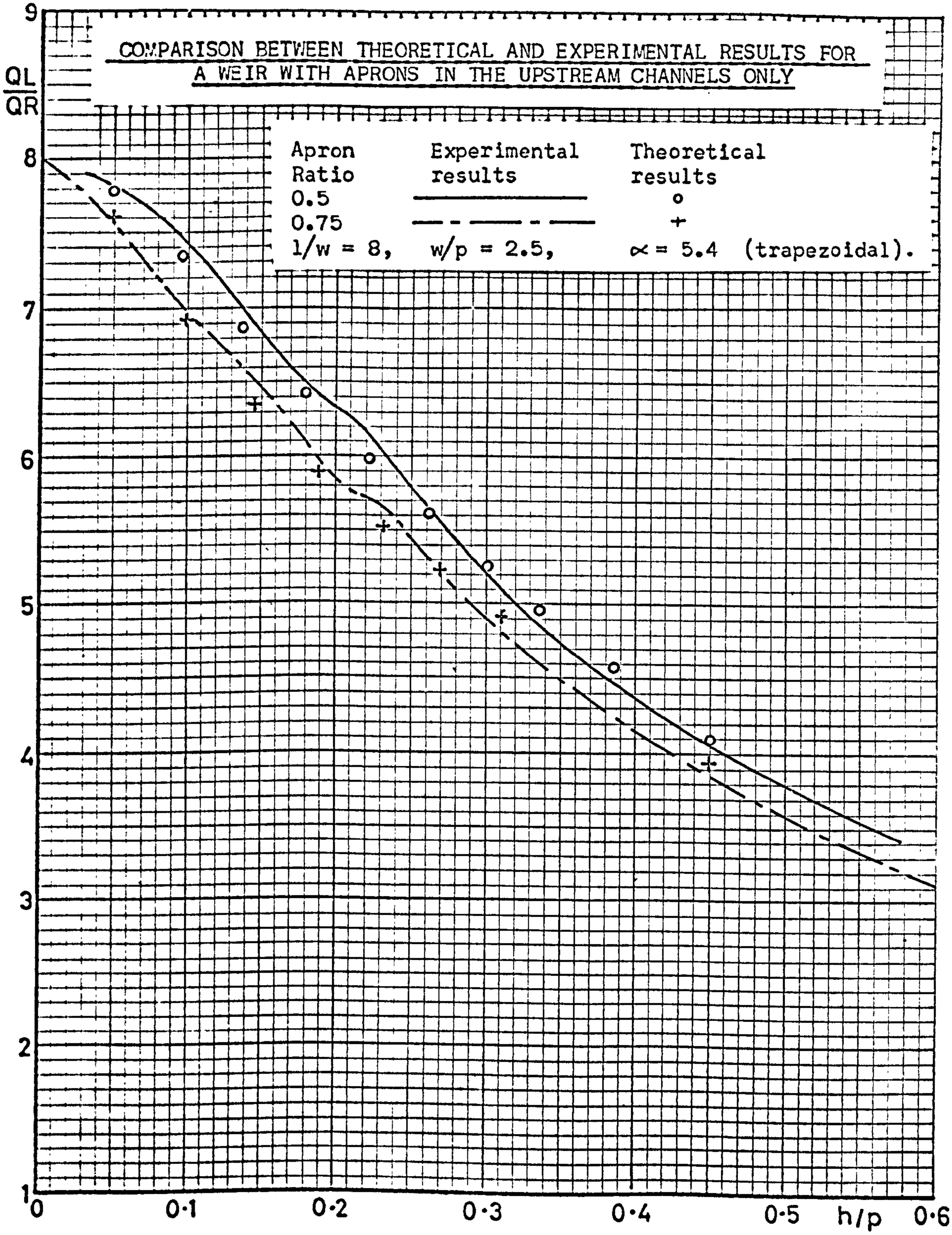

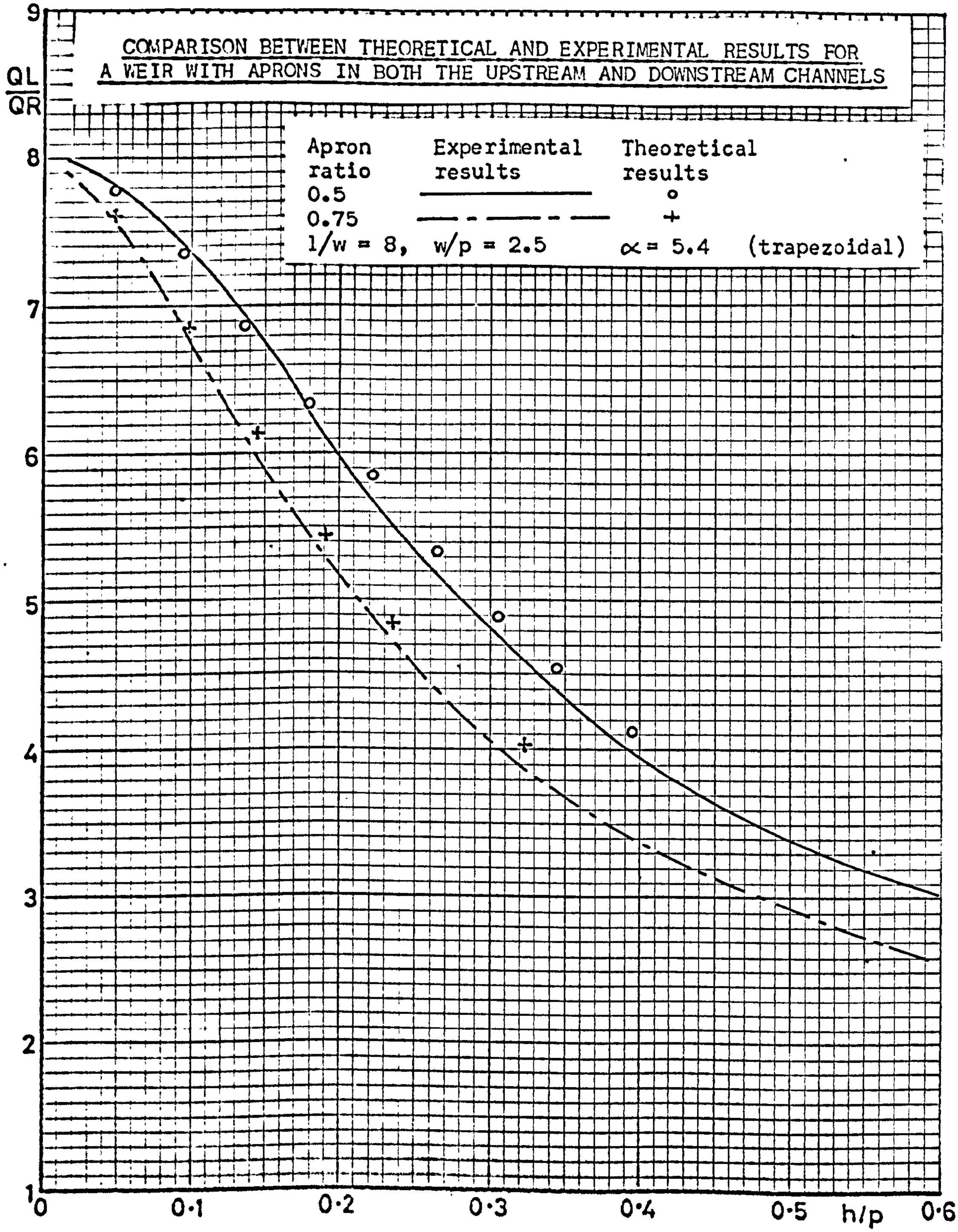
COMPARISON BETWEEN THEORETICAL AND EXPERIMENTAL RESULTS FOR A WEIR WITH APRONS IN BOTH THE UPSTREAM AND DOWNSTREAM CHANNELS
QL/QR
Apron ratio
Experimental results
Theoretical results
0.5
0.75
1/w = 8, w/p = 2.5
∝ = 5.4 (trapezoidal)
9
8
7
6
5
4
3
2
1
0
0·1
0·2
0·3
0·4
0·5
h/p
0·6

Figure 90

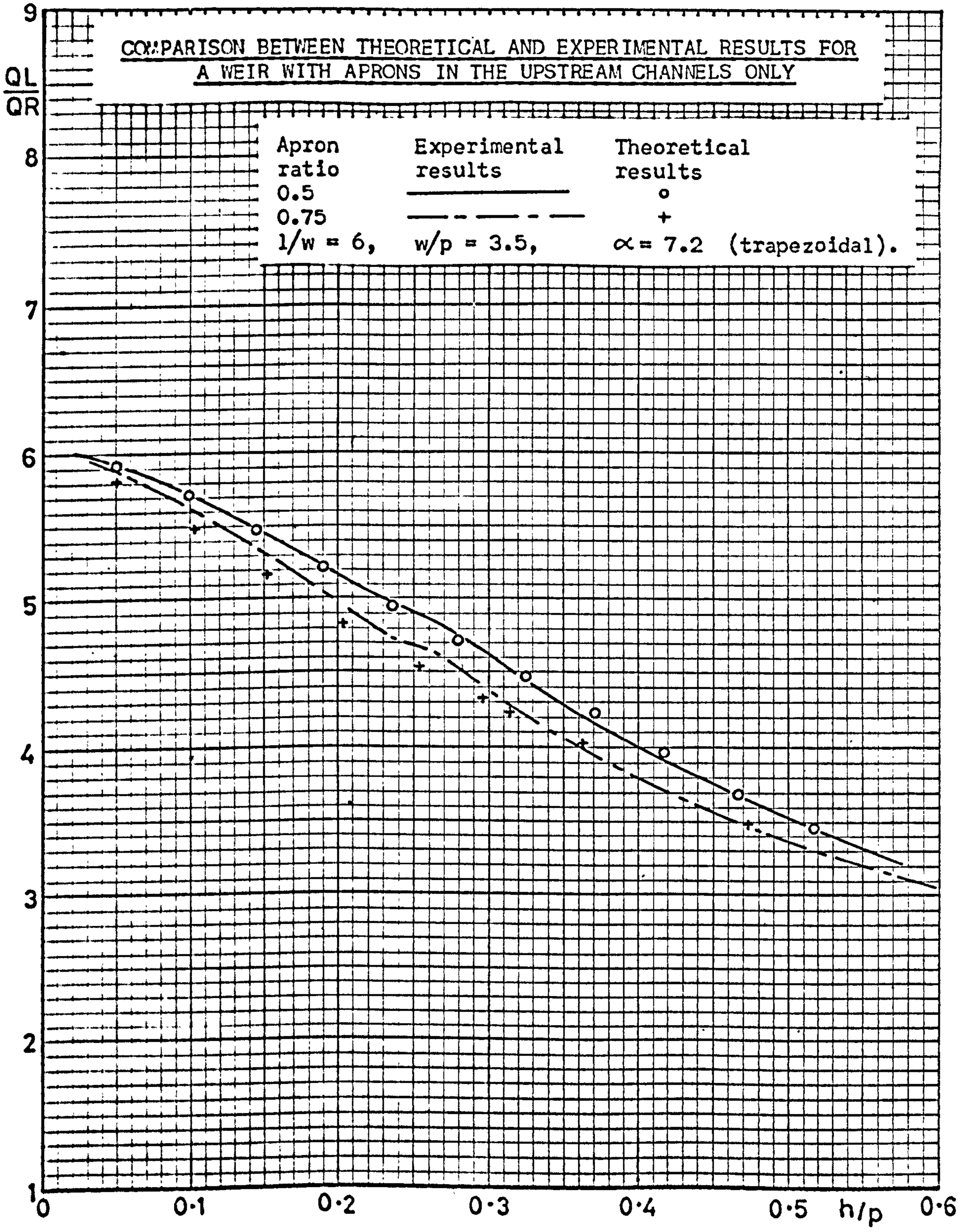
COMPARISON BETWEEN THEORETICAL AND EXPERIMENTAL RESULTS FOR A WEIR WITH APRONS IN THE UPSTREAM CHANNELS ONLY
Apron ratio
Experimental results
Theoretical results
0.5
0.75
o
+
l/w = 6, w/p = 3.5, ∝ = 7.2 (trapezoidal).
QL/QR
9
8
7
6
5
4
3
2
1
0
0·1
0·2
0·3
0·4
0·5
h/p
0·6

Figure 91

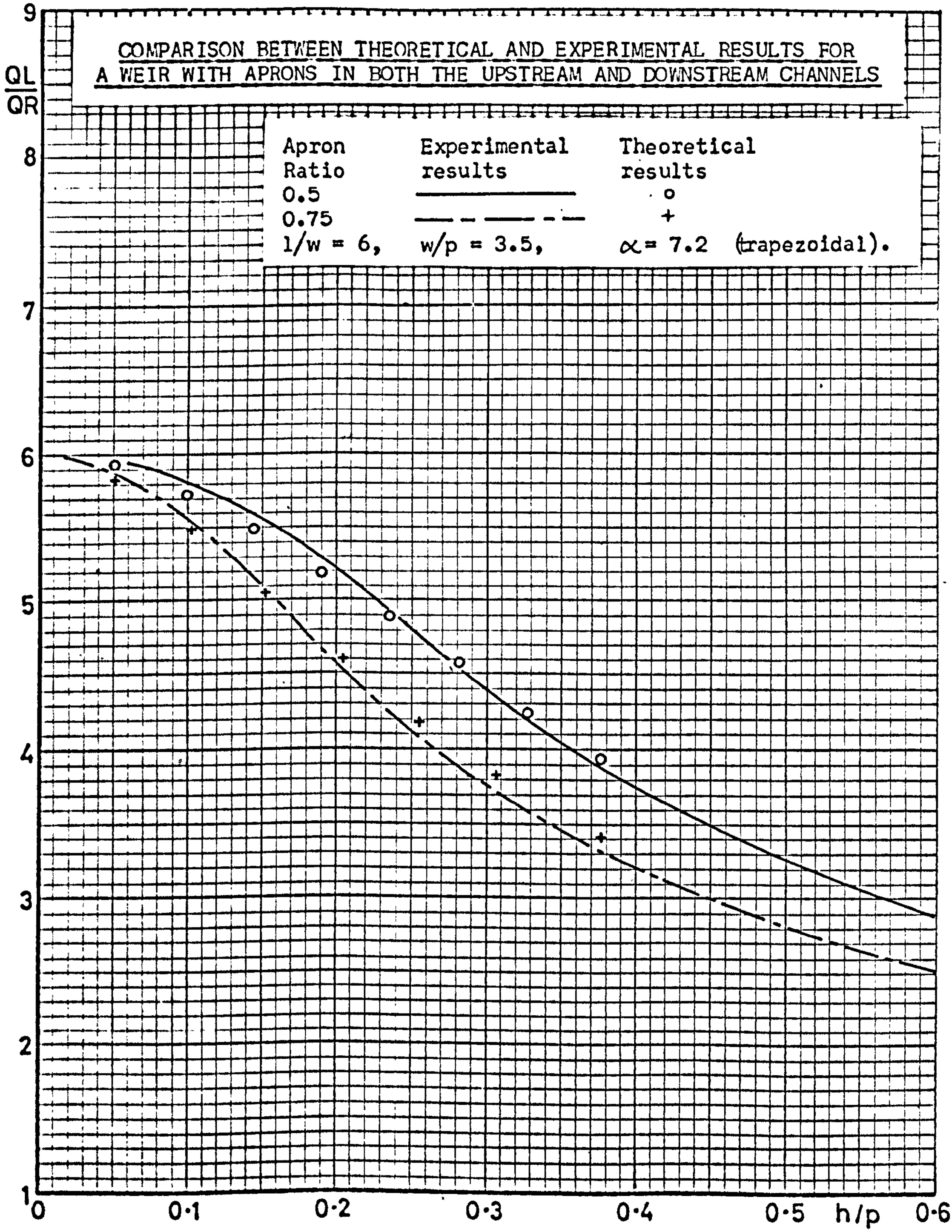
COMPARISON BETWEEN THEORETICAL AND EXPERIMENTAL RESULTS FOR
A WEIR WITH APRONS IN BOTH THE UPSTREAM AND DOWNSTREAM CHANNELS
Apron Ratio
Experimental results
Theoretical results
0.5
0.75
1/w = 6, w/p = 3.5, ∝ = 7.2 (trapezoidal).
QL/QR
9
8
7
6
5
4
3
2
1
0
0·1
0·2
0·3
0·4
0·5
h/p
0·6

Figure 92

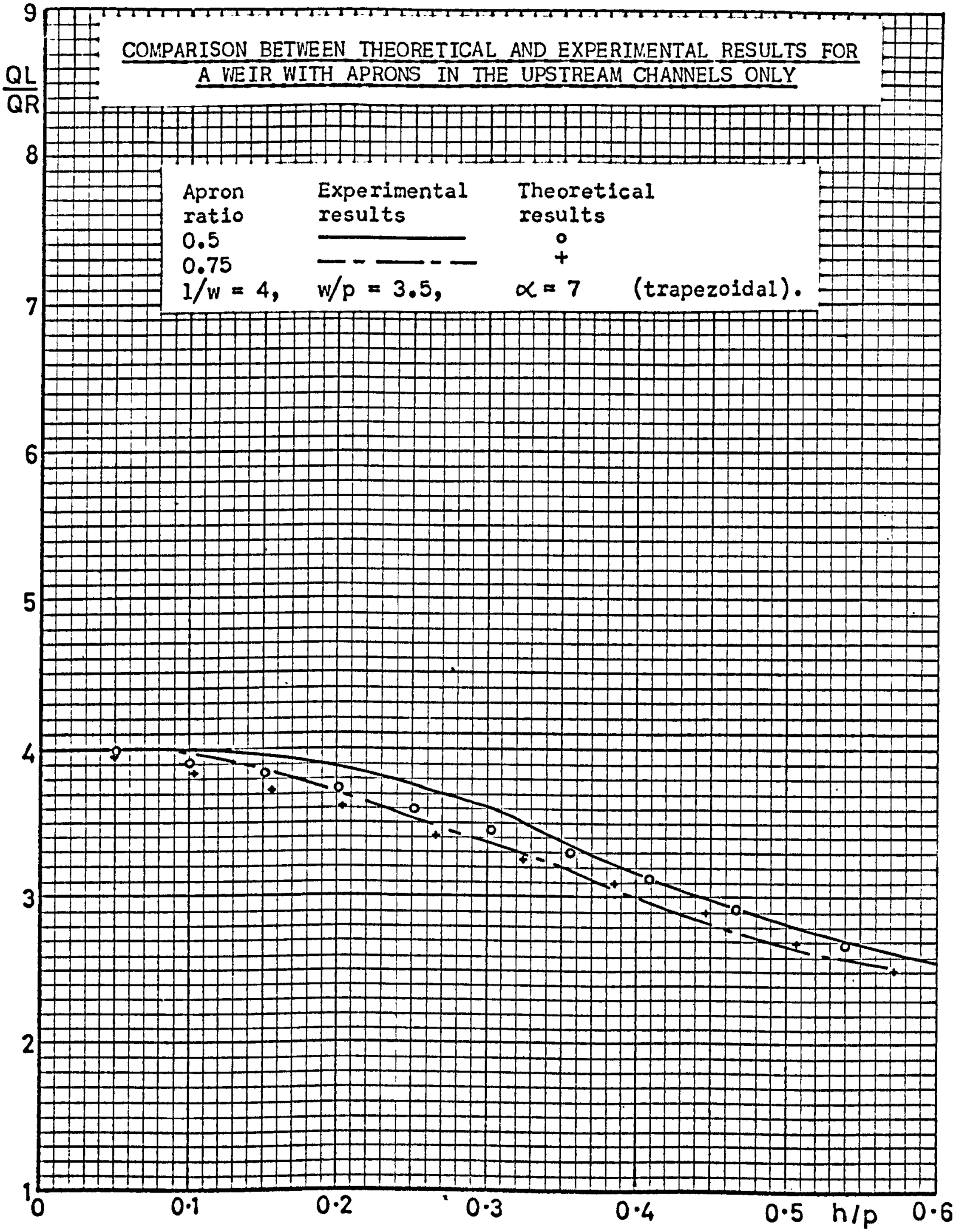
COMPARISON BETWEEN THEORETICAL AND EXPERIMENTAL RESULTS FOR A WEIR WITH APRONS IN THE UPSTREAM CHANNELS ONLY
QL/QR
Apron ratio
Experimental results
Theoretical results
0.5
0.75
1/w = 4, w/p = 3.5, ∝ = 7 (trapezoidal).
9
8
7
6
5
4
3
2
1
0
0·1
0·2
0·3
0·4
0·5
h/p
0·6

Figure 93

COMPARISON BETWEEN THEORETICAL AND EXPERIMENTAL RESULTS FOR A WEIR WITH APRONS IN BOTH THE UPSTREAM AND DOWNSTREAM CHANNELS

Apron ratio	Experimental results	Theoretical results
0.5	———	o
0.75	— - — - —	+

1/w = 4, w/p = 3.5, α = 7 (trapezoidal).

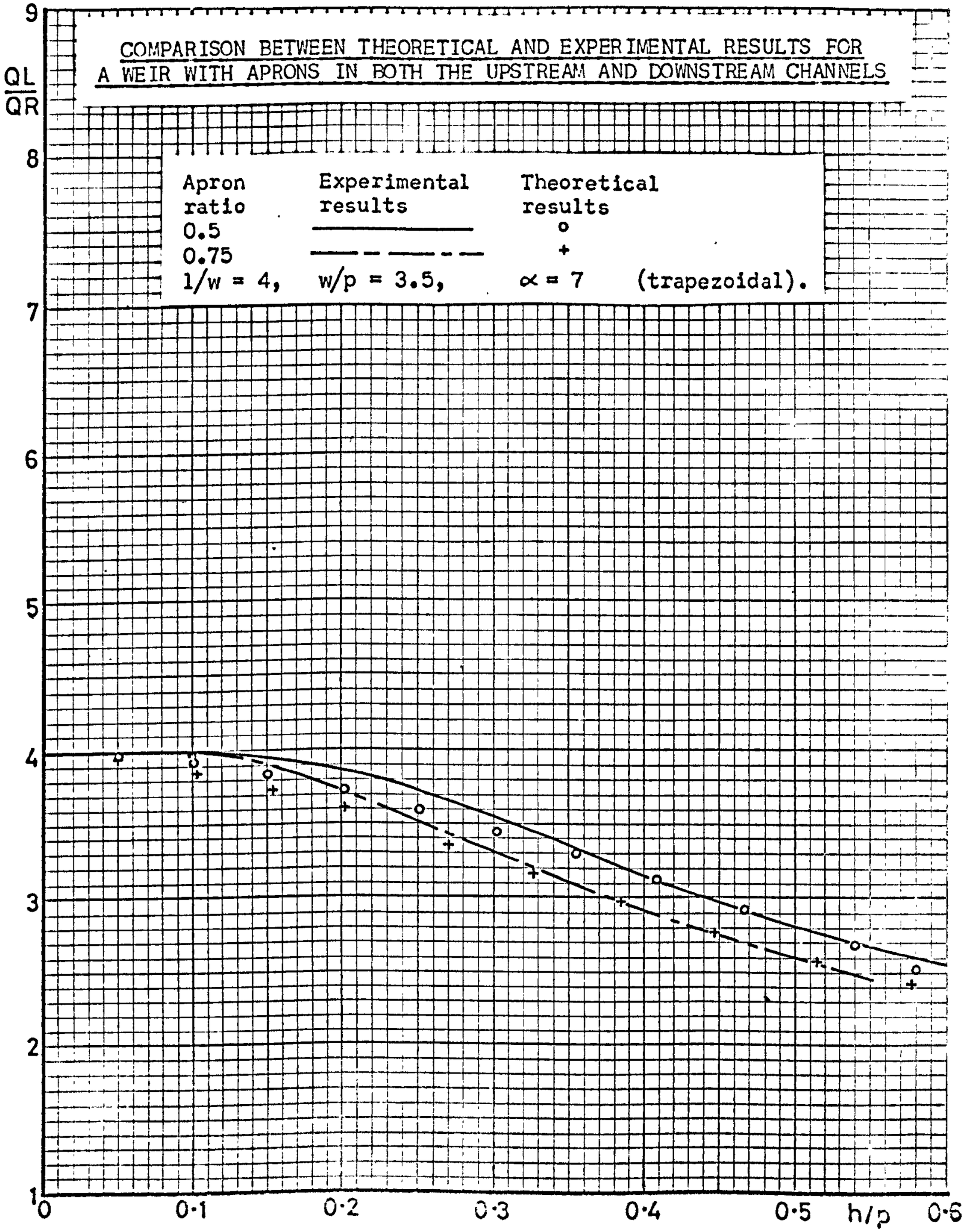

Figure 94

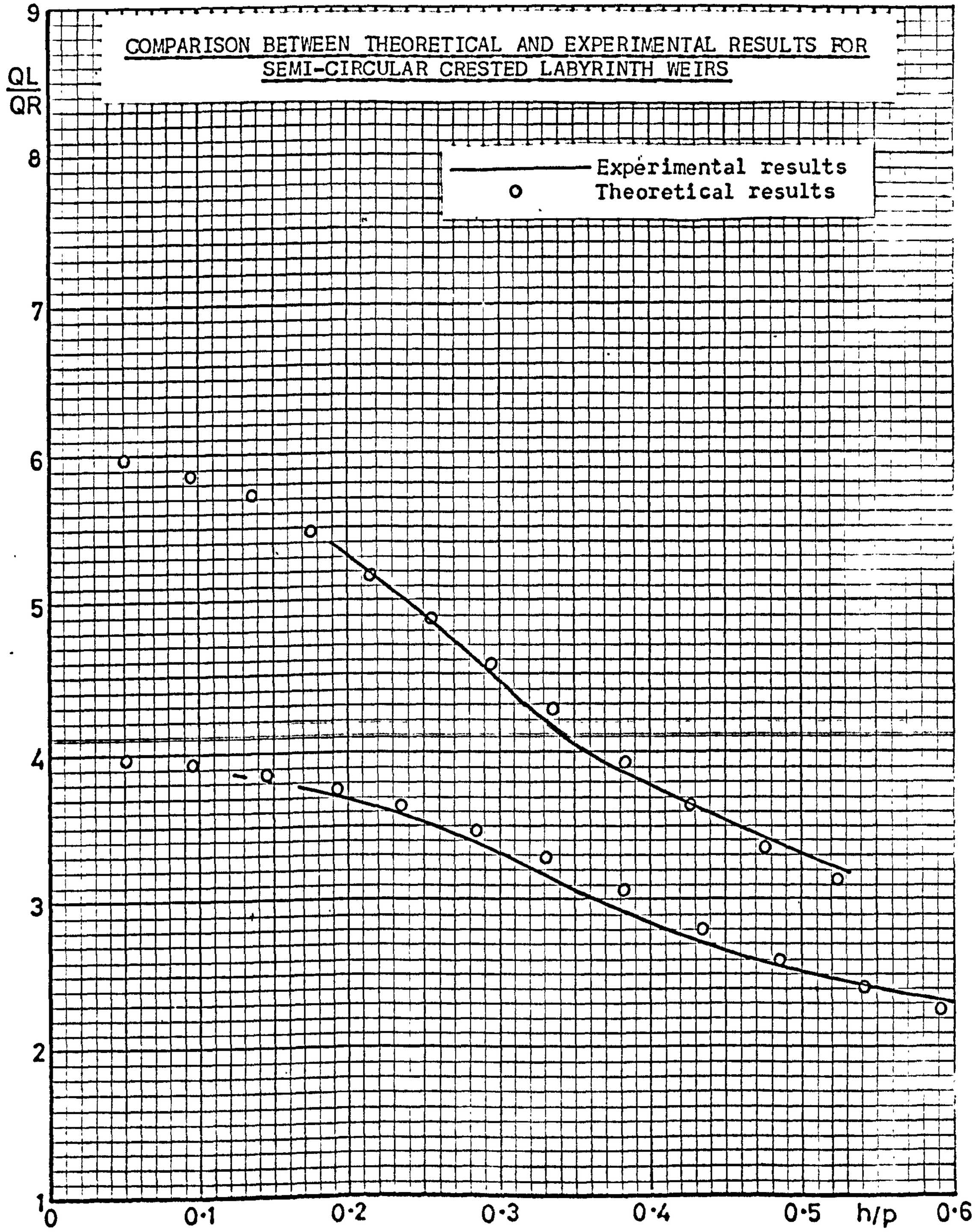
COMPARISON BETWEEN THEORETICAL AND EXPERIMENTAL RESULTS FOR SEMI-CIRCULAR CRESTED LABYRINTH WEIRS
QL/QR
Experimental results
Theoretical results
9
8
7
6
5
4
3
2
1
0
0·1
0·2
0·3
0·4
0·5
h/p
0·6

Figure 95

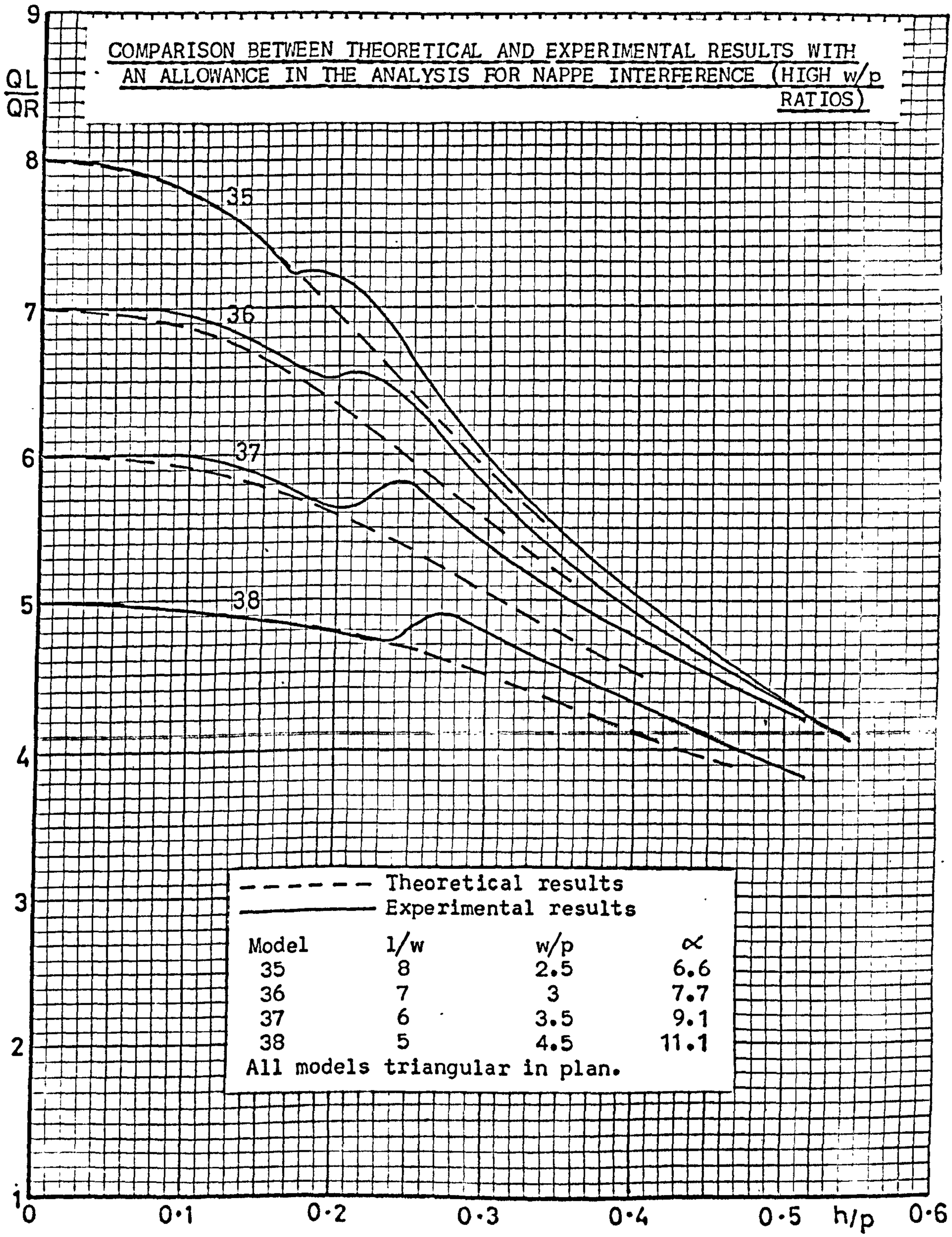
COMPARISON BETWEEN THEORETICAL AND EXPERIMENTAL RESULTS WITH AN ALLOWANCE IN THE ANALYSIS FOR NAPPE INTERFERENCE (HIGH w/p RATIOS)
QL/QR
9
8
7
6
5
4
3
2
1
35
36
37
38
0
0·1
0·2
0·3
0·4
0·5
h/p
0·6
Theoretical results
Experimental results
Model l/w w/p ∝
35 8 2.5 6.6
36 7 3 7.7
37 6 3.5 9.1
38 5 4.5 11.1
All models triangular in plan.

Figure 96

COMPARISON BETWEEN THEORETICAL AND EXPERIMENTAL RESULTS WITH AN ALLOWANCE IN THE ANALYSIS FOR NAPPE INTERFERENCE (w/p = 2)

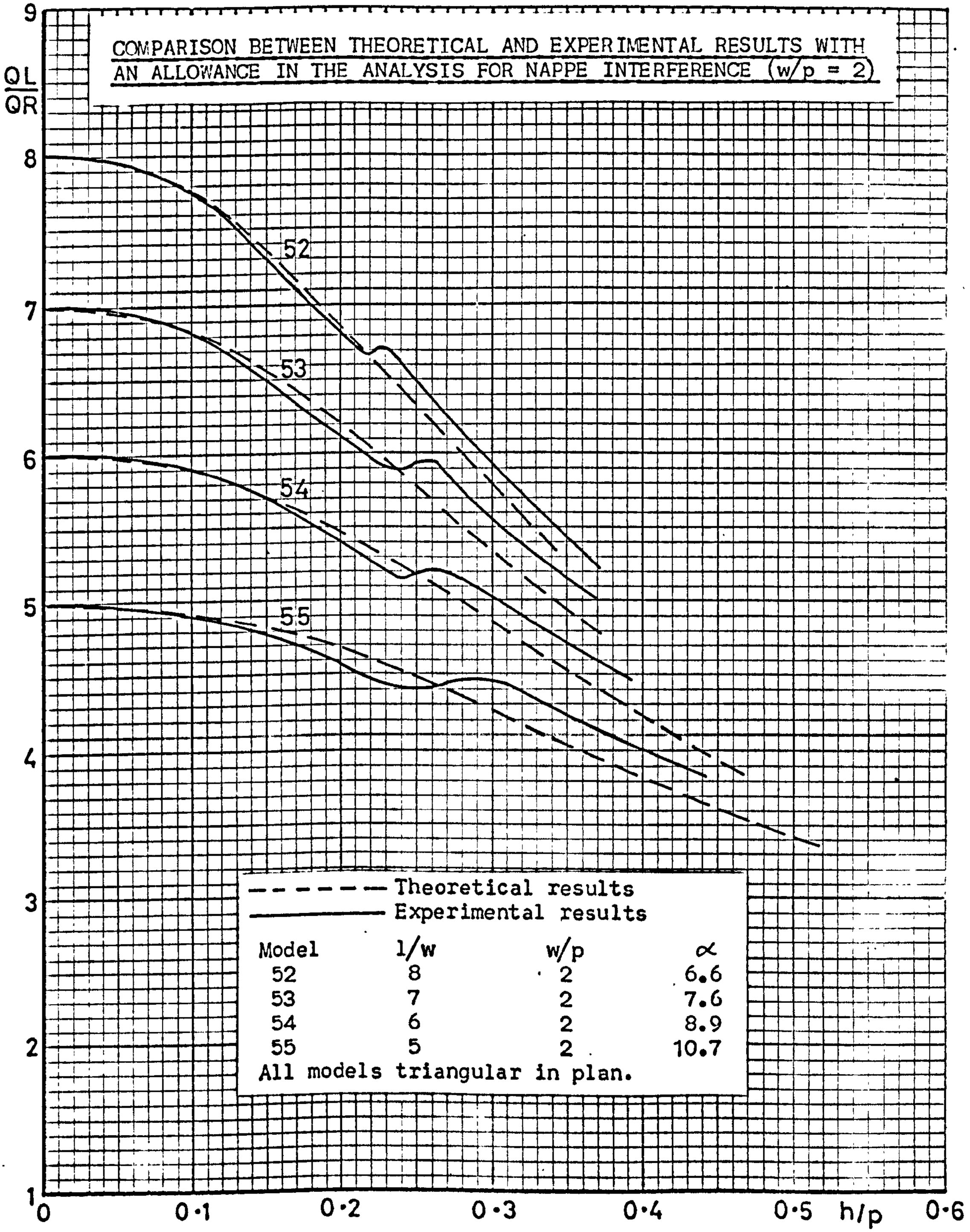

- - - - - - Theoretical results
——— Experimental results

Model	l/w	w/p	∝
52	8	2	6.6
53	7	2	7.6
54	6	2	8.9
55	5	2	10.7

All models triangular in plan.

Figure 97

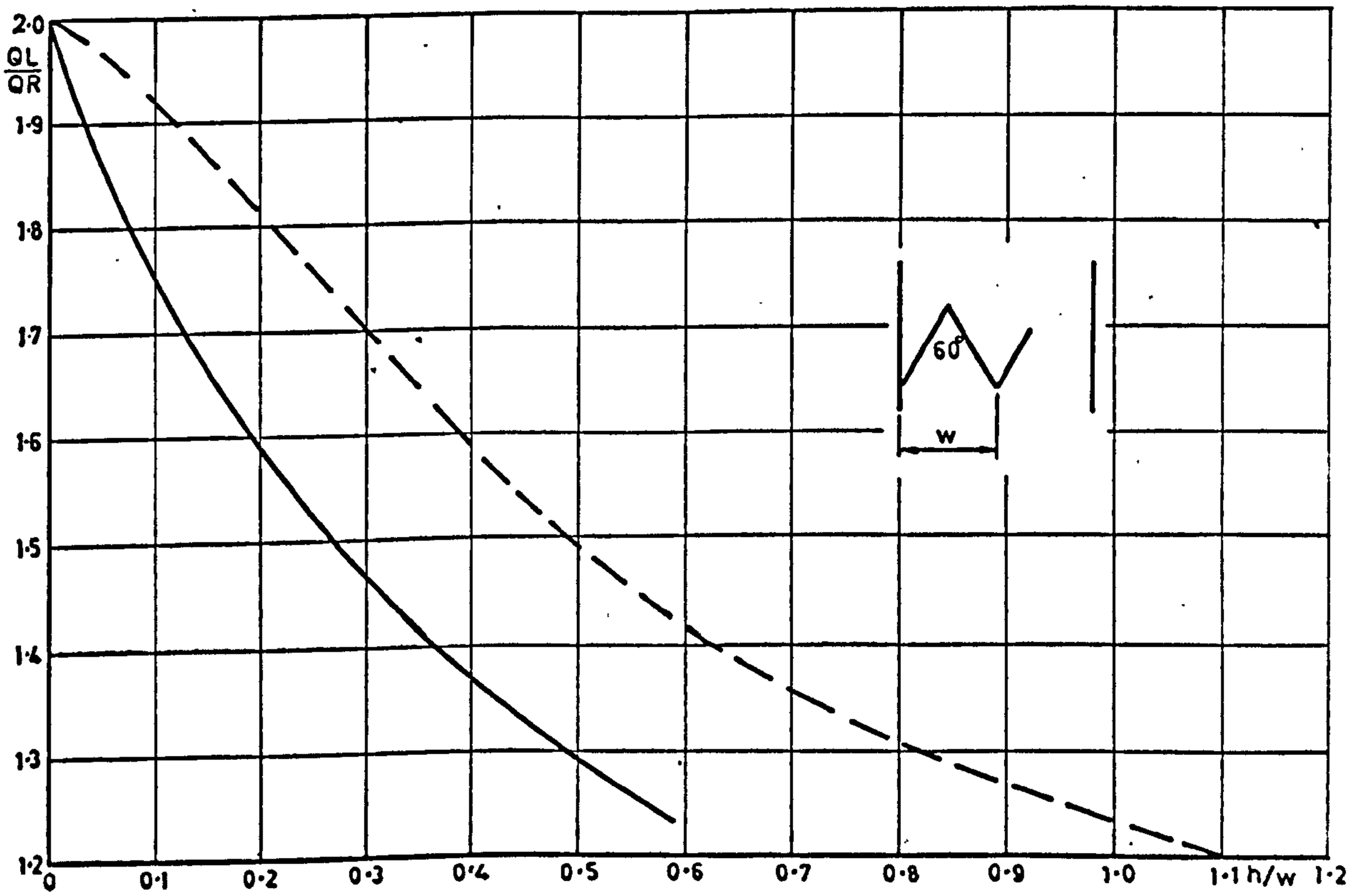

COMPARISON BETWEEN THEORETICAL AND EXPERIMENTAL RESULTS FOR SMALL w/p RATIOS

THE THEORETICAL EFFECTS OF VARIATION OF THE w/p RATIO

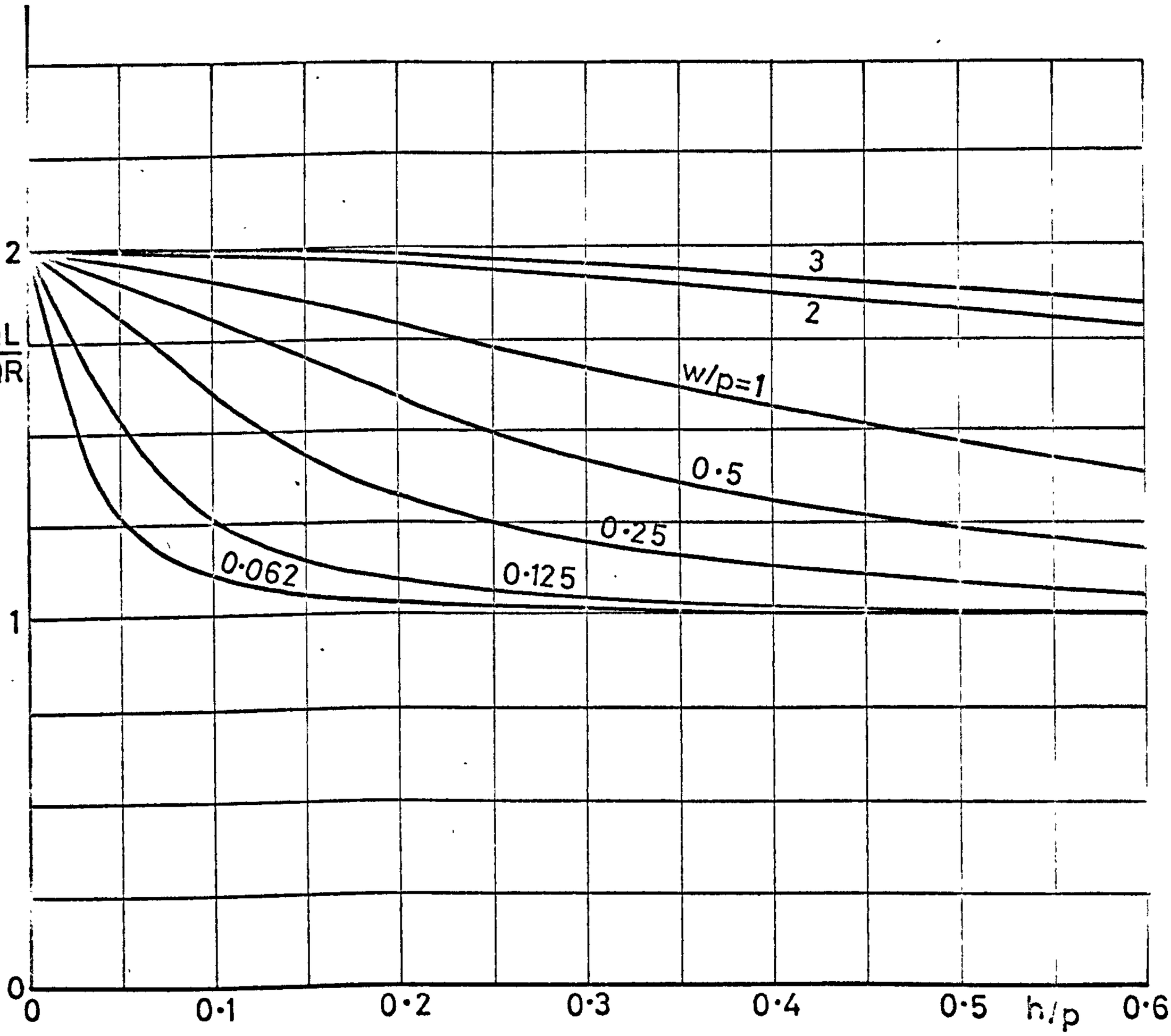

Results obtained from the theoretical analysis with inclusion of an allowance for nappe interference. Length magnification = 2 and plan form triangular.

Figure 99

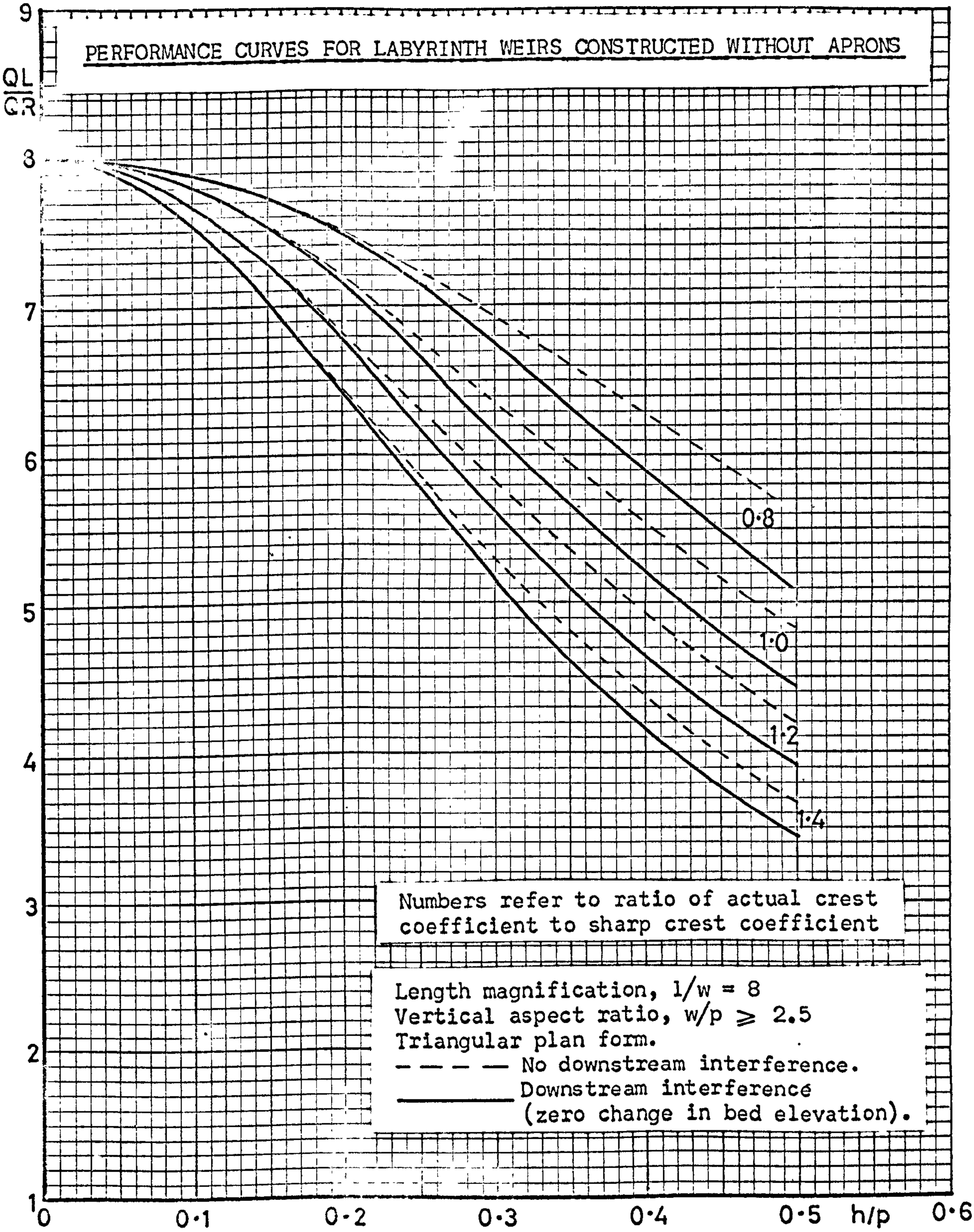
PERFORMANCE CURVES FOR LABYRINTH WEIRS CONSTRUCTED WITHOUT APRONS
QL/QR
9
8
7
6
5
4
3
2
1
0·8
1·0
1·2
1·4
Numbers refer to ratio of actual crest coefficient to sharp crest coefficient
Length magnification, l/w = 8
Vertical aspect ratio, w/p ⩾ 2.5
Triangular plan form.
— — — — No downstream interference.
——— Downstream interference (zero change in bed elevation).
0
0·1
0·2
0·3
0·4
0·5
h/p
0·6

Figure 100

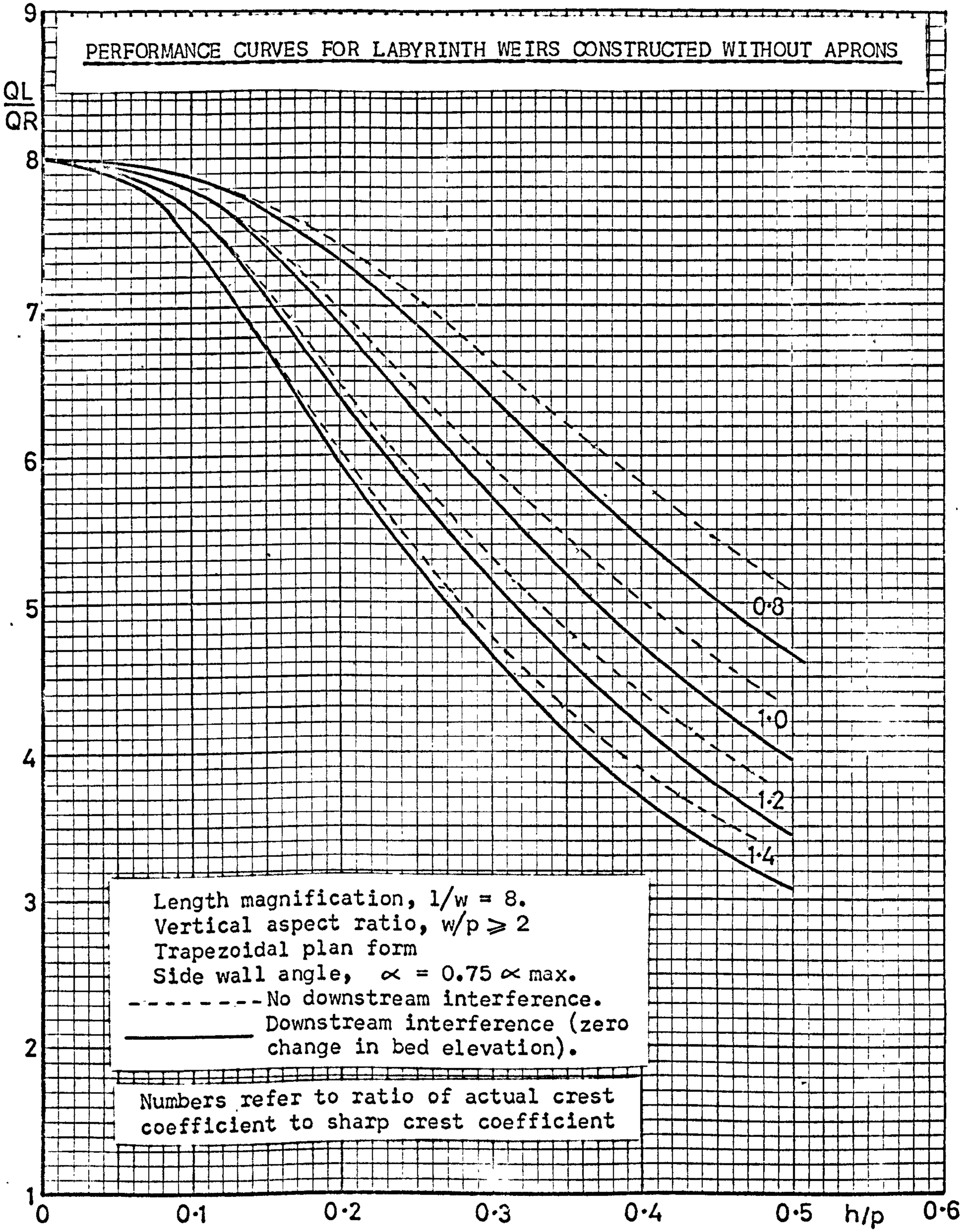
PERFORMANCE CURVES FOR LABYRINTH WEIRS CONSTRUCTED WITHOUT APRONS
QL/QR
9
8
7
6
5
4
3
2
1
0
0·1
0·2
0·3
0·4
0·5
h/p
0·6
0·8
1·0
1·2
1·4
Length magnification, l/w = 8.
Vertical aspect ratio, w/p ⩾ 2
Trapezoidal plan form
Side wall angle, ∝ = 0.75 ∝ max.
---------No downstream interference.
_____ Downstream interference (zero change in bed elevation).
Numbers refer to ratio of actual crest coefficient to sharp crest coefficient

Figure 101

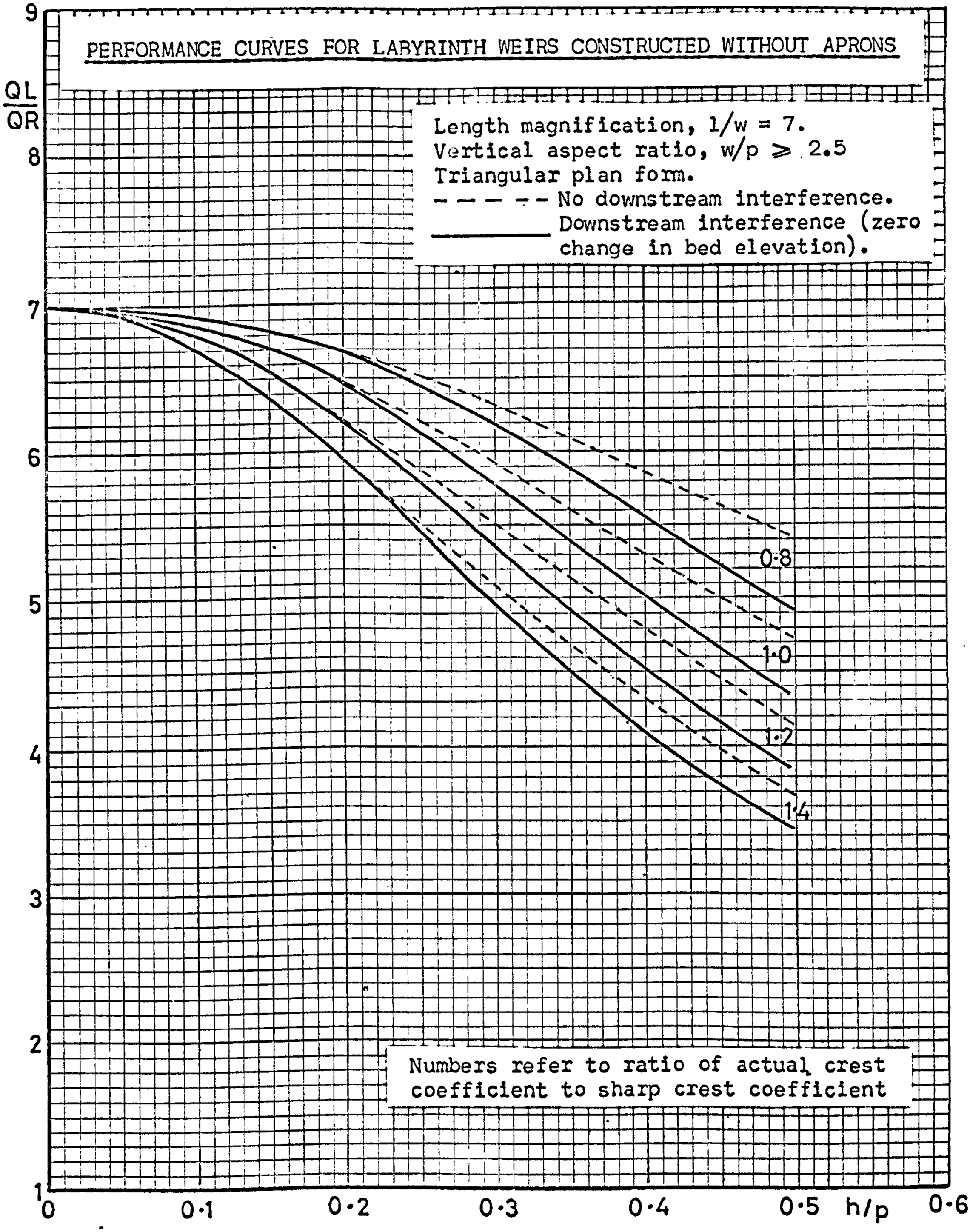
PERFORMANCE CURVES FOR LABYRINTH WEIRS CONSTRUCTED WITHOUT APRONS
QL/QR
Length magnification, l/w = 7.
Vertical aspect ratio, w/p ⩾ 2.5
Triangular plan form.
- - - - - No downstream interference.
——— Downstream interference (zero change in bed elevation).
0·8
1·0
1·2
1·4
Numbers refer to ratio of actual crest coefficient to sharp crest coefficient
9
8
7
6
5
4
3
2
1
0
0·1
0·2
0·3
0·4
0·5
h/p
0·6

Figure 102

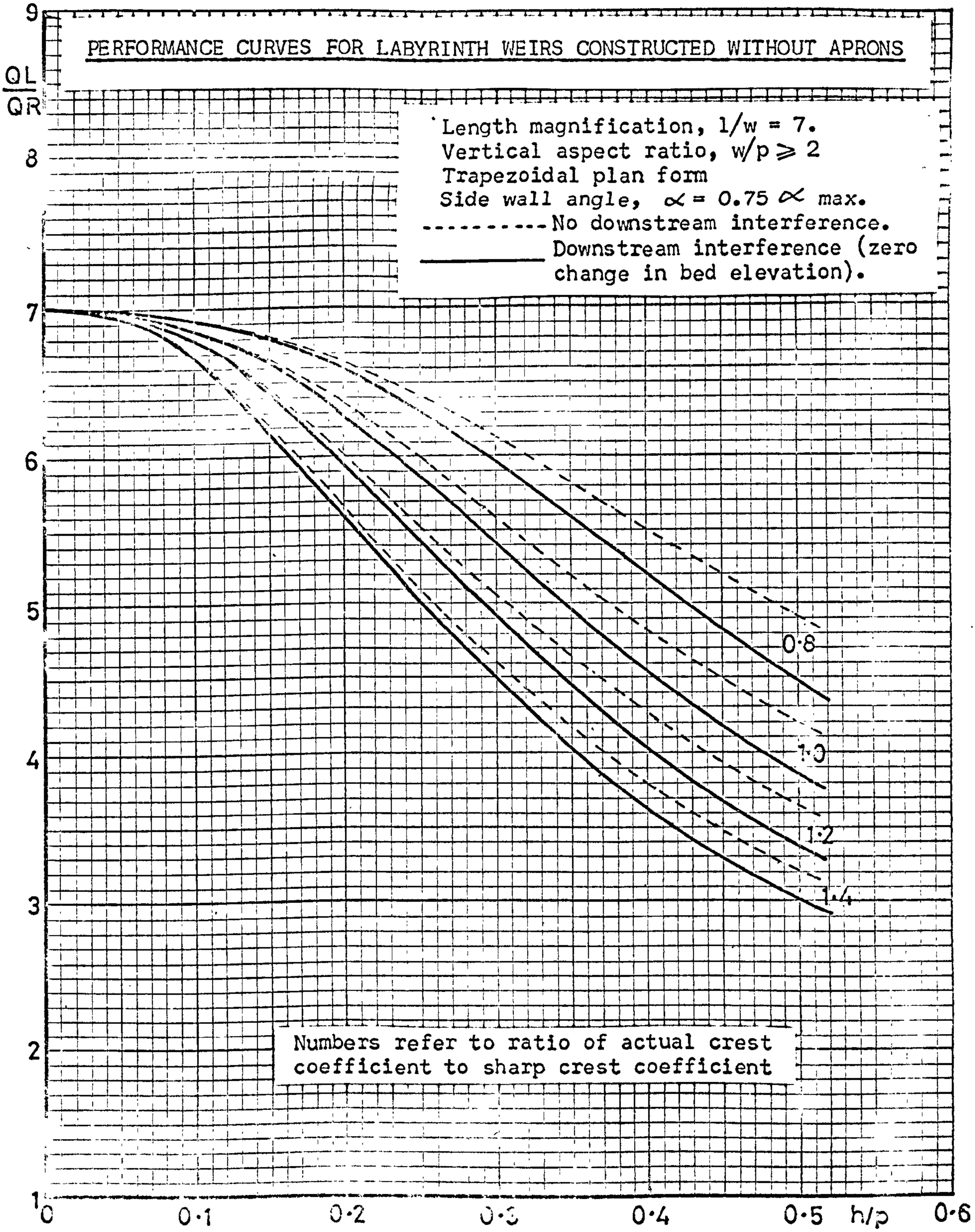
PERFORMANCE CURVES FOR LABYRINTH WEIRS CONSTRUCTED WITHOUT APRONS
QL/QR
Length magnification, l/w = 7.
Vertical aspect ratio, w/p ⩾ 2
Trapezoidal plan form
Side wall angle, ∝ = 0.75 ∝ max.
---------- No downstream interference.
———— Downstream interference (zero change in bed elevation).
0·8
1·0
1·2
1·4
Numbers refer to ratio of actual crest coefficient to sharp crest coefficient
9
8
7
6
5
4
3
2
1
0
0·1
0·2
0·3
0·4
0·5
h/p
0·6

Figure 103

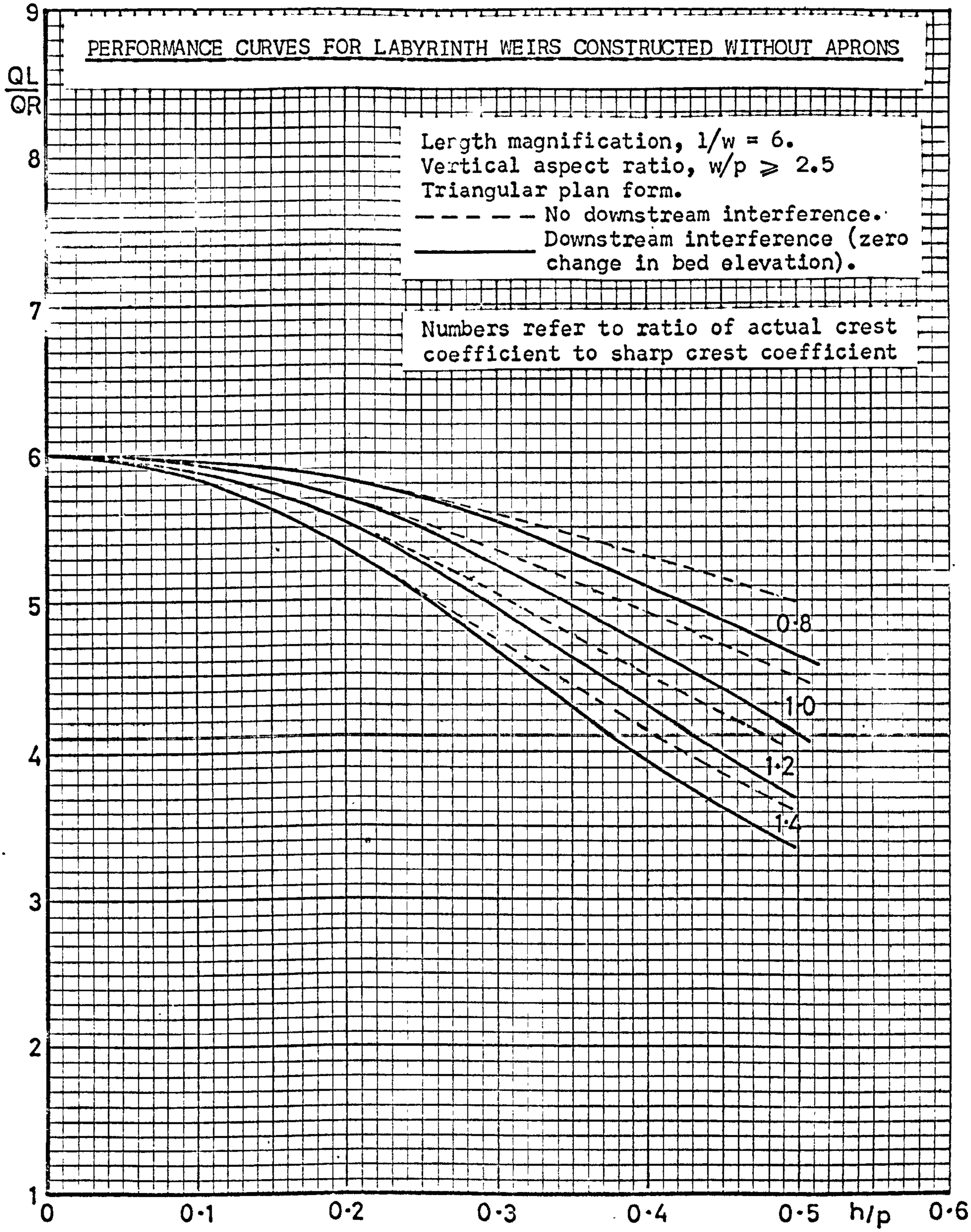
PERFORMANCE CURVES FOR LABYRINTH WEIRS CONSTRUCTED WITHOUT APRONS
QL/QR
Length magnification, l/w = 6.
Vertical aspect ratio, w/p ⩾ 2.5
Triangular plan form.
No downstream interference.
Downstream interference (zero change in bed elevation).
Numbers refer to ratio of actual crest coefficient to sharp crest coefficient
0·8
1·0
1·2
1·4
9
8
7
6
5
4
3
2
1
0
0·1
0·2
0·3
0·4
0·5
h/p
0·6

Figure 104

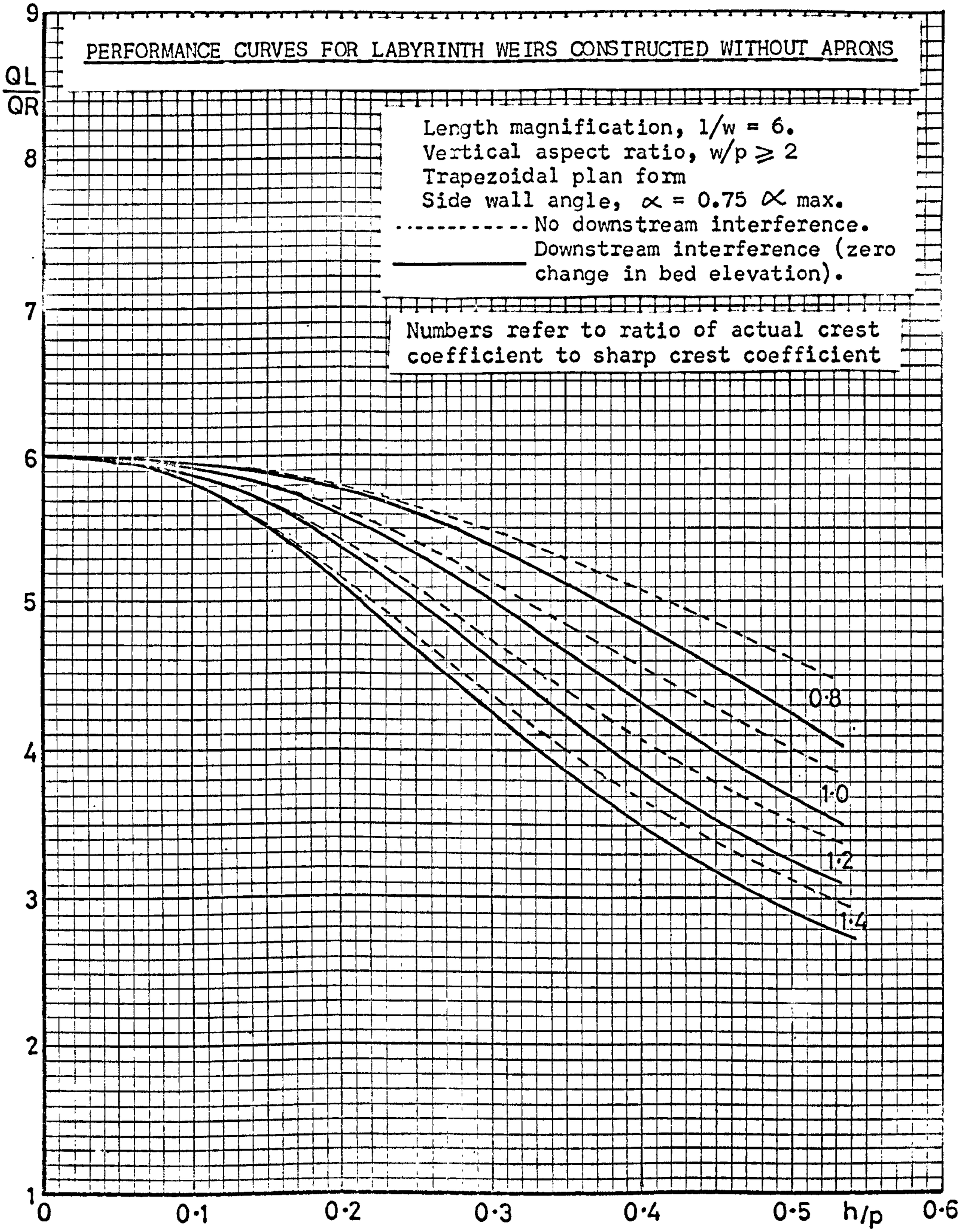
PERFORMANCE CURVES FOR LABYRINTH WEIRS CONSTRUCTED WITHOUT APRONS
QL/QR
Length magnification, l/w = 6.
Vertical aspect ratio, w/p ≥ 2
Trapezoidal plan form
Side wall angle, ∝ = 0.75 ∝ max.
No downstream interference.
Downstream interference (zero change in bed elevation).
Numbers refer to ratio of actual crest coefficient to sharp crest coefficient
0·8
1·0
1·2
1·4
9
8
7
6
5
4
3
2
1
0
0·1
0·2
0·3
0·4
0·5
0·6
h/p

Figure 105

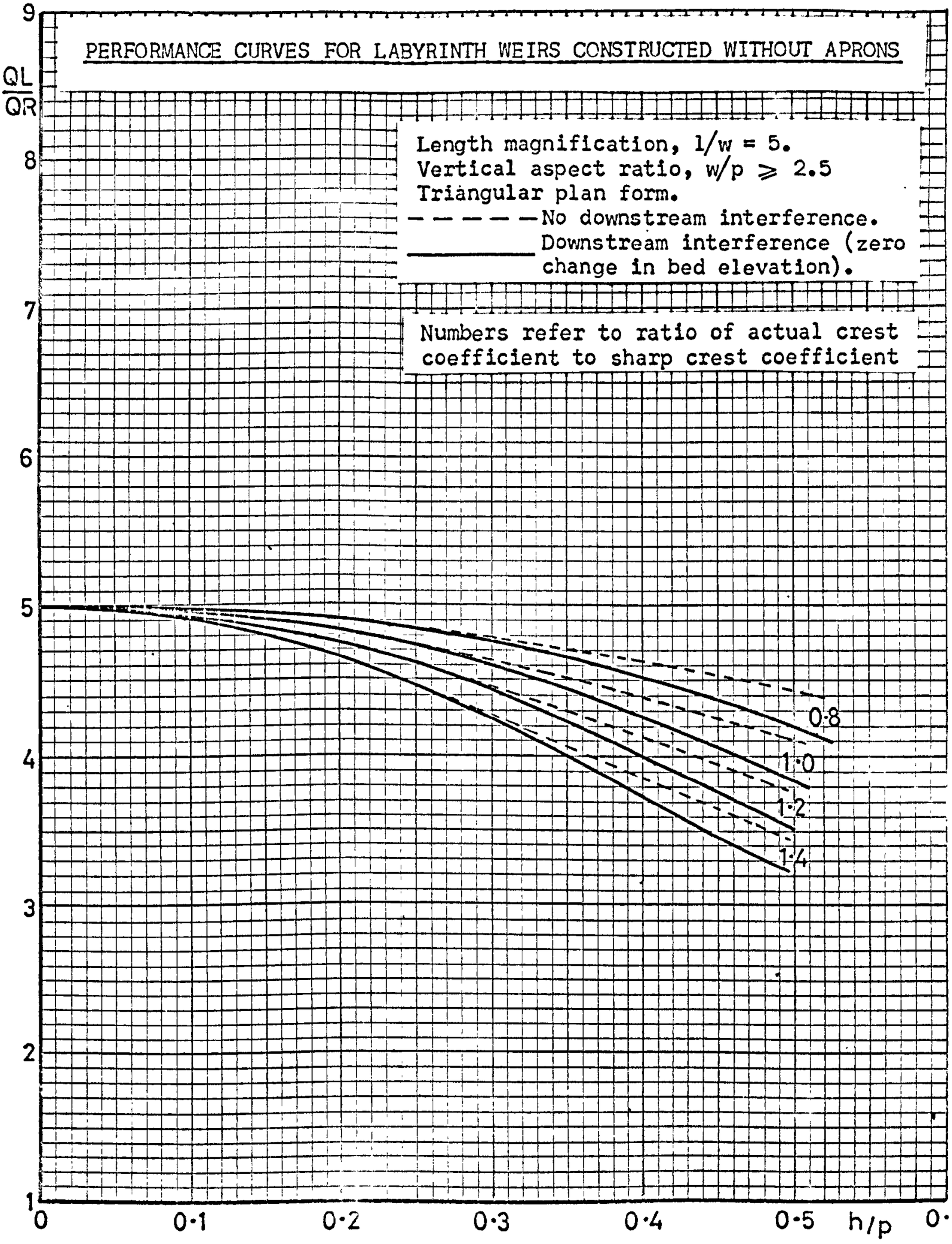
PERFORMANCE CURVES FOR LABYRINTH WEIRS CONSTRUCTED WITHOUT APRONS
QL/QR
Length magnification, l/w = 5.
Vertical aspect ratio, w/p ⩾ 2.5
Triangular plan form.
No downstream interference.
Downstream interference (zero change in bed elevation).
Numbers refer to ratio of actual crest coefficient to sharp crest coefficient
0·8
1·0
1·2
1·4
9
8
7
6
5
4
3
2
1
0
0·1
0·2
0·3
0·4
0·5
h/p
0·6

Figure 106

PERFORMANCE CURVES FOR LABYRINTH WEIRS CONSTRUCTED WITHOUT APRONS

Length magnification, l/w = 5.
Vertical aspect ratio, w/p ⩾ 2
Trapezoidal plan form
Side wall angle, α = 0.75 α max.
----------No downstream interference.
_____ Downstream interference (zero change in bed elevation).

Numbers refer to ratio of actual crest coefficient to sharp crest coefficient

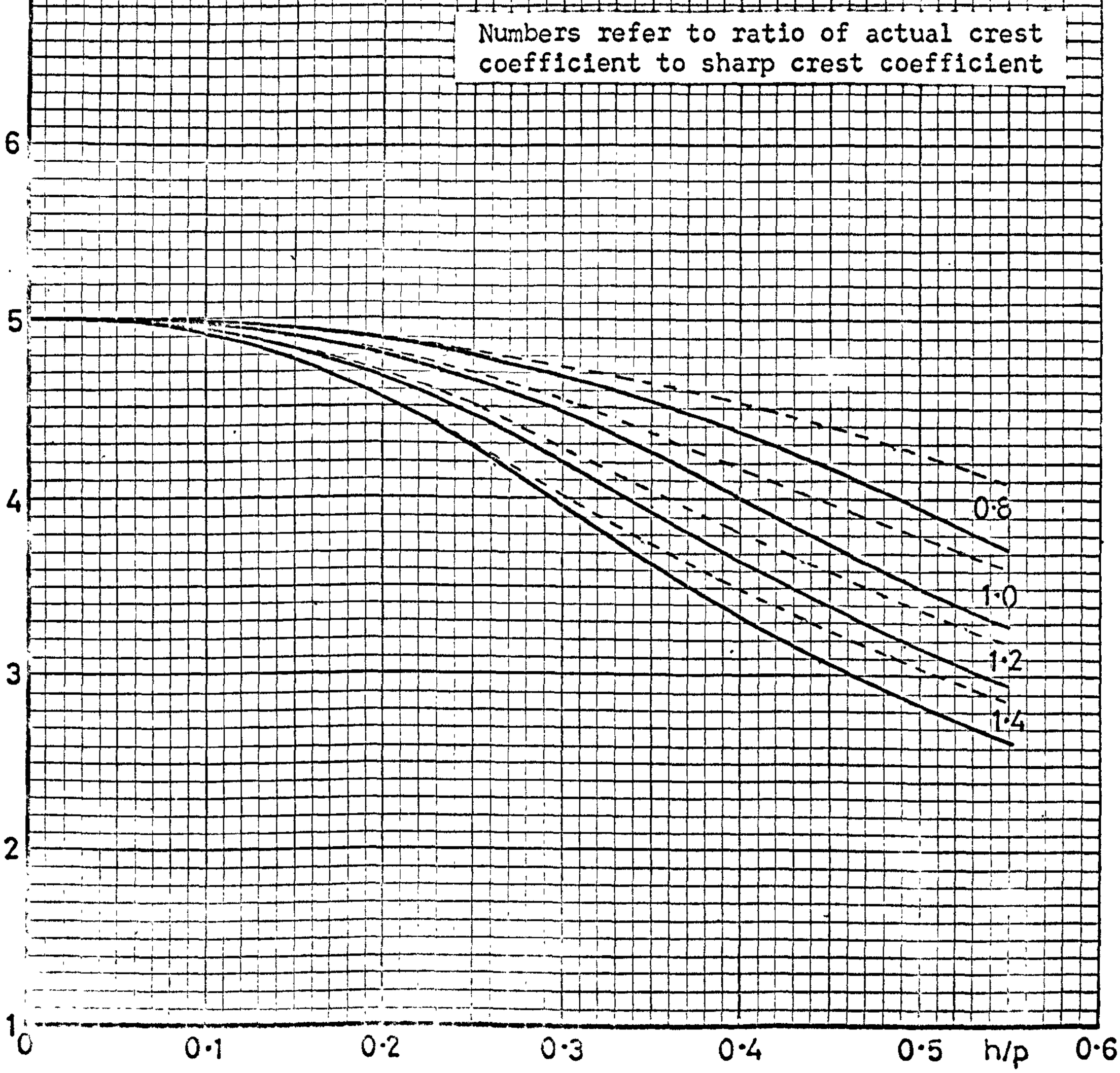

Figure 107

PERFORMANCE CURVES FOR LABYRINTH WEIRS CONSTRUCTED WITHOUT APRONS

Length magnification, l/w = 4.
Vertical aspect ratio, w/p ⩾ 2.5.
Triangular plan form.
— — — — No downstream interference.
———— Downstream interference (zero change in bed elevation).

Numbers refer to ratio of actual crest coefficient to sharp crest coefficient

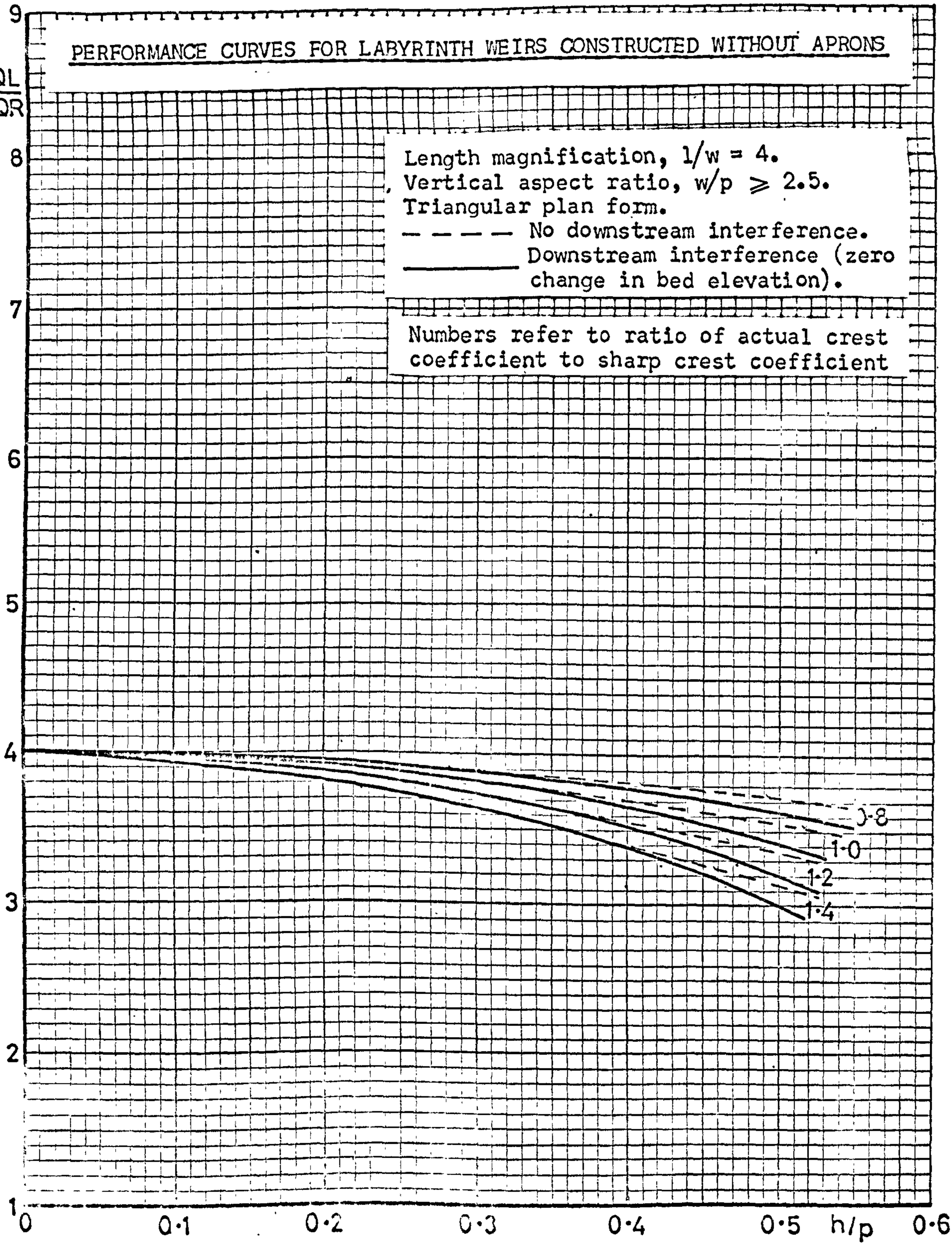

PERFORMANCE CURVES FOR LABYRINTH WEIRS CONSTRUCTED WITHOUT APRONS

Length magnification, l/w = 4.
Vertical aspect ratio, w/p ⩾ 2
Trapezoidal plan form
Slide wall angle, $\alpha = 0.75\,\alpha_{max}$.
---------- No downstream interference.
———— Downstream interference (zero change in bed elevation).

Numbers refer to ratio of actual crest coefficient to sharp crest coefficient

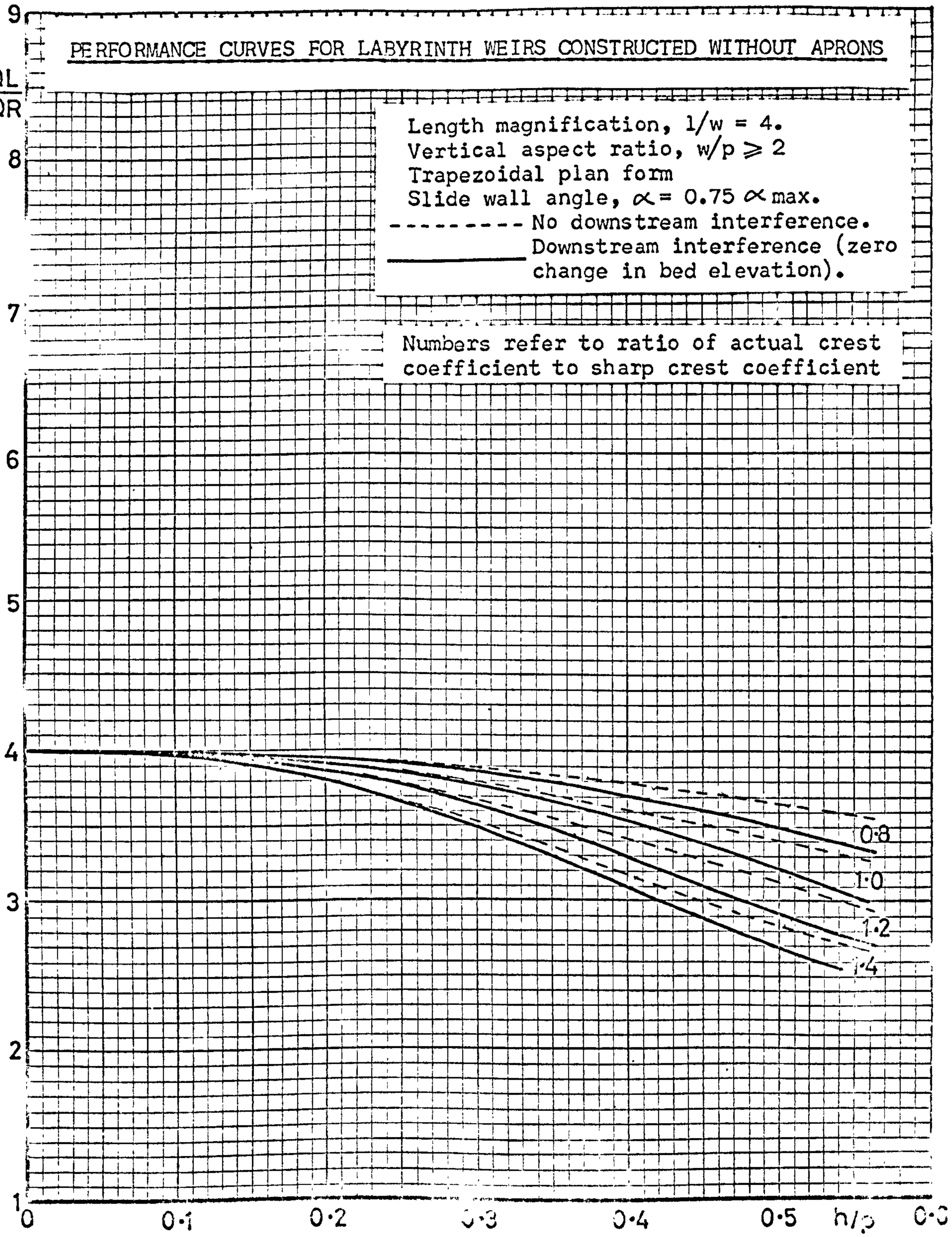

Figure 109

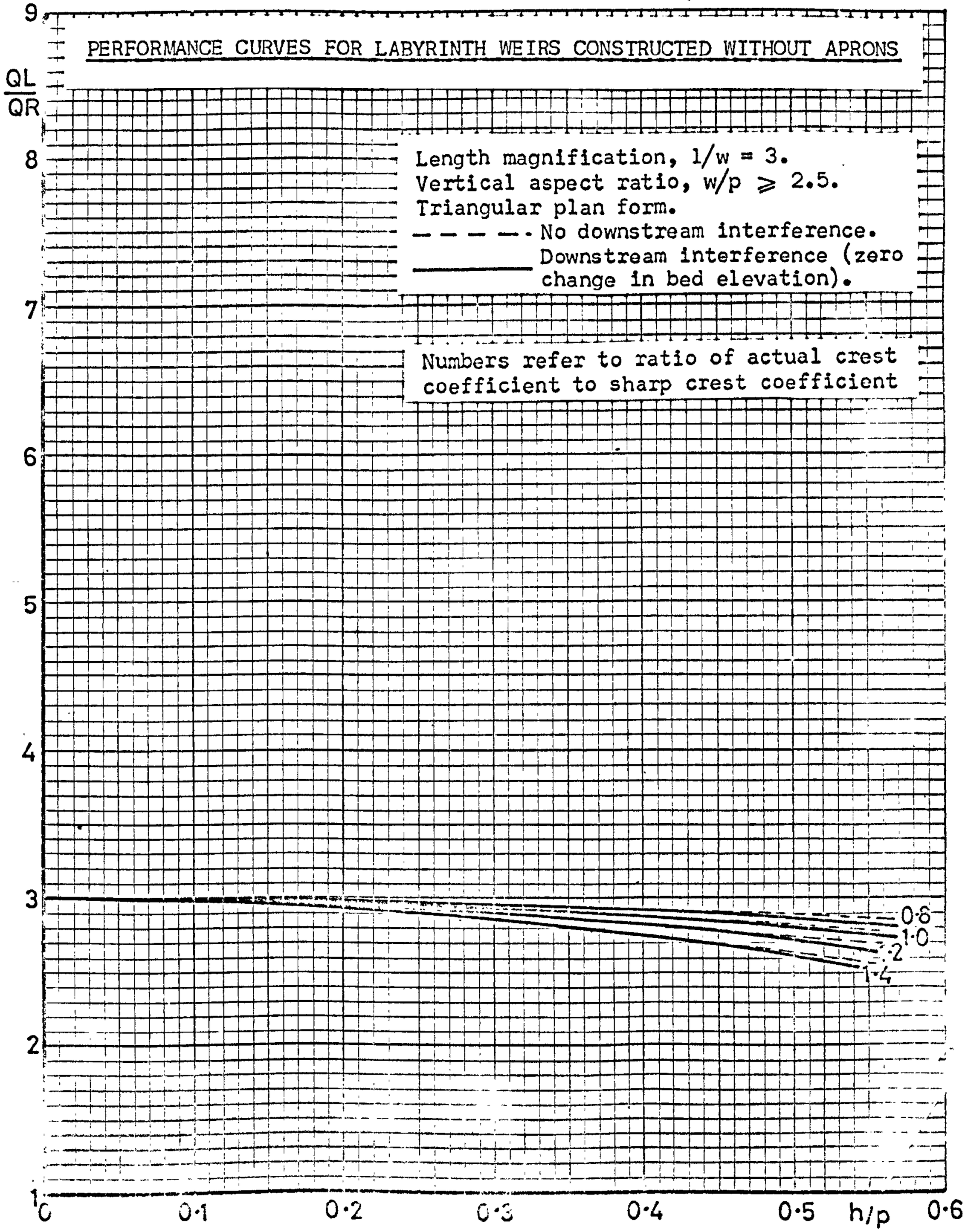
PERFORMANCE CURVES FOR LABYRINTH WEIRS CONSTRUCTED WITHOUT APRONS
QL/QR
Length magnification, l/w = 3.
Vertical aspect ratio, w/p ⩾ 2.5.
Triangular plan form.
- - - - - No downstream interference.
——— Downstream interference (zero change in bed elevation).
Numbers refer to ratio of actual crest coefficient to sharp crest coefficient
9
8
7
6
5
4
3
2
1
0·6
1·0
1·2
1·4
0
0·1
0·2
0·3
0·4
0·5
h/p
0·6

PERFORMANCE CURVES FOR LABYRINTH WEIRS CONSTRUCTED WITHOUT APRONS

Length magnification, $l/w = 3$.
Vertical aspect ratio, $w/p \geqslant 2$
Trapezoidal plan form
Slide wall angle, $\alpha = 0.75\,\alpha_{max}$.
---------- No downstream interference.
_____ Downstream interference (zero change in bed elevation).

Numbers refer to ratio of actual crest coefficient to sharp crest coefficient

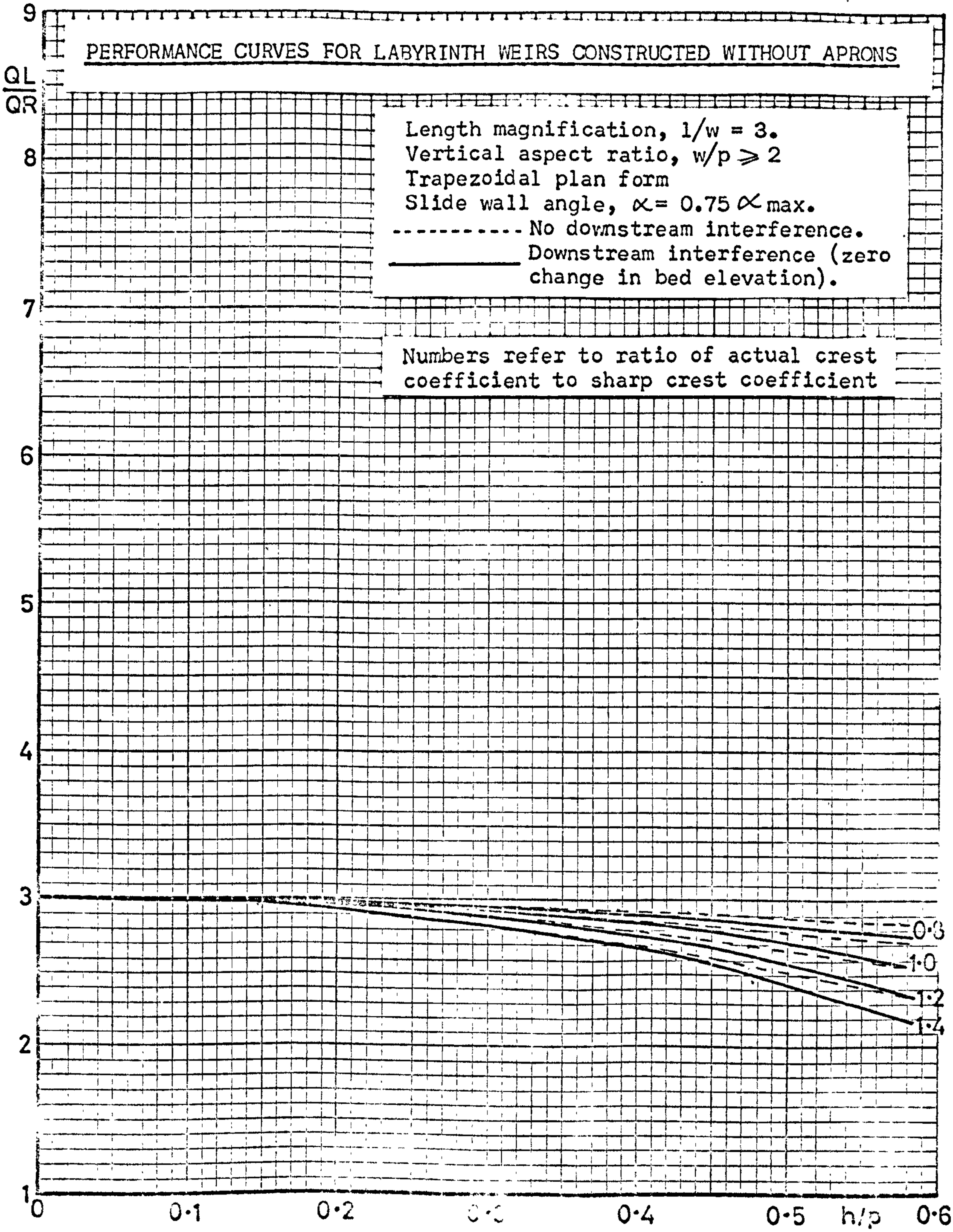

Figure 111

DESIGN CHART 1

TRIANGULAR PLAN FORM WEIRS CONSTRUCTED WITHOUT APRONS

Flow magnification, QL/QR, 'v' head to crest height ratio h/p.

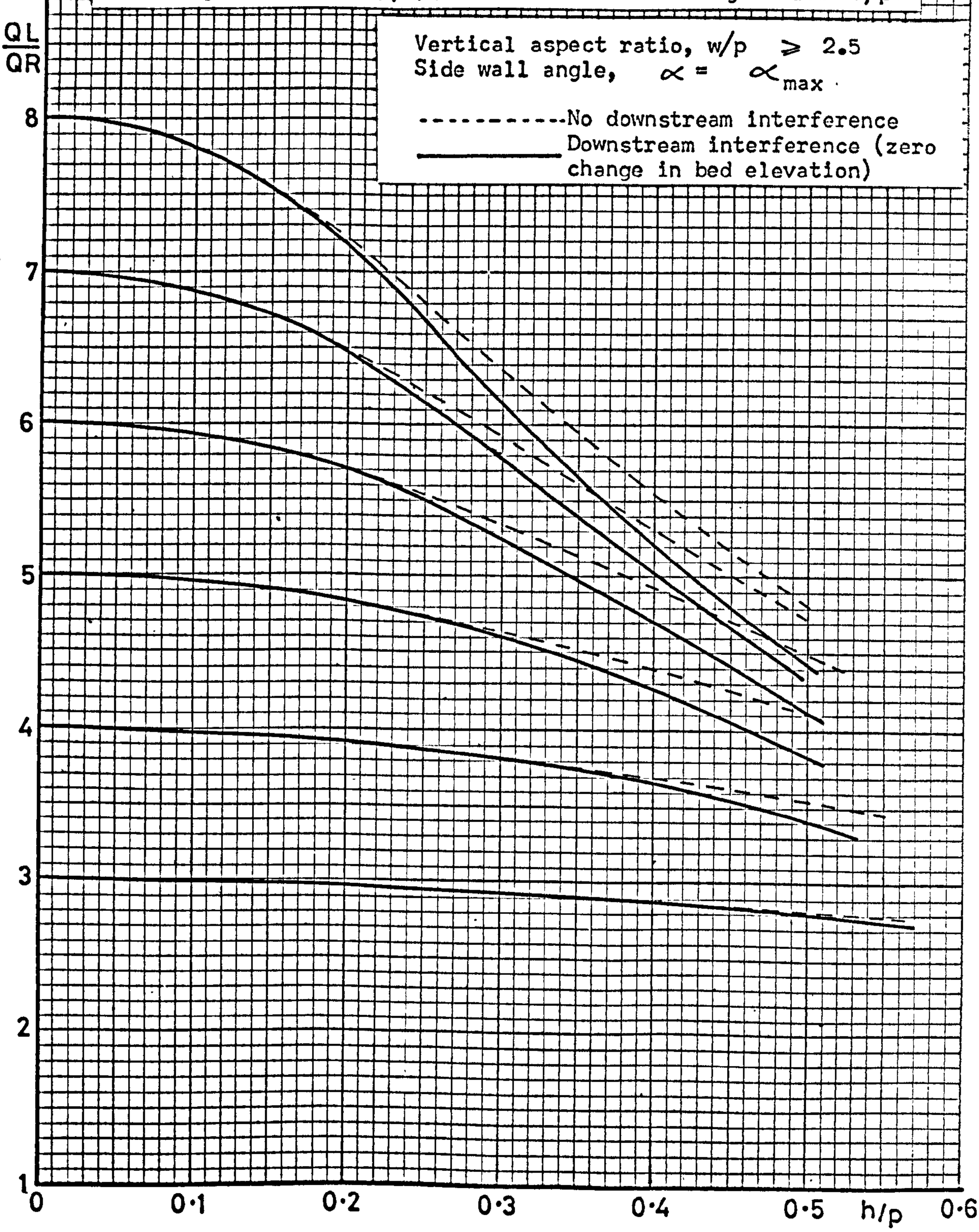

Figure 112

DESIGN CHART 2

TRAPEZOIDAL PLAN FORM WEIRS CONSTRUCTED WITHOUT APRONS

Flow magnification, QL/QR, 'v' head to crest height ratio h/p.

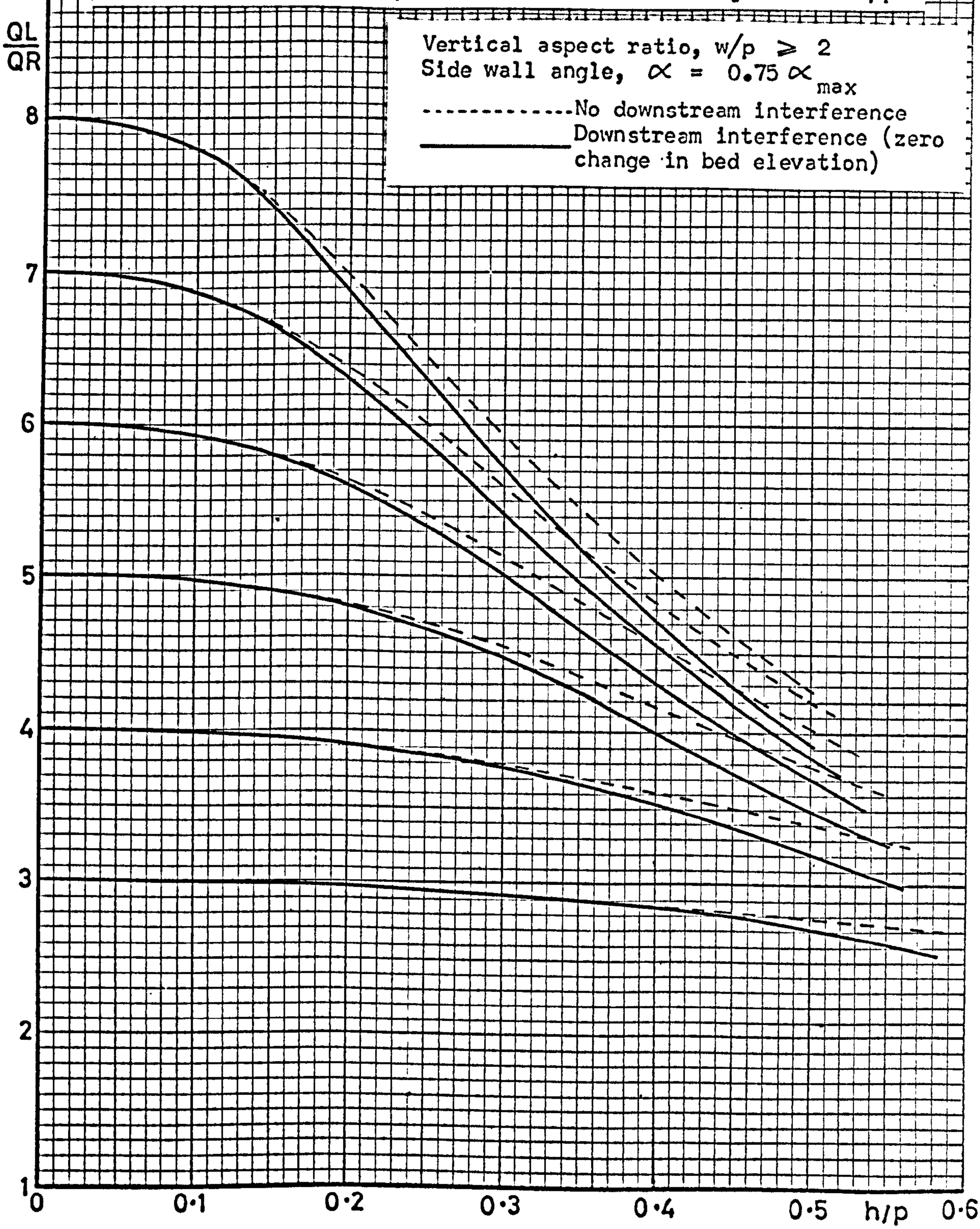

Figure 113

RATIO OF THE SEMICIRCULAR CREST COEFFICIENT TO THE SHARP CREST COEFFICIENT, f , VERSUS HEAD TO CREST HEIGHT RATIO, h/p

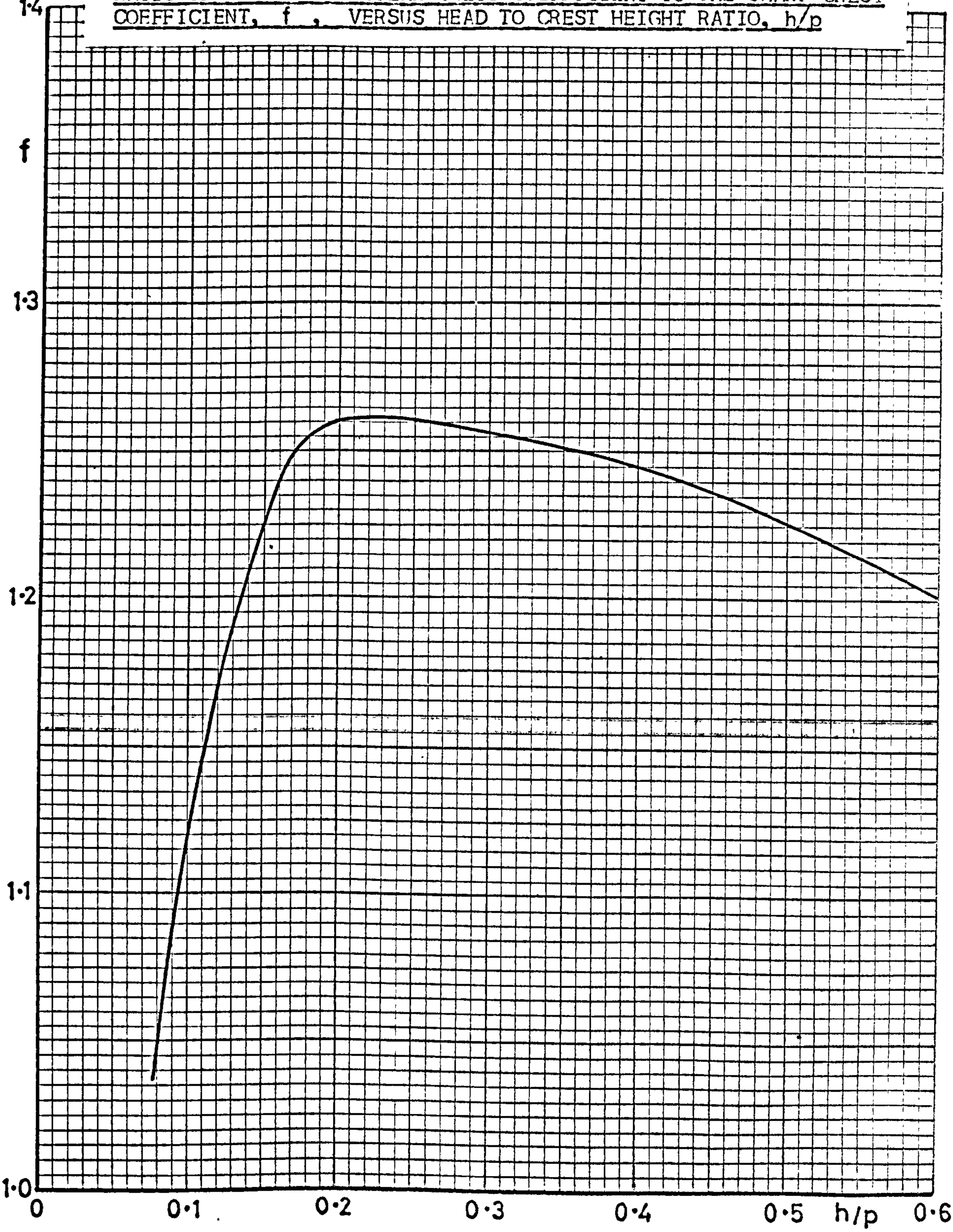

Figure 114

DESIGN CHART 2

TRAPEZOIDAL PLAN FORM WEIRS CONSTRUCTED WITHOUT APRONS

Flow magnification, QL/QR, 'v' head to crest height ratio h/p.

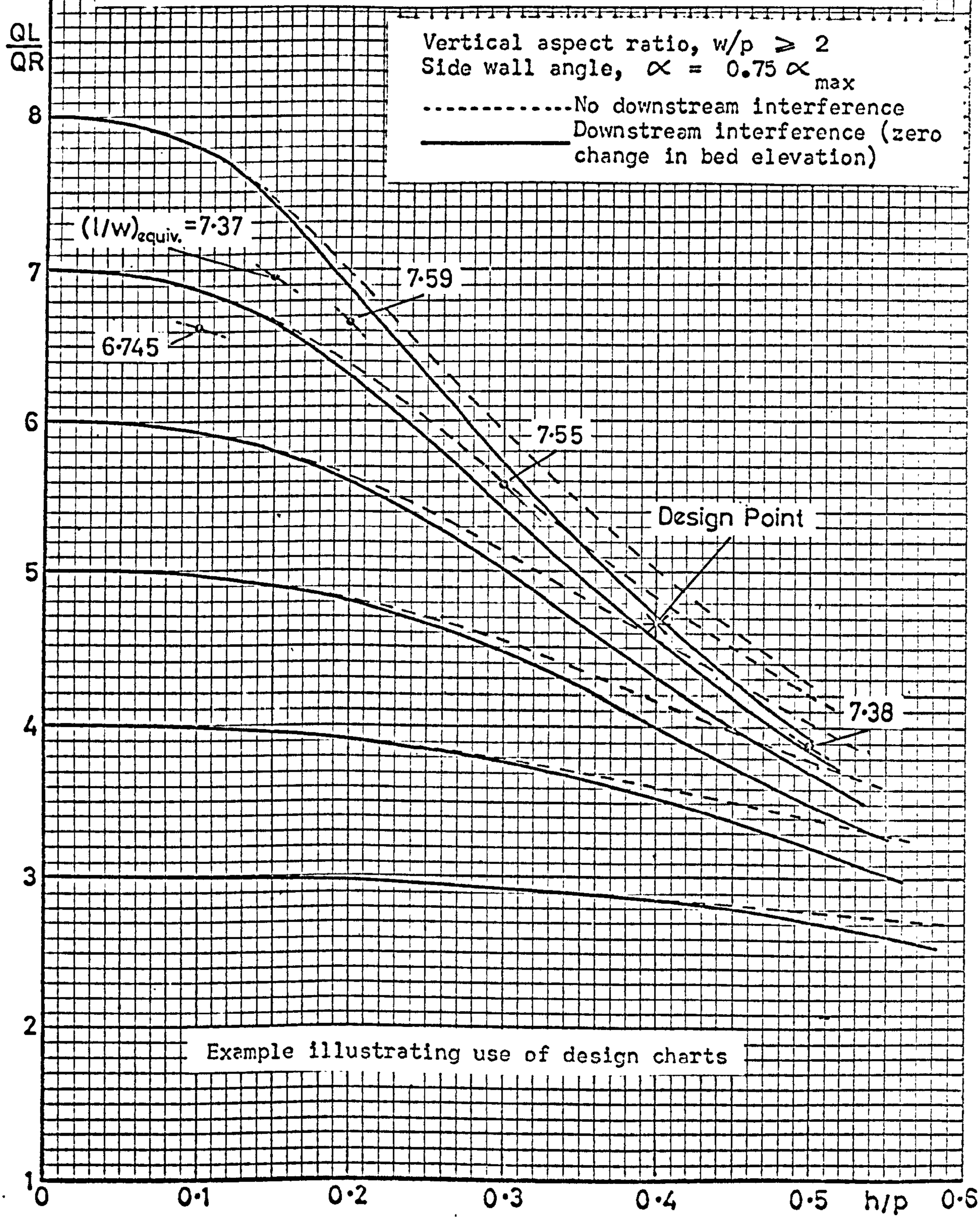

Figure 115

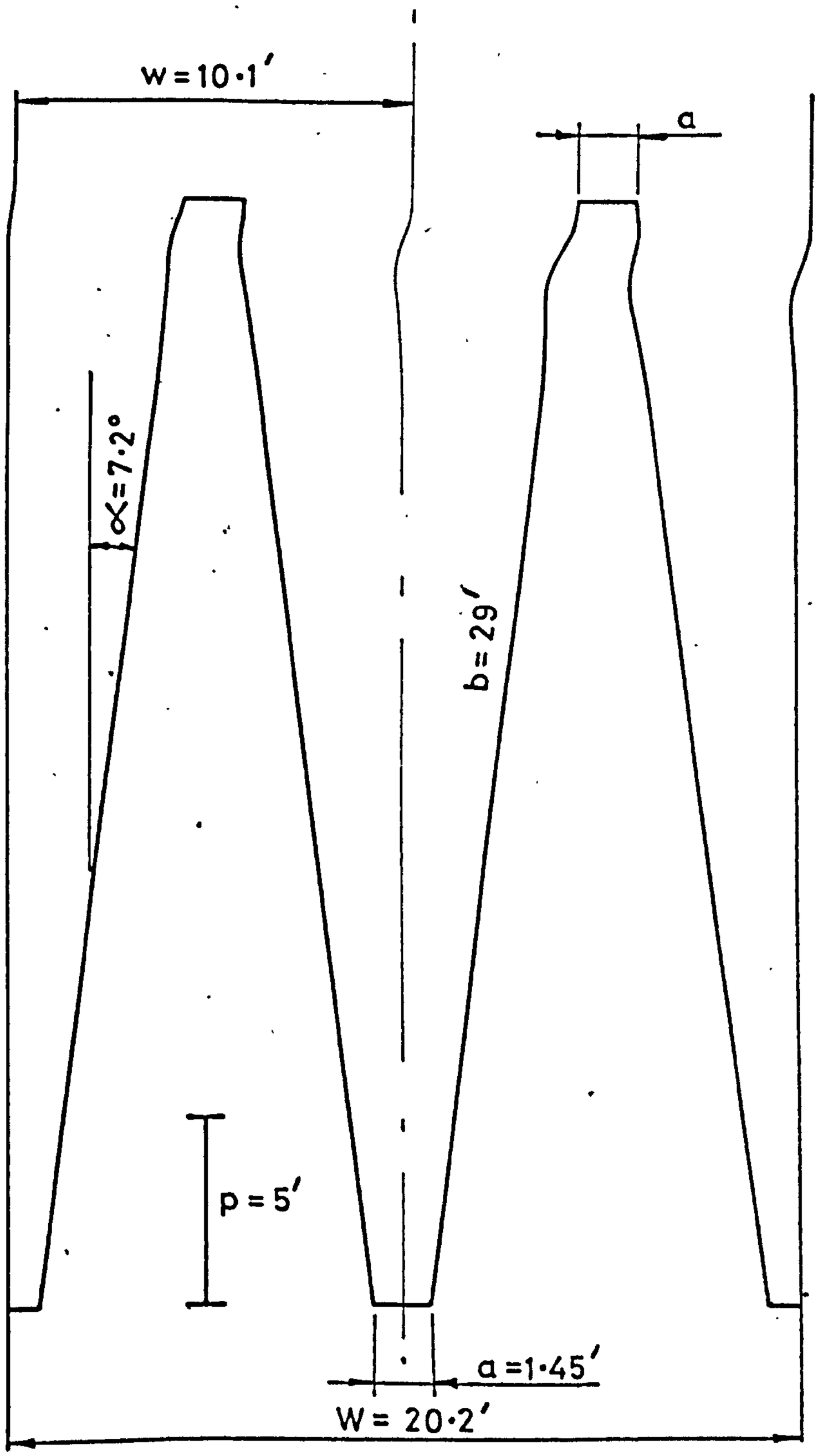

l/w = 6·02 , w/p = 2 , ∝ = 7·2°

SCHEMATIC SHAPE OF THE WEIR DESIGNED IN THE WORKED EXAMPLE

Figure 116

COMPARISON BETWEEN THE PERFORMANCE OF THE WEIR PREDICTED FROM THE DESIGN CHARTS AND EXPERIMENTAL RESULTS FROM MODEL TESTS

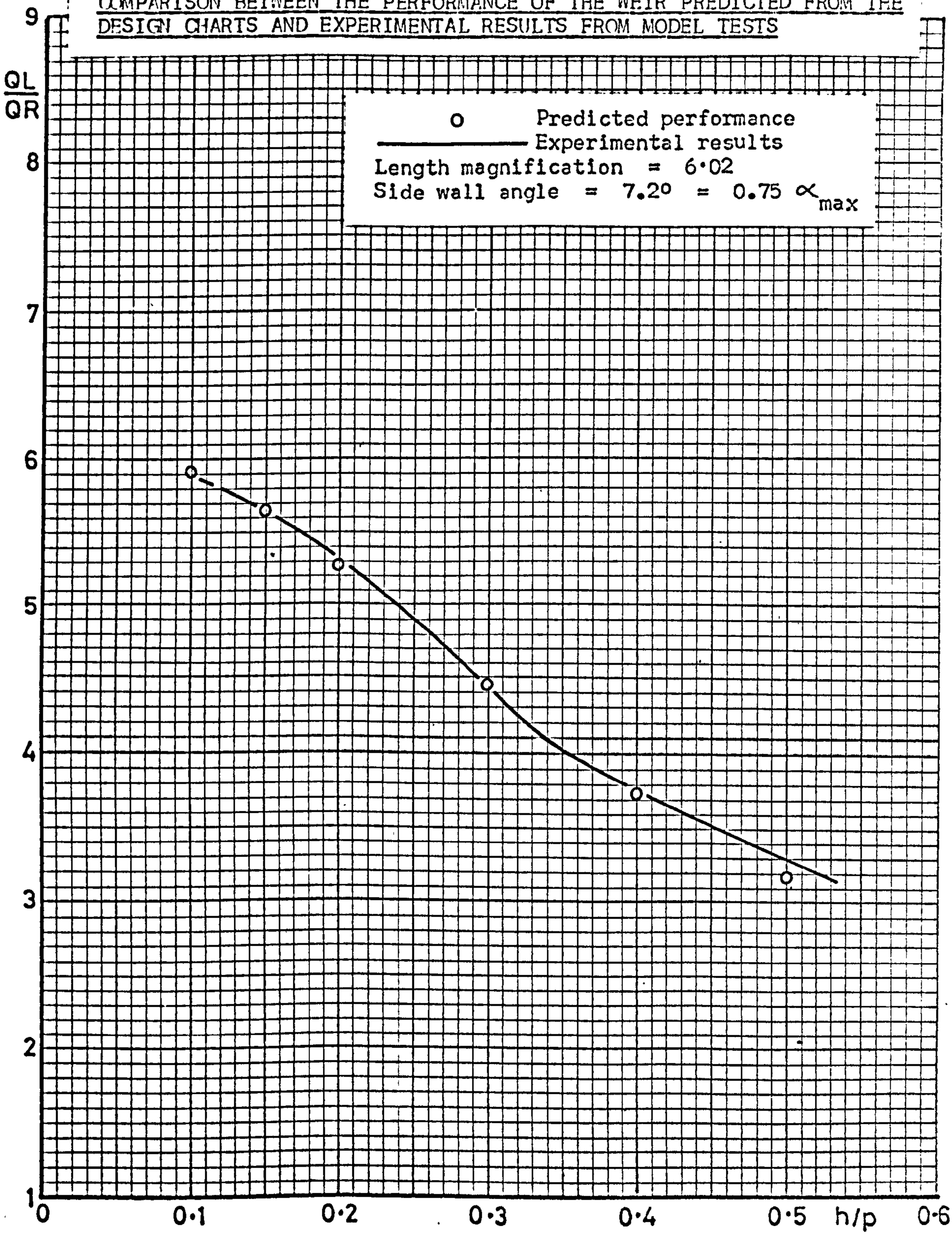

Figure 117

THE DISCHARGE CAPACITY OF THE WEIR DESIGNED IN THE EXAMPLE COMPARED WITH THE DISCHARGE THAT COULD BE OBTAINED WITH A CORRESPONDING LINEAR WEIR